# Development and Performance Prediction of Idaho Superpave Mixes

Prepared for

**Idaho Transportation Department**
Mr. Robert (Bob) Smith, PE
Mr. Michael Santi, PE
Assistant Material Engineer

Prepared by

## NIATT

**National Institute for Advanced Transportation Technology**
**University of Idaho**

Fouad Bayomy, Ph.D., P.E. (PI)
Eyad Masad, Ph.D., P.E. (Co-PI)
Samer Dessoukey, Graduate Assistant
Marhaba Omer, Graduate Assistant

# TABLE OF CONTENTS

Appendix A:    MIX PROPERTIES AND GRADATIONS – Mixes Obtained from the NCHRP 9-16 Project

Appendix B:    Worksheet for Calculating Shear Stress and Contact Energy Index, CEI.

Appendix C:    Job Mix Formula for ITD Mixes (D1, D2 and D3)

Appendix D:    Data for ITD Mixes Gradation, Volumetric Analysis and Calculation of Energy Indices (CEI and TEI)

Appendix E:    APA Test Results for ITD Mixes

Appendix F:    Image Analysis Test Results for ITD Mixes

Appendix G:    e-Files Included on CD-ROM

# LIST OF TABLES

# LIST OF FIGURES

# 1. INTRODUCTION

## 1.1 BACKGROUND

The original proposal for this research project dates back to August 98, in which the research problem statement emphasized that there are many on-going research efforts to address various challenges with asphalt mixes designed by the SHRP Superpave mix design system (AASHTO MP2). The WesTrack test road built in Reno, Nevada is the FHWA largest Superpave field implementation study. The main focus of WesTrack project was to develop a performance-based specification for Superpave mix construction. The state of Idaho faced, like many other states, several issues that are related to the construction and performance of these mixes.

As Idaho is preparing to implement the Superpave mix design system, the proposal identified several issues that need to be resolved, some of which are:

Selecting the appropriate gradation for different mix types,

Binder selection for various climatic regions in the state,

Mix design criteria for different layers and road class,

Incorporation of performance-based criteria for mix design optimization, and

Filed compaction specifications to achieve designated Superpave densities.

There are several on-going national projects to address one or more of these main issues that face not only Idaho, but all agencies that are moving towards Superpave system. For example, a five-year international project sponsored by FHWA is being conducted to develop a "simple" performance test that can be coupled with the Superpave mix design system. NCHRP project 9-16, which is currently being done at the Asphalt Institute, is focusing on prediction of performance by analyzing performance of actually built pavements. NCHRP 9-10 at the

University of Wisconsin, Madison focused on developing new specifications that work with polymer modified binders. NCHRP Report 459 has been recently released which summarized the results of the NCHRP 9-10 project.

The Superpave system was created to replace the long time used Hveem and Marshall methods, and this will not be in place until extensive experience has been established so that agencies can implement it with level of comfort that justify the spending on these superior mixes. Researchers from the University of Idaho NIATT Centre for Transportation Infrastructure (CTI) have teamed with ITD engineers to execute a plan that ensures a successful implementation of the Superpave mix design system. Such a plan involves developing mix design specifications that are relevant to traffic and environment in Idaho, build trial sections to validate developed specifications, and develop a mix design manual with specific data that are relevant to materials and environmental conditions in Idaho.

## 1.2   PROJECT OBJECTIVES

The plan mentioned above is a long-term and needs to be executed in a stepwise approach. ITD main need was to find out a measurable and objective mix design indicator that can be augmented to the volumetric-based Superpave mix design. Thus, for this project, the main objective was to target the first step in the plan mentioned above.  Two main objectives are sought of this project:

Develop a mix design indicator from the gyratory compaction parameters that can be related to pavement performance, especially rutting potential, and

Develop relationship(s) between these parameters and pavement performance.

## 1.3 RESEARCH METHODOLOGY

This research relates to the fundamentals of the development of the Superpave mix design system as represented by the strategic highway research program (SHRP). Based on research done under SHRP, it is concluded that the gyratory compactor reasonably simulates field compaction. One of the unique features of the Superpave volumetric mixture design procedure (AASHTO MP2) is the use of the gyratory densification curves to account for two phenomena: compaction during construction and densification under traffic during pavement service life. Hence, the methodology adopted was to develop gyratory compaction curve indices that relate to performance. This can be achieved through investigating the mix compaction characteristics and its field performance for pavements built with Superpave mixes. For this purpose, various mixes that are being investigated by the Asphalt Institute under the NCHRP project 9-16 were investigated in this study. It is to be noted that, the original plan was to get mixes from the WesTrack test road in Nevada, but this was not possible at the time of conducting the research. Instead mixes from NCHRP 9-16 were procured. For mixes developed for Idaho, performance can be predicted based on the developed relations from the gyratory compaction. If, at or near the end of this phase, a performance test has been recommended by the FHWA project, it can then be used to verify the developed recommendations.

## 1.4 PROJECT TASKS

Task 1: Development of project trial mixes: The original work plan for this project called for developing Superpave trial mixes, which have potential to be used in the state of Idaho. An experiment design was proposed to select two binder grades representing the northern and southern regions of the state and two gradations representing coarse and fine mixes. However, shortly after the initiation of the project, the research team determined that the best way to

implement this development is to use actual mixes that are being used for state projects. Those mixes are discussed in Chapter 6 of this report.

Task 2: Study the relationship between the gyratory compaction curve characteristics and permanent deformation (rutting) in pavements from WesTrack and other states. Develop compaction parameters that can be related to performance. During the execution of this project, WesTrack mixes were found to hard to get. Instead, mixes from NCHRP 9-16 project were obtained from the Asphalt Institute.

Task 3: Assess the sensitivity of the proposed compaction parameters to asphalt mixtures.

Task 4: Conduct gyratory compaction on Idaho mixes and measure the parameters, which are to be developed from tasks 2 and 3.

Task 5: Perform image analysis as well as energy calculations on obtained mix samples to identify regions in the densification curves that correspond to construction and traffic loading. This will assist in linking compaction parameters and aggregate structure to pavement performance.

Task 6: Establish performance criteria based on the developed compaction-performance relationship to be developed in task 5.

Task 7: Prepare a report to document research findings and recommendations for Superpave mix design and construction in the state of Idaho.

## 1.5   MODIFICATIONS TO THE ORIGINAL WORK PLAN

There are two modifications to the original research plan that emerged in order to facilitate the mix preparations and execution of the research plan. These are:

1.  In task 1, three mixes were selected from three ITD projects in Districts 1, 2 and 3 instead of developing trail Superpave mixes. The research team felt this was more

realistic approach to implement the research results. In addition, these mixes were

also verified whether they fit Superpave criteria or not. And, if not, they were

modified to satisfy the Superpave volumetric criteria.

2. Mixes from the asphalt Institute project, NCHRP 9-16, were procured instead of

the WesTrack project (Task 2). This modification was needed because the

WesTrack samples were not available and there was wide variety of mixes that

can be used from the NCHRP 9-16 project, which in fact was a better approach to

the overall project objective.


## 1.6   ORGANIZATION OF THE REPORT

This report documents the developed experimental and analytical procedures for assessing the

mix shear strength and stability during compaction in the Superpave Gyratory Compactor, SGC.

In addition, it briefly describes the work being done on the development of evaluation of Idaho

Superpave mixes.  The report is organized as follows:

The first chapter gives an overview of the problem statement, objectives, tasks, and report

organization.

Chapter two presents a detailed review of the development of the gyratory compactor and its

ability to produce specimen similar to field pavement.  It also discusses different formulas that

have been developed to express the shear stress in an asphalt mix during Superpave gyratory

compaction.  A review of internal structure analysis using imaging technology is also offered in

this chapter.

Chapter three presents detailed analysis of the asphalt mix compaction using the SGC.

Equations for the shear stress and stability index "Contact Energy Index (CEI)" based on energy

calculations are developed in this chapter.  The relationships between the CEI and mix

constituents, internal compaction variables, and mechanical properties are also discussed in chapter 3.

Chapter four presents two and three-dimensional finite element models of the compaction process in the SGC. The shear stress and CEI are calculated using these models and related to experimental measurements.

Chapter five presents the use of image analysis techniques to quantify the internal structure of asphalt mixes. The relationship between the internal structure analysis results and the CEI is investigated in this chapter.

Chapter six addresses the ITD mixes' selection and evaluation.

Chapter seven summarizes the main conclusions and recommendations of this study.

# 2. LITERATURE REVIEW

## 2.1 INTRODUCTION

Permanent deformation is one of the main distresses in asphalt pavements. It occurs due to the shear failure in asphalt mixes and/or underneath supporting layers. The shear strength of an asphalt mix is a result of the aggregate interlock and adhesion provided by the asphalt binder. Several mechanical tests have been developed to evaluate the resistance of an asphalt mix to permanent deformation. Some of these tests are intended to measure material properties that can be used in constitutive models for predicting permanent deformation. Others can only be used to rank asphalt mixes based on their resistance to shear failure under different loading conditions. These tests are conducted on asphalt mix specimens compacted using one of the available devices such as the roller compactor, California kneading compactor, Marshall hammer, and gyratory compactor.

Several attempts have been directed at extracting information about the mix shear strength and resistance to permanent deformation during specimen preparation, and especially in the gyratory compactor. These attempts have been motivated mainly by the need of a rapid method to assess the mix shear strength or stability. Specimens are prepared in the gyratory compactor under a combination of shear and normal forces, and the reaction of the mix to these forces can be analyzed and used as a predictor of its stability.

During the Strategic Highway Research Program (SHRP), the Superpave gyratory compactor (SGC) was developed to prepare specimens and as a tool for quality control in the field.

This chapter summarizes the literature review related to the development and operational characteristics of the gyratory compactors. It discusses some of the features of the gyratory

compactors developed prior to SHRP. Then, the chapter offers discussion on the development of the Superpave gyratory compactor during SHRP. The emphasis is on the characteristics of the Australian Servopac gyratory compactor used in this study.

In addition, the chapter presents a review of previous studies targeted at extracting information on the mix stability during gyratory compaction. These studies focused on analyzing the compaction curves, or measuring the shear strength of the mix as compaction progresses. The experimental results from these studies are discussed, and the limitations of the analysis methods are presented. Finally, the application of image analysis techniques in qualifying the internal structure of gyratory compacted specimens is presented.

## 2.2   DEFINITION OF ASPHALT MIX

Asphalt concrete mix, often referred to as Hot Mix Asphalt (HMA), is a paving material that consists of asphalt binder and mineral aggregate. The asphalt binder, either an asphalt cement or modified asphalt cement, acts as the binding agent that glues aggregate particles into a dense mass and to waterproof the mixture. When bound together, the mineral aggregates act as a stone framework to import strength and toughness to the system. The performance of the mixture is affected by both the properties of the individual components and their combined reaction in the system.

## 2.3   DEVELOPMENT OF GYRATORY COMPACTORS

The researchers of the Strategic Highway Research Program (SHRP) had several goals in developing a laboratory compaction method. Most importantly they wanted to realistically compact mix specimens to densities achieved under actual pavement climate and loading condition. The compaction device was needed to be capable of measuring compactability so that

potential tender mix behavior and compaction problem could be identified. In addition, a high priority of SHRP was a device portable enough for use in mixing facility and quality control operation. Since no existing compactor achieved all these goals, the Superpave Gyratory Compactor (SGC) was developed. The basis for the SGC was some of the operational characteristics of the Texas gyratory compactor, the Corps of Engineering gyratory compactor, and French gyratory compactor. The development and characteristics of these compactors are discussed in the following subsections.

### 2.3.1 Texas Gyratory Compactor

Gyratory compaction has been used in asphalt mixture design since the 1930's when a procedure was developed by Texas Department of Transportation. The original gyratory compaction procedure was done manually. A mold, constructed from a section of 4-inch inside diameter pipe, was placed between two parallel plates. The plates were spaced one half inch further apart than the mold height, which allowed the mold to be, tilted approximately 6 degree until the diagonal corners contacted the upper and lower plate, (*Huber 1996*).

A study by *Consuegra et al. (1989)* evaluated different compactors and ranked the Texas gyratory first in terms of its ability to produce compacted mixtures with engineering properties similar to those of field cores, because of its operational simplicity, and the potential to use the large gyratory models capable of fabricating large-size aggregate.

A similar study conducted by *Button et al. (1994)* found the Texas gyratory to have the advantage over other laboratory compaction mechanism in producing specimens similar to pavement cores in their mechanical properties. A study by *Sousa at al. (1991)* showed that the mechanical properties of field cores lied between those of the Texas gyratory compacted specimens, and the California kneading compacted specimens.

### 2.3.2 Corps of Engineers Gyratory Compactor

During the post World War II the Corps of Engineers began developing a testing machine based on the gyratory compaction process. The Gyratory Testing Machine (GTM) was designed to measure forces during the compaction process, as shown later these forces were used to calculate the shear strength of the mix. It was postulated that the change in angle during compaction could be related to permanent deformation performance. The GTM was used to design asphalt mixes for heavy-duty airfield pavements, (*Huber 1996).*

The Corps of Engineering GTM has been recognized as a research tool for years by many agencies around the world and for mix design and quality control of asphalt pavement construction. The GTM process has been adopted in ASTM D 3387 standard. According to *Mc Rea (1962)* the kneading compaction used in the GTM produces a specimen that has stress-strain properties that are more representatives of the actual compacted asphalt pavement structure than an impact hummer compaction. This conclusion was reached based on previous studies that compared the mechanical properties of GTM specimens with field cores (Ruth and Schaub 1966). *Murfee and Manzione (1992)* indicated that the GTM is still preferable to the Marshall method of mix design for pavement subjected to heavy loads

As reported by *Crawley (1993)*, the research conducted by the Mississippi Department of Transportation (MDOT) indicated that the GTM shear strength properties were more sensitive to variations in the mixture proportions than was Marshall stability. *Ruth et al. (1992)* reported that the GTM provides rapid assessment of a mixture's shear resistance as related to changes in asphalt content, aggregate gradation, and density.

### 2.3.3  French Gyratory Compactor (LCPC Compactor)

During the 1960's and early 1970's, the development of the French gyratory compactor protocol occurred. In the early 1970's LCPC replaced the Marshall method of mix design with a new method using the French compactor. Extensive studies investigated the shape of the gyratory densification curves and the effects of aggregate gradation, mineral filler content, and asphalt properties on the position and slope of the curve. During the same time, studies were done to investigate the compaction characteristics of mixture under rollers and relate the results to densification properties of the mixture in the compactor, (*Huber 1996)*. As a result, the current LCPC mix design standardizes the relationship between the compaction effort on the road based on the number of gyrations in the laboratory to the number of roller passes in the field. This relationship was established based on investigating the compaction characteristics under rollers and related the results to densification properties of the mixture in the compactor, (*Moutier 1997)*. As opposed to the GTM, the French compactor operates under a preset gyration angle, and the mold is heated during the compaction.

### 2.3.4  Superpave Gyratory Compactor

The decision to develop the Superpave gyratory compactor was based on NCHRP 9-5 Study. This study focused on compaction methods and developed a preliminary mix design and analysis system using pre-SHRP performance related tests, *(Huber 1996)*.

The Superpave Gyratory Compactor (SGC) is a transportable device whose primary function is to fabricate test specimens by simulating the effect of traffic on an asphalt pavement, produce large specimens to accommodate large size aggregates, and allow monitoring the densification during compaction. According to a study by *Consuegra et al. (1989)* the Superpave gyratory compactor provides specimens that are much more representative of actual in-service pavements. The level or amount of compaction is dependent on the environmental conditions and traffic levels expected at the job site.

Studies conducted at the Asphalt Institute during SHRP investigated the effect of angle of gyration, speed of gyration and vertical pressure on mix densification, *(SHRP 1994)*. Density was most influenced by the angle of gyration. Speed of gyration showed little effect on density, while vertical pressure had a small effect on the density achieved.

As mentioned earlier the ability to evaluate the rate of densification was selected as a desirable characteristic during SHRP research. The constant angle and constant vertical pressure of the Texas gyratory compactor allowed the densification curves to be developed. Early testing showed that a high angle, five degrees, produced a very rapid rate of compaction and produced densification curves, which were difficult to measure. An angle of one degree was then selected which matched the LCPC protocol. Subsequent work indicated that the rate of densification was not sufficient; hence, the final angle selected for Superpave was 1.25 degrees, *(SHRP 1994)*.

The current Superpave gyratory compactor operates at a constant pressure of 600 kPa. The mixture is compacted by a gyratory kneading action using a compaction angle of 1.25 degrees and operating at 30 rpm. By knowing the mass of the specimen being compacted and the height of the specimen, specimen density can be estimated during the compaction process. This is accomplished by dividing the specimen mass by the specimen volume. The current mix design requires that percent air voids in the gyratory specimens meet certain criteria at different number of gyrations in order for the aggregate blend and optimum asphalt binder to be acceptable.

### 2.3.5 Servopac Gyratory Compactor

Australia in 1992 adopted the gyratory compactor as a standard method for preparing asphalt mix specimen. The first Australian gyratory compactor, the Gyropac, was produced in 1992. Following a period of investigation and development, *Australian Standard AS1289.2.2 (1995)*, for preparing asphalt specimens by gyratory compaction. Subsequently, a number of State Road Authorities have replaced the Marshall compaction method in their standard asphalt specification documents with gyratory compaction, (*Butcher 1998*).

The Australian gyratory compactor meets the standards of the Superpave gyratory compactor in terms of angle, pressure and monitoring of specimen height during compaction. It is discussed here in a separate section in order to highlight its additional features that make it an attractive machine for measuring the shear stress at the mix during compaction.

The second generation Australian gyratory compactor, the Servopac, is a servo-controlled gyratory compactor, designed to apply a static compressive vertical force to an asphalt specimen, whilst simultaneously applying a gyratory motion to a cylindrical mold containing the asphalt, (*Butcher 1998).* The Servopac was designed to maintain the gyratory angle constant during compaction, and to provide a means to simply and quickly adjust the critical compaction variables (pressure, angle). It is Discussed in the following chapter, the forces applied to a specimen during compaction. These forces recorded by the machine can be used to calculate the shear stress of the mix, and predict its stability, (*Butcher 1998).*

## 2.4  SHEAR STRESS PARAMETERS

The gyratory compactor actuators exert forces on the specimen during compaction in order to apply the vertical pressure and angle of gyration. The response of the mix to these forces can be monitored and used to evaluate the mix stability. Two main approaches can be identified in the literature in order to achieve this objective. The first approach is analyzing the compaction curve characteristics, and relating them to mix stability. The second approach relies on developing experimental tools and analysis methods to measure the shear stress during compaction and relating them to stability. The following sections discuss these two approaches.

### 2.4.1  Compaction Curve Characteristics

An experiment conducted under SHRP contract A-001 evaluated the ability of the SGC to discern changes in key mix properties, *(SHRP 1994).* Results of height measurements taken

during the compaction process were used to calculate changes in specimen density expressed as a percent of the maximum specific gravity $G_{mm}$ %.  A plot was made of the percent maximum specific gravity versus the log of the number of gyrations. This compaction or densification curve is characterized by three parameters. $C_{10}$ is the percent maximum specific gravity after 10 gyrations, and $C_{230}$ is the percent maximum specific gravity after 230 gyrations.  The slope of the densification curve, K, is calculated from the best-fit line for all data points assuming that the curve is approximately linear.

A comparison of $C_{10}$, $C_{230}$, and K found that they were sensitive to changes in asphalt content, gradation or aggregate type.  Based on the results of this experiment, it was found that the slope of the compaction curve, K, was affected by asphalt content and the aggregate percent passing the 75 μm sieve.  The position of the curve however, varied as the experiment variables changed.  Other studies have also related K to mix performance; *Rand (1997)* for example, showed that K is strongly related to the amount of asphalt and coarse aggregates in the mix. A study in France compared the K values for two mixes with known permanent deformation in the field, (*Moutier 1997*).  This study illustrated that higher K values were associated with better performance in the field.

It is noted that most of the studies on the SGC used the average slope of the compaction curve.  However, one of the unique features of the Superpave volumetric mixture design procedure developed by *SHRP (AASHTO MP2 1996)* is the use of the gyratory densification curves to account for the two phases of compaction in situ:

(a) Compaction during construction using rollers at high temperatures, and

(b) Densification under traffic at ambient temperatures.

It is well recognized that a good mixture should be easy to compact during construction, but should show adequate resistance to permanent deformation under traffic. Therefore, in order to be able to effectively evaluate permanent deformation potential, compaction properties should be evaluated relative to these distinct phases. The compaction curve characteristics should be analyzed to identify mixes that:

(a) can be successfully compacted during construction, but

(b) can resist traffic induced densification and alternate plastic flow.

### 2.4.2  Shear Stress Measurements

Other measurements that might be derived from the gyratory compaction are based on the resistance to deformation and the amount of energy required to compact the mix. Compaction in the gyratory compactor occurs due to two mechanisms; vertical pressure at the top of the specimen and shear displacement induced by the gyratory movement.

*McRea (1965)* proposed a formula to determine the shear stress in the asphalt mixture during compaction in the GTM, the formula is based on a simplicity equilibrium analysis of the mix and the mold by taking the moment about the lower center of the mix (0). (Figure 2.1)
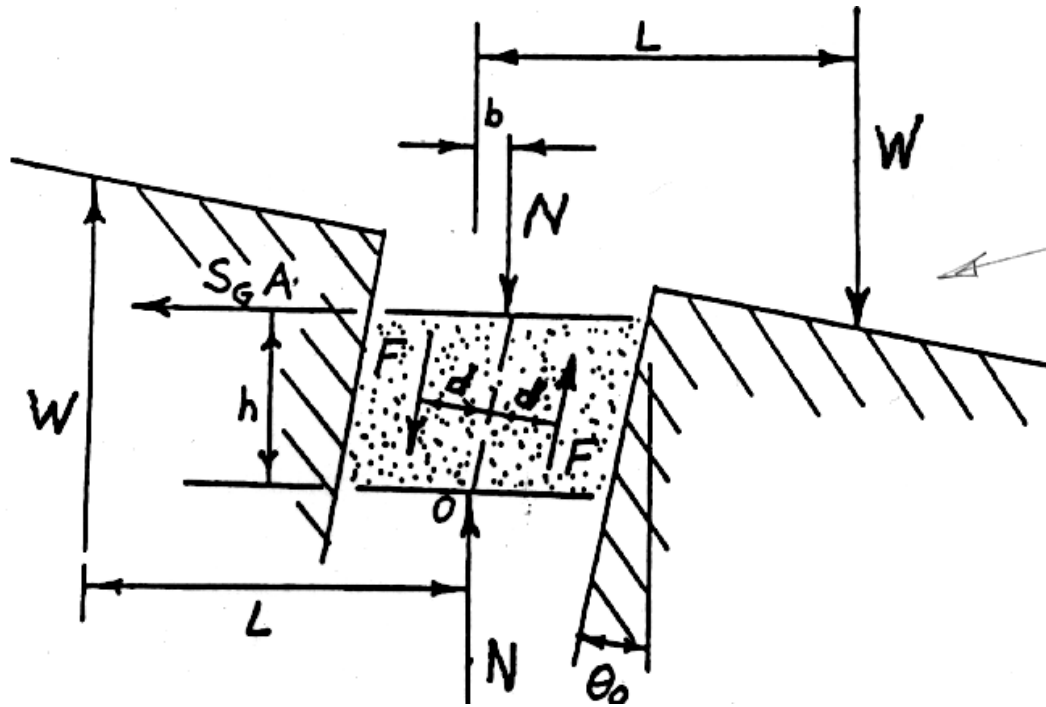
Figure 2.1 Parameters used for Calculating the Shear Stress ( *McRea 1965*).

$$S = \frac{2(W * L - F * d) + (N * b)}{A * h} \qquad (2.1)$$

Where, S is the shear stress, F is the friction force between the aggregate particles, d is the distance of the resultant friction from the center, N is the applied vertical pressure, A and h are the sectional area and the height respectively, W is the applied forced to proceed the angle, and L is the moment arm to point (0). *Mc Rea (1965)* neglected the distance b -arguing that it is too small- and the friction force F, then he obtained the following equation:

$$S = \frac{2 * W * L}{A * h} \qquad (2.2)$$

It is noted that the free body diagram in **Figure 2.1**, includes external and internal forces which is incorrect. Also, the derivation neglects the friction between the mold and the mix. These assumptions are believed to affect the validity of equation (2.2), and limit its applicability.

16

A study by *Kumar and Goetz (1974)* was performed to evaluate:

1) the GTM design method, and

2) the relationship between densification and the mixture properties, and

3) the job mix formula tolerance limits.

They noted that the gyratory shear results (i.e. equation 2.2) on gravel mixtures indicated in general that coarse gradation and low percent asphalt combinations were different as compared with fine gradation and high percent asphalt combinations. *Kumar and Goetz (1974)* showed that the difference in gyratory shear values was insignificant with respect to variations in percent asphalt content. They also indicated that the GTM was sensitive to study the changes in mixture properties caused by small variations in gradation and asphalt content.

*Sigurjonsson and Ruth (1990)* conducted a study to evaluate the sensitivity of the GTM to minor changes in asphalt content and aggregate gradation. They showed that the combined effect of aggregate particle shape, surface texture, and gradation of the aggregate blend could be evaluated for level of attainable shear strength (equation 2.2) and for sensitivity to slight changes in mix proportions. Also, a minimum S value of 54 psi (372 kPa) should be required for any mixture densified for 200 revolutions. They estimated that a dense-grade structural mix should have a minimum shear stress value of 56 psi (386 kPa) when the pavement lift thickness is greater than 50 mm. They also showed that the GTM densification testing procedure provides information on the shear resistance of the mix regardless of the factors influencing its behavior (e.g., air void content, aggregate characteristics, asphalt content, and VMA).

A study by *Ruth et al. (1991)* used the GTM air roller testing procedure to evaluate asphalt mixtures and to identify undesirable mixtures which would be susceptible to excess permanent deformation. Regression analyses were used to show the relationships between the

gyratory shear (S) value and physical properties of the mixture. *Ruth et al. (1991)* used two different sources of aggregate, different aggregate blends, and asphalt AC-30. These mixes conformed to Florida DOT specifications. They concluded that the GTM compaction and densification testing procedure provided rapid assessment of a mixture's shear resistance as related to change in asphalt content, aggregate gradation, percent of natural sand and density. Figure 2.2 shows the influence of binder content sensitivity on gyratory shear measurements in the GTM, while S of 372 kPa at 200 gyrations was thought by them to be applicable for light to medium traffic conditions.
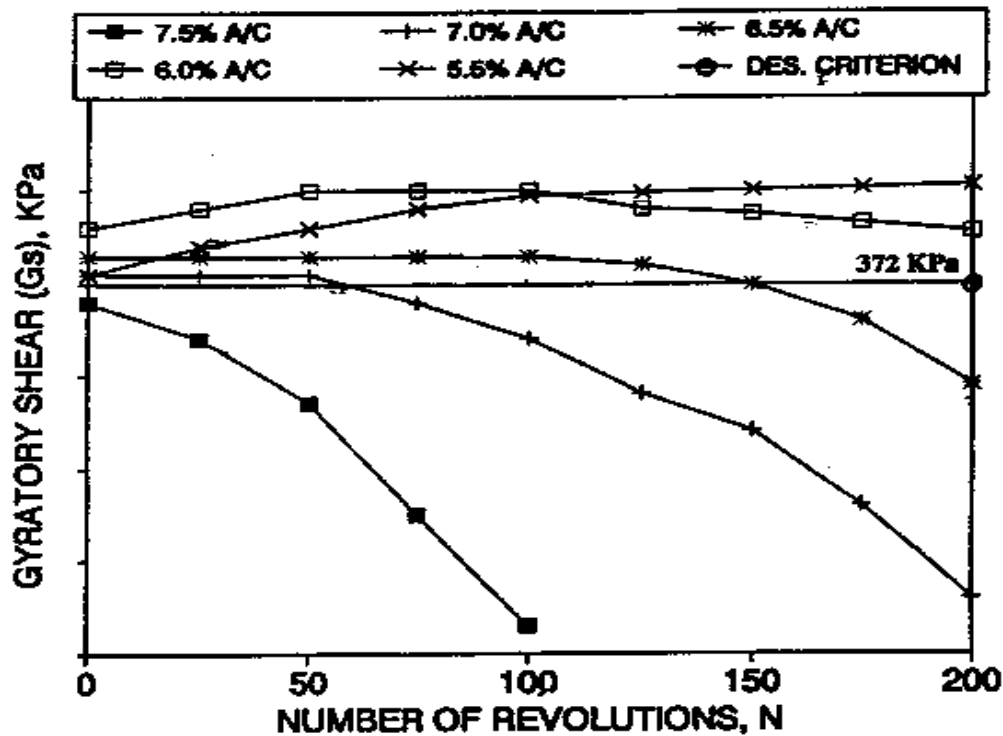


**Figure 2.2** Typical GTM Densification Results, (Ruth et al. 1991)

*De Sombre et al. (1998)* used a gyratory compactor from Finland to estimate the shear stress and the compaction energy for different asphalt mixes. They stated that energy is transferred to the specimen through the moment needed to apply the gyratory action.  A load cell located on the piston of the compactor measures the lateral load needed to create this moment as shown in **Figure 2.3**. *De Sombre et al. (1998)* measured this moment and used it in conjunction with the sample geometry to calculate the shear stress in the sample at any point in time.  The shear stress was calculated using a similar equation to 2.2.
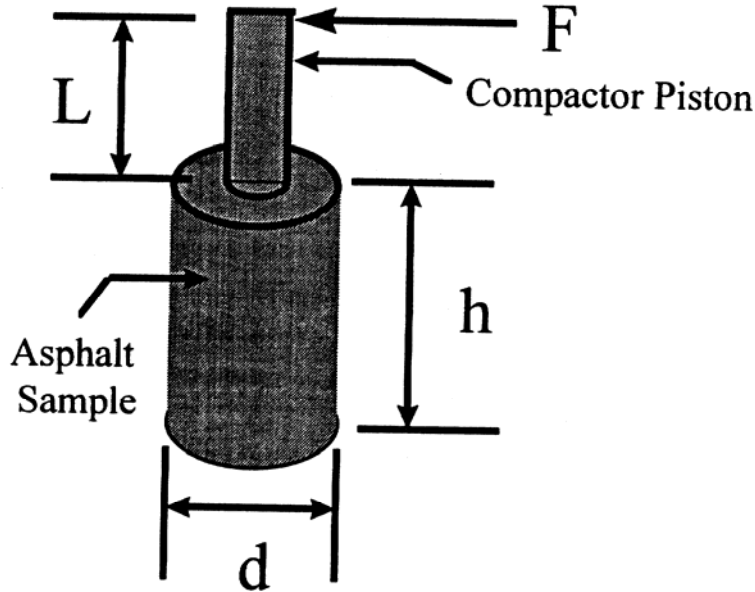


**Figure 2.3** Parameters for the Calculation of Shear Stress (De Sombre et al.1998).

*De Sombre et al. (1998)* argued that the change in height during compaction can be used to calculate the amount of power required during compaction.

$$\text{power} = \frac{\sum p \cos \alpha \times \Delta h \times r^2 \times \pi}{t}$$
(2.3)

19

where:

p = pressure in cylinder,

α = gyratory angle,

Δh = change in height per cycle,

r = radius of cylinder and

t = time.

A study conducted at the Department of Transport in Australia had shown that the shear stress evolution calculated using equation (2.2) was a function of the applied angle and mix components, *(Butcher 1998)*. At an angle of gyration greater than or equal to $1.00^o$, the shear stress increased with compaction until a maximum value is reached when it began to decrease with further increase in the compaction level as shown in **Figure 2.4**. In general, the reduction of shear stress was shown to be more significant in mixes with softer asphalt (AC14) that were more susceptible to permanent deformation as shown in **Table 2.1**. This study also used the change in voids at maximum shear stress as a parameter to distinguish among mixes. **Figure 2.5** shows that mixes with different asphalt grades experienced distinct changes in percent air voids at maximum shear stress. Other studies have also illustrated the relationship between the change of shear stress with compaction and the change in mix design components *(Gauer 1996, Moutier 1996)*.
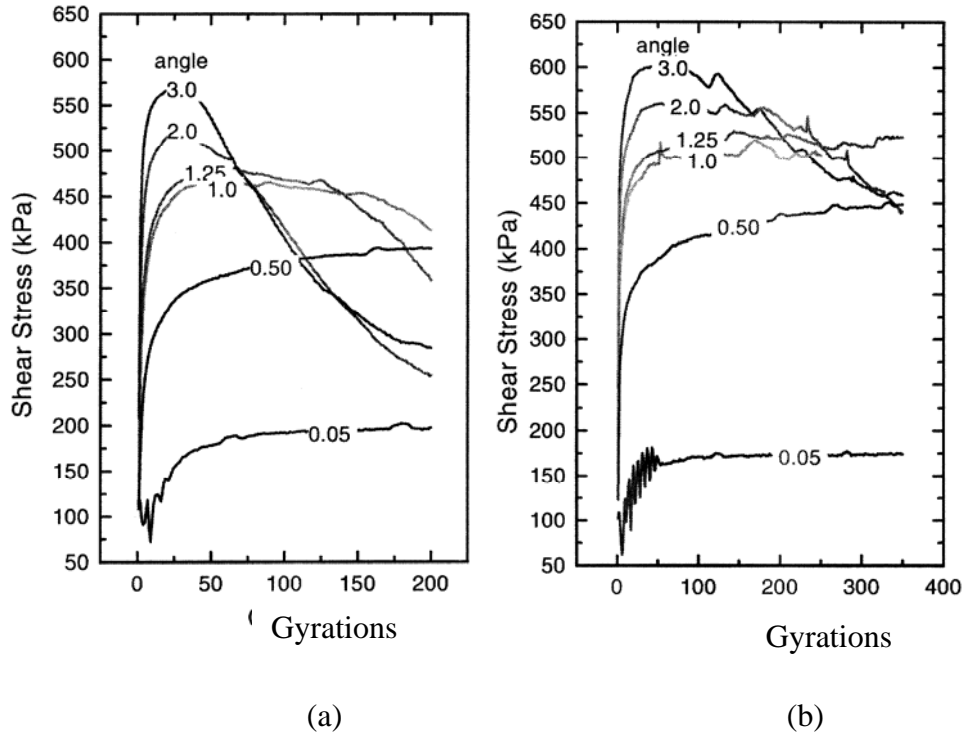
Figure 2.4 Shear Stress Measurements at Different Compaction Levels; (a) AC14 (soft asphalt) (b) AC 20 (stiff asphalt) (*Butcher 1998*).

**Table 2.1** Maximum Shear Resistance at Different Angles and Binder Type (*Butcher 1998*)

| Angle (Deg.) | Vertical Stress (kPa) | AC14 | | AC20 | |
|---|---|---|---|---|---|
| | | Max. Shear Stress (kPa) | Voids (%) | Max. Shear Stress (kPa) | Voids (%) |
| 0.05 | | 175 (est.*) | - | 225 (est.*) | - |
| 0.50 | | 405 (est.*) | - | 450 (est.*) | - |
| 1.00 | | 467 | 5.1 | 502 | 4.3 |
| 1.25 | 600 | 481 | 4.4 | 529 | 4.0 |
| 1.50 | | - | - | 534 | 4.5 |
| 2.00 | | 515 | 4.4 | 561 | 4.9 |
| 3.00 | | 571 | 4.1 | 601 | 4.3 |
| 2.00 | 400 | 365 | 5.6 | 398 | 5.7 |
| 2.00 | 240 | 231 | 5.6 | 250 | 4.6 |

*\* Maximum shear resistance not achieved and values estimated.*

21
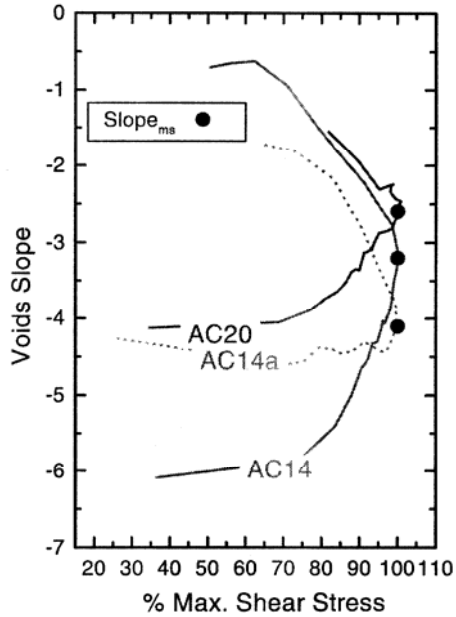
**Figure 2.5 The Change in Percent Air Voids at Maximum Shear Stress (Butcher 1998).**

*Butcher (1998)* showed that these results appear to confirm the universal nature of the first stage of shear stress development during compaction. Further confirmation appeared to be in the French work by *Moutier (1997)* as represented in Figure 2.6. A suggested explanation for the evolution of shear stress as offered by *Moutier (1997)* was that the shear force increased gradually as the percent compaction increased. The particles tried to interlock to each other with the assistance of the sufficient binder content. Further compaction may lead the binder to get out between the particles and lead to particles fracture or deformation.

Another study was carried out by *Mallick (1999)* to develop a method for using the SGC and the GTM compaction data to identify unstable mixes during the construction process by extracting parameters from the compaction curve. Five projects were selected in this study including construction of wearing courses on I-90 in Idaho, I-40 in New Mexico, US-280 and AL-86 in Alabama and I-385 in South Carolina, knowing the aggregate type and gradation,
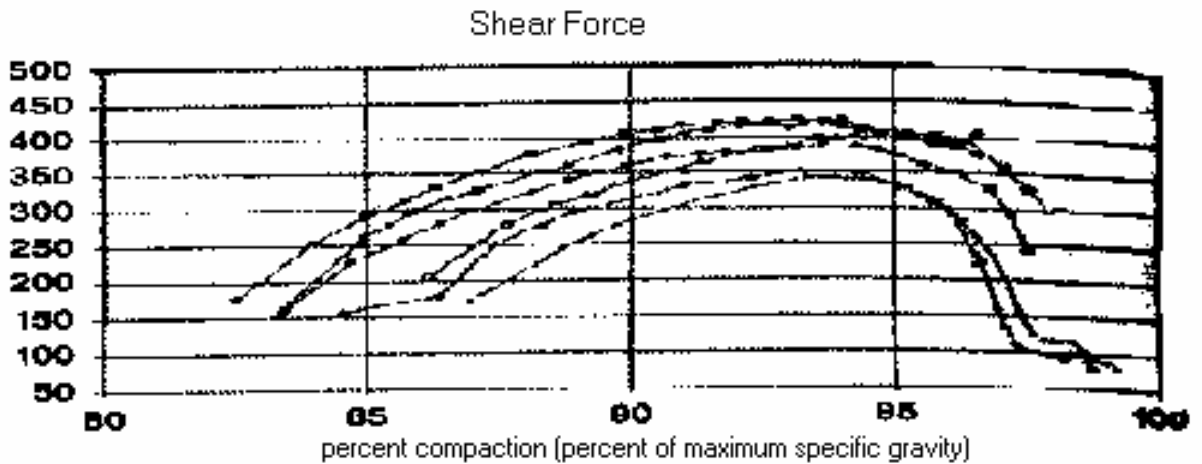
Figure 2.6 French maximum shear stress by *Moutier (1997)*

asphalt binder type and content, and traffic levels of these projects. All of these mixes were compacted with the SGC operated at 600 kPa and a 1.25-degree angle, and all mixes except the I-385 were compacted with the GTM operated at 800 kPa and a 1-degree angle.

The shear stress measurements in the GTM are shown in **Figure 2.7.** The results show that the I-90 mix is inferior to the other mixes. In the SGC, *Mallick (1991)* identified inferior mixes during compaction process by calculating the gyratory ratio between the number of gyrations required by the Superpave gyratory compactor to compact a mix to 98 and 95 percent of theoretical maximum specific gravity. He presented the results in **Figure 2.8** to show the relationship between rutting in the field and the gyratory ratio.

A method for using the Superpave Gyratory Compactor (SGC) results to select optimum mixture design introduced by *Bahia et al. (1998)*. The method divided the measured densification curve into two zones. The first zone represents the compaction characteristics related to the construction stage; the second zone represents the densification under traffic.

23
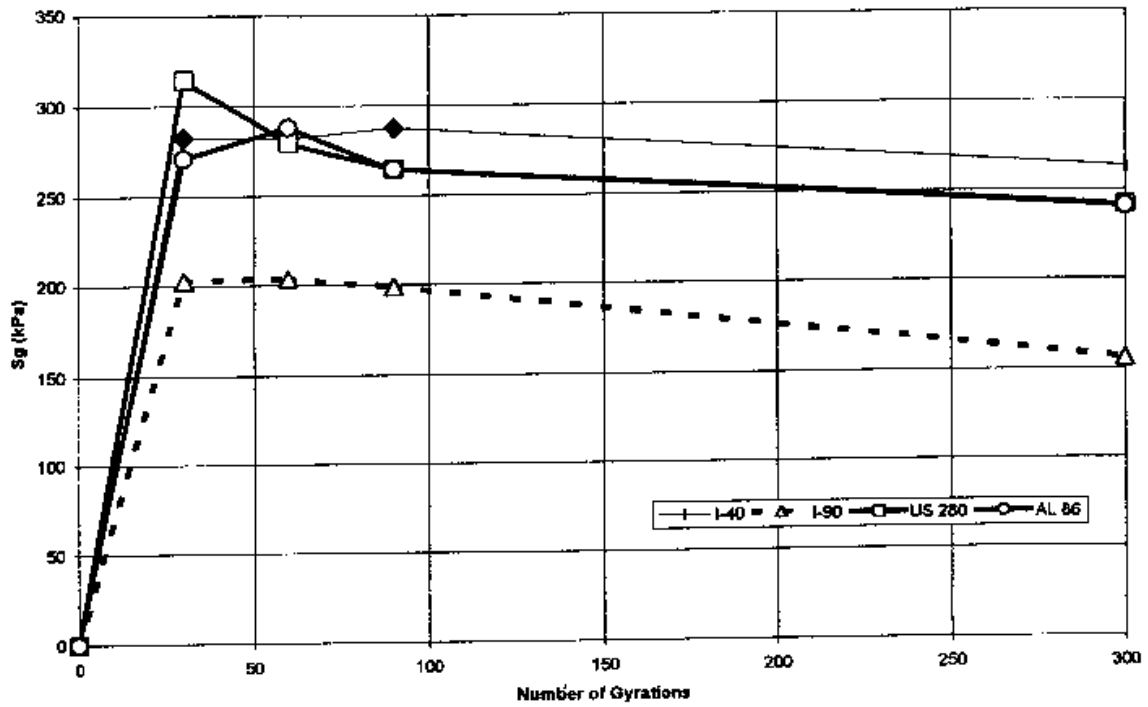
**Figure 2.7** Plot of Gyratory Shear (Sg) Versus Number of Gyrations (Mallick 1999)
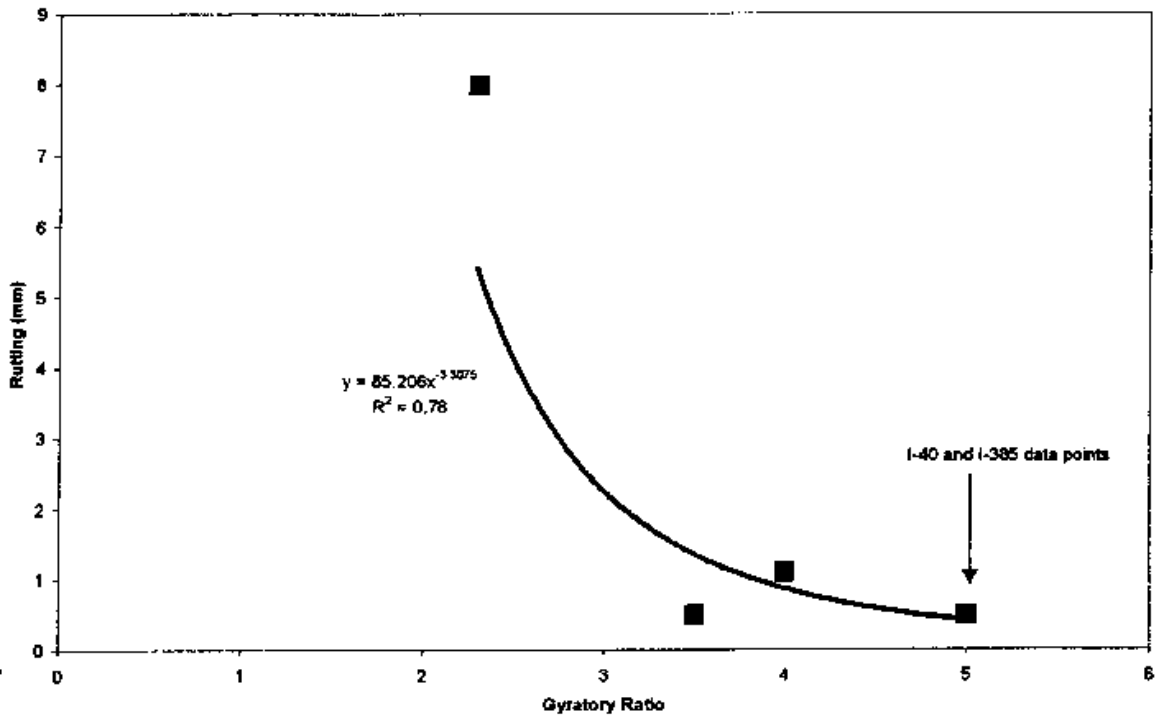


**Figure 2.8** Plot of Rutting Versus Gyratory Ratio (Mallick 1999)

Bahia et al. (1998) found that the densification curve measured by the SGC could be used to calculate densification indices that represent the performance of mixture during construction and during in-service. They also introduced the Compaction Energy Index (CEI) and the Traffic Densification Index (TDI) to evaluate the potential performance of mixture during construction and in-service. The values of CEI and TDI for different gradations tested showed that finer gradations, above or passing through the restricted zone, require significantly less energy to compact to 8% air voids, also these mixtures offered more resistance to densification between 8% and both of 4% and 2% air voids. This indicated that finer blends could be more favorable for construction and can perform better under traffic densification. They showed the importance of fine aggregate angularity for some mixture and also suggested that blends with high content of rounded sand may offer reasonable performance.

Guler et al. (2000) conducted a study for the purpose of developing a device that can be used in the SGC and allow shear measurements. The device consists of three load cells placed $120^o$ apart on the top plate of the SGC called the Gyratory Load Cell Plate Assembly (GLPA). Illustration of the GLPA and its components are shown in **Figure 2.9** and **Figure 2.10**. They reported that the energy balance for the mixture sample at any gyration cycle could be written using the following equation:

$$W = U \tag{2.4}$$

where W= work of external forces; U= total strain energy of sample. The above equation was written in the following form:

$$M\theta = S\gamma V \tag{2.5}$$

where M = applied moment during gyration; θ = gyration angle (radians); γ = shear strain; S = frictional resistance; and V = sample volume at any cycle. The forces measured by the GLPA and the top vertical actuator, were used to calculate the resultant force (R) and force eccentricity (e), as shown in **(Figure 2.11).**
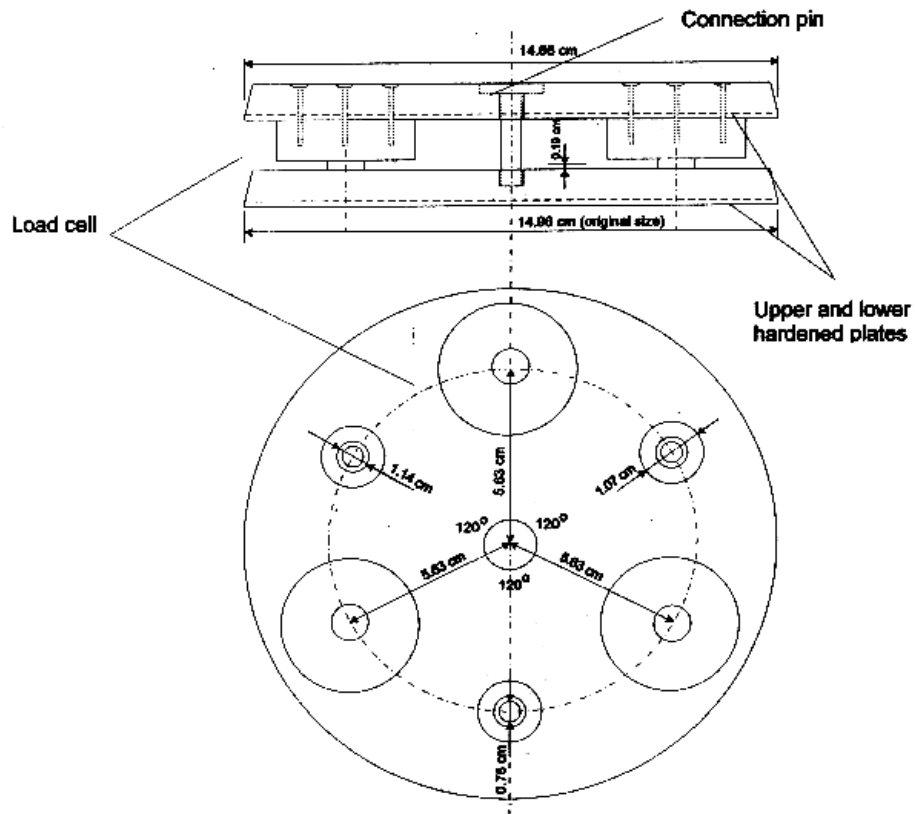


**Figure 2.9** Gyratory Load Cell Plate Assembly *(Guler et al. 2000)*
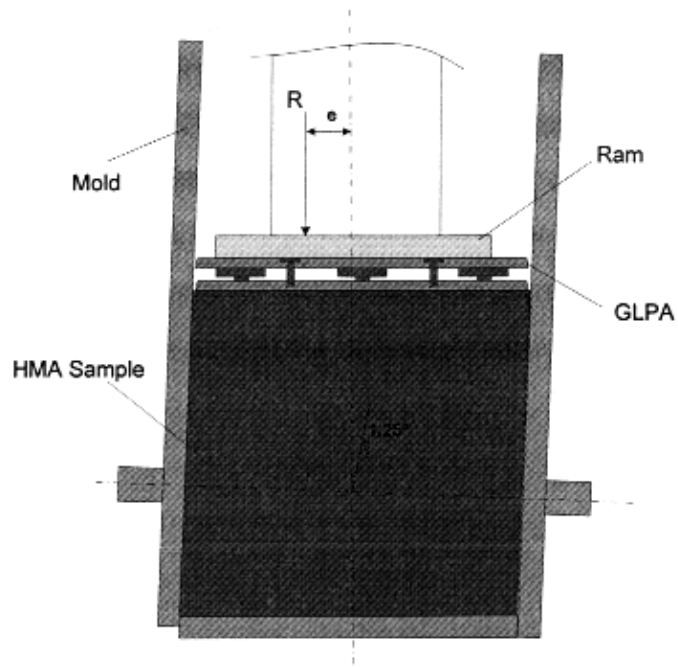
**Figure 2.10** Gyratory Load Cell Plate Assembly Placed on the Mold During Gyration Process
*(Guler et al. 2000)*
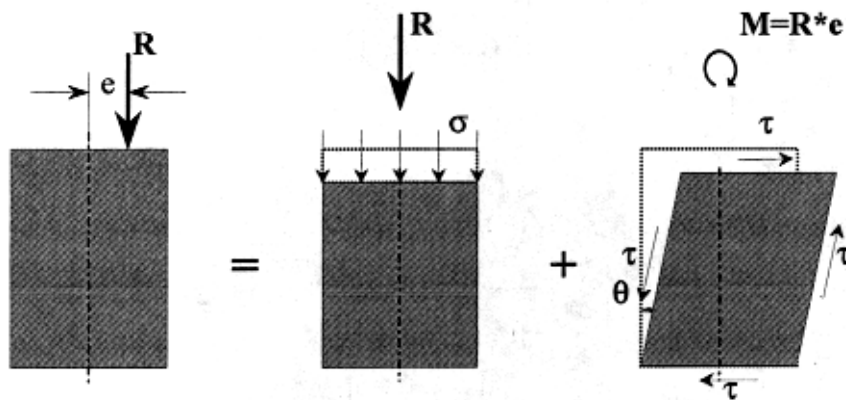


**Figure 2.11** Applied External Forces and The Stress Distributions Used in Energy Relations
*(Guler et al. 2000)*

They suggested that two-dimensional distribution of the eccentricity of the resultant load could be used to calculate the effective moment required to overcome the shear resistance of mixture and tilt the mold to the 1.25 degrees. *Guler et al. (2000)* stated that this effective moment is a direct measure of the resistance of asphalt mixtures to distortion and densification.

27

As shown in **Figure 2.9** the moment M needed to apply the angle can be calculated by multiplying the resultant ram force R, by the average eccentricity, e, for a given gyration cycle. *Guler et al. (2000)* stated that θ and γ in equation (2.5) are equal, and the shear stress can be calculated as follows:

$$S = \frac{R \cdot e}{A \cdot h} \qquad (2.6)$$

where A = sample cross section area; and h = sample height at any gyration cycle. They presented experimental results showing that the derived frictional resistance is sensitive to the asphalt content, aggregate gradation, and fine aggregate angularity. Careful analysis of the derivation provided by *Guler et al. (2000)* reveals that the shear stress in Equation (2.6) is actually the frictional stress between the mold and the mix. This equation does not represent the mix shear strength. Also U and W in equations 2.4 and 2.5 are both calculated from external forces and U does not represent the energy dissipated.

## 2.5  ANALYSIS OF THE INTERNAL STRUCTURE

Digital image analysis provides the capacity of rapid measurement of particle distribution and characteristics. Several studies established the effect of aggregate contacts on the shear strength properties *Oda (1972, 1977)*. It is also well documented that aggregate orientation is an important factor that controls the shear strength and the stiffness of granular materials. For example, *Tobita (1989)* showed that the yielding behavior of unbound granular materials is controlled by aggregate distribution. Also, *Masad et al. (2001)* showed that the asphalt mix stiffness could be expressed in terms of parameters that describe aggregate orientation.

Image analysis techniques usually treat particles as two-dimensional objects because only the two dimensional projection of the particles is captured and measured. The principle of the technique is that an image is digitizing into picture elements (usually 512x512 pixels). Each pixel has an intensity value (gray level) that is scaled from 0-255 (black - white). Features of interest are measured by their corresponding gray level. For example, after proper contrast has been achieved so that the gray levels of all the phases can be distinguished from one another. It is a simple matter to count all the pixels that fall within a certain range of intensities. This provides a measure of area fraction of each phase. For particle analysis, when proper contrast is achieved so that particles can be distinguished from the background, numerous measurements for each particle can be made in near real time

*Yue et al. (1995)* work showed that internal structure characteristics such as gradation, shape, and orientation of coarse aggregates in asphalt mixes could be accurately measured using the digital image processing technique. The main objective of the *Yue et al. (1995)* work was to quantitatively, capture the difference in the internal structure of asphalt mixtures compacted using different methods of compaction, and to relate the internal structure to the performance of the mix. *Eriksen and Wegan (1993)* conducted microscopic analysis of air voids in AC mixtures at the Danish Road Institute. However efforts were directed at specimen preparation technique instead of digital image analysis.

*Masad et al. (1998, 1999a, 1999b)* focused on developing image analysis techniques to quantify the internal structure of asphalt concrete based on aggregate orientation, aggregate gradation, aggregates contacts, aggregate segregation, and air voids distribution. These measurements were used to quantify the internal structure of asphalt concrete specimens prepared by the Superpave gyratory compactor at different levels of compaction and test its

29

ability to duplicate field conditions. Twelve specimens were compacted in the gyratory at

different number of gyrations (8, 50, 100, 109, 150, and 174 gyrations) where two specimens

were prepared at each level of compaction; these specimens were then cut vertically. In addition,

five field cores were recovered from pavement directly after construction and prior to trafficking.

Comparison of the internal structure of gyratory compacted specimens with field cores

showed that gyratory specimens reached the initial aggregate orientation of field cores at higher

number of gyrations (100 gyrations). Whereas they reached the average percent air voids in the

field cores at a much lower number of gyrations (20 gyrations), **Figure 2.12**.
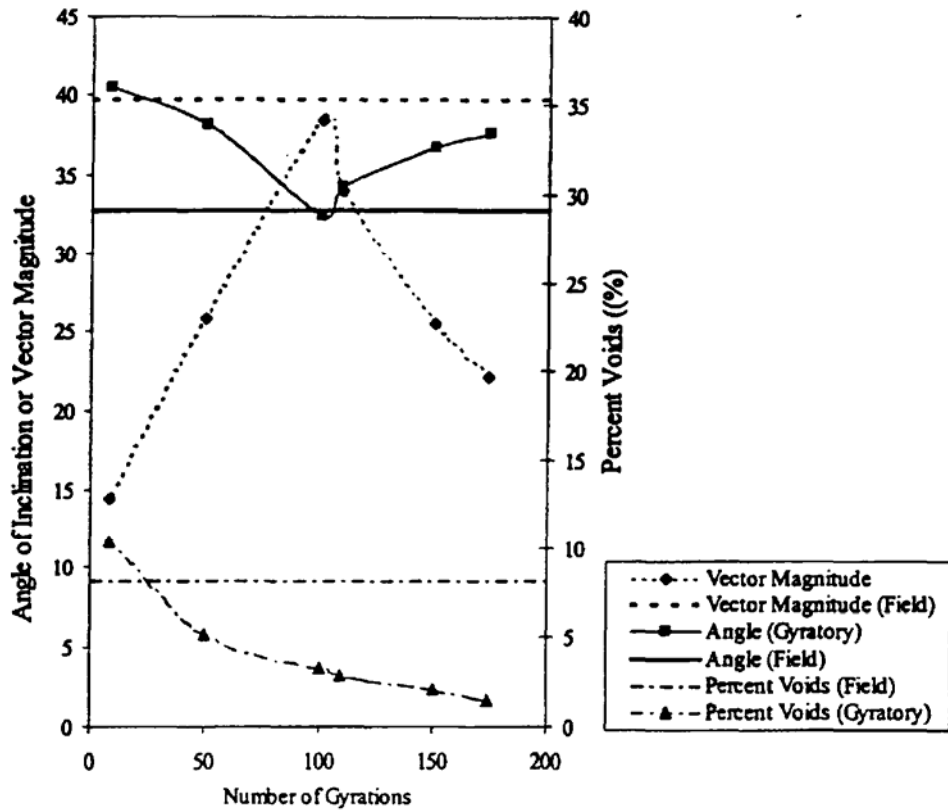


**Figure 2.12** Variation of Vector Magnitude, Angle of Inclination, and Percent Air Voids with
Compaction (*Masad et al. 1999*)

*Masad et al. (1998)* also showed that in the mix evaluation, there was a tendency in the

aggregate orientation to increase up to a certain level of compaction (100 gyrations), after which,

aggregate structure tended to have more random orientation. Air voids distribution was found to be non-uniform, more voids were noticed at the top and bottom of the specimens, whereas the specimens compacted more in the middle portion, **Figure 2.13**.
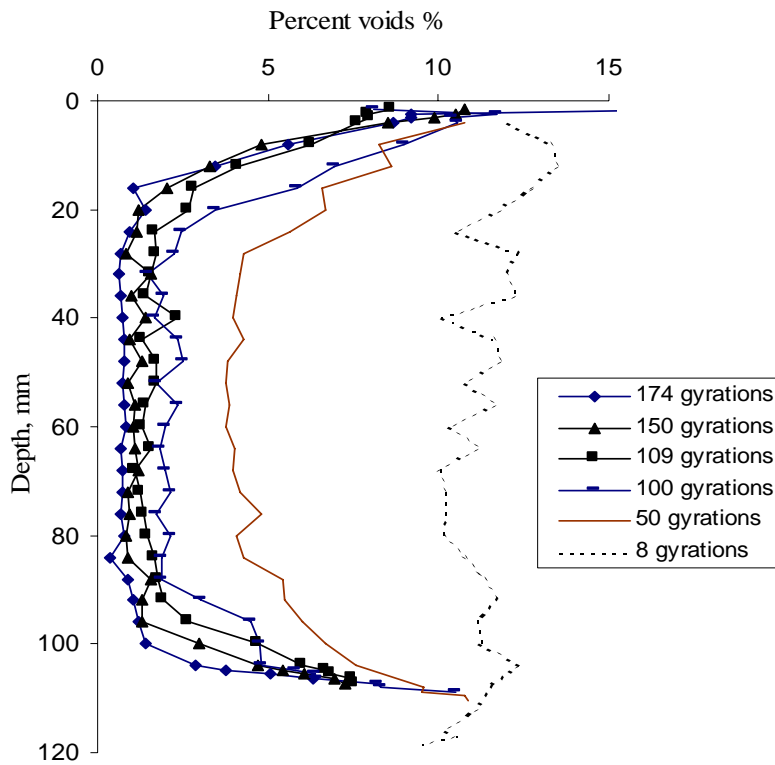


**Figure 2.13** Distribution of Air Voids in Gyratory Specimens at Different Number of Gyrations
*(Masad et al. 1999)*

*Masad et al. (1998)* work emphasized that the new image analysis techniques were useful tools to describe and compare asphalt materials produced using different laboratory equipment and mix designs. In addition, these procedures would improve mechanical modeling by providing consistent and accurate quantifying parameters of internal structure to be included in constitutive relationships. Coarse aggregate gradation of gyratory compacted specimens was

well captured using the image analysis techniques and there was no change in aggregate gradation during compaction, **Figure 2.14.**
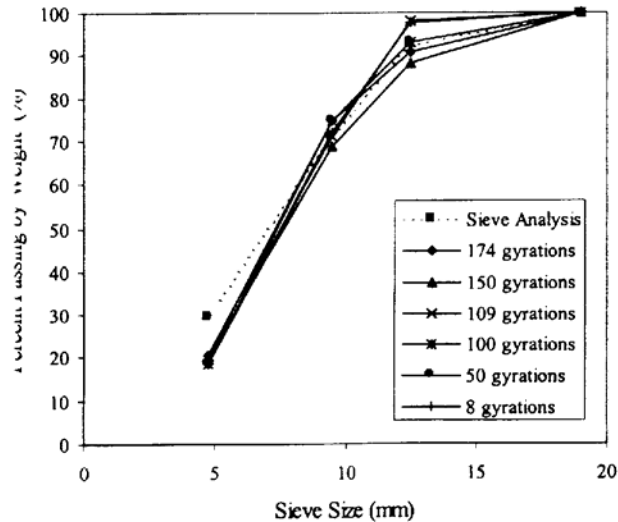


Figure 2.14 Accuracy of Calculating Aggregate Gradation Using

Image Analysis (Masad et al. 1999)

*Tashman et al. (2001)* evaluated the ability of the Superpave gyratory compactor to simulate the internal structure of HMA in the field, and the influence of different field compaction patterns on the produced internal structure. They concluded that the compaction variables in the compactor (angle, pressure, height, and temperature) influenced the internal structure in laboratory specimens. They recommended a set of variables to improve the simulation of the gyratory compactor to field conditions.

## 2.6  SUMMARY

The literature review shows that the Superpave gyratory compactor has been developed during SHRP to compact HMA specimens with relatively large aggregate size, and to achieve compaction under the influence of shear and normal stresses, which is believed to be similar to

field conditions. Several studies have used different types of gyratory compactors in order to evaluate the mix shear strength during compaction. This shear strength was related the mix resistance to permanent deformation. A critical review of these studies has revealed their limitations especially in the derivation of the shear stress formula, and accounting of all forces acting on HMA during compaction. There is a need to develop a new procedure to evaluate the mix stability and shear strength based on the response of the mix to the forces applied during compaction.

The review above indicated that image analysis techniques are powerful methods to quantify the internal structure of asphalt mixes. These methods have already been used to measure aggregate orientation, contacts, segregation, and air void distribution. In this study, image analysis techniques will be used to relate the aggregate structure parameters to HMA stability and shear strength.

This is a blank Page

# 3. ANALYSIS OF HMA STABILITY USING THE SGC

## 3.1 INTRODUCTION

This chapter presents detailed analysis of the HMA compaction using the Servopac Gyratory Compactor (SGC). The compaction forces are analyzed in order to derive a mathematical expression of the shear stress inside the mix. The shear stress value is used to calculate the compaction energy, which is divided into two regions according to the type of dominating strain. The volumetric strain dominates the first region, while the shear strain dominates the second region. Analytical procedure is developed to identify these two regions. An index termed the "Contact Energy Index" is developed to measure the stability of mixes. The contact energy index is used to analyze mixes with different constituents such as percent of binder, percent of natural sand, type of aggregate, gradation, and nominal maximum aggregate size. The effect of the gyratory compaction variables such as the angle of gyration, and vertical pressure on the contact energy index is investigated in order to determine the variables that would best discern among mixes with different constituents. The contact energy indices are compared to mechanical properties and permanent deformation of HMA.

## 3.2 SERVOPAC GYRATORY COMPACTION METHODOLOGY AND ANALYSIS

### 3.2.1 Compaction Mechanism

The compaction device used in this study is the Servopac gyratory compactor produced by Industrial Process Controls (IPC) in Australia, which is a Servo-controlled multi-axis pneumatic loading system designed for the laboratory production of asphalt specimens. The compaction is achieved by the simultaneous action of static compression and shearing resulting

from the motion of the centerline of the upper boundary test specimen. Thus, the line connecting the middle of the lower and upper boundaries generates a conical surface of revolution, while the ends of the specimen remain perpendicular to the axis of the conical surface, **(Figure 3.1)**.
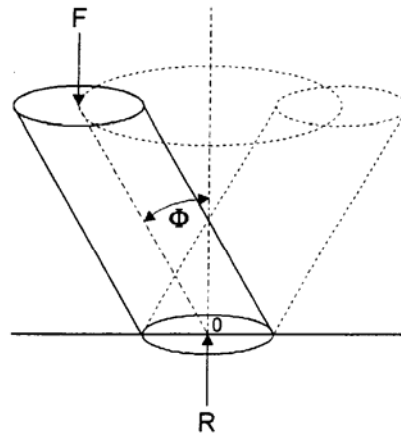


**Figure 3.1** Test Specimen Motion Diagram *(IPC Operating and Maintenance Manual 1996)*.

The vertical compressive force is applied using a digital servo controlled, pneumatic actuator, where a load cells is used to measure the vertical force. The vertical actuator is connected to an intermediate plate via the load cell. This mechanism allows the top platen to move freely in the horizontal plane.

In addition, there are three actuators located 120 degrees apart around the perimeter of the mold carrier ring. The electronic control system sends a sine wave via a servo valve to each of these actuators. The three sine waves are 120 degrees out of phase from each other as shown in **Figure 3.2**. The amplitude of the sine wave controls the angle magnitude, and its frequency controls the gyration rate. The feedback signal comes from the displacement transducer, which bears directly on the bearing that connects the actuator rod to the mold carrier ring. All forces

acting on the specimen and the mold during compaction are shown in **Figure 3.3**. (*IPC PTY LTD 1996*)
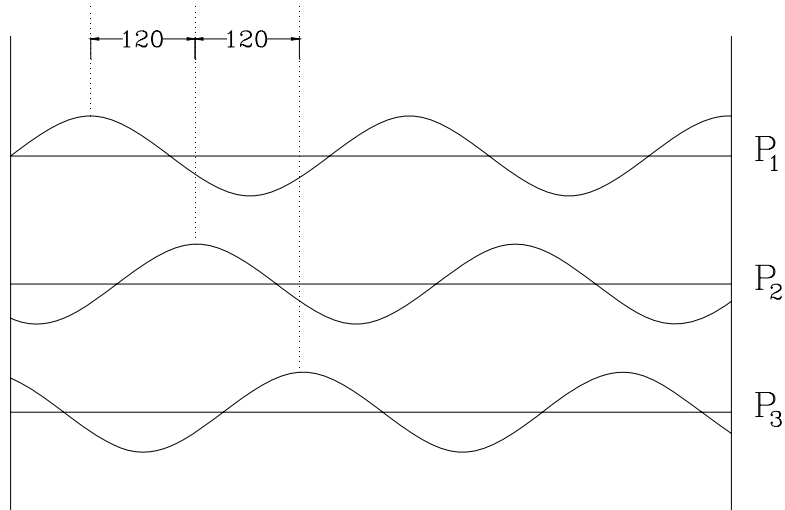


**Figure 3.2** Actuator Forces Acting by Sine Wave with 120° out of Phase
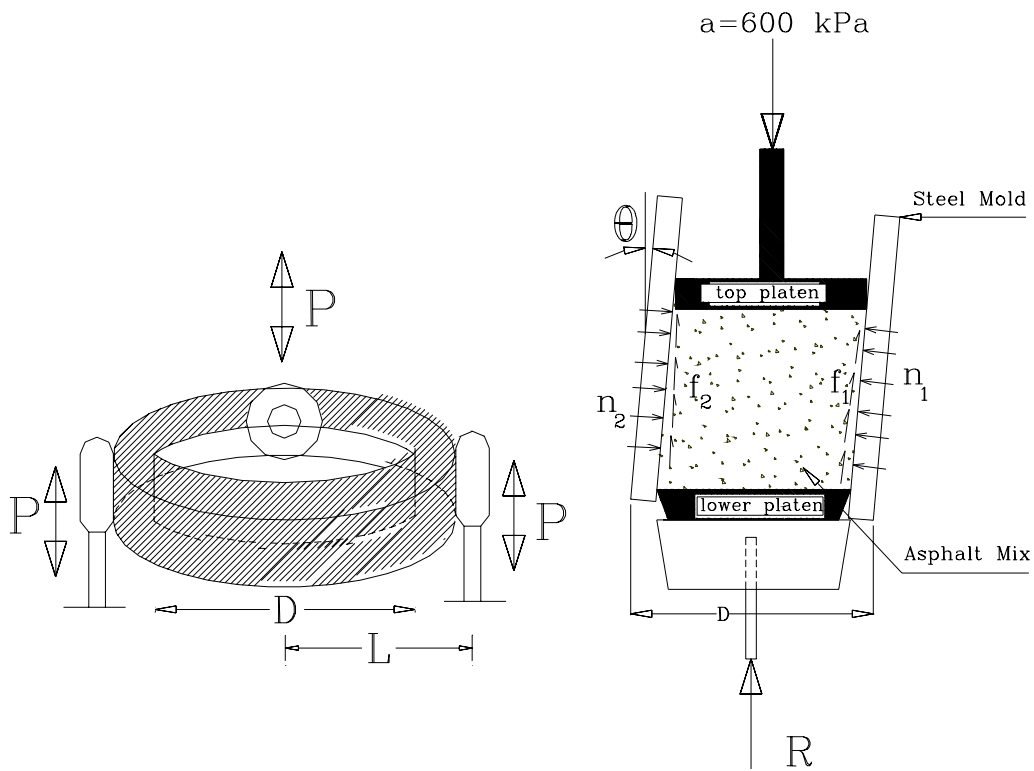


**Figure 3.3** A Schematic Diagram of the Compactor Components.

### 3.2.2 Analysis of Shear Stress During Compaction

Several equations have been used to calculate the shear stresses in a mix during compaction. These equations have essentially similar forms as they all rely on the force or momentum needed to apply the gyration angle as a measure of shear stress (McRea 1965, *De Sombre et al. 1998, Butcher 1998, Guler et al. 2000*). As demonstrated in the previous chapter, the shear stress equation used in the GTM and the Servopac gyratory compactor was derived using a free body diagram. This section presents a derivation of the shear stress in a gyratory specimen during compaction in the Servopac machine. Consider a specimen inclined at a certain angle of gyration, where the actuator P1 is applied at its maximum value (the amplitude of the sinusoidal force). Points of application of the forces on the bottom plate are shown in Figure 3.4. The force "A" is the result of the constant pressure "a" applied by the upper actuator on the specimen during the compaction process. As it can be seen in Figure 3.4, the mix weight "Wm" and the force "A" are at different offsets from the specimen centeroid due to the applied gyration angle. By taking the summation of moment around the P3-R line to be equal to zero, the following equation is derived P2:

$$P_2 = \frac{P_1 d_1 + A d_3 + W_m d_4}{d_2}$$

(3.1)

where:

$d_3 = \delta \sin \pi/3$

$\delta = h \tan \theta$

$\theta$ : the angle of gyration,

h: the specimen height, and

$d_4 = \frac{1}{2} d_3$

Because of symmetry as shown in **Figure 3.2**, P2 is equal to P3 when P1 is at the amplitude. P1 is measured using a load cell in the Servopac; therefore P2 and P3 can be calculated using Equ. (3.1).
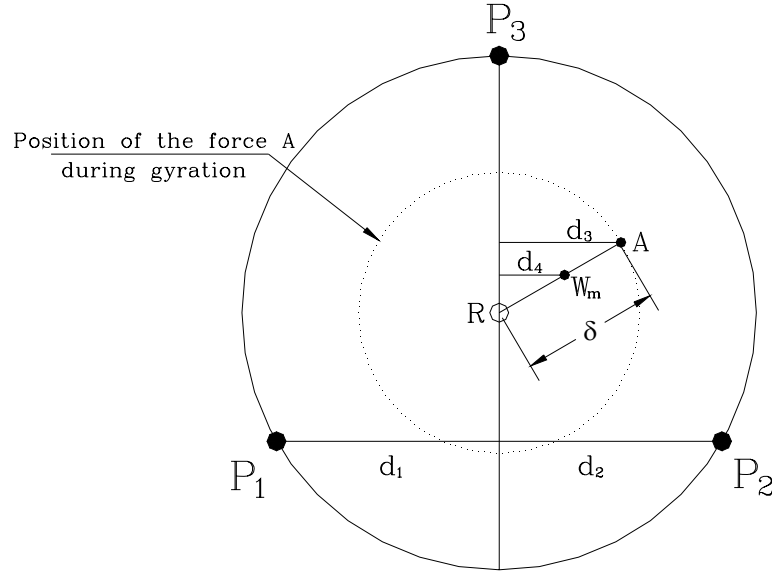
Figure 3.4 Plan View of the Forces Acting on the Specimen and the Mold.

The shear stress varies within the specimen depth. For the purpose of comparing the shear stress in different mixes, the location at which the shear stress is calculated should be specified. In this study, the average shear stress at the middle of the specimen is calculated. This location is selected in order to avoid the high change in the shear stress along the boundaries due to friction with upper and lower plates. Consider the free body for the top half of a specimen shown in **Figure 3.5**, where the shear force $S_\theta$ can be expressed by taking the summation of forces in the horizontal direction

$$S_\theta = (N_2 - N_1)\cos\theta + (F_1 + F_2)\sin\theta \qquad (3.2)$$

38

where $N_1$, $N_2$ are the normal forces acting on half the specimen surface, and $F_1$, $F_2$ are the resultant frictional force acting on half the specimen surface. It is assumed here that these normal and frictional forces are uniformly distributed and the friction factor between the specimen and the mold is constant during compaction. Due to the dynamic motion of the specimen with the mold, Eq. (3.2) is valid only when the angle is fully applied (when one of the actuators reaches its maximum height). The normal and frictional forces can then be calculated as follows:

$$
\left.
\begin{aligned}
N_1 &= \pi r \frac{h}{2} n_1, N_2 = \pi r \frac{h}{2} n_2 \\
F_1 &= \pi r \frac{h}{2} f_1, F_2 = \pi r \frac{h}{2} f_2
\end{aligned}
\right\}
\tag{3.3}
$$

where $n_1$, $n_2$ represent the average normal stresses, and $f_1$, $f_2$ are the average frictional stresses. r* refers to the vertical pressure acts at bottom of the specimen. Generally, small letter refers to acting stress, and capital letter refers to acting force.
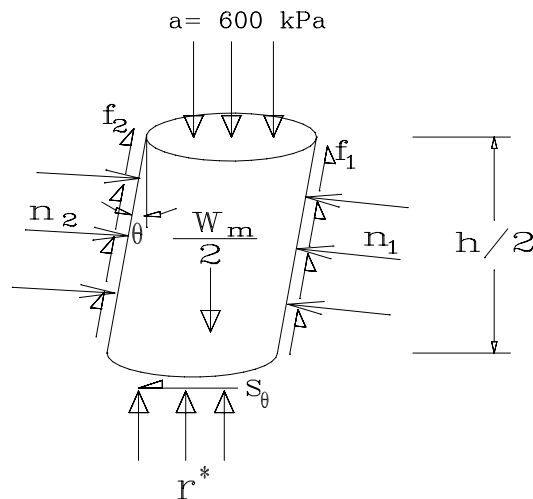


**Figure 3.5** Plan View of the Forces Acting on the Specimen and the Mold.

Similarly, taking the summation of forces in the vertical direction results in the following equilibrium equation:

$$R* = (A + \frac{W_m}{2}) - (F_1 + F_2)\cos\theta + (N_2 - N_1)\sin\theta \qquad (3.4)$$

where R* is force acting on the bottom of the top half of a specimen, A is the applied vertical force which is kept constant during compaction, and $W_m$ is the weight of the specimen. Assuming that the specimen is subjected to vertical compressive stress along its horizontal cross section. This assumption is motivated by the high vertical stress 600 kPa, and the small-applied angle of gyrations θ. It is noted that $R^* \neq A + \frac{W_m}{2}$ because of the presence of the frictional and normal forces acting on the mold. Also, R* is not located exactly at the center of the specimen because of the applied angle, (**Figure 3.6**). Calculating the moment around the center "o" gives another formula for determining R* as follows:

$$R* = \frac{1}{x_\theta}\left[(N_2 - N_1)\frac{h}{4\cos\theta} - (N_2 + N_1)r\sin\theta + (F_2 - F_1)r\cos\theta + (A + \frac{w_m}{2})\frac{h}{2}\tan\theta\right] \qquad (3.5)$$
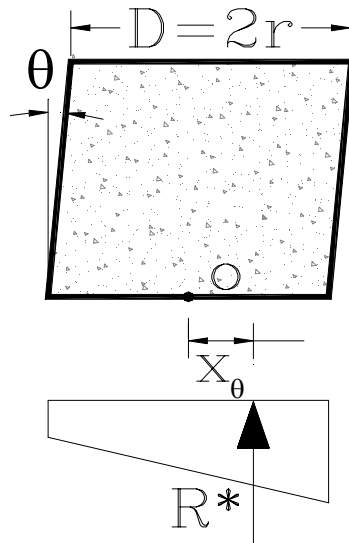


**Figure 3.6** Illustration of the Location of the Resultant Vertical Force
at the Bottom of the Top Half of the Specimen.

where $x_\theta$ is the distance from the center to the point where the force R* is acting. The

value of $x_\theta$ increases with an increase in the applied angle. The maximum value for $x_\theta$ is one

third of the specimen radius (r/3), which occurs when the applied angle causes triangular stress

distribution at the bottom of the specimen. The minimum value of $x_\theta$ is zero at which the angle

of gyration is zero.

Consider the free body diagram of the mold shown in **Figure 3.7**. The summation of

forces in the vertical direction gives the following expression:
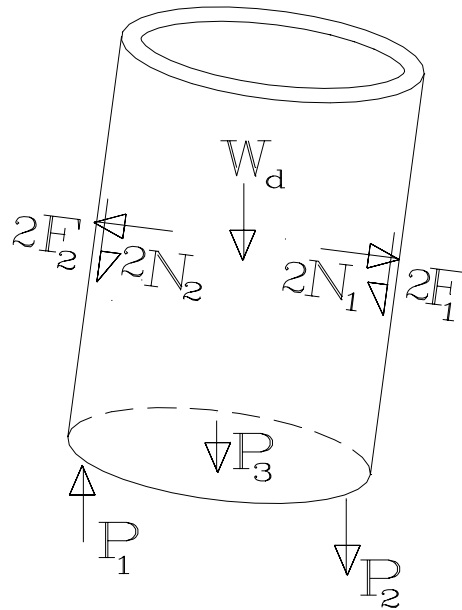


**Figure 3.7** The Forces Acting on the Mold at Angle $\theta$ and the Change in the
Direction of $P_2$ and $P_3$ is to Satisfy the Equilibrium.

$$\sum P - W_d = 2(N_1 - N_2)\sin\theta + 2(F_1 + F_2)\cos\theta \qquad (3.6)$$

where $\sum P$ is the summation of the forces applied to the mold from the actuators and $W_d$ is

the weight of the mold. As mentioned earlier, $P_2$ and $P_3$ are 120 degrees out of phase from $P_1$,

and consequently, they have different sign than $P_1$ when it is at the maximum value. Therefore, the summation of the actuator forces is expressed as follows:

$$\Sigma P = P_1 - P_2 - P_3 \tag{3.7}$$

Mathematical manipulations of Eqs. (3.4), (3.5) and (3.6) give the following expressions:

$$N_2 - N_1 = \frac{\left[A + \dfrac{W_m}{2}\right]\left(x_\theta - \dfrac{h}{2}\tan\theta\right) - \dfrac{1}{2}\left[\Sigma P - W_d\right]\left(x_\theta - \dfrac{r}{\mu}\tan\theta\right)}{\dfrac{h}{4\cos\theta} + \mu r\cos\theta - r\dfrac{\sin^2\theta}{\mu\cos\theta}} \tag{3.8}$$

$$N_1 + N_2 = \frac{\Sigma P - W_d}{2\mu\cos\theta} + (N_2 - N_1)\frac{\tan\theta}{\mu} \tag{3.9}$$

The normal and frictional forces are assumed to be related through a constant frictional factor $\mu$ ( $N_1 = \mu F_1$, $N_2 = \mu F_2$ ) in the derivation of Eqs. (3.8) and (3.9). The friction factor was taken a value of 0.28 based on a study by *Abou-Chakra and Tuzun (1999)* to determine the coefficient of friction between coarse and fine granular materials and a smooth wall. Substituting Eq. (3.9) in Eq. (3.2) results in the following equation for the shear force:

$$S_\theta = (N_2 - N_1)\cos\theta + \frac{1}{2}(\Sigma P - W_d)\tan\theta + \frac{(N_2 - N_1)\sin^2\theta}{\cos\theta} \tag{3.10}$$

The term $\dfrac{\sin^2\theta}{\cos\theta}$ can be neglected because it is too small relative to the other components. Therefore, the shear force has the following expression:

$$S_\theta = (N_2 - N_1)\cos\theta + \frac{1}{2}(\Sigma P - W_d)\tan\theta \tag{3.11}$$

where ($N_2$-$N_1$) is calculated using Eq. (3.8). The above equation indicates the shear forces increases with an increase in the applied angle, and an increase in the applied actuator forces. The expression in Eq. (3.11) can be used to calculate the shear stress by dividing over the cross-section area at all gyrations during compaction.

### 3.2.3 Derivation of Shear Compaction Energy for Stability Analysis

The conservation of energy principle states that the total rate of work done to the system by all external sources must equal the rate of increase of the total energy of the system. This principle is also called the first law of thermodynamics. The conservation of energy can be written in the following form:

$$\rho \frac{du}{dt} = \sigma_{ij} D_{ji} + \rho r - q_{i,i} \qquad (3.12)$$

where $\rho$ is the material density, $\dfrac{du}{dt}$ is the rate of change of the internal energy per unit volume, $\sigma_{ij}$ is the stress tensor, Dji is the deformation rate, $\rho r$ is the heat supplied by internally distributed sources, and qi,i is the heat provided by the flow of thermal energy through the boundary into the system or continuous body. If the deformation is assumed to occur under isothermal conditions, the equation of energy conservation becomes:

$$\rho \frac{du}{dt} = \sigma_{ij} D_{ji} \quad (3.13)$$

The term $\sigma_{ij} D_{ji}$ represents the mechanical work done by the external forces not converted into kinetic energy. The applications of the conservation of energy to the gyratory compaction are discussed here. The time increment used in Eq. (3.13) represents the time

needed to complete one gyration.  If the deformation induced within each gyration is considered to be all plastic deformation, then the change in the internal energy in each gyration (du) is equivalent to the dissipated energy due to volumetric and shear strain as follows:

$$du = dv + ds \qquad (3.14)$$

where dv is the change in the internal energy due volumetric deformation, and ds is the change in the internal energy due to shear deformation.  A typical compaction curve from the gyratory compaction is shown in Figure 3.8. It can be divided into two parts; the first one has a steep change in percent air voids with an increase in number of gyrations.  In this part (part A), most of the applied energy is used in inducing volumetric permanent deformation (reduction in percent air voids).  Also, in the first part, the aggregates do not experience significant amount of shearing force.  In the second part (part B), however, most of the energy applied by the induced angle does not cause significant volumetric change (small change in percent air voids).  However, most of this energy is consumed in overcoming the shear resistance between the particles.  Therefore, the energy calculations for assessing the mix stability under shear loading should focus on the second part of the compaction curve.

In a discrete time domain where each gyration is considered a time increment, a measure of energy can be calculated as follows:

$$Total \; Energy \; index = \sum_{N_{G1}}^{N_{G2}} S_\theta \cdot d \qquad (3.15)$$

where $S_\theta$ is the shear force at N number of gyrations derived from equation (3.11) and angle $\theta$ and d is the vertical deformation (Specimen Diameter $\times$ tan$\theta$).  The summation is conducted over the "Part B" of the compaction curve.  It should be noted that the quantity in Eq.

(3.15) does not represent the actual compaction energy, as it does not account for all the forces acting on a specimen multiplied by the deformations in the directions of these forces. The complexity of the applied stresses and induced deformations makes it difficult if not impossible to account for all forces and their associated deformations. However, since the shear force in Eq. (3.11) is a result of all the applied forces, and the deformation d is also the resultant of all deformations, equation (3.15) is a reasonable index of the compaction energy.

The applied energy in "Part B" is either used in developing more contacts among the aggregates and cause reduction in percent air voids, or is dissipated by aggregate sliding as the aggregate structure fails to develop more contacts. In order to capture this phenomenon in evaluating the mix stability, another index is introduced that captures the energy used in reducing the percent air voids or developing contacts:

$$Contact\ Energy\ index = \sum_{N_{G1}}^{N_{G2}} S_\theta \cdot d_e \qquad (3.16)$$

where $d_e$ is the change in height at each consecutive gyrations in Part B of Figure 3.8. For consistency, units were taken N.mm, because the vertical deformations are too small.

## 3.3  EXPERIMENTS AND RESULTS

Two experiments have been conducted to evaluate the ability of the developed shear stress and energy indices to discern among different mixes. The first experiment evaluated the influence of changes in the mix constituents including asphalt binder content, percent of natural sand, nominal maximum aggregate size, aggregate source, and type of gradation on the energy indices. The second experiment was targeted at evaluating the influence of changes in compaction variables on the energy indices to determine the variables that have the best ability in

discerning among the mixes. Mixes were prepared at WCAT (Washington Center of Asphalt Technology) and the compaction process using the Servopac was done at University of Idaho.
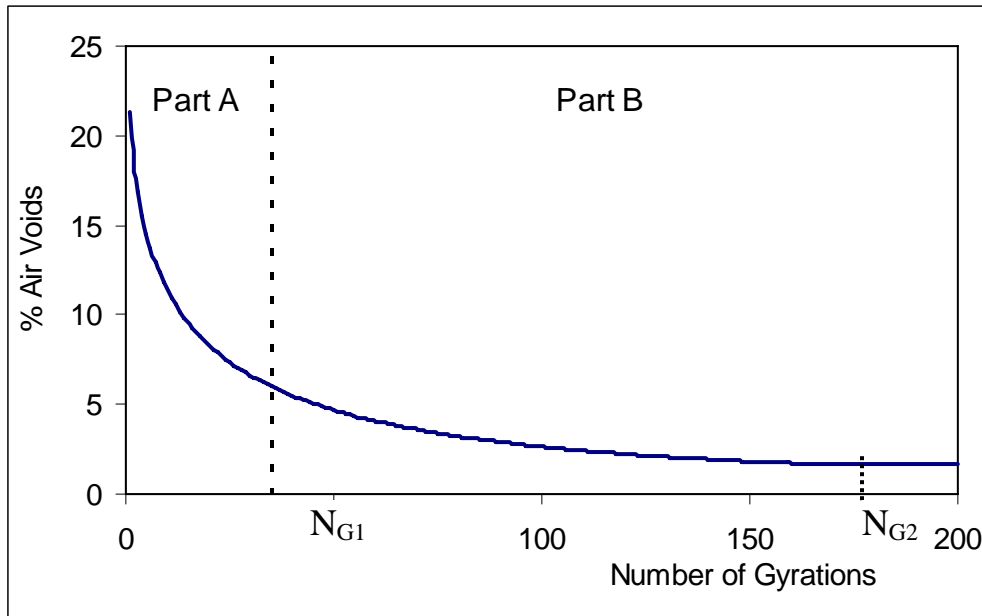


**Figure 3.8** A Schematic Diagram Shows the Two Zones of the Compaction Curve

### 3.3.1 The Effect of Mix Constituents on Energy Indices

The first experiment consists of 16 mixes as shown in

Table 3.1. The aggregate gradations are shown in Figure 3.9. The optimum asphalt content was selected to achieve a target of 4% air void at Ndes gyrations. The actual percent air voids varied between 3.5% and 4.5%. In order to study the effect of excess asphalt content, all mixes were prepared at the optimum asphalt content and 0.8% more than the optimum value. All the mixes were prepared at a temperature of 325° F, and compacted at a temperature of 300° F. All specimens were compacted to a maximum number of gyrations (Nmax) of 160. This level of compaction corresponds to a Superpave traffic level of 3 to 10 million equivalent single axle loads (*AASHTO 2001*). A summary of mix properties is shown in

Table 3.1. In this Table, the coarse gradation indicates that the gradation curve passes below the restricted zone, while the fine gradation passes above the restricted zone. More details on aggregate gradations and properties are provided in Appendix A.

**Table 3.1** The Experimental Matrix of Asphalt Mixes with Different Constituents

| Aggregate | Gradation | Size, mm | % Fine Aggregate | Design AC, % | Mix label |
|---|---|---|---|---|---|
| Limestone | Coarse | 9.5 | 0 | 5.3 | A |
| | | | 40 | 5.7 | B |
| | | 19 | 0 | 4.4 | C |
| | | | 40 | 4.7 | D |
| | Fine | 9.5 | 0 | 6.2 | E |
| | | | 40 | 6.3 | F |
| | | 19 | 0 | 4.7 | G |
| | | | 40 | 5.2 | H |
| Gravel | Coarse | 9.5 | 0 | 6.3 | I |
| | | | 40 | 5.9 | J |
| | | 19 | 0 | 5.4 | K |
| | | | 40 | 4.8 | L |
| | Fine | 9.5 | 0 | 6.7 | M |
| | | | 40 | 6.3 | N |
| | | 19 | 0 | 5.0 | O |
| | | | 40 | 5.4 | P |

Prior to the analysis of the compaction energy, the repeatability of the compaction procedure should be evaluated in order to determine the number of specimens needed to represent each mix. Two specimens from each of the C, D, K, and L mixes were compacted using the same vertical pressure (600 kPa), angle of gyration (1.5o), rate of gyration (30 gyrations/minute). The compaction curve results are shown in Figure 3.10. The two replicates from each mix followed almost the same compaction curve. Also, as shown in **Table 3.2**, the maximum difference in percent air voids was about 0.5%, which is within the experimental error

that is usually experienced in the laboratory. Consequently, it was decided to use only one specimen to represent each mix at a given set of compaction variables.
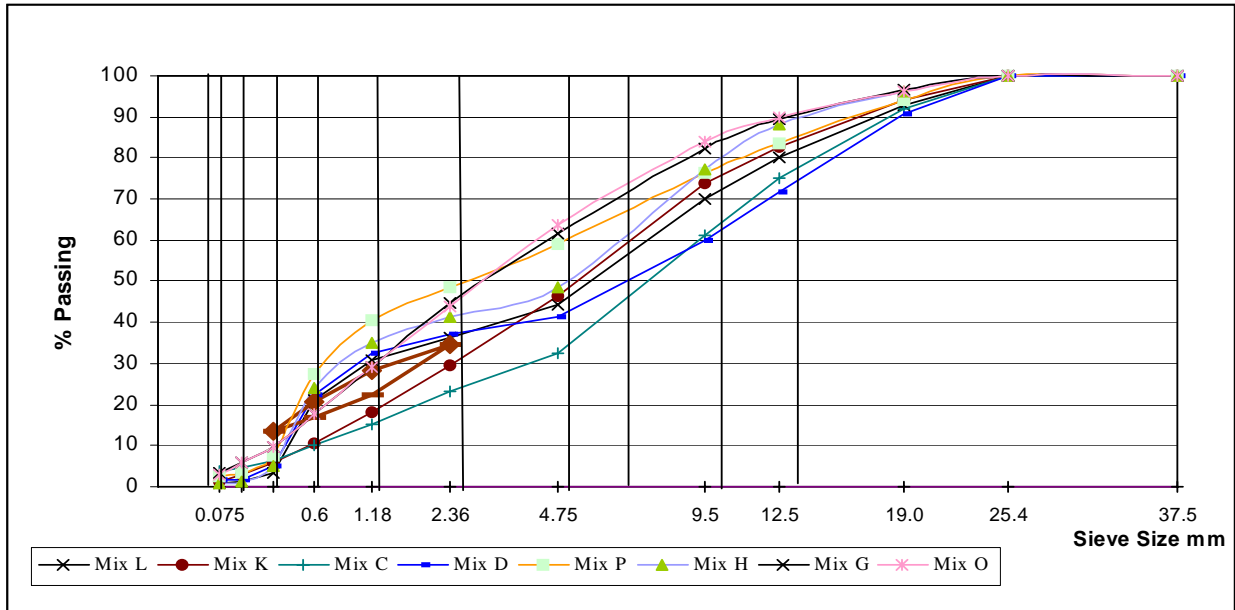


**A:** Mixes with 19.0 mm NMAS Raised to the Power of 0.45.
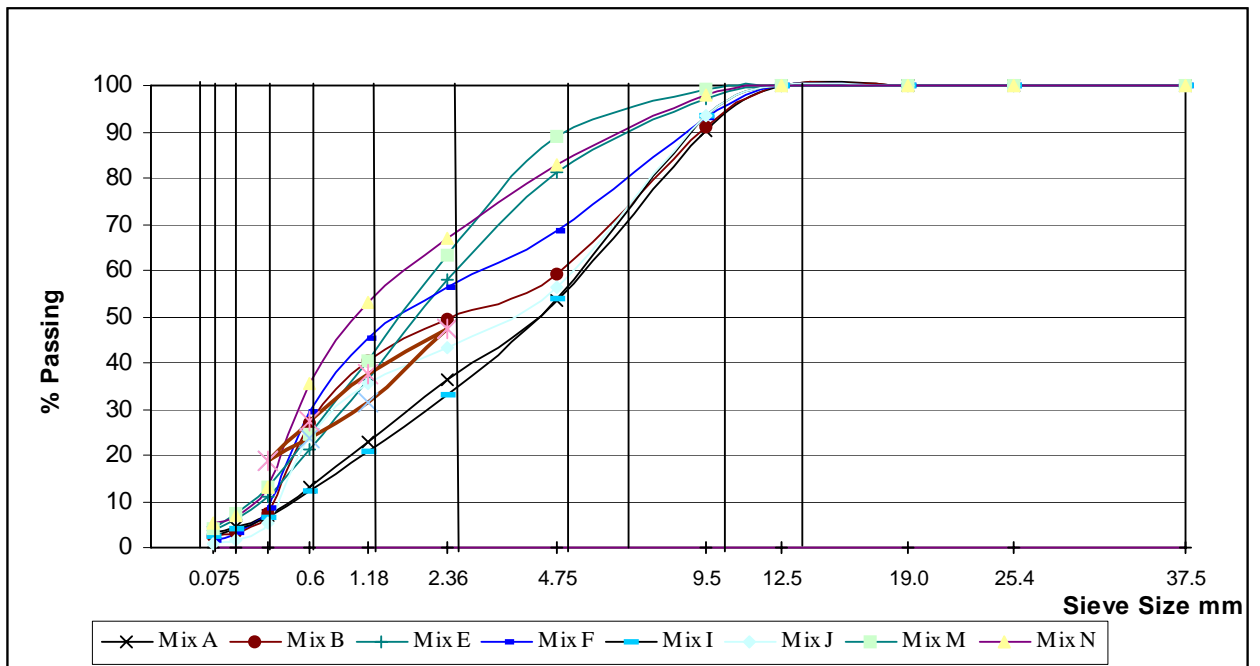


**B**. Mixes with 9.5 mm NMAS Raised to the Power of 0.45.

**Figure 3.9** Aggregate Gradation for Mixes with 19.0 mm & 9.5 mm NMAS Raised to the Power of 0.45.
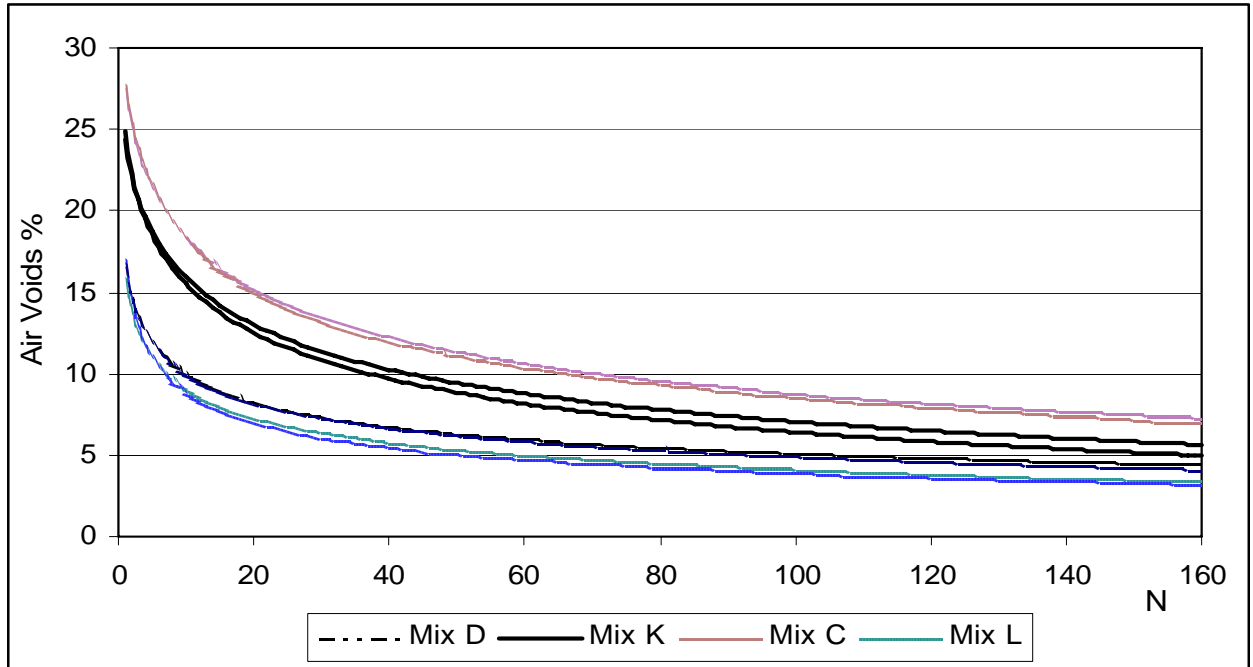


**Figure 3.10** The Changing in the Compaction Curve with Two Replicate Samples.

**Table 3.2** The Average Difference in Percent Air Voids among Replicates

| Mix # | Average Diff. % |
|-------|-----------------|
| C | 0.26 |
| D | 0.17 |
| K | 0.59 |
| L | 0.26 |

As mentioned earlier, the compaction energy is calculated in the shear deformation part (Part B of the compaction curve shown in Figure 3.8). Therefore, a criterion is needed to establish the start and the end of part B. The number of gyrations ($N_{G1}$) that indicates the beginning of part B is defined by fitting a polynomial of the sixth degree to the compaction curve and determines the slope at each gyration. Then, $N_{G1}$ is taken as the point at which the change in the slope of two consecutive gyrations is less or equal to 0.001%. The approach followed here to

determine the number of gyrations that defines the end of Part B ($N_{G2}$) was first to determine the mix with the lowest "160- $N_{G1}$" value, and then to add this value to $N_{G1}$ of each mix. This approach ensures that the same and maximum number of gyrations possible ($N_{G2}$- $N_{G1}$) is used in calculating the energy indices for all mixes. The maximum number of gyrations is needed in order to capture the shear stress behavior along a large number of gyrations. For example, Figure 3.11 shows the difference of shear stress behavior for two specimens with different binder content. The beginning of the shear compaction region ($N_{G1}$) occurs at about 80 gyrations. The difference between the energy indices of these two mixes is best captured by taking the maximum $N_{G2}$ value possible which is 160 gyrations in this case. However, $N_{G2}$ of 160 gyrations cannot be applied for all mixes since they do not all have the same $N_{G1}$.

An example of data required for the calculation of the shear stress and the energy indices is shown in Appendix B.
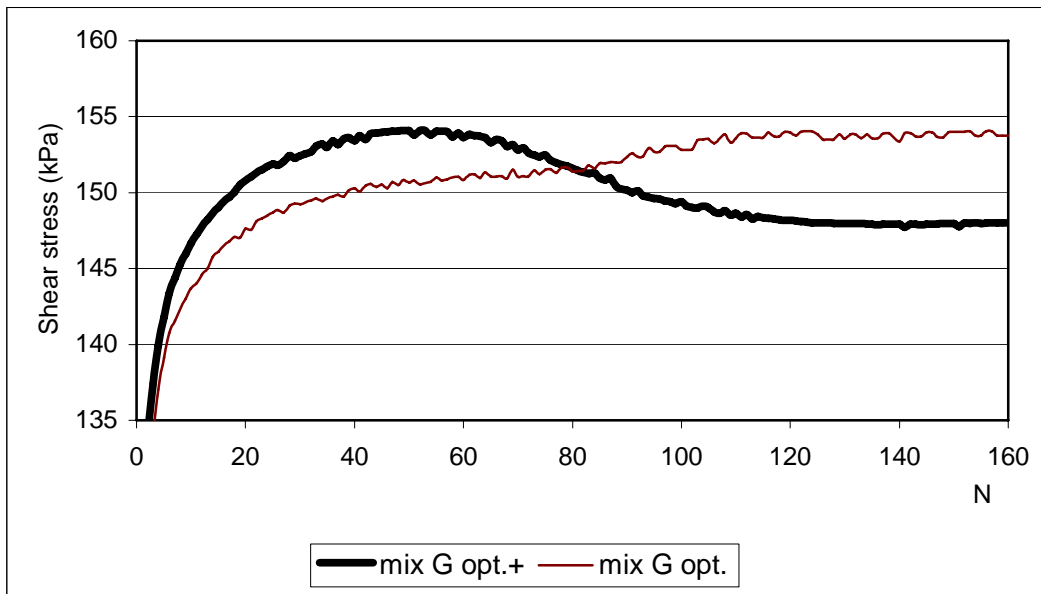


**Figure 3.11** Examples of Shear Stress Curves for Asphalt Mixes During Compaction.

Two different binder contents were used to investigate the effect of the binder content on the energy indices. The first one was the optimum value determined from the Superpave mix design procedure. The second one was 0.8% higher than the optimum value, which is referred to hereinafter as optimum plus. It was noticed that most of the optimum plus mixes reached a peak value at which it started to decrease with further compaction. The rate of reduction was a function of the aggregate gradation. However, most of the mixes with optimum asphalt content reached a maximum shear stress and stabilized at that value with further compaction. An example of this phenomenon is shown in Figure 3.11. A comparison between the shear indices is presented in Figure 3.12 and **Table 3.3**. It is evident that the total energy index did not show a certain pattern in comparing the optimum and optimum plus mixes. However, the contact energy index was always higher for mixes with optimum asphalt content. This indicates that the applied energy was used to develop contacts in the optimum mixes, while it was dissipated in aggregate sliding in the optimum plus mixes.

**Table 3.3** Energy Indices of Mixes with Different Asphalt Content.

|       | Total E.I. | | ratio | Contact E.I. | | ratio |
|-------|--------|---------|----------|-------|--------|----------|
| Mix # | opt.   | opt.+   | opt/opt+ | opt.  | opt. + | opt/opt+ |
| mix a | 1402.89 | 1397.47 | 1.004 | 25.80 | 22.43 | 1.150 |
| mix b | 1289.80 | 1322.17 | 0.976 | 11.15 | 8.82  | 1.264 |
| mix c | 1315.44 | 1336.67 | 0.984 | 24.20 | 20.16 | 1.200 |
| mix d | 1306.94 | 1292.29 | 1.011 | 9.82  | 8.57  | 1.146 |
| mix e | 1400.21 | 1383.36 | 1.012 | 23.12 | 23.24 | 0.995 |
| mix f | 1293.79 | 1303.36 | 0.993 | 10.62 | 9.97  | 1.065 |
| mix g | 1238.65 | 1251.00 | 0.990 | 28.20 | 8.88  | 3.177 |
| mix h | 1344.64 | 1287.33 | 1.045 | 9.27  | 8.63  | 1.074 |
| mix I | 1348.73 | 1403.00 | 0.961 | 24.49 | 22.49 | 1.089 |
| mix j | 1274.62 | 1249.19 | 1.020 | 10.17 | 7.95  | 1.279 |
| mix k | 1432.65 | 1419.30 | 1.009 | 29.03 | 25.33 | 1.146 |
| mix L | 1283.52 | 1356.96 | 0.946 | 10.45 | 8.82  | 1.185 |
| mix m | 1245.30 | 1249.52 | 0.997 | 21.59 | 9.12  | 2.368 |
| mix n | 1446.35 | 1427.85 | 1.013 | 20.41 | 17.89 | 1.141 |
| mix o | 1428.27 | 1400.26 | 1.020 | 20.58 | 20.54 | 1.002 |
| mix p | 1319.32 | 1357.94 | 0.972 | 9.62  | 8.95  | 1.075 |
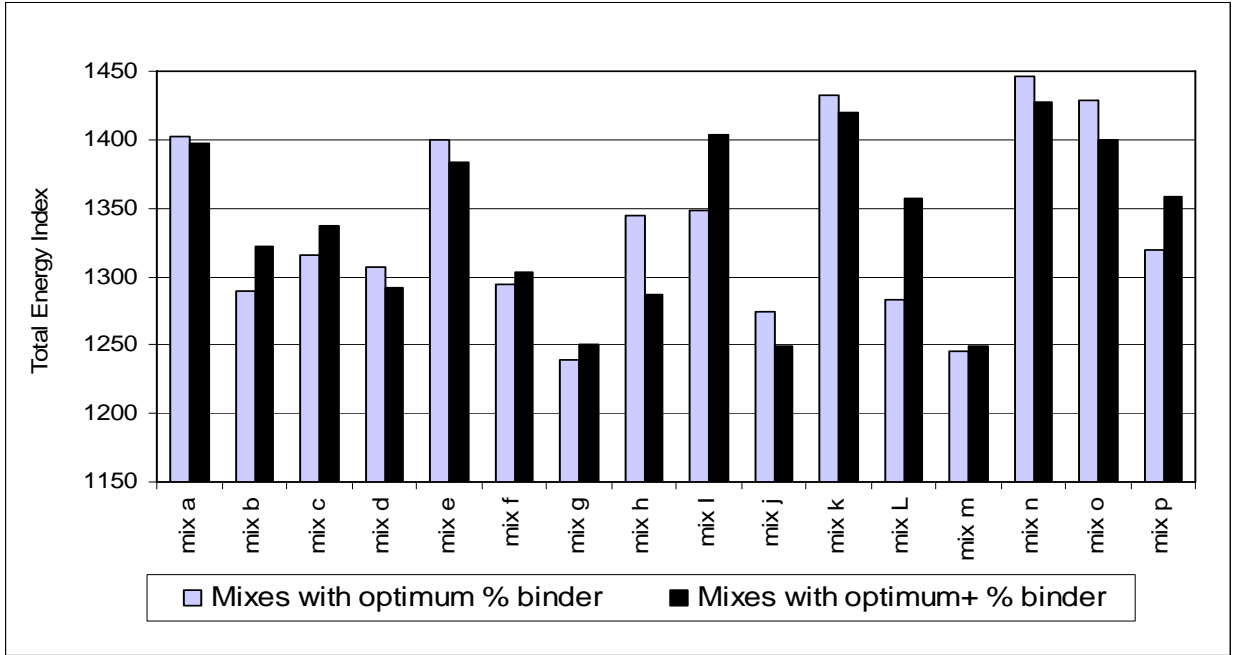
**A:** The Total Energy Index.
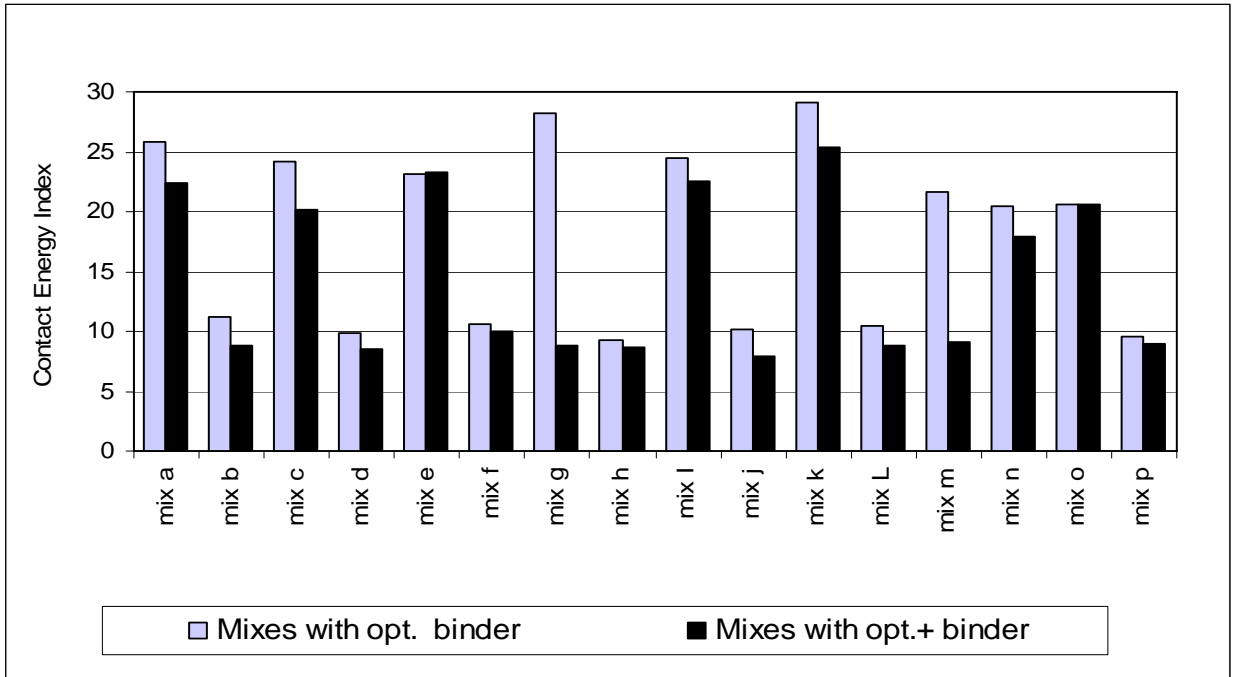


**B:** Contact Energy Index.

**Figure 3.12** Comparison among Mixes with Different Asphalt Content in Terms of Total & Contact Energy Index.

*Effect of the aggregate type*

Two types of aggregates were used in this evaluation; limestone and gravel. A comparison between the energy indices of the gravel and limestone mixes is shown in Figure 3.13 (**a**, **b)** and **Table 3.4**. It is evident that both the total and contact energy indices were higher for the limestone than for the gravel mixes. This indicates that more energy was needed to compact the limestone mixes, and the part of this energy that was transferred to developing more aggregate contacts was higher for the limestone mixes as well. It is well known that limestone has more texture and angularity than gravel, which explains the higher stability of the limestone mixes as indicated by the energy indices.

**Table 3.4** Energy Indices of Mixes with Different Aggregate Type

| Limestone Mix # | Total E.I. | Contact E.I. | Gravel Mix # | Total E.I. | Contact E.I. % | Total E.I. Ratio | Contact E.I. Ratio |
|---|---|---|---|---|---|---|---|
| mix a | 1382.50 | 21.39 | mix l | 1358.75 | 24.59 | 1.017 | 0.870 |
| mix b | 1291.82 | 8.16 | mix j | 1249.19 | 7.95 | 1.034 | 1.026 |
| mix c | 1336.67 | 24.59 | mix k | 1318.68 | 23.02 | 1.014 | 1.068 |
| mix d | 1337.76 | 10.01 | mix L | 1293.46 | 9.39 | 1.034 | 1.066 |
| mix e | 1360.86 | 14.35 | mix m | 1352.85 | 9.12 | 1.006 | 1.574 |
| mix f | 1303.36 | 10.72 | mix n | 1282.01 | 12.11 | 1.017 | 0.885 |
| mix g | 1399.87 | 21.92 | mix o | 1428.27 | 20.58 | 0.980 | 1.065 |
| mix h | 1375.81 | 8.63 | mix p | 1319.32 | 8.33 | 1.043 | 1.036 |
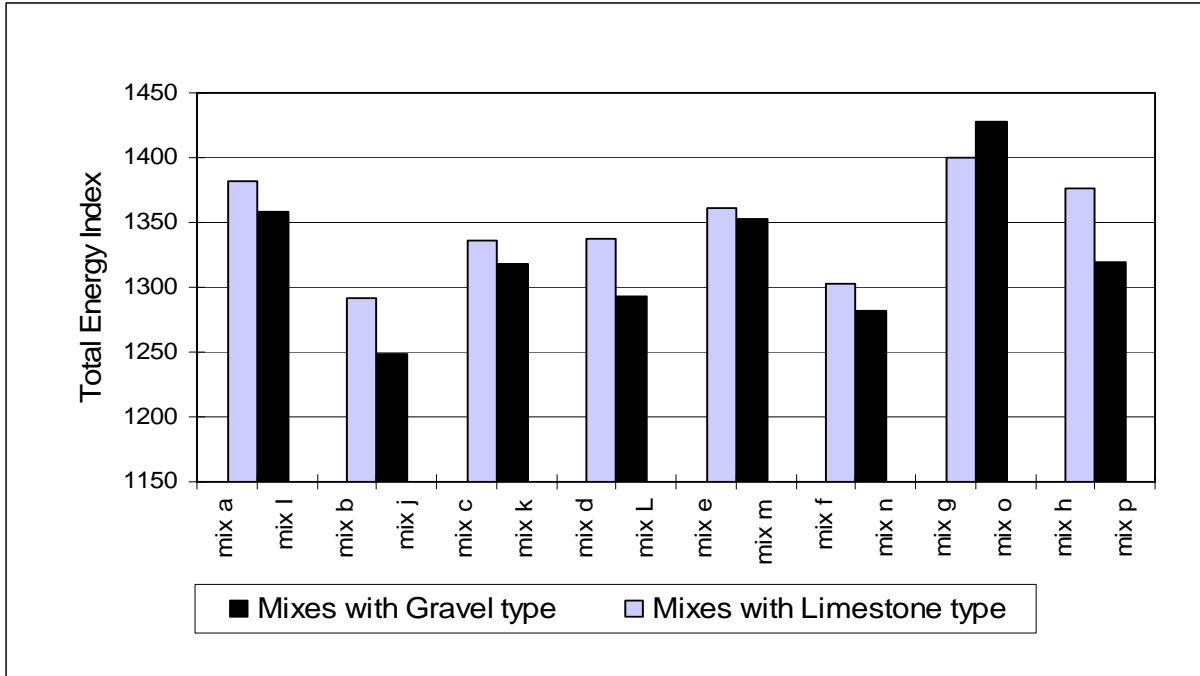
**A:** Total Energy Index.
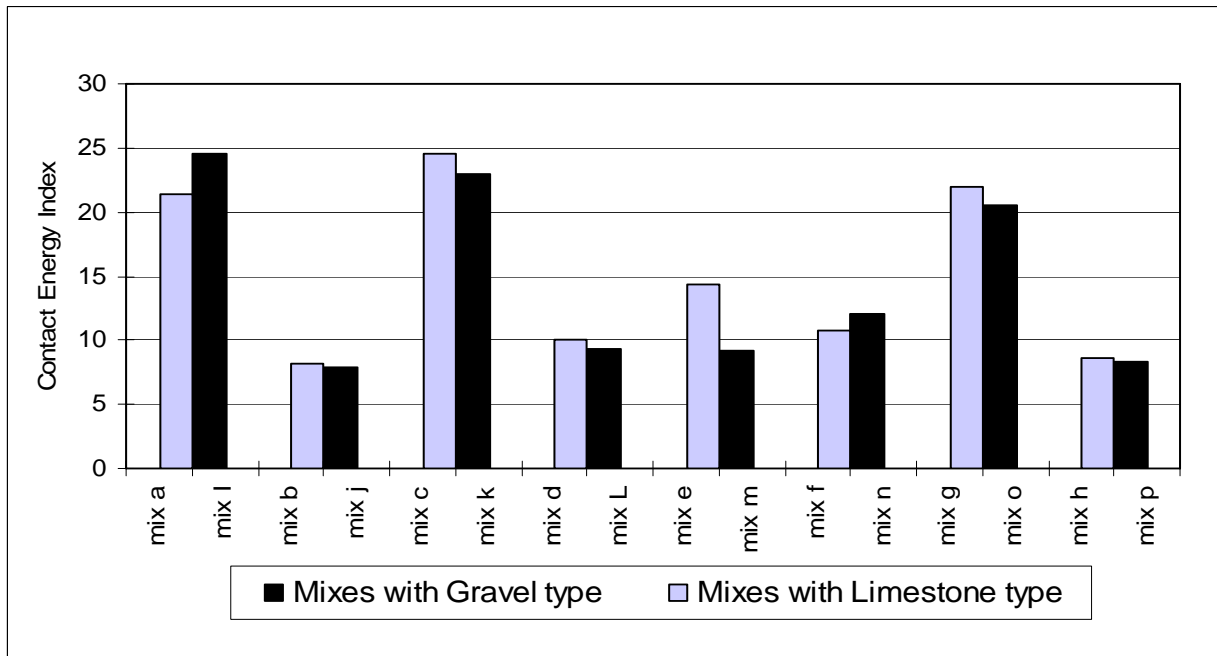


**B:** Contact Energy Index.

**Figure 3.13** Comparison among Mixes with Different Aggregate Type in terms of Total & Contact Energy Indices.

*Effect of the Nominal Maximum Aggregate Size (NMAS)*

The nominal maximum aggregate size (NMAS) is defined as the sieve size larger than the first sieve to retain more than 10 percent of the material.  The analysis results in Figure 3.14**a** indicate that the majority of the mixes with 19.0 mm NMAS required higher energy to compact.  However, the contact energy index results in Figure 3.14**b** show no trend in favoring one NMAS over the other in developing contacts and strong aggregate structure.  A comparison between the mixes is shown in **Table 3.5.**

**Table 3.5** Energy Indices of Mixes with Different NMAS.

| 9.50 mm agg. Mix # | Total E.I. | Contact E.I. | 19 mm agg. Mix # | Total E.I. | Contact E.I. | Total E.I. Ratio | Contact E.I. Ratio |
|---|---|---|---|---|---|---|---|
| mix a | 1402.89 | 22.28 | mix c | 1385.83 | 20.16 | 0.99 | 0.91 |
| mix b | 1289.80 | 8.74 | mix d | 1337.76 | 8.57 | 1.04 | 0.98 |
| mix e | 1400.21 | 22.66 | mix g | 1420.07 | 8.88 | 1.01 | 0.39 |
| mix f | 1293.79 | 9.89 | mix h | 1375.81 | 8.63 | 1.06 | 0.87 |
| mix l | 1358.75 | 22.59 | mix k | 1381.66 | 25.20 | 1.02 | 1.12 |
| mix j | 1314.75 | 7.95 | mix L | 1303.40 | 8.77 | 0.99 | 1.10 |
| mix m | 1352.85 | 9.12 | mix o | 1407.98 | 23.47 | 1.04 | 2.57 |
| mix n | 1318.12 | 17.49 | mix p | 1339.28 | 8.95 | 1.02 | 0.51 |
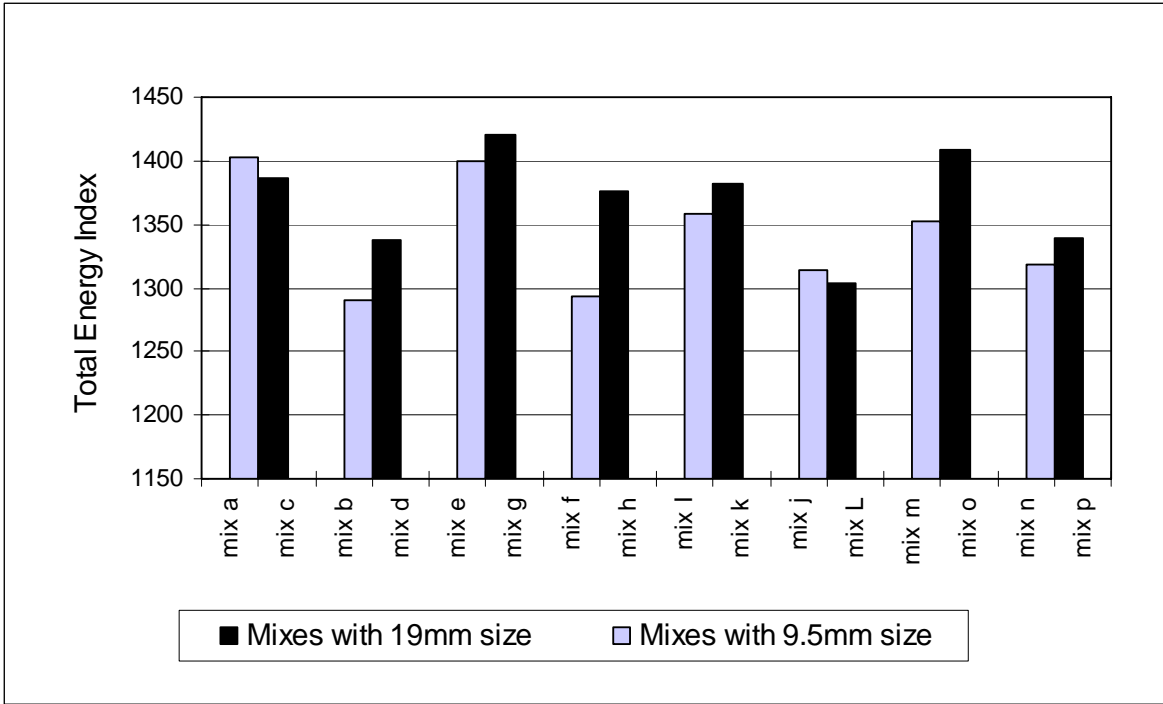
**A:** Total Energy Index.
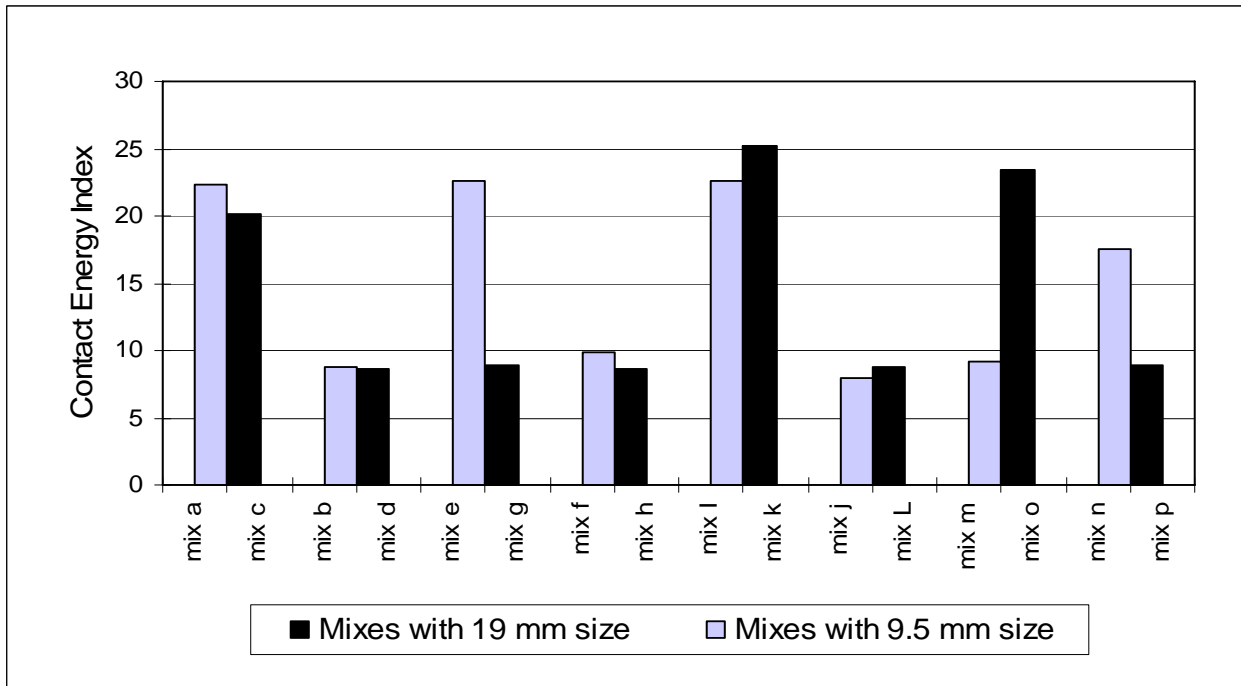


**B**: Contact Energy Index.

**Figure 3.14** Comparison among Mixes with Different Aggregate NMAS in terms of Total & Contact Energy Indices.

Two different gradations were used in this study, below the restricted zone (BRZ) and above the restricted zone (ARZ).  The BRZ gradation is usually referred to as coarse gradation, while the ARZ gradation is referred to as fine gradation.  There have been several studies to evaluate the influence of the location of the aggregate gradation curve with respect to the restricted zone on mix stability and performance *(Chowdry et al. 2001, Hand and Epps 2001)*. These studies came to the conclusion that there is no trend between the mix stability and location of the gradation curve below or above the restricted zone.  The energy indices results shown in **Figure 3.15** and **Table 3.6** are in agreement with these findings as no relationship was found between the energy indices and gradation shape.

**Table 3.6** Energy Indices of Mixes with Different Aggregate Gradation Shape.

| B.R.Z (Coarse) Mix # | Total E.I. | Contact E.I. % | A.R.Z (Fine) Mix # | Total E.I. | Contact E.I. % | Total E.I. Ratio | Contact E.I. Ratio |
|---|---|---|---|---|---|---|---|
| mix a | 1433.35 | 22.43 | mix e | 1400.21 | 23.11 | 1.024 | 0.970 |
| mix b | 1339.31 | 8.82 | mix f | 1323.18 | 9.89 | 1.012 | 0.892 |
| mix c | 1385.83 | 19.75 | mix g | 1389.80 | 8.88 | 0.997 | 2.225 |
| mix d | 1337.76 | 8.57 | mix h | 1375.81 | 8.60 | 0.972 | 0.996 |
| mix I | 1358.75 | 22.36 | mix m | 1343.10 | 9.12 | 1.012 | 2.452 |
| mix j | 1314.75 | 7.95 | mix n | 1288.45 | 17.29 | 1.020 | 0.460 |
| mix k | 1412.24 | 25.33 | mix o | 1428.27 | 23.83 | 0.989 | 1.063 |
| mix L | 1333.34 | 8.82 | mix p | 1339.28 | 8.82 | 0.996 | 1.000 |
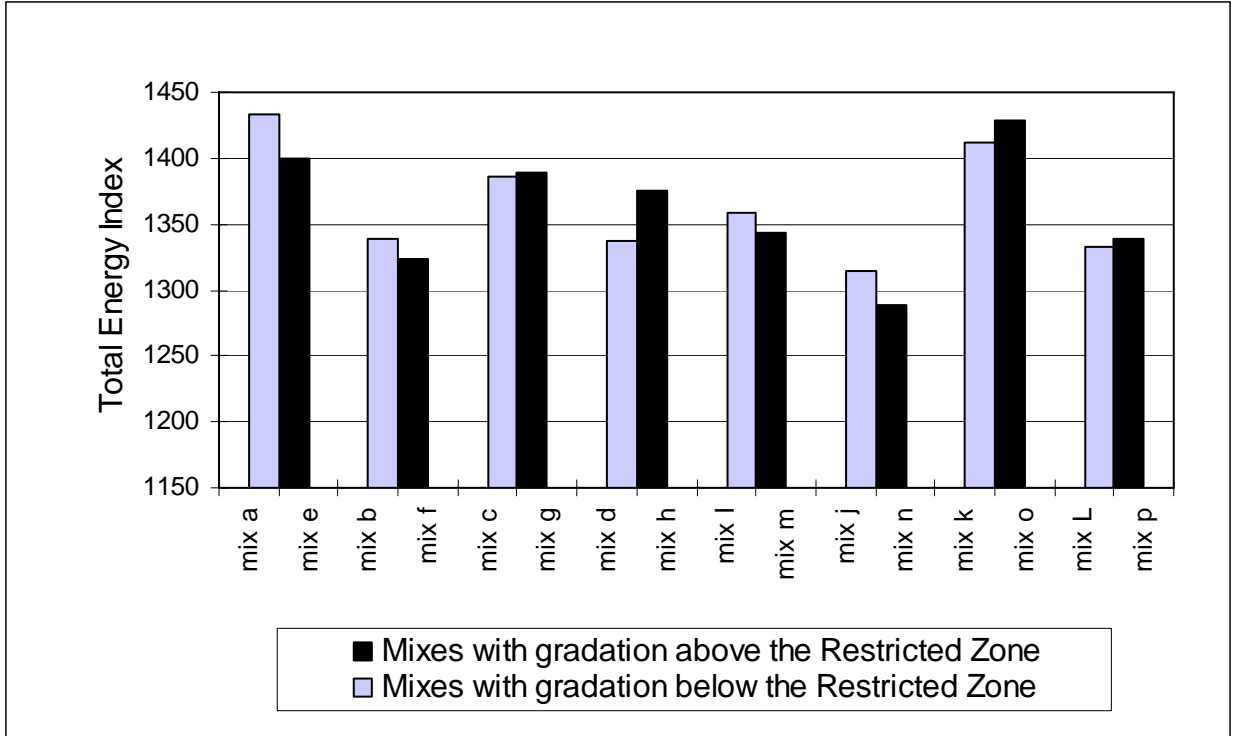
**A:** Total Energy Index.
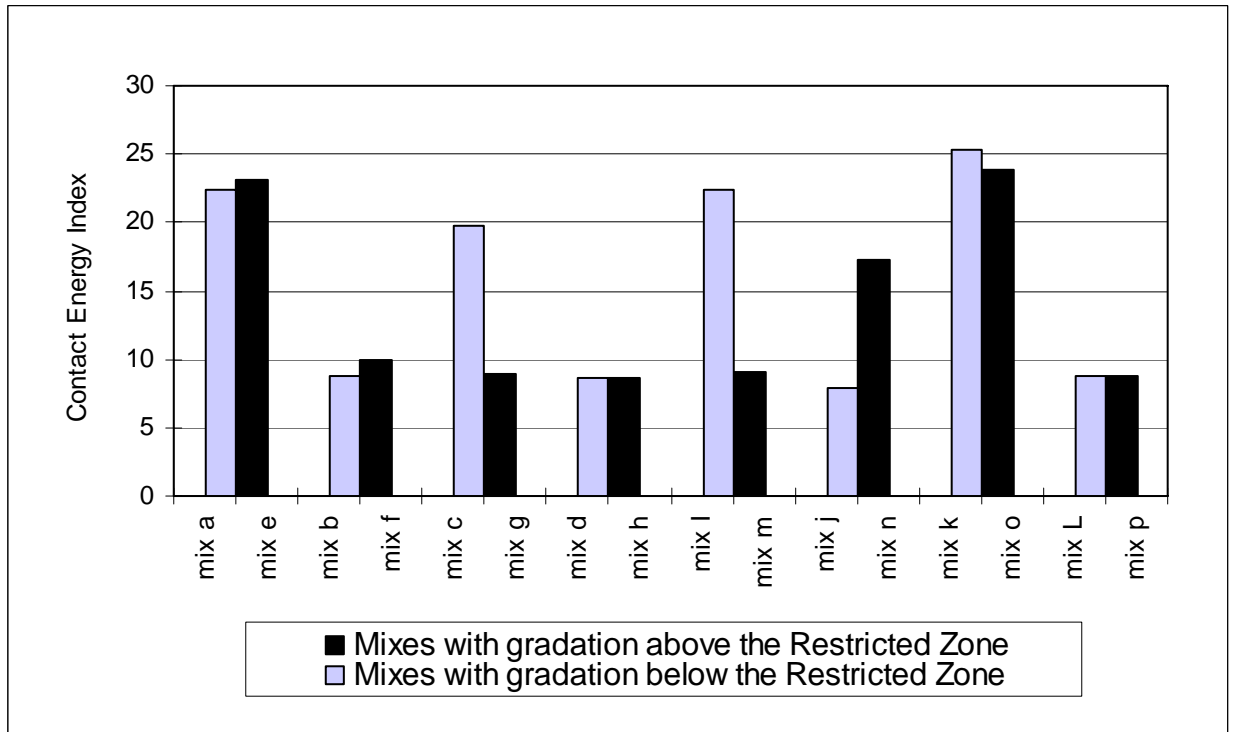


B: Contact Energy Index.

Figure 3.15 Comparison among Mixes with Different Aggregate Gradation Shape in terms of Total & Contact Energy Indices.

Mixes with 0% and 40% natural sand were tested in this study.  Figure 3.16 and **Table 3.7** show that the total energy index did not distinguish between mixes with and without natural sand.  However, the results show that the contact energy index was higher for all mixes without natural sand compared with those included 40% natural sand. It is evident that the contact energy index captures the influence of natural sand on mix stability.  Most natural sands and especially the one used in this study have rounded shape with very small texture, therefore, mixes with natural sand are expected to be less stable than the mixes that do not include natural sand.

**Table 3.7.** Energy Indices of Mixes with Different Percent of Natural Sand.

| 0% Natural Sand Mix # | Total E.I. | Contact E.I. % | 40% Natural Sand Mix # | Total E.I. | Contact E.I. | Total E.I. Ratio | Contact E.I. Ratio |
|---|---|---|---|---|---|---|---|
| mix a | 1392.69 | 25.80 | mix b | 1369.03 | 11.35 | 1.017 | 2.274 |
| mix c | 1295.35 | 24.05 | mix d | 1337.76 | 10.01 | 0.968 | 2.403 |
| mix e | 1331.37 | 22.91 | mix f | 1323.18 | 10.72 | 1.006 | 2.138 |
| mix g | 1319.21 | 28.63 | mix h | 1375.81 | 9.35 | 0.959 | 3.064 |
| mix I | 1301.86 | 24.20 | mix j | 1249.19 | 10.27 | 1.042 | 2.357 |
| mix k | 1361.27 | 28.61 | mix L | 1343.27 | 10.70 | 1.013 | 2.673 |
| mix m | 1352.85 | 21.91 | mix n | 1367.43 | 20.05 | 0.989 | 1.093 |
| mix o | 1367.34 | 20.35 | mix p | 1339.28 | 9.62 | 1.021 | 2.114 |

The effect of natural sand can also be seen in compaction curves.  **Figure 3.17a** shows that mixes with natural sand started at smaller percent air voids.  The slopes of the compaction curves are plotted in **Figure 3.17b**, in which the slope is calculated for each 10 gyrations.  It is clear that mixes with 0% natural sand had higher slopes than mixes with 40% natural sand.  This observation is especially true in the shear compaction range (Part B in **Figure 3.17**), which starts between 30 to 50 gyrations.  As mentioned earlier, an increase in the slope in Part B indicates an increase in the portion of the applied energy transferred into developing contacts among aggregates.
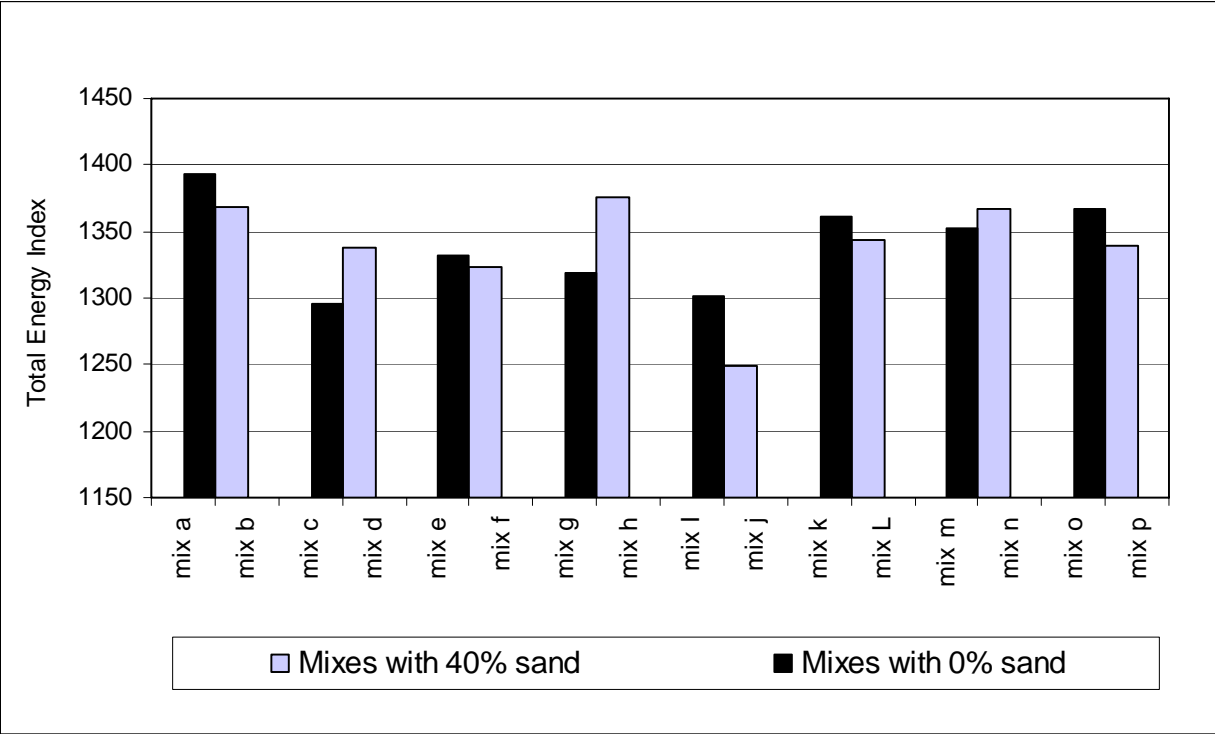
A: Total Energy Index.
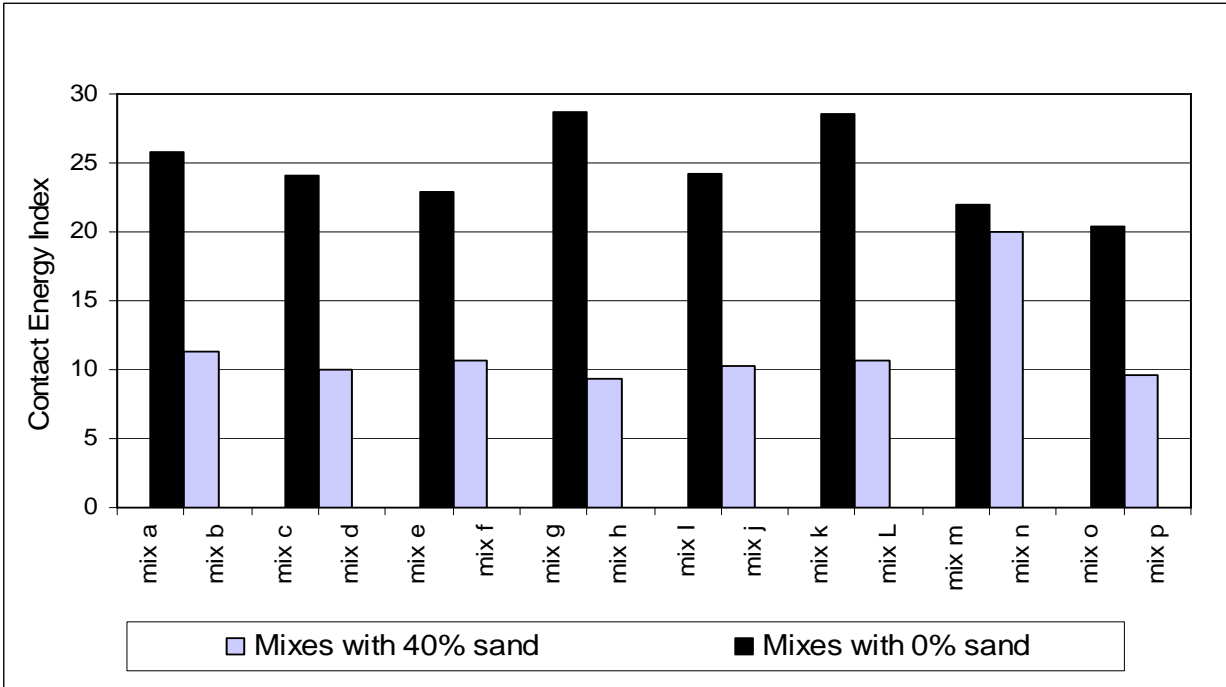


**B:** Contact Energy Index.

**Figure 3.16** Comparison TEI and CEI among Mixes with Different % Natural Sand.

60
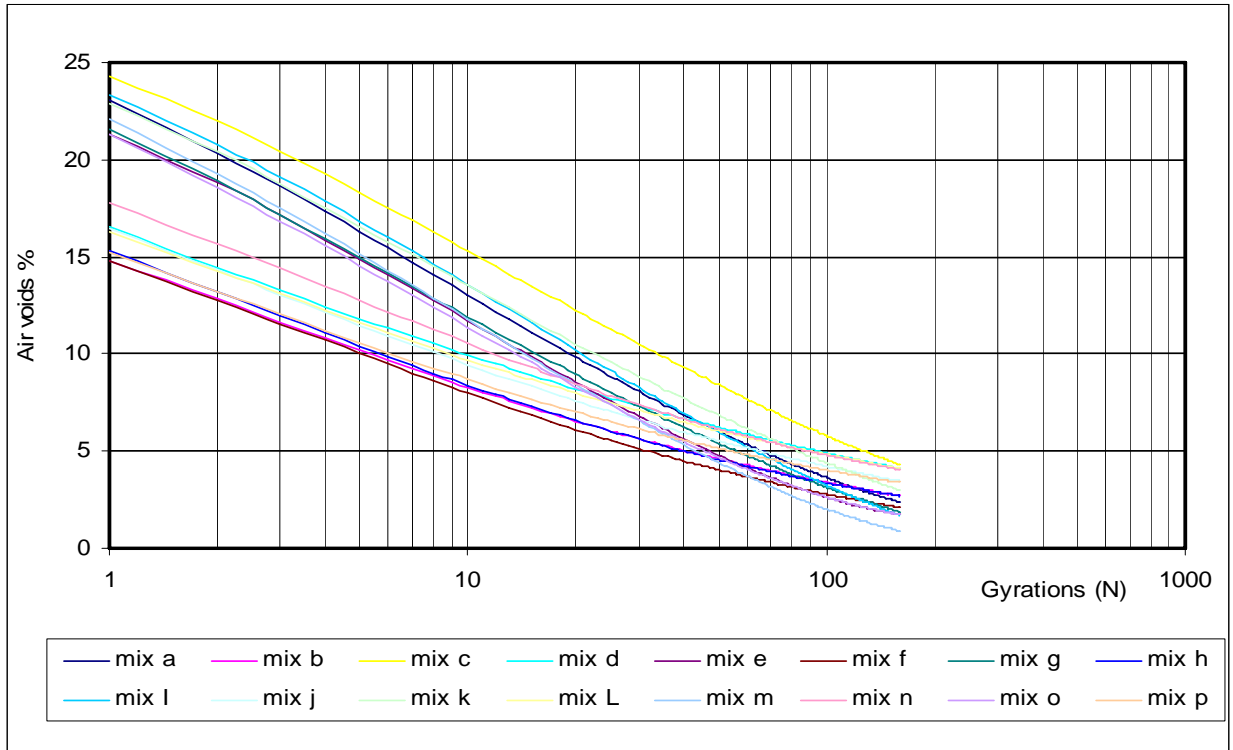
**A:** Compaction Curves of Mixes with Different Percent Natural Sand.
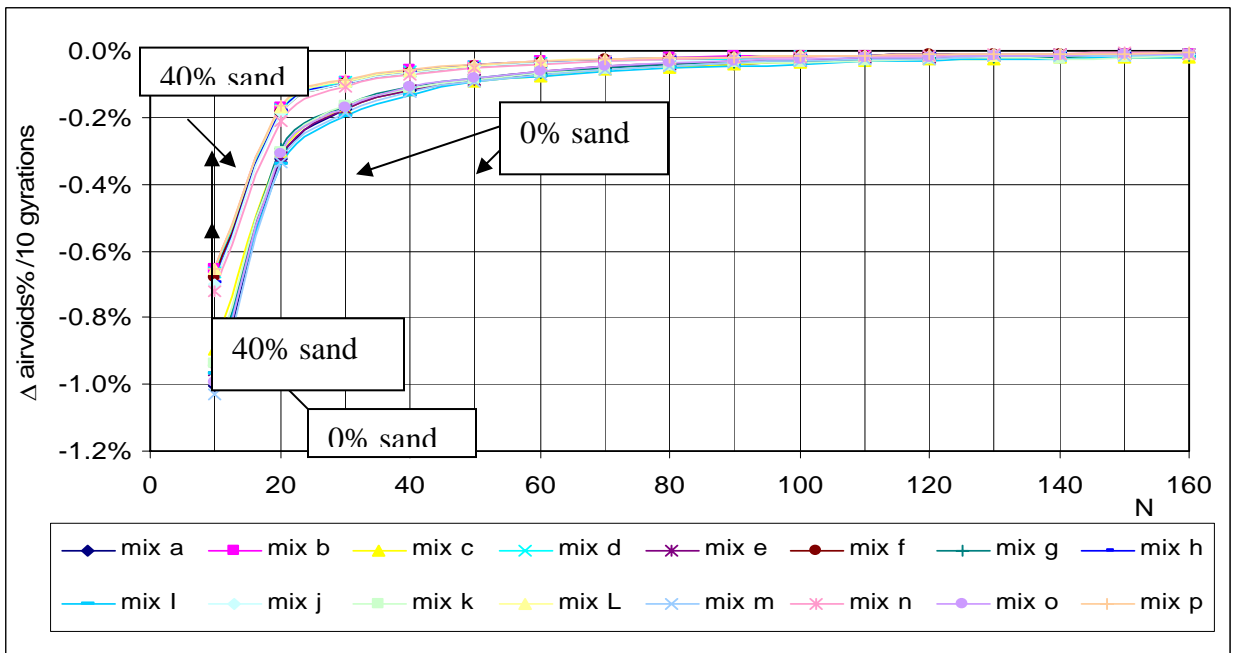


**B**. Slopes of Compaction Curves.

**Figure 3.17** Compaction Curves and Their Slopes for Mixes with Different Percent Natural Sand

### 3.3.2 The Effect of Compaction Variables on Energy Indices

The previous section evaluated the influence of mix constituents on the energy indices. This evaluation was conducted using the same set of compaction variable (Angle = 1.5o, Pressure = 600 kPa). However, *Butcher et al. (1998)* showed that the shear stress in a mix changes as a function of the angle of gyration. As shown in **Figure 2.4,** the shear stress at small angles ($\theta < 1.0$) increases with the number of gyrations until reaches a constant value, indicating that the material reaches a stable state at low angles of gyrations. However, the shear stress curve has different characteristics at higher angle values as it increases up to a maximum value beyond which the shear stress tends to decrease with further compaction. It can be seen in **Figure 2.4,** that two different mixes (a and b) might behave similarly at low angle but different at high angle such as 3o. Mix "a" takes almost 50 gyrations to start showing unstable behavior, while instability in mix b is triggered at 100 gyrations.

In this section, the influence of changes in compaction pressure and angle of gyration on the energy indices is investigated using four mixes (C, D, K, and L). This is necessary to determine if there exists a set of compaction variables that have the best ability to differentiate among mixes with different constituents. Five specimens of each of the four mixes were compacted at 0, 0.75, 1.5, 2.25, 3.0°. Mixes compacted at 0° angle collapsed right after taking them from the mold, which emphasized the influence of shear action induced by the angle of gyration on developing aggregate contacts, as shown in **Figure 3.18**. The difference in shear stress among the mixes increased with an increase in the angle of gyration. It is also noticed that the shape of the compaction curve for mix k changed with an increase of angle of gyration from 0.75 to 3.00. **Figure 3.19** shows that the shear stress increased remarkably with an increase in angle of gyration.
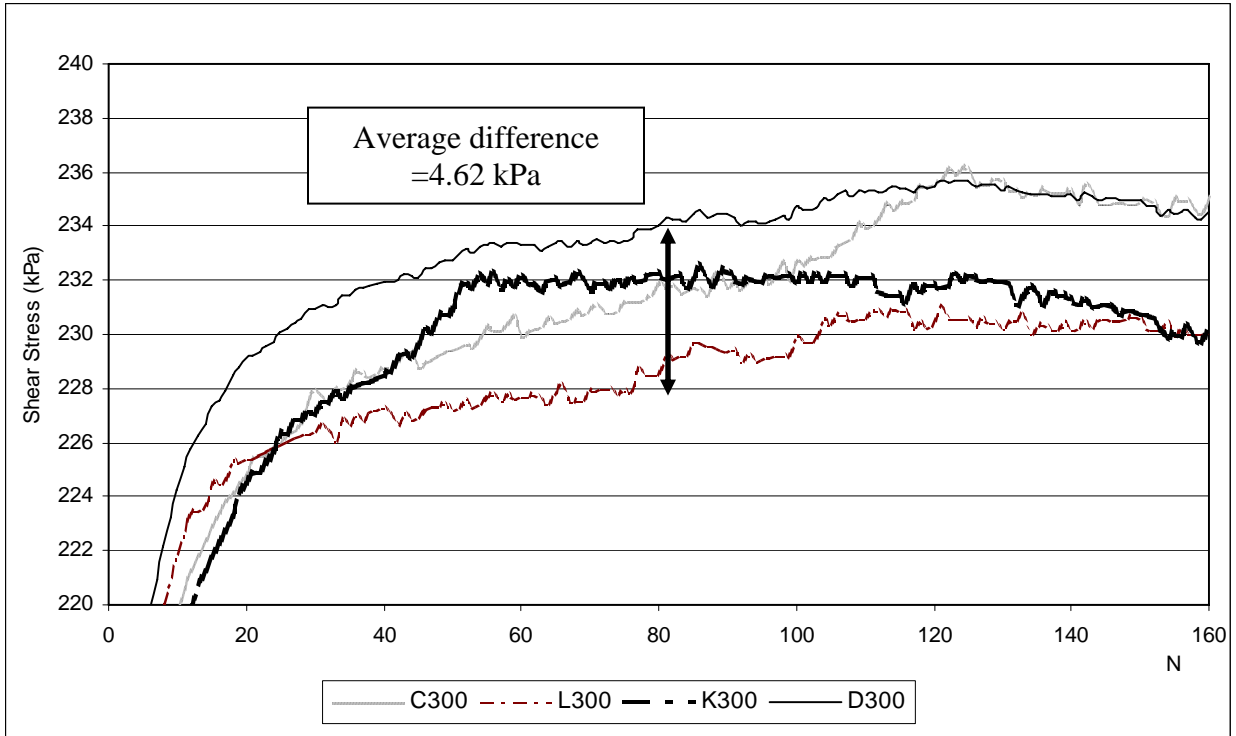
**Figure 3.18a**. Shear Stress Curves at an Angle of 3.00°
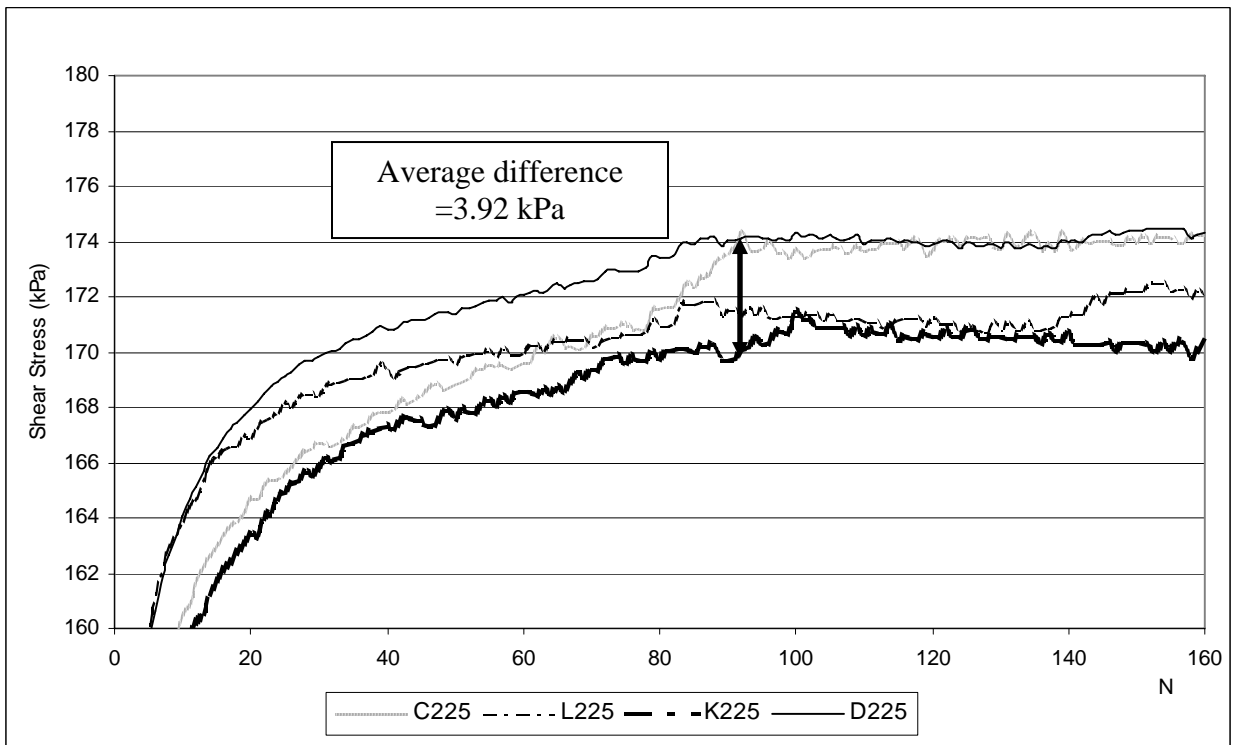


**Figure 3.18b**. Shear Stress Curves at an Angle of 2.25°
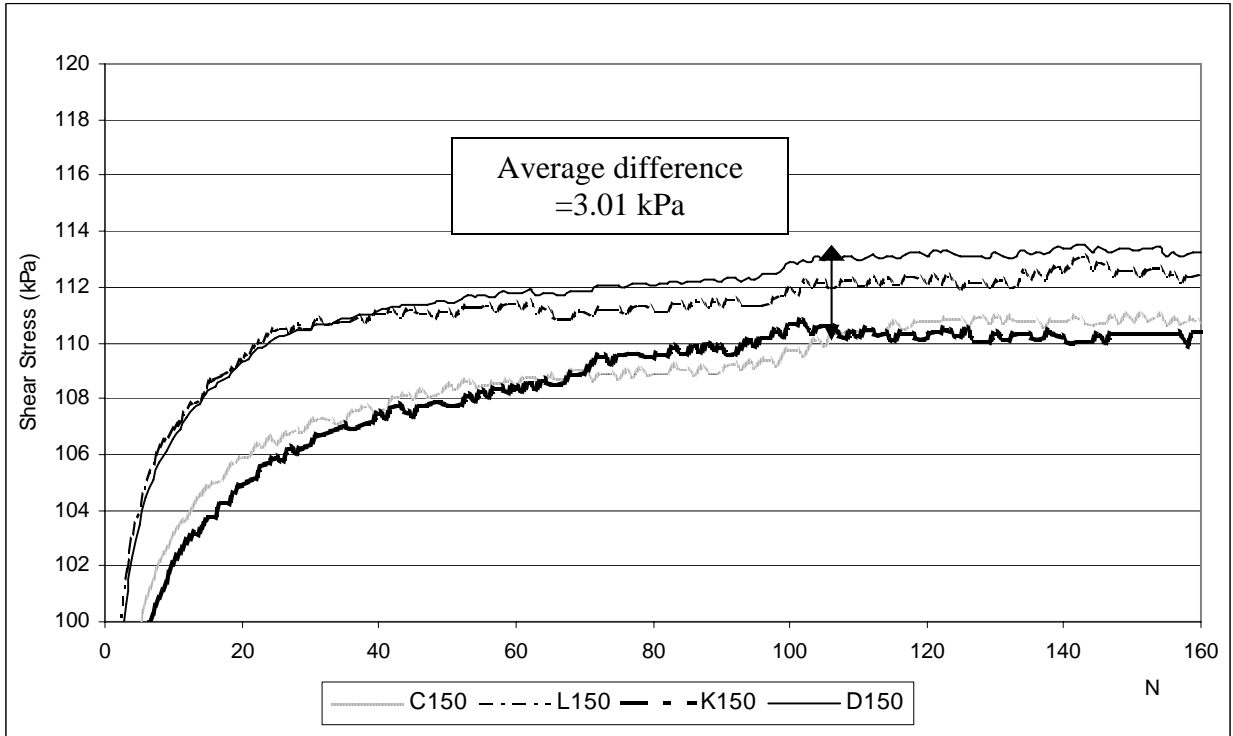
**Figure 3.18c**. Shear Stress Curves at an Angle of 1.50°
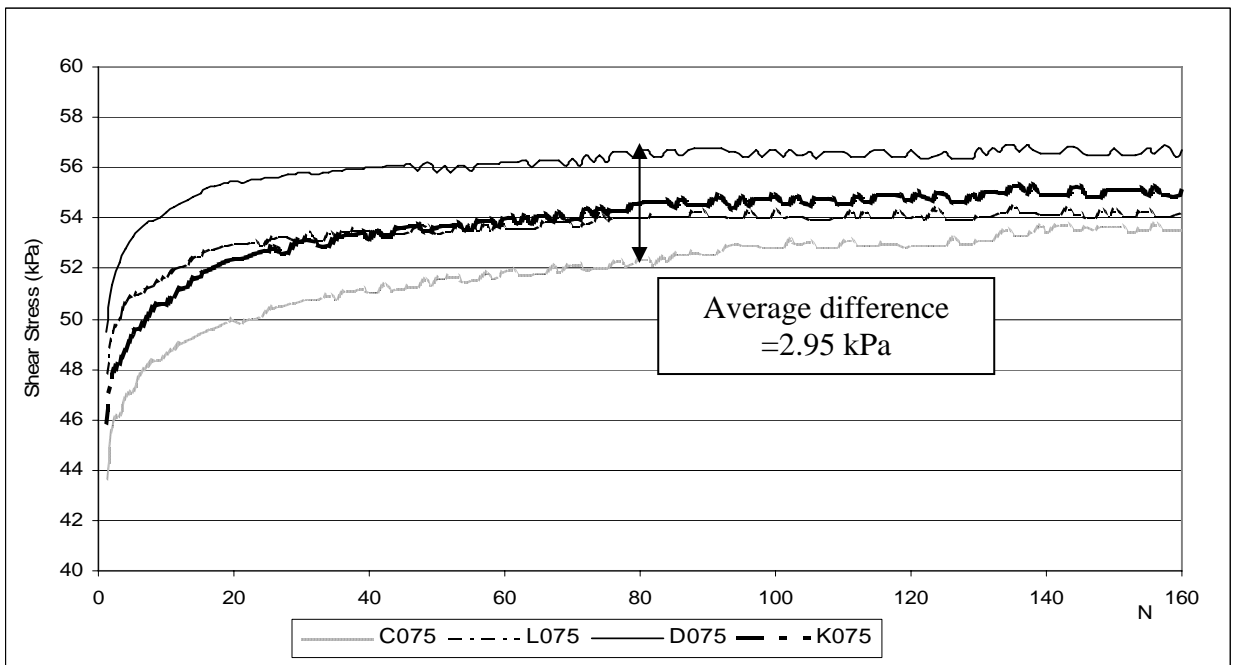


**Figure 3.18d**. Shear Stress Curves at an Angle of 0.75°

**Figure 3.18** Shear Stress Curves at Different Angles of Gyrations (3.00, 2.25, 1.5 and 0.75°)
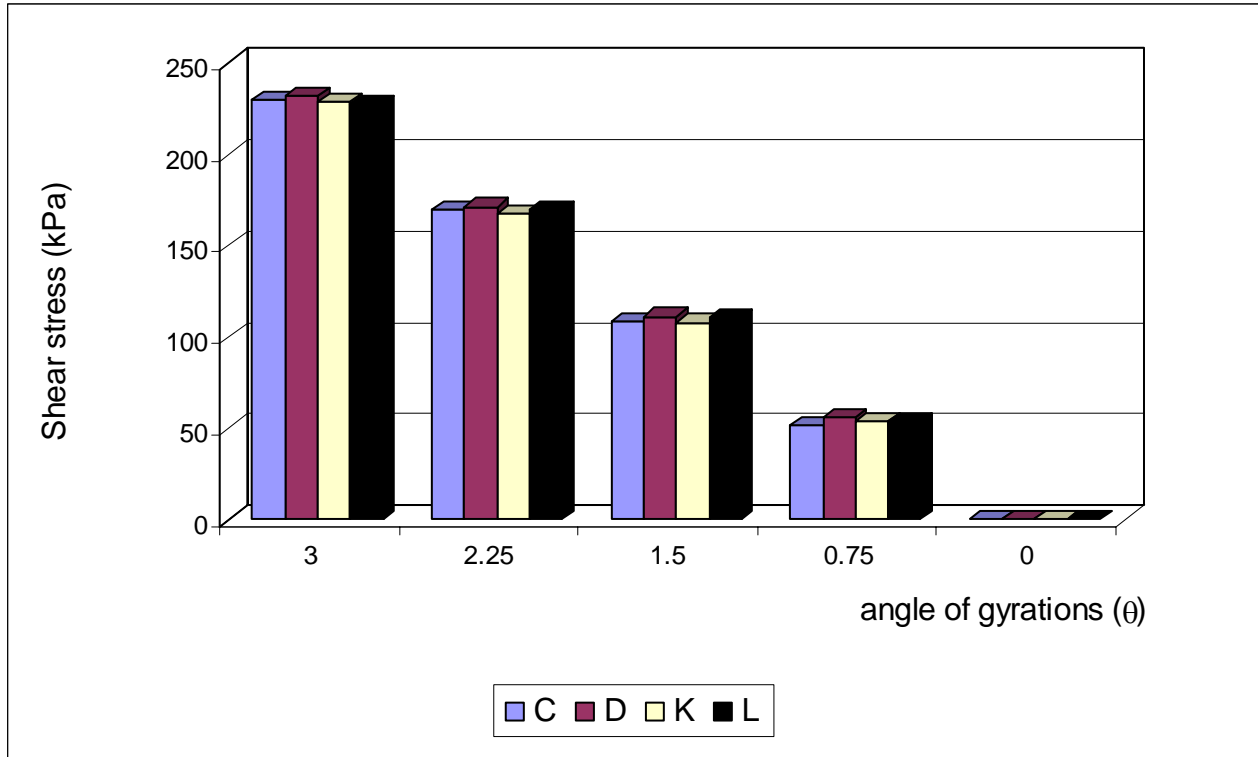
**Figure 3.19** Maximum Shear Stress at Different Angles of Gyrations.

Both the total and contact energy indices were calculated at all angles for the four mixes (**Figure 3.20** and **Table 3.8**). As can be seen the total energy index was almost the same for all mixes at a given angle of gyration. The contact energy indices for the four mixes had the same order at all angles, in spite of the increase in their values with an increase in angle. The ratio of contact energy index of mix C to that of D and of mix K to that of L remained almost the same at different angles. This result suggests that the angle of gyration affects the shear stress but does not change the order of the mixes in terms of stability.
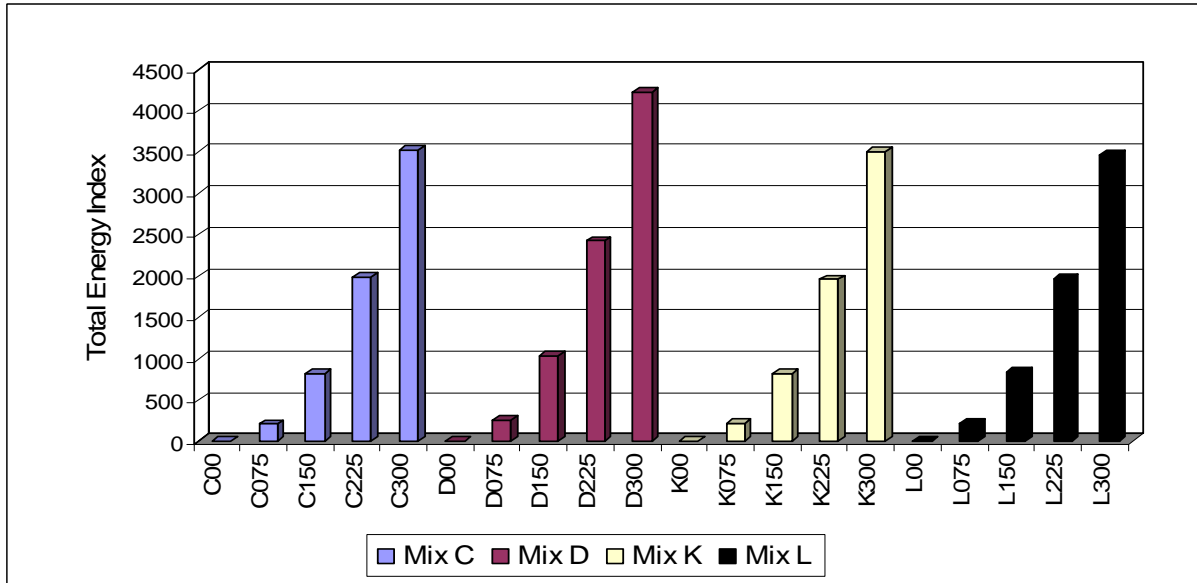
**A:** The Total Energy Index.
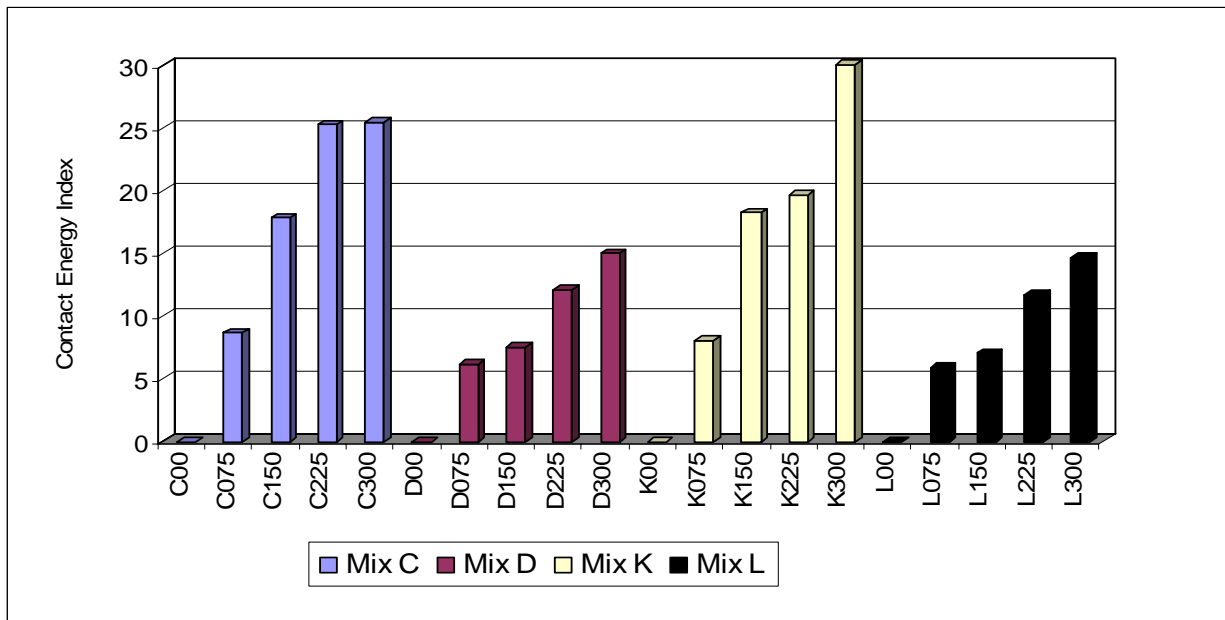


B: The Contact Energy Index

**Figure 3.20** The Total & Contact Energy Indices at Different Angles of Gyrations.

66

.

**Table 3.8** Energy Indices at Different Angle of Gyrations.

| E.I. @ angle | Total E.I. | | | | Contact E.I. | | | |
|---|---|---|---|---|---|---|---|---|
| | Mix C | Mix D | Mix K | Mix L | Mix C | Mix D | Mix K | Mix L |
| 0.00 | 0.01 | 0.01 | 0.00 | 0.00 | 0.00 | 0.00 | 0.00 | 0.00 |
| 0.75 | 207.54 | 261.31 | 214.32 | 212.61 | 8.67 | 6.14 | 8.06 | 5.89 |
| 1.50 | 825.87 | 1035.72 | 825.88 | 843.01 | 17.84 | 7.53 | 18.24 | 7.05 |
| 2.25 | 1982.38 | 2428.39 | 1960.31 | 1972.71 | 25.24 | 12.08 | 19.62 | 11.73 |
| 3.00 | 3524.14 | 4220.72 | 3500.16 | 3470.16 | 25.43 | 15.01 | 32.73 | 14.69 |

The vertical pressure is another factor that influences the compaction process. An increase in pressure leads to an increase in confinement during compaction. Specimens from the C, D, K, and L mixes were compacted at pressures of 450 kPa, 600 kPa, and 750 kPa at 1.5 and 2.25 angles. The results in **Figure 3.21a** show that the total energy index was almost the same for all mixes at given pressure and angle values, while the contact energy index decreased with a decrease in the pressure and angle values as shown in **Figure 3.21b**. The rank of the contact energy index remained almost the same at the different combinations of pressure and angle. The mixes without natural sand C and K showed higher stability than their counterpart mixes with natural sand D and L. These results suggest any combination of the pressure and angle would be suitable to characterize the mixes.

**Table 3.9** Energy Indices at Different Angles and Pressures.

| | Total E.I. | | | | | |
|---|---|---|---|---|---|---|
| Angle | 1.50 | | | 2.25 | | |
| Pressure | 450 | 600 | 750 | 450 | 600 | 750 |
| C | 982.83 | 1361.72 | 1606.75 | 2108.16 | 2907.77 | 3664.91 |
| D | 1035.72 | 1414.39 | 1658.11 | 2189.90 | 3133.69 | 3784.86 |
| K | 978.96 | 1354.86 | 1657.57 | 2099.51 | 3122.75 | 3605.88 |
| L | 1003.82 | 1370.49 | 1716.48 | 2108.05 | 2909.42 | 3718.85 |
| | Contact E.I. | | | | | |
| Angle | 1.50 | | | 2.25 | | |
| Pressure | 450 | 600 | 750 | 450 | 600 | 750 |
| C | 12.76 | 20.51 | 18.75 | 14.01 | 28.17 | 28.49 |
| D | 7.37 | 10.58 | 11.48 | 8.88 | 13.63 | 17.44 |
| K | 13.53 | 19.08 | 17.71 | 14.27 | 27.86 | 25.57 |
| L | 7.05 | 9.95 | 11.90 | 8.66 | 13.58 | 17.12 |
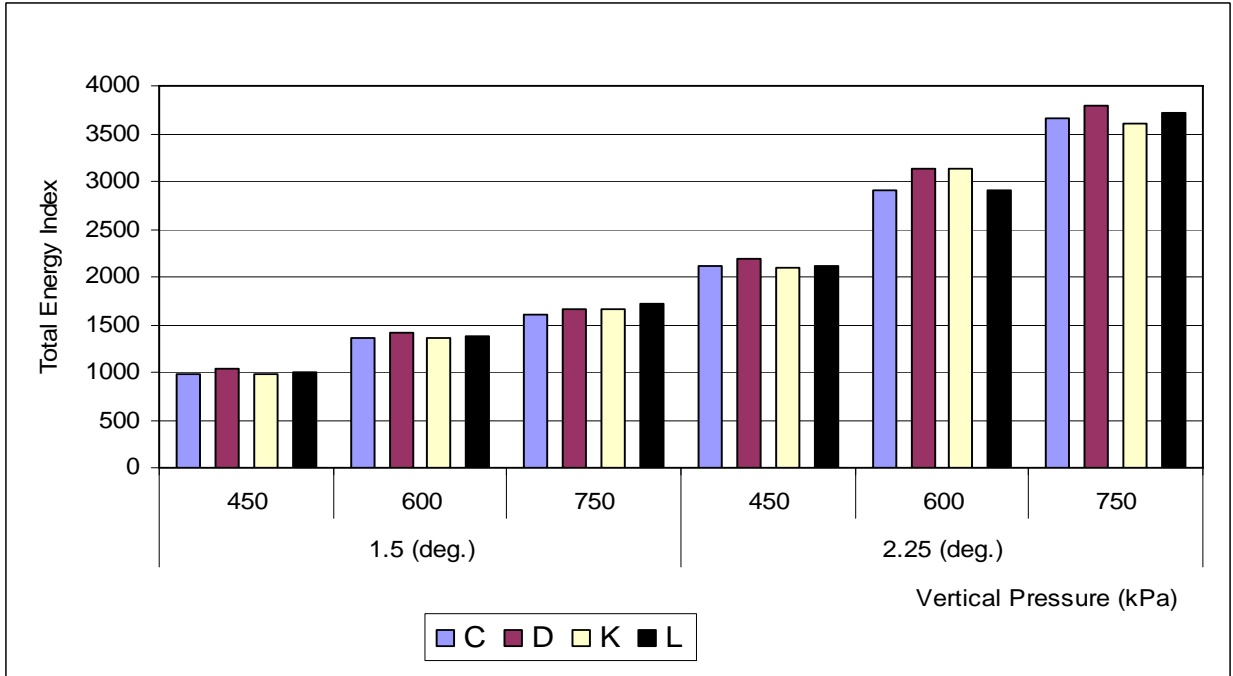
**A:** The Total Energy Index
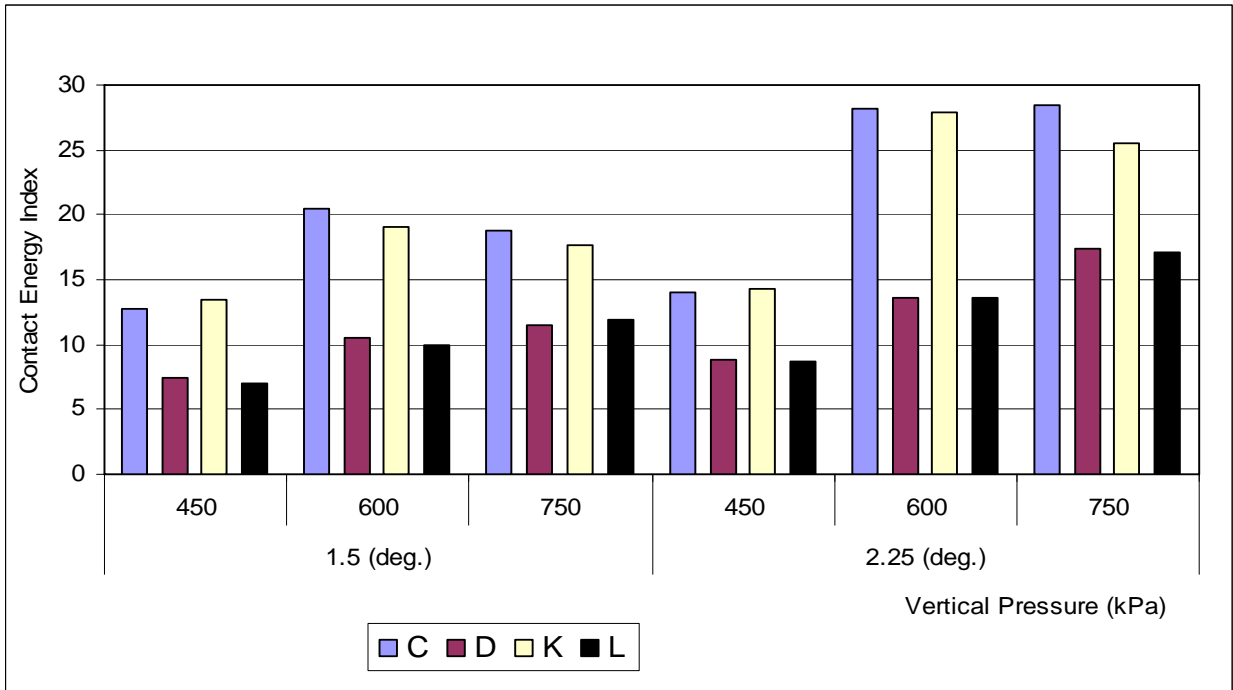


**B: The Contact Energy Index**

**Figure 3.21** The Total & Contact Energy Indices at Different Pressures and Angles of Gyrations.

## 3.4  COMPARISON OF CONTACT ENERGY INDEX WITH MIX MECHANICAL PROPERTIES

The Superpave shear test was used to measure the viscoelastic properties; namely the dynamic shear modulus G* and phase angle δ of four mixes (C, D, K, and L) of two temperatures (40C, and 52C).  All measurements were conducted on mixes with optimum asphalt content.  The viscoelastic properties and contact energy indices at an angle of 1.5o and a pressure of 600 kPa are shown in **Table 3.10**.  Each of the viscoelastic properties is an average of three measurements.  The comparison focuses on G*/sinδ since it has been recommended as a parameter to evaluate the mix resistance to permanent deformation *(Romero and Mogawer 1998a, and b)*.  It can be seen that both G*/sinδ and the contact energy index were higher for mixes without natural sand (C and K), compared with their counterpart mixes that included 40% natural sand (D and L).  The contact energy index was higher for mixes with limestone compared with those that included gravel. In general, this limited data show that good correlation exists between the contact energy index predictions and G*/sinδ.

**Table 3.10** Comparison between the Viscoelastic Properties and Contact Energy Index

| Mix # | G* | | δ | | G*/sinδ | | Contact |
|-------|------|------|------|------|---------|---------|---------|
|       | 40C | 52C | 40C | 52C | 40C | 52C | E.I. |
| C | 545031.8 | 206360.3 | 39.6 | 44.3 | 854618.8 | 295539.5 | 17.84 |
| D | 532877.0 | 188875.1 | 43.1 | 46.7 | 780314.9 | 259696.2 | 7.53 |
| K | 653159.4 | 273335.5 | 37.1 | 45.3 | 1083127.9 | 384240.5 | 18.24 |
| L | 506535.1 | 192294.6 | 43.3 | 50.6 | 738910.7 | 248672.1 | 7.05 |

## 3.5  COMPARISON WITH PERFORMANCE AND MECHANICAL PROPERTIES

Three compacted mixtures specimens from each of three SPS-9 projects from 1992 were received. These mixes were analyzed and tested using different experiments by *Michael Anderson et al. (2000)*. The energy indices were calculated to all mixes and averaged for each

project then compared to the findings and results presented by *Anderson et al. (2000)*. The
following table presents the mixes description:

**Table 3.11** Summary of the 1992 SPS-9 mixtures

| Project | Mix Label |
|---|---|
| Wisconsin IH-94 | S-4 (2) |
| | S-4 (5) |
| | S-4 (7) |
| Wisconsin IH-43 | S-3 (84) |
| | S-3 (89) |
| | S-3 (90) |
| Indiana IH-65 | S-3 (2) |
| | S-3 (4) |
| | S-3 (5) |

These mixes were tested with the Static Shear Creep Testing (SSCH), and Shear

Frequency Sweep Testing (FSCH) at two different temperatures. SSCH determined the average

maximum shear strain ($\gamma$max) and the FSCH determined the average shear stiffness (G*) and

phase angle ($\delta$).  In addition, field rutting measurements were obtained after six years of service.

These measurements were presented by *Anderson et al. (2000)* in terms of the rutting rate

parameter expressed in mm/ESAL1/2, Table 3.12.  As reported by *Anderson et al. (2000)* all

mixes would be considered to have minimal rutting since they all had a rutting rate less than

0.00584 mm/ESAL1/2.

The relationships between the CEI and the mechanical properties are shown in **Figure
3.22.**  In general, the results show that the CEI increases with an increase in G* and G*/sin$\delta$, and

a decrease in maximum shear strain. This shows the potential of the CEI in reflecting the mix

stability and shear strength. The CEI index is also the highest for the mixes from IH-43, which

has the lowest rutting rate, **Table 3.12**.  However, the CEI is almost the same for IH-94 and IH-
65 although these two sections have different rutting rates. It should be noticed that the three

sections did not experience significant rutting that would allow complete verification of the

ability of the CEI to predict the field permanent deformation.

**Table 3.12** Performance and Experimental Data Presented by *Anderson et al. (2000)* on SPS-9 Sections.

| Project | IH-43 | IH-94 | IH-65 |
|---|---|---|---|
| Rut Depth (mm) | 2 | 2 | 5 |
| ESAL | 3.58E+06 | 7.39E+06 | 1.65E+07 |
| Ruttin rate | | | |
| $(mm/ESAL^{1/2})$ | 1.06E-03 | 7.36E-04 | 1.23E-03 |
| Total energy index | 1052.76 | 1077.18 | 1051.24 |
| Contact energy index | 28.47 | 25.91 | 25.59 |
| Temperature T1 ( C) | 38 | 38 | 39 |
| Temperature T2 ( C) | 22 | 21 | 23 |
| SSCH ($\gamma_{max}$) | | | |
| T1 ( C) | 1246.00 | 932.00 | 2060.00 |
| T2 ( C) | 370.00 | 453.00 | 1187.00 |
| FSCH (G* kPa) | | | |
| T1 ( C) | 863176 | 656499 | 370655 |
| T2 ( C) | 3422942 | 2344772 | 1811702 |
| FSCH ($\delta$ degree) | | | |
| T1 ( C) | 33.90 | 35.70 | 43.70 |
| T2 ( C) | 8.90 | 16.40 | 25.40 |
| G*/sin$\delta$ | 1547.62 | 1125.03 | 536.50 |
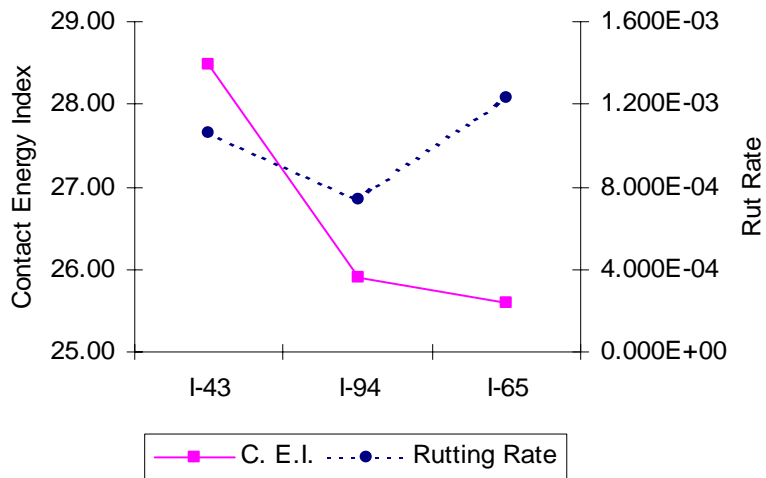
Figure 3.22a. Rutting Rate Versus Contact Energy Index
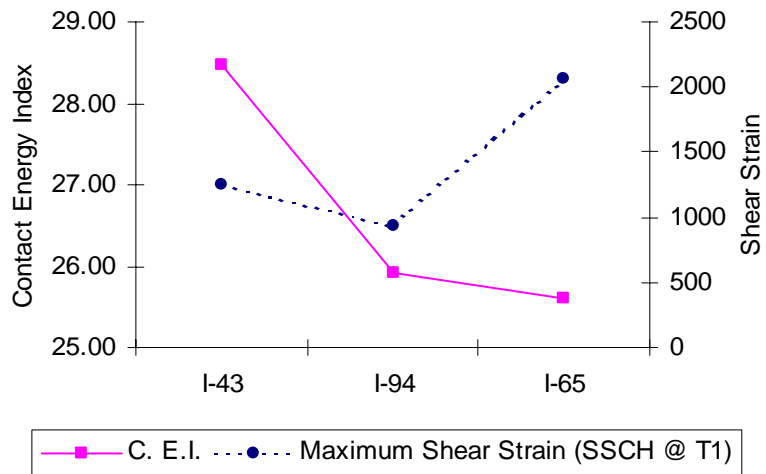


Figure 3.22b. Maximum Shear Strain at $T_1$ Versus Contact Energy Index
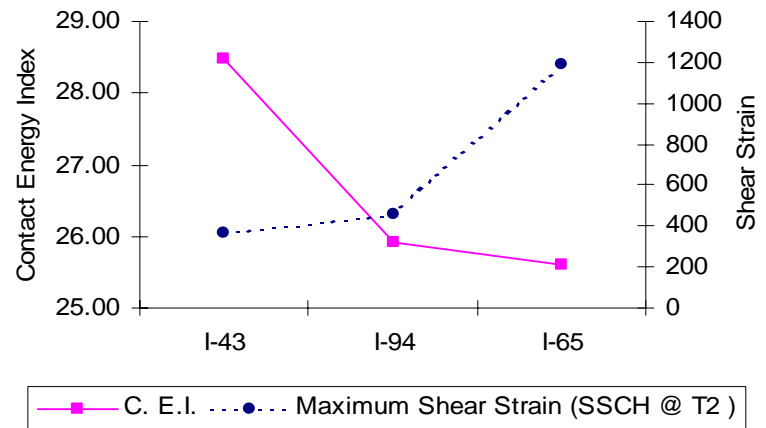


Figure 3.22c. Maximum Shear Strain at $T_2$ Versus Contact Energy Index
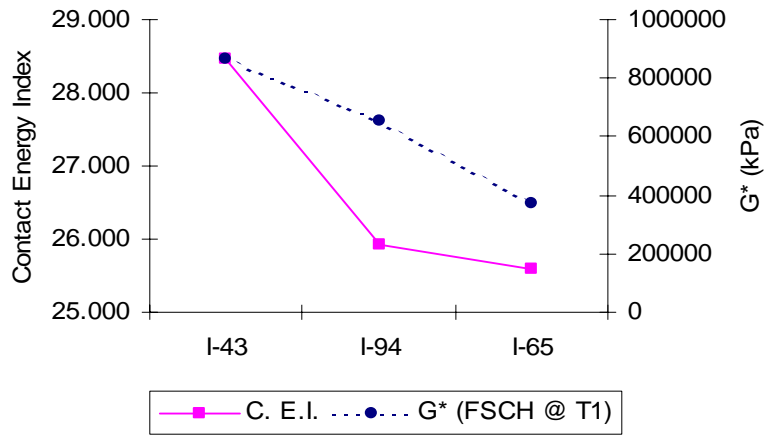
Figure 3.22d. Stiffness Modulus G* at $T_1$ Versus Contact Energy Index
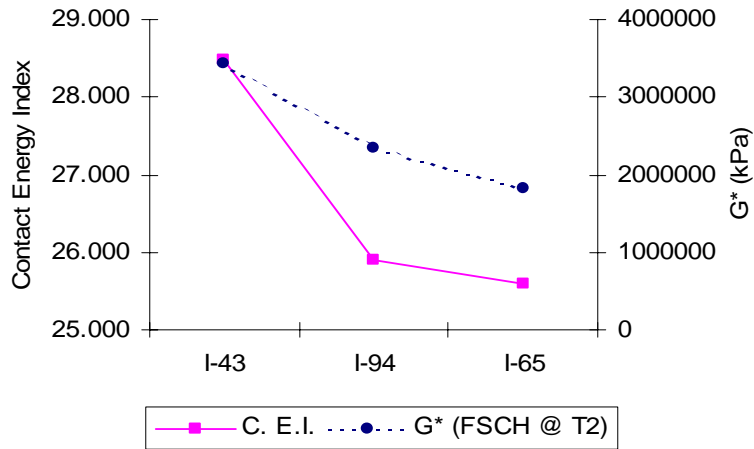


Figure 3.22e. Stiffness Modulus G* at $T_2$ Versus Contact Energy Index
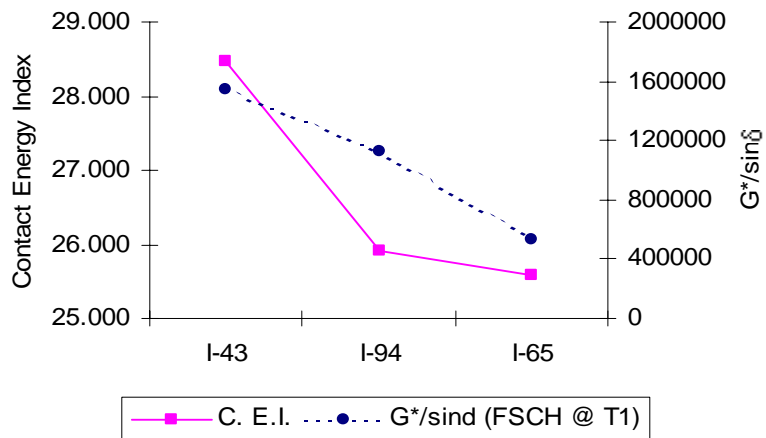


Figure 3.22f. Stiffness Parameter G*/Sinδ at $T_1$ Versus Contact Energy Index

**Figure 3.22** Relationships between the CEI and the mechanical properties

## 3.6  SUMMARY

The compaction process in Servopac has been analyzed and a new equation for calculating the shear stress in the mix is developed.  The shear stress is used to develop energy indices that account for the total energy needed to compact a specimen (Total Energy Index), and the energy used to develop contacts among the aggregates (Contact Energy Index). The energy indices were determined for mixes with different asphalt content, percent natural sand, aggregate gradation, nominal maximum aggregate size, and aggregate type.  The contact energy index was found to capture the influence of binder content, percent of natural sand, and aggregate type on mix stability.  The value of the contact energy index was less for mixes with natural sand, excess binder content, and smooth surface aggregates.

The influence of the compaction pressure and angle of gyration on the energy indices was investigated in order to determine the best combination that would capture the difference among mixes with different constituents.  It was found that an increase in pressure or angle would increase the value of the energy indices.  However, the order of mixes in terms of their contact energy index value was not affected by changing the pressure or angle values.  Therefore, the values recommended in the current Superpave procedure (angle = 1.25, pressure = 600 kPa) would be effective in capturing the influence of mix constituents on the value of the contact energy index.

The Superpave shear test was used to measure $G^*$, $G^*/\sin\delta$ and maximum shear strain of three mixes at two different temperatures.  In general, the CEI was in agreement with the values of the mechanical properties.  The results show that the CEI increases with an increase in $G^*$ and $G^*/\sin\delta$, and a decrease in maximum shear strain. The CEI was able to distinguish between the mix that had the lowest rutting rate and the other two mixes.

This is a blank Page

# 4.  THE FINITE ELEMENT ANALYSIS (FEA) IN DETERMINING THE SHEAR STRESS

## 4.1  INTRODUCTION

This chapter presents two-dimensional (2-D) and three-dimensional (3-D) models of the

Superpave gyratory compactor. The general geometry and loading conditions that are converted

to finite element models are illustrated in Figure 4.1.  The HMA material properties are selected

such that the specimen vertical deformation in the model is similar to the laboratory

measurements.   The shear stress and contact energy index are calculated using the finite element

models and the results are compared with values obtained using the experiments and analysis

procedures given in Chapter 3 of this report.  The 3-D finite element model is shown to be able

to simulate the gyration action, and give results similar to laboratory measurements.
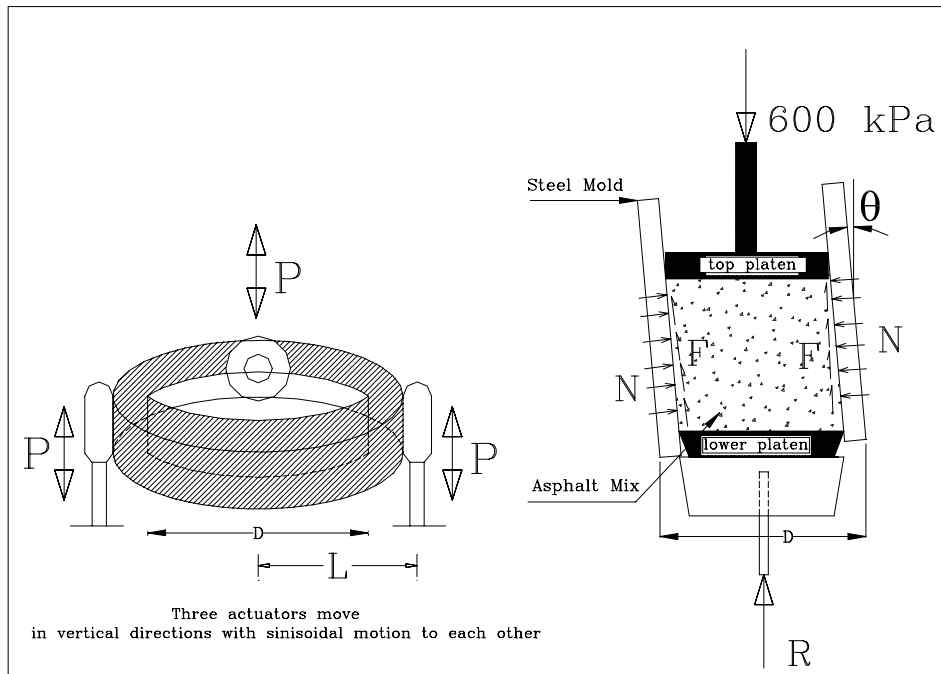


**Figure 4.1** A Schematic Diagram of the Gyratory Compactor.

## 4.2  FINITE ELEMENT ANALYSIS METHODOLOGY

FEA uses a complex system of points called nodes, which make a grid called a mesh. This mesh is programmed to contain the material and structural properties, which define how the structure will react to certain loading conditions. Nodes are assigned at a certain density throughout the material depending on the anticipated stress levels of a particular area. Regions, which will receive large amounts of stress usually, have a higher node density than those, which experience little or no stress. Points of interest may consist of: fracture point of previously tested material, fillets, corners, complex detail, and high stress areas. The mesh acts like a spider web in that from each node, there extends a mesh element to each of the adjacent nodes. This web of vectors is what carries the material properties to the object, creating many elements.

## 4.3  DESCRIPTION OF THE FINITE ELEMENT PROGRAM: *(ADINA 2000)*

The finite element program ADINA was used to develop a model of an asphalt mix specimen during the compaction process in the Servopac gyratory compactor. ADINA (Automatic Dynamic Incremental Nonlinear Analysis) is a commercial finite element program. It has been developed by ADINA R & D, Inc founded in 1986 by *K. J. Bathe* and associates. The exclusive mission is the development of the ADINA System for the analysis of solids; structures, fluids and fluid flow with structural interactions. Numerous types of elements, constitutive material definition and loading procedures are included within the program. The ADINA (version 7.4) is capable of solving dynamic and static analyses for a variety of material behavioral properties, from simple (elastic) to complex (plastic, visco-elastic, etc), in either two or three dimensions with the capability of linear and nonlinear analyses. For the engineering problems developed in this section, the following capabilities of ADINA were used in this analysis. For material property definition, the elastic modulus and poisson ratio is defined based on the incremental

deformation of a specimen at a certain gyration. The model was loaded by a constant uniform pressure at the top while subjected to confining pressure and friction along the both sides. The boundary conditions are maintained at the base to prevent any vertical movement.

## 4.4   2-DIMENSIONAL FINITE ELEMENT MODEL

Two-dimensional solid element with plane strain type was used to model the specimen, the model consists of a quadratic quadrilateral (iso-parametric) element contains 8-nodes distributed along the corners and the mid spans of the sides is used to model an asphalt specimen, the nodal variable is displacement and each node has two degrees of freedom (uy, uz) as shown in Figure 4.2. The reason for choosing the rectangle quadrilateral element is the geometrically isotropic characteristic, better than triangle elements in terms of the linear variation over the entire element, appropriate for bending behavior, and the compatibility along boundaries among the rectangular elements is guaranteed. The term quadratic refers to two types of numerical integration methods, full and reduced integration. For full integration, the number of integration points should be sufficient to integrate the virtual work expression exactly at least for linear material behavior, use of full integration is the only sure way to avoid mesh instability. For reduced integration the number of integration points should be sufficient to exactly integrate the contributions of the strain field that are one order less than the order of interpolation. The advantage of the reduced integration elements is the accuracy to find the stresses and strains at specific locations, and maintain the simplicity and save on computational time.
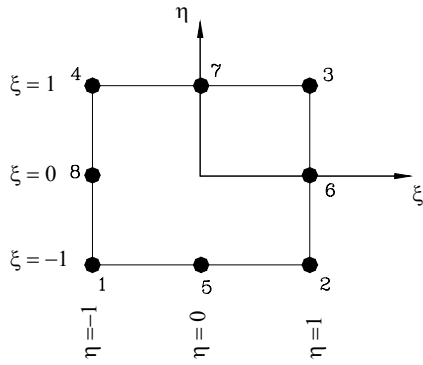
Quadratic plane element with straight sides and mid-sides nodes in the parent coordinate system
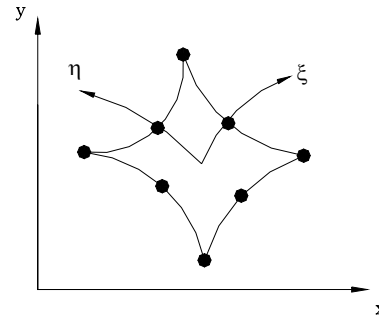
The quadratic element defined in global coordinate with deformed sides

**Figure 4.2** Element Type Used in 2-Dimensional Model

The steel mold accepts no lateral deformation, and rotates as a rigid body with fixity at one end, so it works as a cantilever. Therefore, the most appropriate model is a beam element with constant cross section in rectangle shape with width 0.01m and unit height. The element consists of 2-nodes composed together to form segment. The interaction between the specimen and the steel mold was modeled by defining contact surface along the boundaries, with the characteristic of not tied element to allow the relative movement of specimen with no penetration. In order to define the frictional plane, which is represented by a line in 2-D modeling, two types of surfaces has to be defined in "contact pair" menu i.e., two contact-surfaces, which are either initially in contact or are anticipated to come into contact during analysis. One contact-surface is termed the "contactor" contact-surface and must be deformable, i.e., has contact segments associated with the boundary surfaces of deformable finite elements (i.e., with nodes with free displacement degrees of freedom) within the model, which is the specimen in this case. The other contact-surface, which makes up the contact pair, is termed the "target" contact-surface. The target contact-surface may be deformable or have prescribed displacement, which is taken as the mold in this case. The nodes given on the frictional plane are

constrained not to penetrate into the target surface. Generally, the target surface is chosen as the surface with coarser mesh, while the boundaries of the specimen are the contactor surface, (*ADINA Modeling Guide 2000).*

When surfaces are in contact, they usually transmit shear stress as well as normal pressure. These tractions are considered in a local basis system defined by the normal to the contacting surface n and shear component $n_r$ Figure 4.3. The friction factor defines the relation between the normal pressure and shear stress. The Coulomb friction coefficient µ introduced by ADINA, maintain that the surfaces do not slide over each other as long as the shear stress magnitude is less than the friction coefficient µ multiplied by the normal stress. The coefficient of friction was set to 0.28 to extract consistent results with previous analysis in chapter (3). The two-dimensional contact surfaces are planar and lying in the global YZ plane, with all X coordinates equal to zero. Two-dimensional contact surfaces are formed of a series of linear contact segments and each segment is bounded by two nodes. Two successive nodes along a two-dimensional contact surface define a contact segment. A two-dimensional contact surface is an open surface while the segments do not form a closed path. The contact surface can be defined over only a part of a two-dimensional solid boundary if the remaining portion of the boundary does not take part in any contact interactions. Each two-dimensional contact surface must be formed by at least two nodes (i.e., one segment) so that the surface segment normal and tangential vectors n and $n_r$ can be calculated.
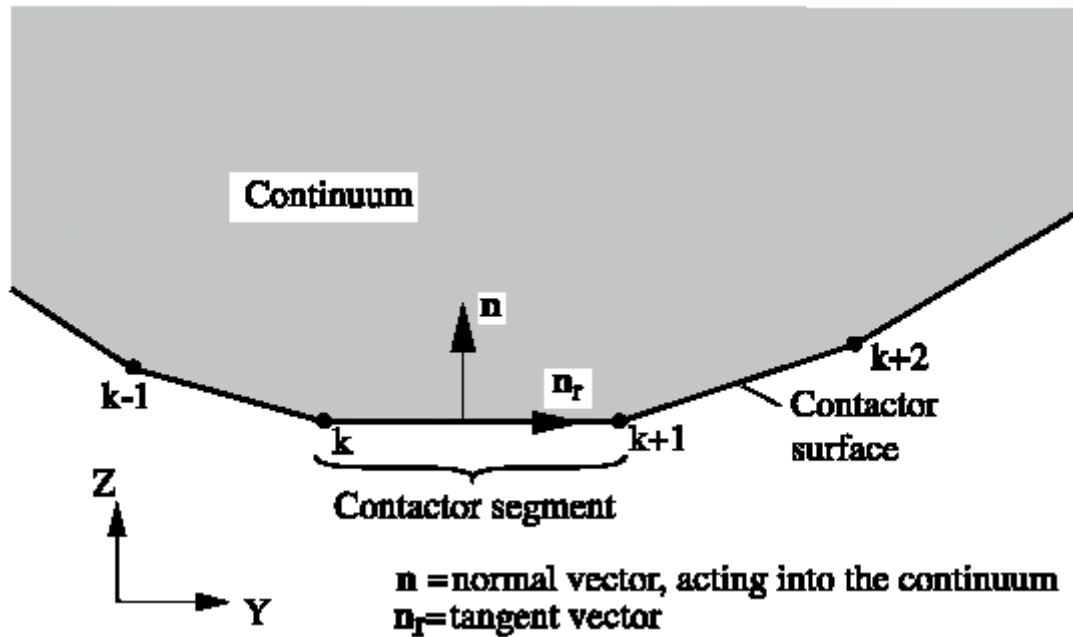
**Figure 4.3** Normal and Tangential Vectors of a Contactor Segment in 2-D Analysis. (*ADINA Modeling Guide 2000)*

### 4.4.1  Material Modeling

Different types of materials are available through ADINA material library such as elastic, plastic, viscoelastic, creep and concrete. Two different material types are defined in this analysis, the specimen and the mold. The mold is defined as an elastic isotropic material with high young's modulus ($2x10^{11}$ N/m$^2$) to prevent any lateral deformation developed from the confining pressure. The Poisson ratio is taken 0.3 as a typical value for metal. For asphalt specimen, since the infinitesimal deformation at each gyration occurs during the compaction, the behavior of the specimen can be practically assumed to be quasi-elastic behavior at each gyration. The specimen subject to constant vertical stress induced a decrease in the strain as the gyrations increased. The elastic properties were set to values such that the vertical deformation in the model is very close to the measured deformation value.

## 4.4.2  Boundary Conditions

In order to model the asphalt specimen as effectively as possible and simulate the effect of vertical pressure and lateral displacement, appropriate boundary conditions were applied to the model; all the nodes at the bottom of the specimen were restrained in the Y and Z-directions. As well as the lower node of each beam elements at the lower left and lower right edges. The top fiber of the specimen is set free to move in the Y-Z plane, to allow both vertical deformation and horizontal displacement from the actuators movement. The fixity at the bottom of the beam element occurs due to the attachment to the mold carrier, which prevents lateral displacement and vertical movement. (Figure 4.4)

Two different types of loading were applied to the model, first a uniform constant pressure at the top of the specimen with magnitude $6x10^5$ N/m$^2$. The load was applied directly in a period of one second. A lateral displacement was also applied at the top of the mold to simulate the motion in the gyratory compactor. The lateral deformation was determined such that the vertical inclination angle is equal to the angle of gyration. A detailed model with the element types, boundary conditions, and loading is presented in Figure 4.4. In this figure the solid line between the specimen and the mold indicates the position of friction line while the direction of the arrows is perpendicular to the relative movement of the friction direction. The character "B" indicates the boundary condition at the bottom fiber, which prevents the displacement $u_2$, $u_3$, while $u_2$ is the displacement in the Y-direction, and $u_3$ is the displacement in the Z-direction. The specimen is represented by 10X10 2-D solid elements. The prescribed lateral displacement is acting at the top of the beam elements, which is responsible for applying the angle of gyration. Another vertical pressure uniformly distributed along the top fiber is also presented.

Figure 4.5 show the distribution of the shear stress $\tau_{yz}$ along the all height at two different deformation values. The average of the shear stress is taken at the middle height and middle width far from the effect of boundary contact. This value is compared next with the shear stress calculated in chapter three. Figure 4.5**c** shows the distributions of the Z-displacement and the contact force along the boundary with the beam elements.

### 4.4.3  Analysis and Results

The 2-Dimensional model is used to determine the shear stress at the middle height of a specimen under the same loading and boundary conditions that exist in the gyratory compactor. A parametric study is conducted in order to calculate the shear stress at different pressure and angle values and compare with the numerical results to those calculated in chapter three. The parametric study includes changing the pressure (450, 600 and 750 kPa) and angle values (0.75, 1.50, 2.25 and 3.00°). The elastic properties are determined such that the vertical deformation in the model is equal to the measured value. The vertical deformation is averaged for each four gyrations. **Figure 4.6** (**a-h)** show the relationship between the shear stress derived mathematically using equation (3-11) and the finite element results.

The results as shown in Table 4.1 indicate that measurement are matching with a tolerance not exceeding than ±10%, for all cases at small number of gyrations (less than 19 gyrations), However the 2-D finite element model represents higher shear stresses than measurements at a number of gyrations higher than 19.

**Figure 4.4** 2-Dimensional Model with Boundary Conditions
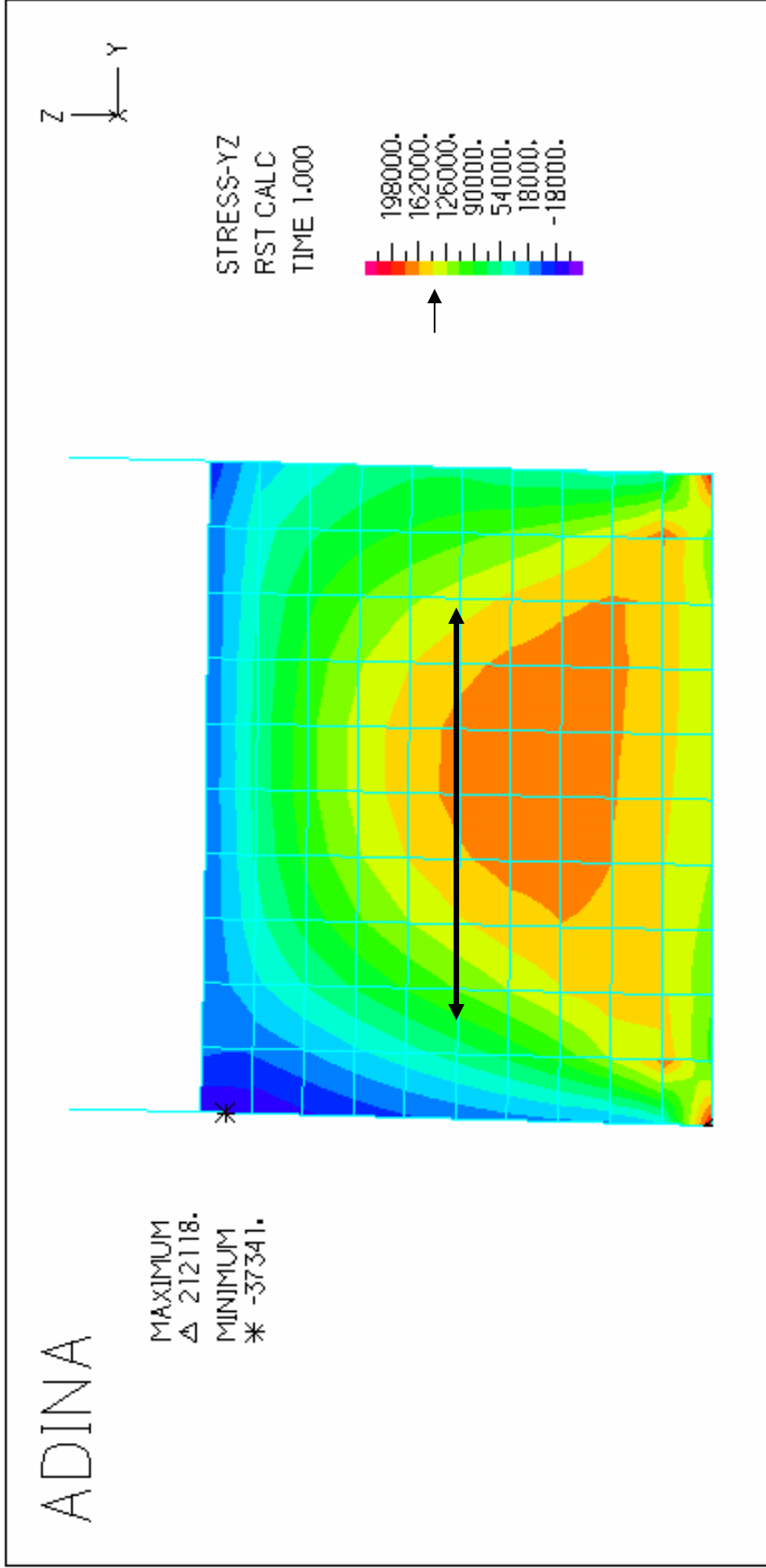
**Figure 4.5a.** Shear Stress Distribution for a Deformation of 1.97 mm
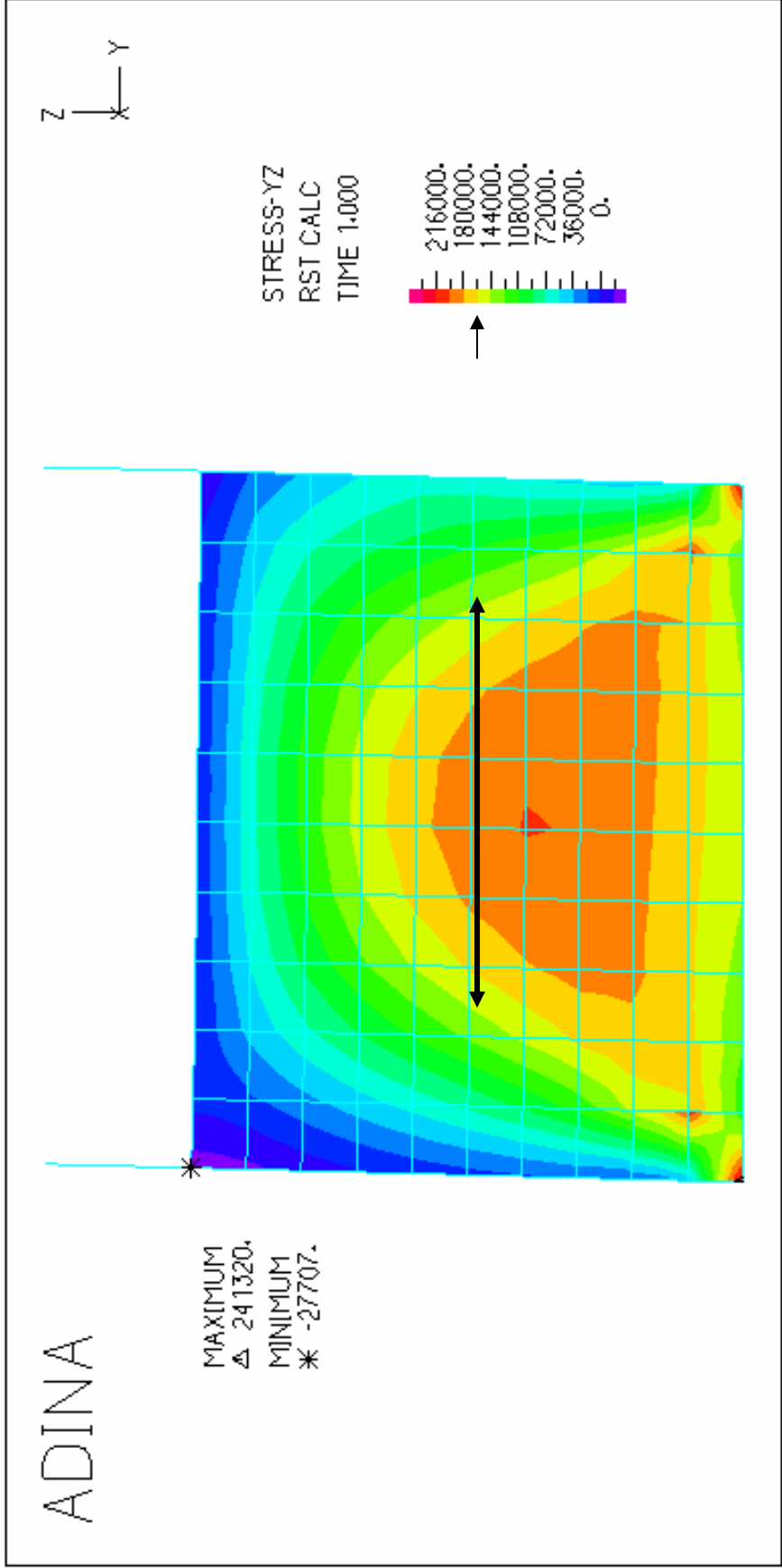
**Figure 4.5b.** Shear Stress Distribution for a Deformation of 1.74 mm
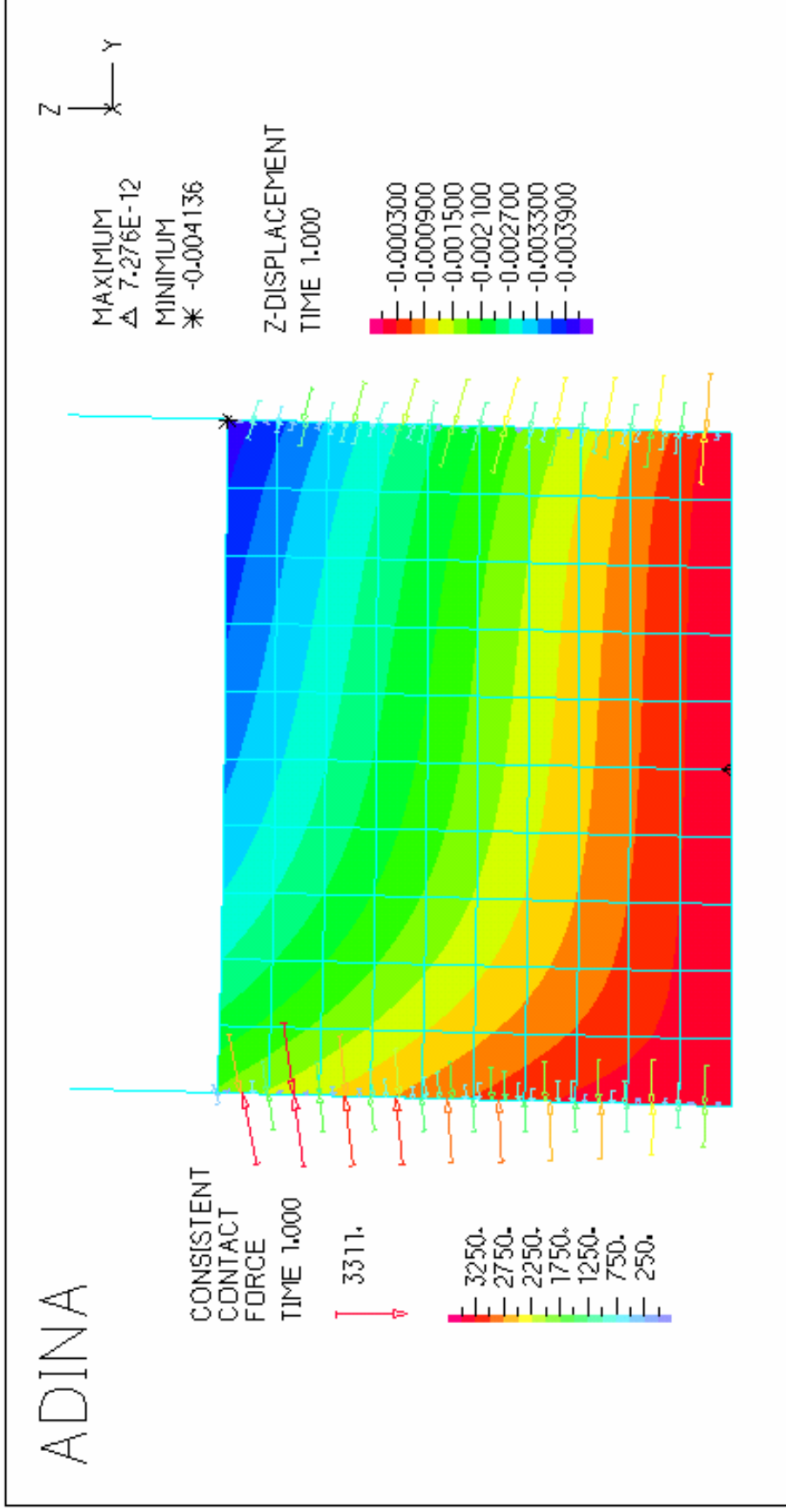
**Figure 4.5c.** Layout of the Vertical Displacement and Contact Force Distribution

Figure 4.5(a, b & c): Shear Stress Distribution for a Deformation of 1.97 mm & Layout of the Vertical Displacement and Contact

Force Distribution
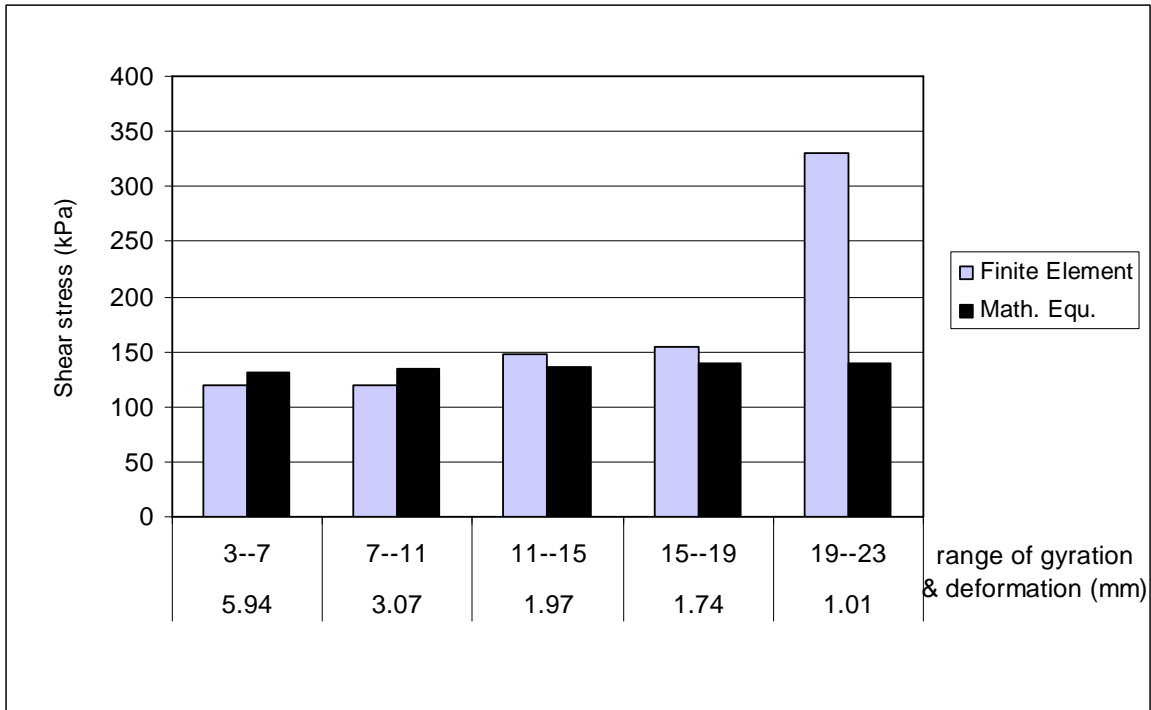
**Figure 4.6a**. Shear Stress Derived at Compaction with Pressure= 600 kPa and angle θ=1.50°
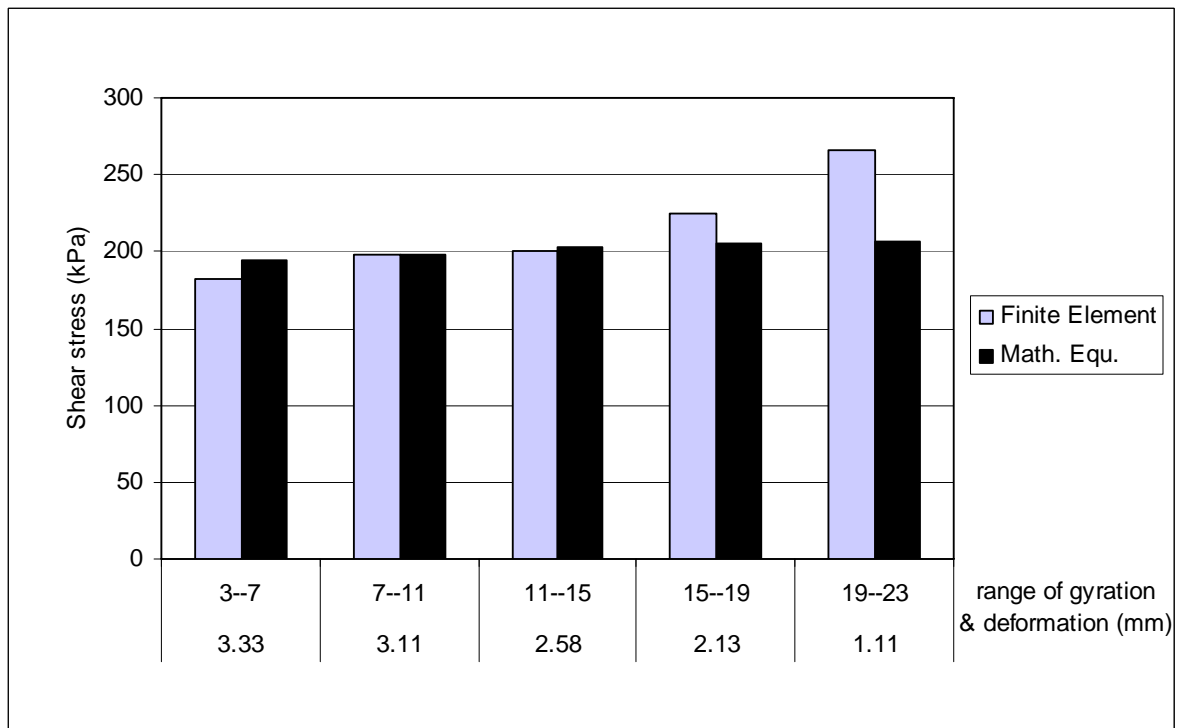


**Figure 4.6b**. Shear Stress Derived at Compaction with Pressure= 600 kPa and angle θ=2.25°
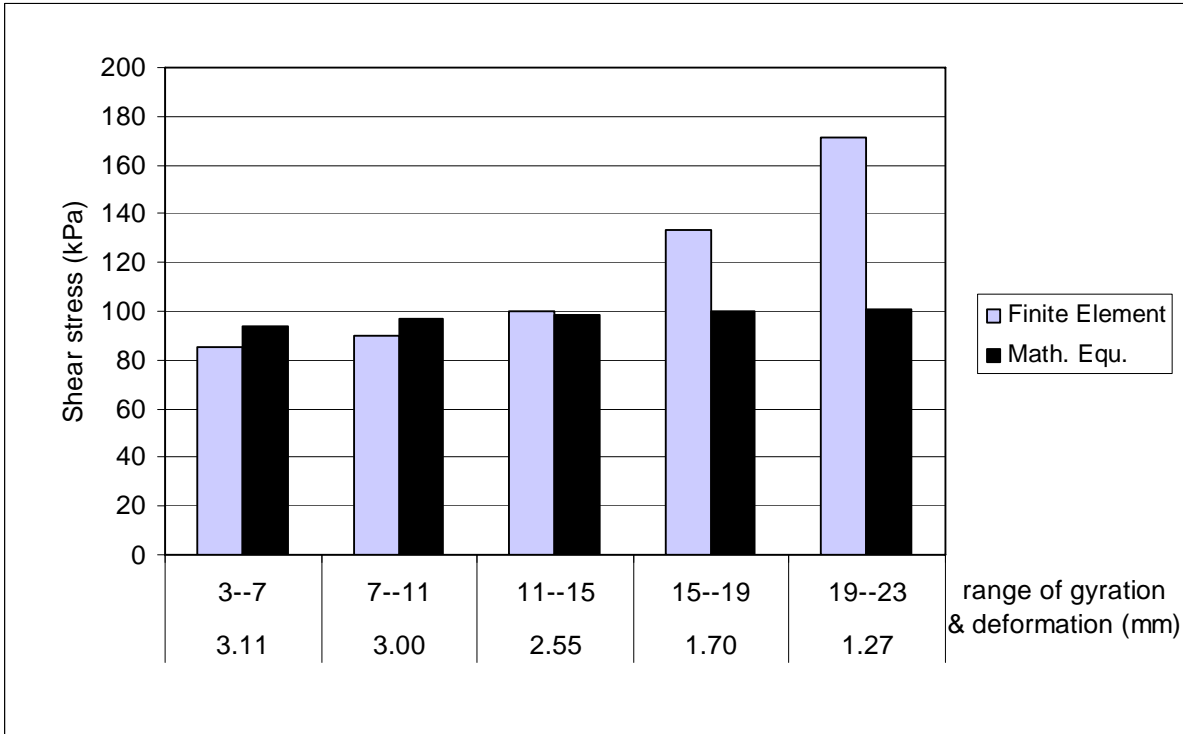
**Figure 4.6c**. Shear Stress derived at Compaction with Pressure= 450 kPa and angle $\theta$=1.50°
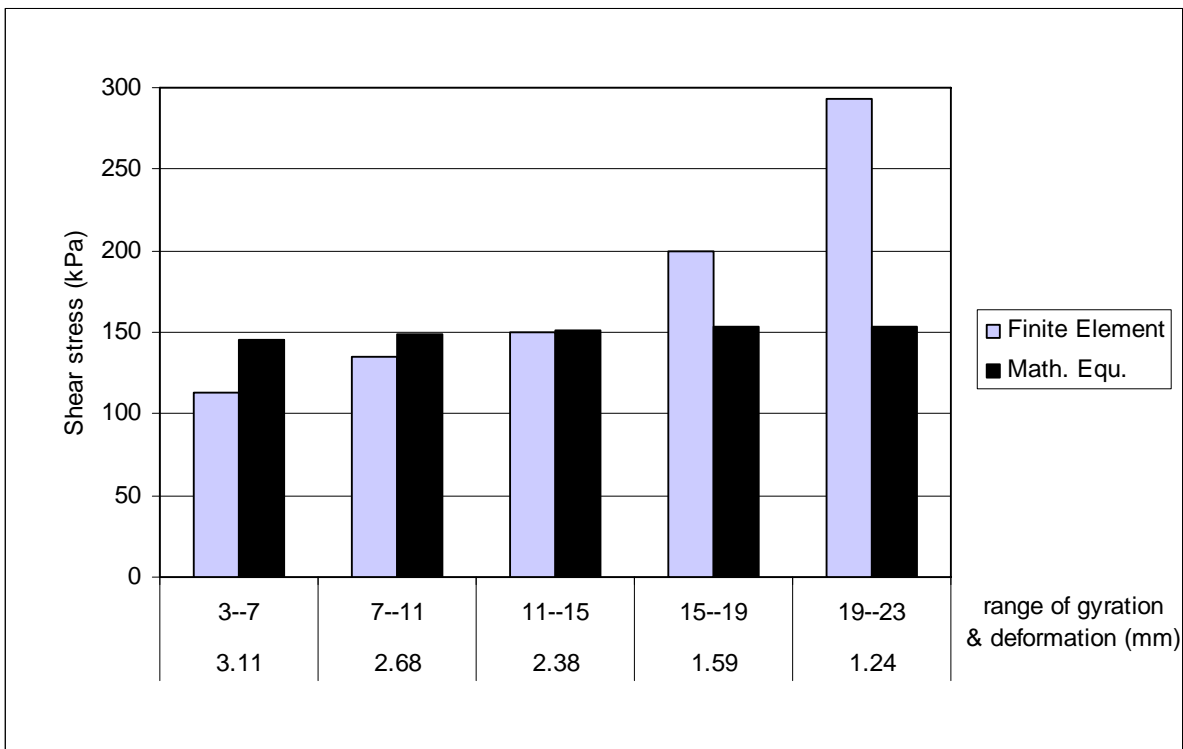


**Figure 4.6d**. Shear Stress Derived at Compaction with Pressure= 450 kPa and angle $\theta$=2.25°
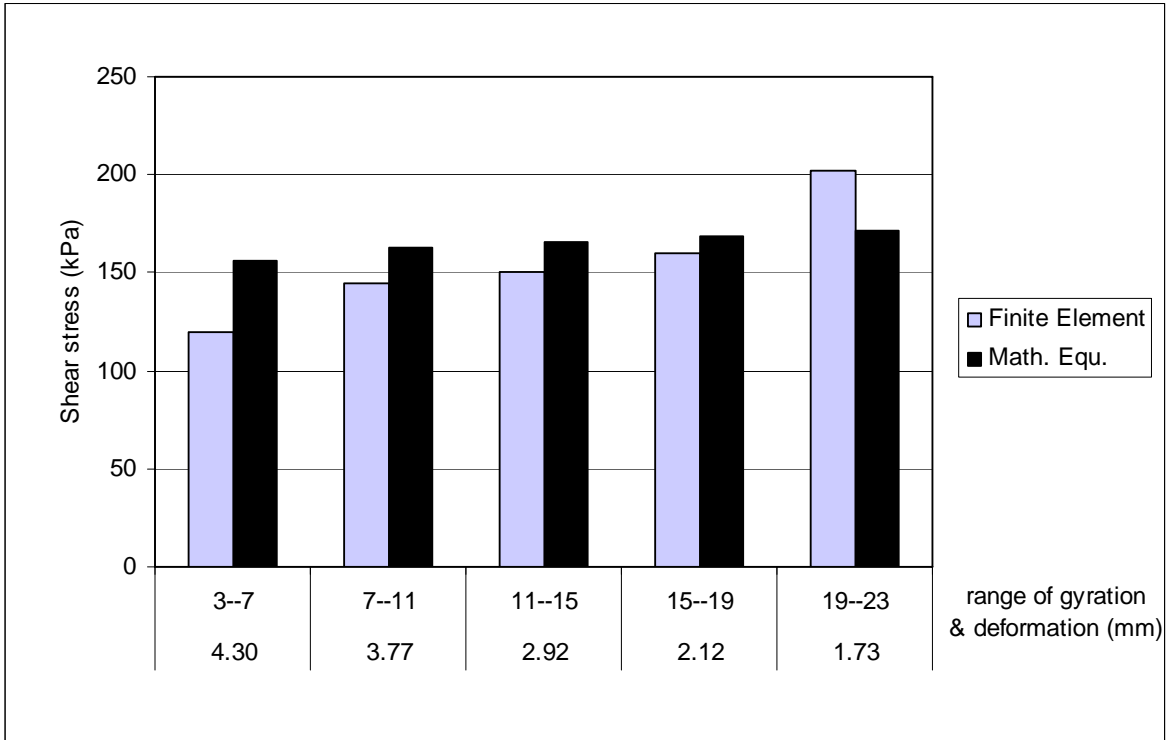
**Figure 4.6e**. Shear Stress Derived at Compaction with Pressure= 750 kPa and angle θ=1.50°
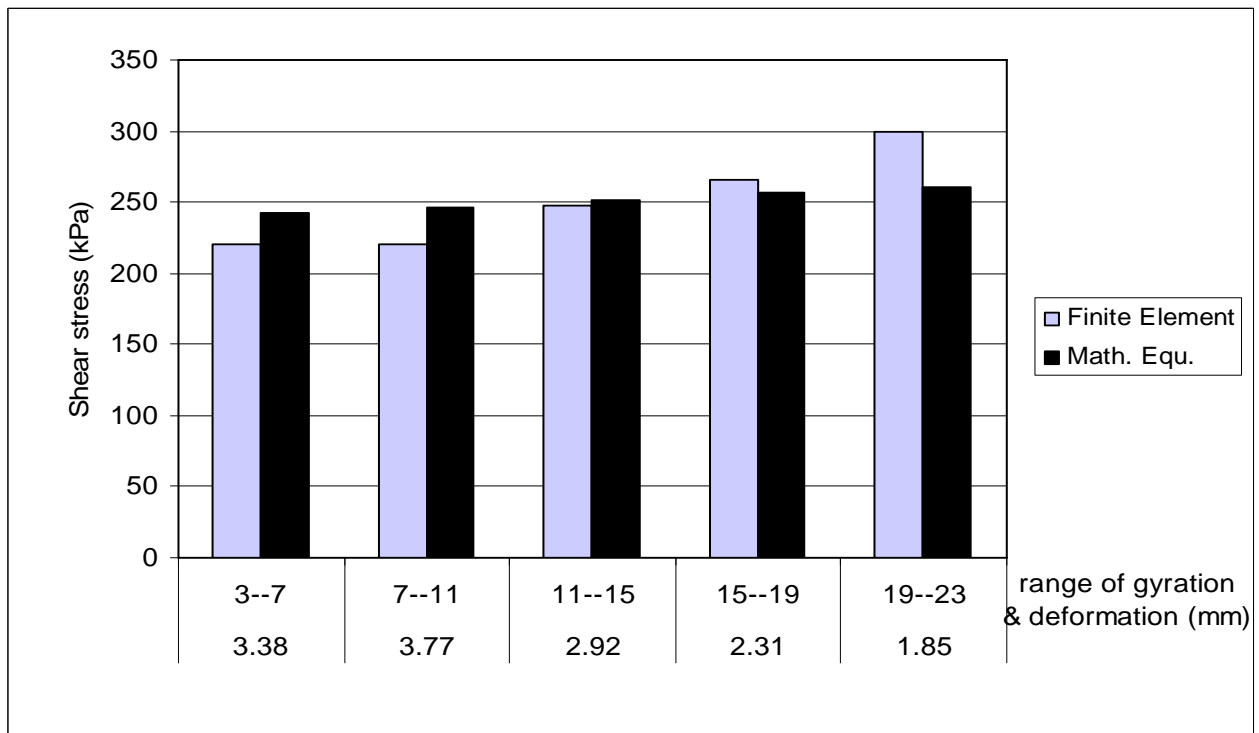


**Figure 4.6f**. Shear Stress Derived at Compaction with Pressure= 750 kPa and angle θ=2.25°
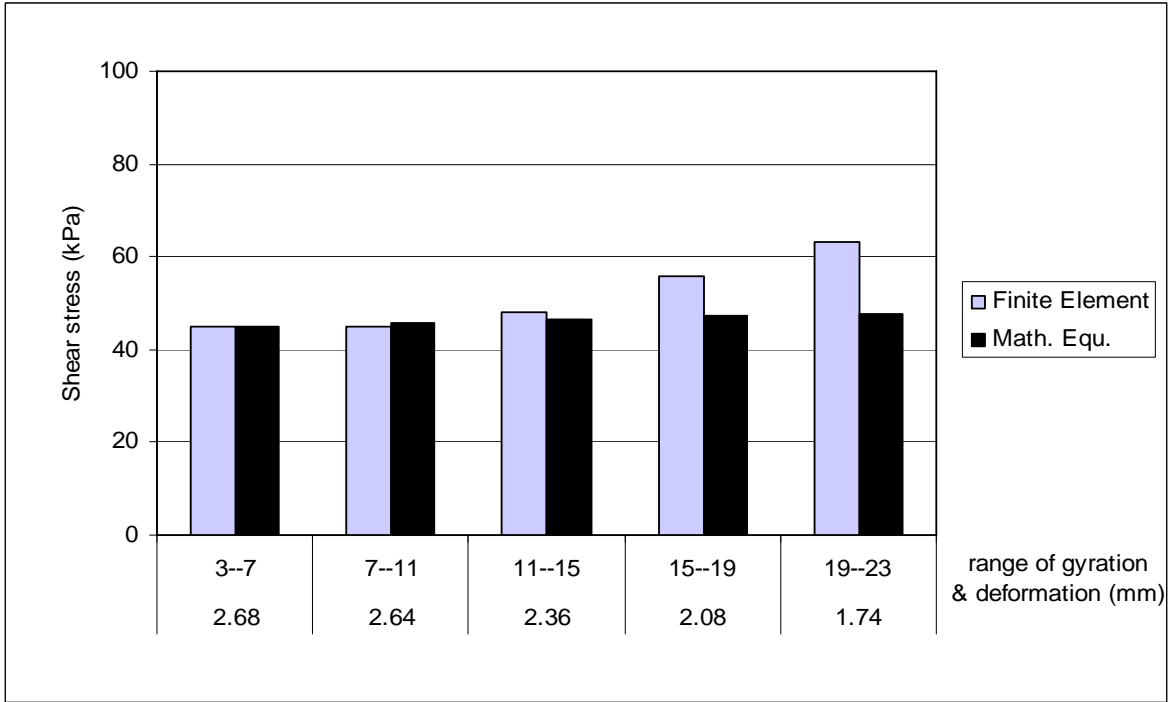
**Figure 4.6g**. Shear Stress Derived at Compaction with Pressure= 450 kPa and angle θ=0.75°
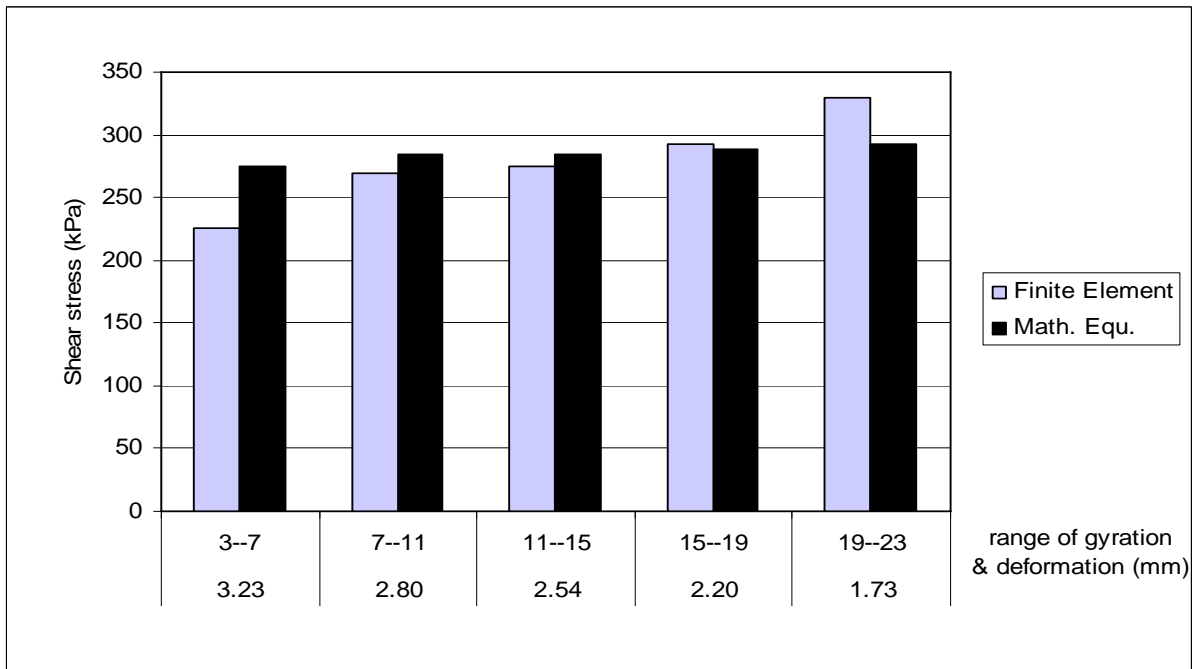


**Figure 4.6h**. Shear Stress Derived at Compaction with Pressure= 600 kPa and angle θ=3.00°

**Figure 4.6(a-h):** Shear Stresses Derived at Compaction with different combinations of contact pressure and angle of Gyrations

**Table 4.1** The Tolerance in Determining the Shear Stress Mathematically Versus the Finite Element

| VI. deformation (mm) | gyration range | Finite Element | Math. Equ. | % error |
|---|---|---|---|---|
| Compaction @ pressure= 600 kPa and angle θ=1.50 | | | | |
| 5.94 | 3--7 | 120.00 | 130.71 | -8.19 |
| 3.07 | 7--11 | 120.00 | 134.68 | -10.90 |
| 1.97 | 11--15 | 147.60 | 136.86 | 7.85 |
| 1.74 | 15--19 | 154.72 | 138.59 | 11.64 |
| 1.01 | 19--23 | 330.00 | 139.68 | 136.25 |
| Compaction @ pressure= 600 kPa and angle θ=2.25 | | | | |
| 3.33 | 3--7 | 182.5 | 194.24 | -6.04 |
| 3.11 | 7--11 | 198 | 198 | 0.00 |
| 2.58 | 11--15 | 200 | 203 | -1.48 |
| 2.13 | 15--19 | 225 | 205 | 9.76 |
| 1.11 | 19--23 | 266 | 206 | 29.13 |
| Compaction @ pressure= 450 kPa and angle θ=1.50 | | | | |
| 3.11 | 3--7 | 85 | 94 | -9.57 |
| 3.00 | 7--11 | 90 | 97 | -7.22 |
| 2.55 | 11--15 | 100 | 98.51 | 1.51 |
| 1.70 | 15--19 | 133 | 99.62 | 33.51 |
| 1.27 | 19--23 | 171 | 100.43 | 70.27 |
| Compaction @ pressure= 450 kPa and angle θ=2.25 | | | | |
| 3.11 | 3--7 | 113 | 145.2 | -22.18 |
| 2.68 | 7--11 | 135 | 149 | -9.40 |
| 2.38 | 11--15 | 150 | 151.5 | -0.99 |
| 1.59 | 15--19 | 200 | 153 | 30.72 |
| 1.24 | 19--23 | 293 | 154 | 90.26 |
| Compaction @ pressure= 750 kPa and angle θ=2.25 | | | | |
| 3.38 | 3--7 | 220 | 242 | -9.09 |
| 3.77 | 7--11 | 220 | 246.87 | -10.88 |
| 2.92 | 11--15 | 247.5 | 252 | -1.79 |
| 2.31 | 15--19 | 266 | 257 | 3.50 |
| 1.85 | 19--23 | 300 | 260 | 15.38 |
| Compaction @ pressure= 750 kPa and angle θ=1.50 | | | | |
| 4.30 | 3--7 | 120 | 156 | -23.08 |
| 3.77 | 7--11 | 145 | 162.54 | -10.79 |
| 2.92 | 11--15 | 150 | 166 | -9.64 |
| 2.12 | 15--19 | 160 | 169 | -5.33 |
| 1.73 | 19--23 | 202.5 | 171 | 18.42 |
| Compaction @ pressure= 450 kPa and angle θ=0.75 | | | | |
| 2.68 | 3--7 | 45 | 44.81 | 0.42 |
| 2.64 | 7--11 | 45 | 45.7 | -1.53 |
| 2.36 | 11--15 | 48 | 46.4 | 3.45 |
| 2.08 | 15--19 | 56 | 47.2 | 18.64 |
| 1.74 | 19--23 | 63 | 47.6 | 32.35 |
| Compaction @ pressure= 600 kPa and angle θ=3.00 | | | | |
| 3.23 | 3--7 | 225 | 275 | -18.18 |
| 2.80 | 7--11 | 270 | 284.5 | -5.10 |
| 2.54 | 11--15 | 275 | 285 | -3.51 |
| 2.20 | 15--19 | 293 | 289.07 | 1.36 |
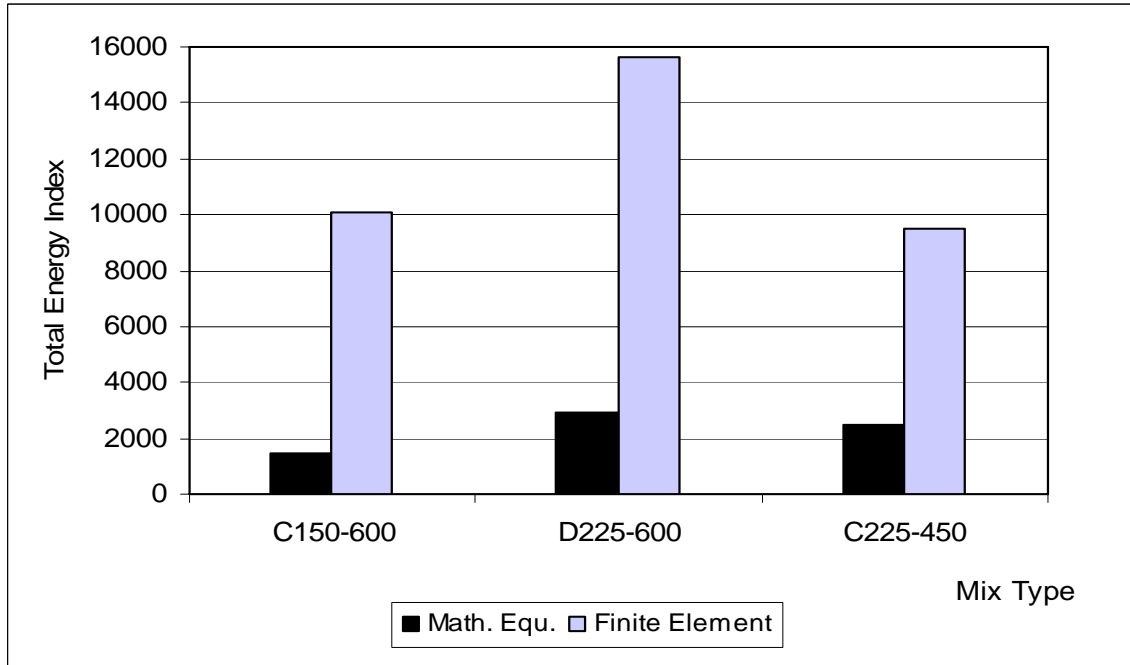
**Figure 4.7a**. Determination of the Total Energy Index in the Finite Element
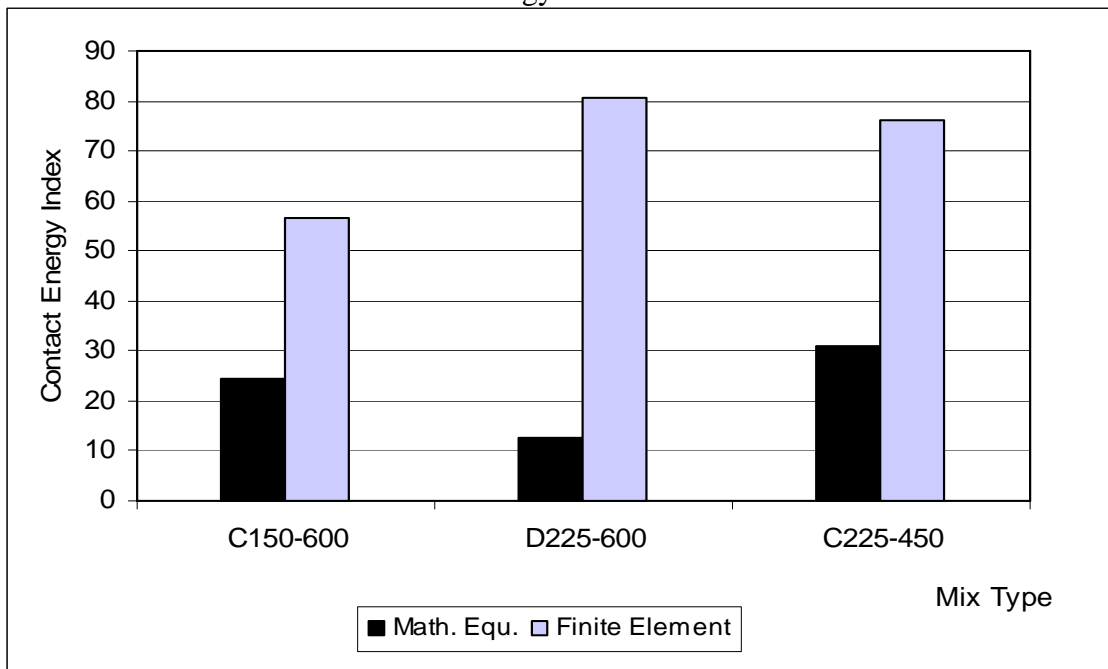


**Figure 4.7b**. Determination of the Contact Energy Index in the Finite Element

**Figure 4.7 (a, b):** Determination of the Total and Contact Energy Indicies in the Finite Element

## 4.5 3-DIMENSIONAL FINITE ELEMENT MODEL

This section discusses the development of a 3-D finite element model. The model in this case was similar to the real shape of the mold with the attachment components including actuators and hinges, which are responsible of the gyratory motion. A three-solid that has 4-nodes was used in this model. Figure 4.8.

Figure 4.8 **4-node Tetrahedral Element. (*ADINA Modeling Guide***
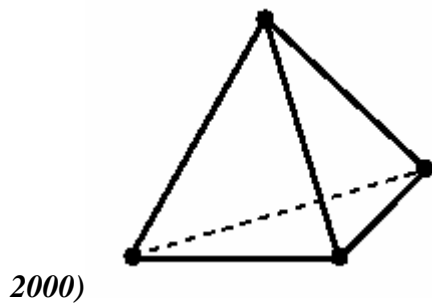


*2000)*

**Figure 4.8** 4-node Tetrahedral Element. (*ADINA Modeling Guide 2000*)

The mold was modeled as a hollow cylinder with thickness of 1 cm, height of 25 cm and internal diameter of 15 cm, attached by a mold carrier consists of another hollow cylinder (ring) of internal diameter of 16 cm and height of 5 cm. The mold carrier is connected to three spheres 120° apart with diameter of 1 cm as represented in Figure 4.9. All these parts are attached together to construct one body. Also, rings that surround the spheres similar to the gyratory actuators are modeled. These rings are responsible for applying the force on the spheres as shown graphically in Figure 4.10. The specimen was modeled as a disc element (solid cylinder) of diameter 15 cm, placed inside the hollow cylinder which the lower face is 2 cm apart form the cylinder bottom face, the 2 cm is reserved for the lower plate. The model including all the elements and the attached parts is shown in Figure 4.11.

Notice that the rigidity of the top platen that transfers the vertical pressure to the specimen is responsible for the uniform and constant displacement at the top of the specimen at each gyration. This is considered in the model by using the constraint equation option available in ADINA. This equation ensures that all points in the plate move the same value in Z-direction as shown in Figure 4.12.
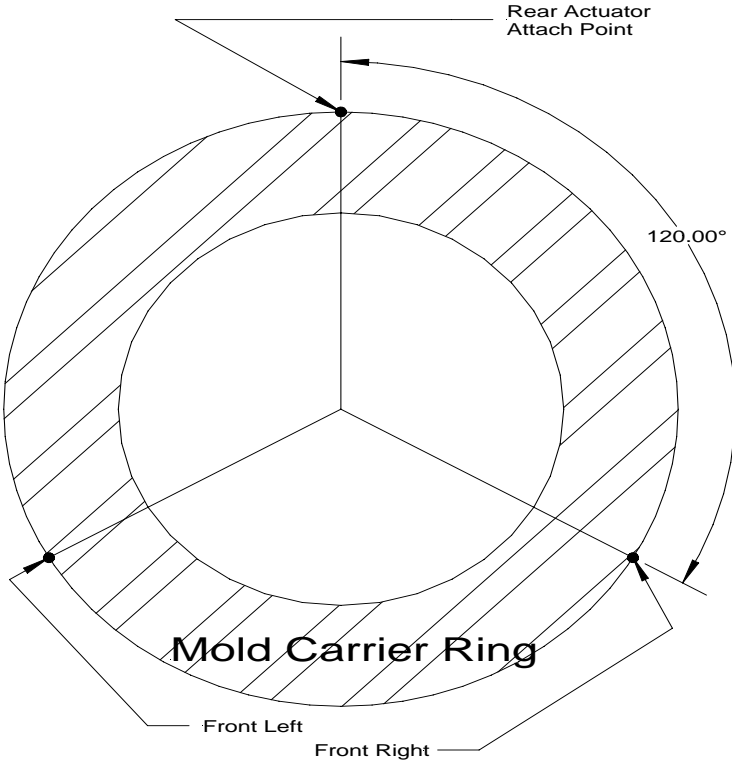


**Figure 4.9**. The Mold Carrier with the Attaching Spheres (Actuator Positions).
(IPC PTY LTD 1996)
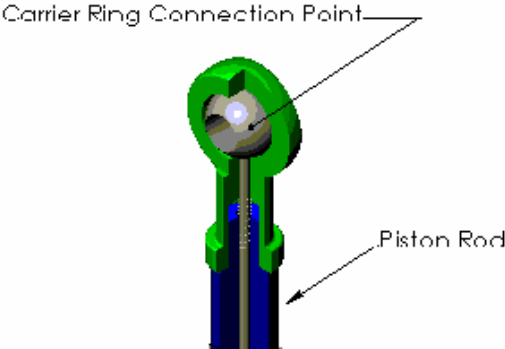
**Figure 4.10**. The Sphere Surrounding by the Fixed Ring (Actuator Assembly).

(IPC PTY LTD 1996)

ADINA

PRESCRIBED
PRESSURE
TIME 1.000

600000.

PRESCRIBED
DISPLACEMENT
TIME 1.000

0.004300

$U_1 \; U_2 \; U_3 \; \theta_1 \; \theta_2 \; \theta_3$
B ⟋ ⟍ - - - -
C - - - - - -
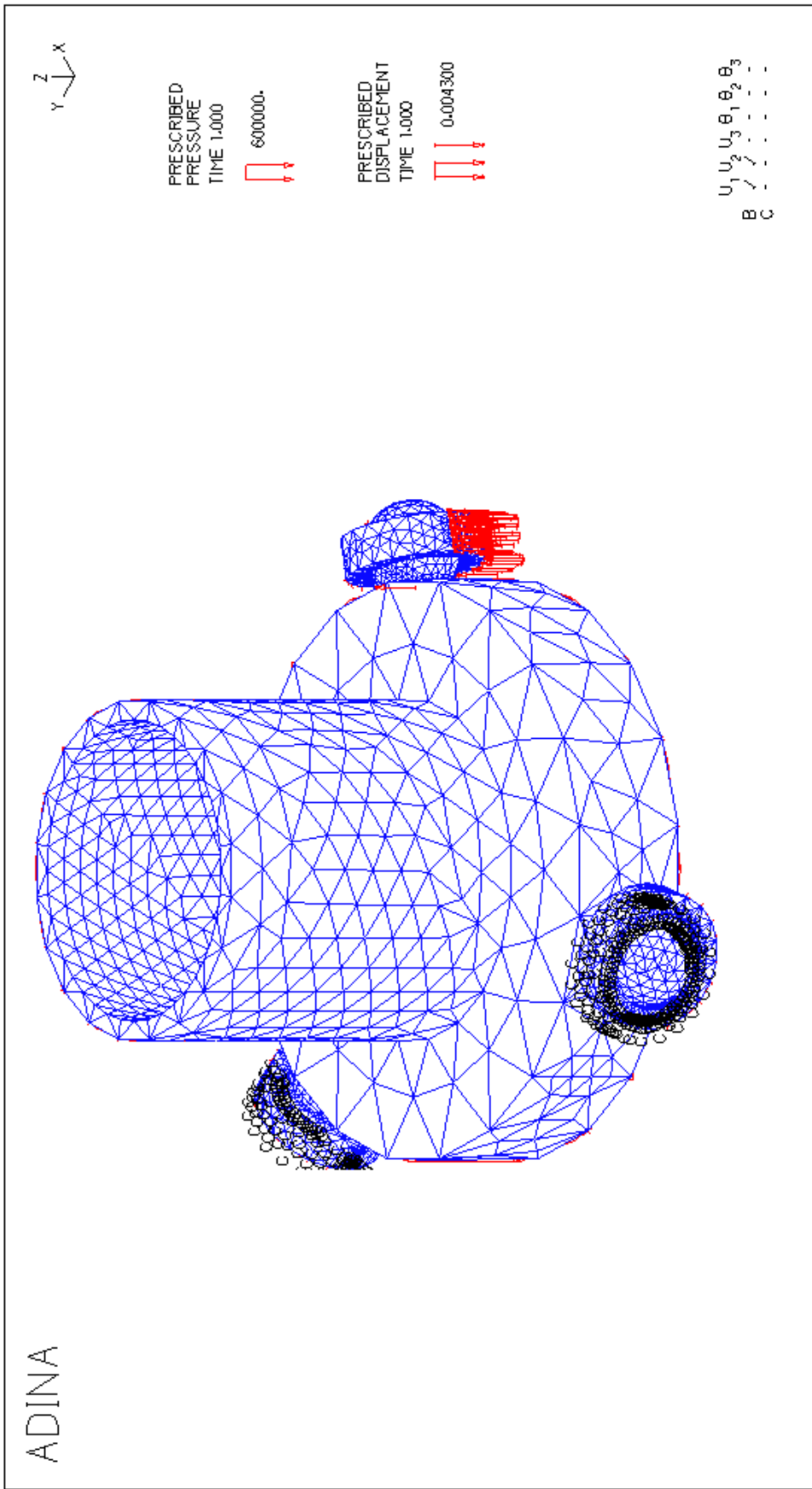
**Figure 4.11.** 3-Dimensional Model with the Loading and Boundary Conditions
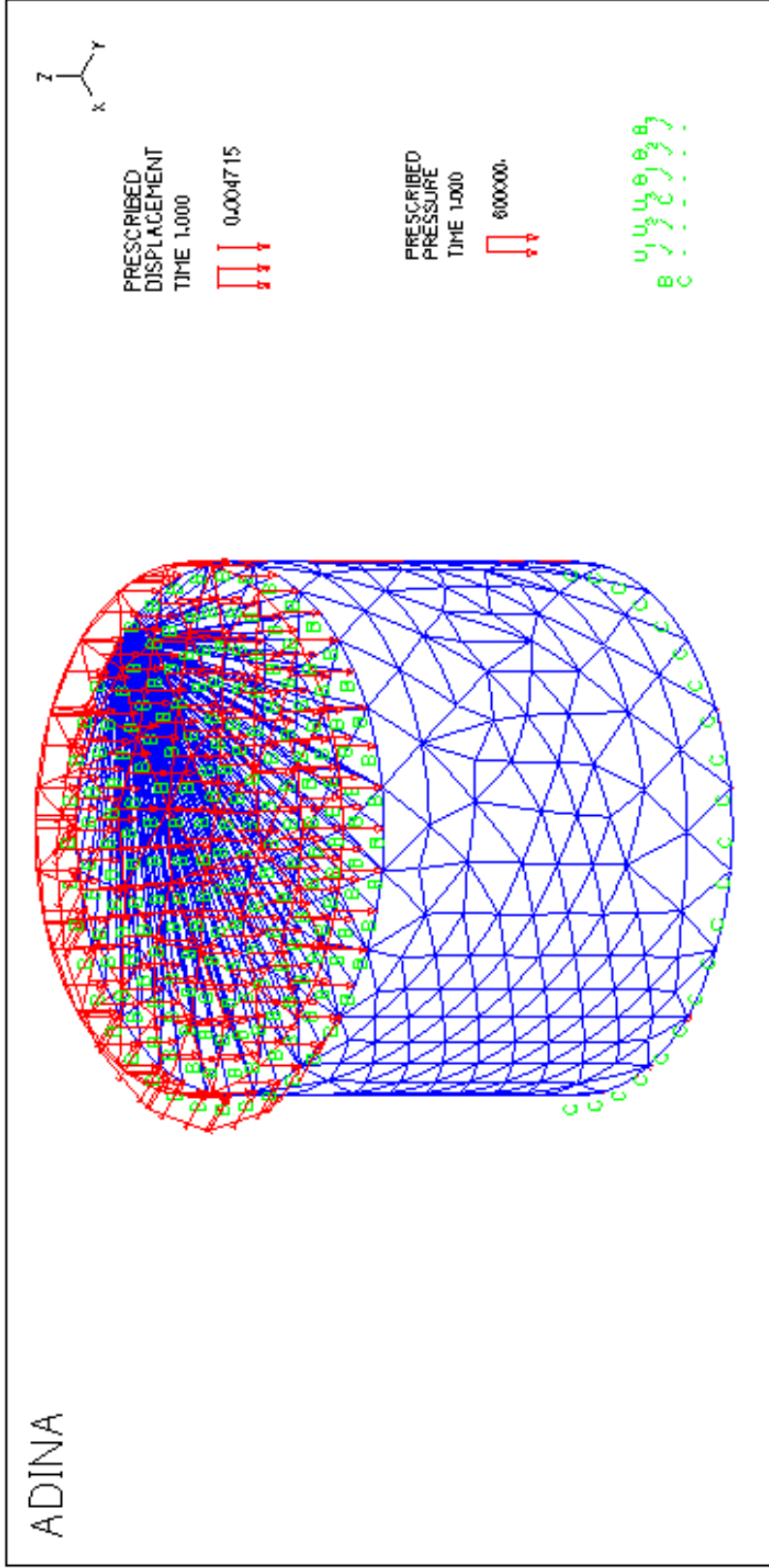
**Figure 4.12. 3-Dimensional Model in Cross Sectional View Describes the Boundary Conditions.**
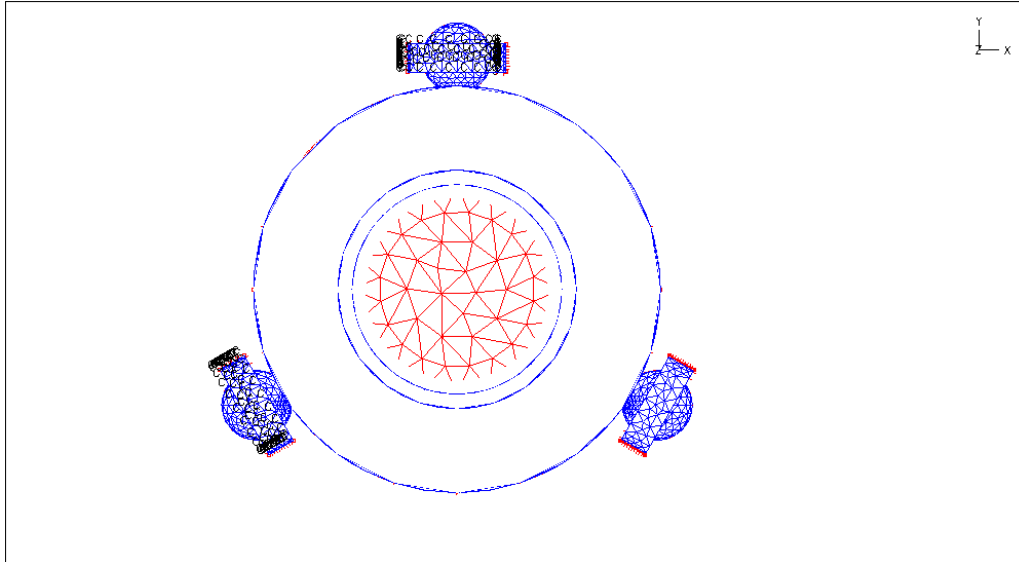
**A:**. 3-Dimensional Model in Plan View.
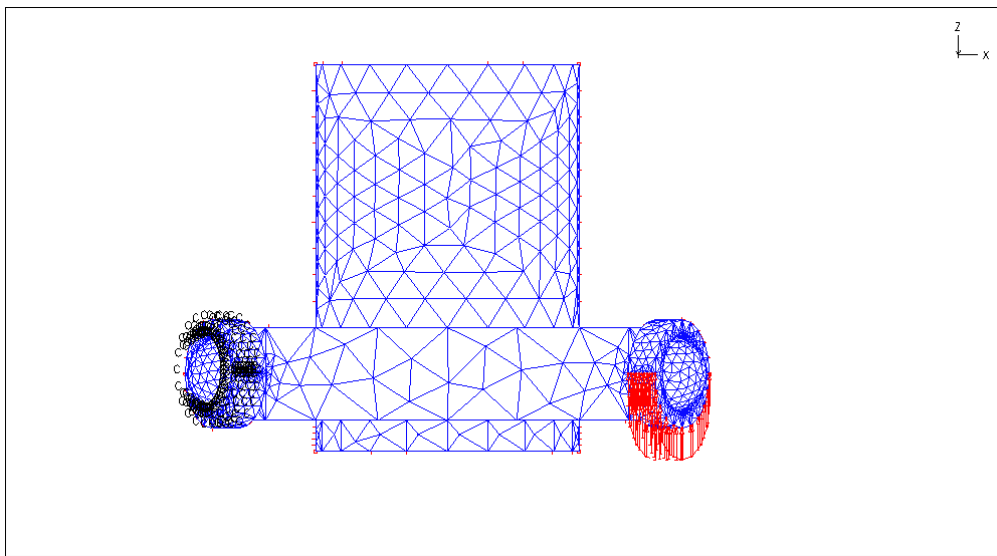


**B:** 3-Dimensional Model in Side View

Figure 4.13: 3-Dimensional Model in Plan and SideView.

Figure 4.13 show the model in different views to describe the element connectivity. The

interaction between the specimen and the steel mold was modeled by defining contact surface

along the boundaries, with the characteristic of not tied element to allow the relative movement

of specimen with no penetration. The frictional plane was defined here between the specimen

boundary and the internal surface of the mold. Each two faces attached together composed

"contact pair", the contactor in this case is the specimen (deformable) and the target is the mold.

The nodes given on the frictional plane were constrained not to penetrate into the target surface.

Another frictional plan was defined between the spheres and the surrounding rings. The friction

factor μ at the spheres was taken 0.80 for stability purpose, and around the specimen was 0.28.

The contact between the surfaces causes the development of shear stress and normal pressure.

These tractions are considered in a local basis system defined by the normal to the contacting

surfaces, n and two shear components r and s. (

Figure 4.14)



3-D contact surface
segment (area = A)

N3

N4

N2

r

n

s

N1

Normal to the segment
at (r = 0, s = 0)

Segment contact force = F
(integration of segment tractions)

Average normal traction = $[(F \cdot n)n]/A$

Average tangential traction = $[F - (F \cdot n)n]/A$
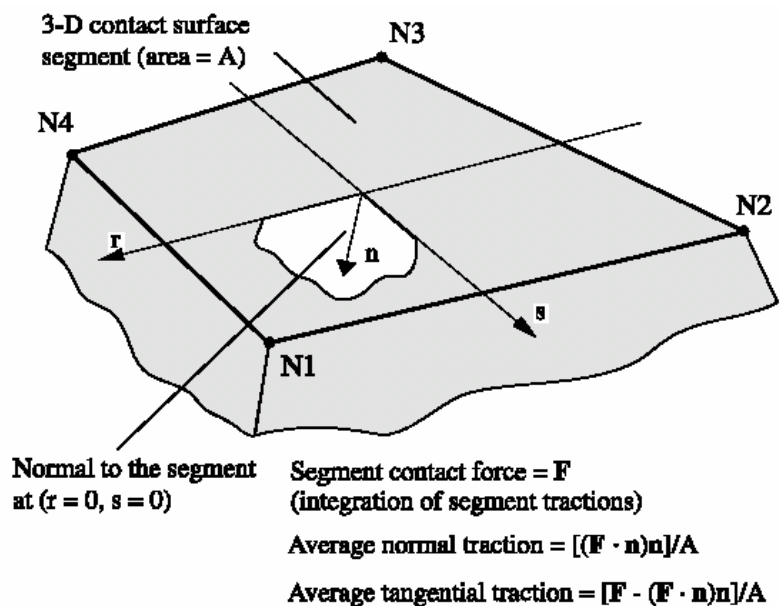
Figure 4.14 Calculation of Average Normal and Two Tangential Tractions for a Contactor Segment. (*ADINA Modeling Guide 2000*)

### 4.5.1  Material Modeling Properties

The model is defined similar to the 2-D in which the mold is an elastic isotropic material with modulus of elasticity ($2 \times 10^{11}$ N/m$^2$) to prevent any lateral deformation developed from the confining pressure, with the poisson ratio defined for metal (0.3). The elastic properties are determined such that the vertical deformation in the model is equal to experimental measurement. The Poisson's ratio is set to be constant with a value of 0.35.

### 4.5.2  Boundary Conditions

The displacement field consists of six components $u_1$, $u_2$, $u_3$, $\theta_1$, $\theta_2$ and $\theta_3$ defined for each element in the model instead of two components only in the 2-D $u_1$, $u_2$. Two types of fixity are defined in the 3-D model; the first one at the lower face of the specimen, which has only two displacement components in the X-Y plane $u_1$ and $u_2$ while the other components are zero as indicated by the character "B" in Figure 4.11. The second fixity was defined at the rings, which holds the whole body. The fixity was defined only at two rings and the third kept free in order to apply the angle of gyration as indicated by the character "C".

Two different types of loading were applied on the model. The first was a uniform constant pressure at the top face of the 3-D solid element (specimen) with magnitude $6 \times 10^5$ N/m$^2$, and direction downward. At the meantime, a vertical displacement acting upward was applied at one of the rings with no fixity to induce the angle.

### 4.5.3  Analysis and Results

The average shear stress measurement was taken around the specimen centeroid away from the edges. Typical shear stress distribution at the middle height is shown in Figure 4.15. The rectangle shape illustrates the calculated area of stresses. The variability in stresses around the edges can be seen in Figure 4.15. The analysis was carried out using different angles and pressures, angles of 1.50°, 2.25°, and pressures 450, 600 kPa for two different mixes. The shear stress results are shown on **Figure 4.16** and examples of the comparison between the 3-D FE results and experimental measurement for mixes at different angles, pressures are shown in Figure 4.17.

The results from ADINA show the same trend of shear stress with the mathematical formula, at a wide range of gyrations. In addition, the energy indices determined by the Finite element are much closed to the mathematical formula. Figure 4.17.
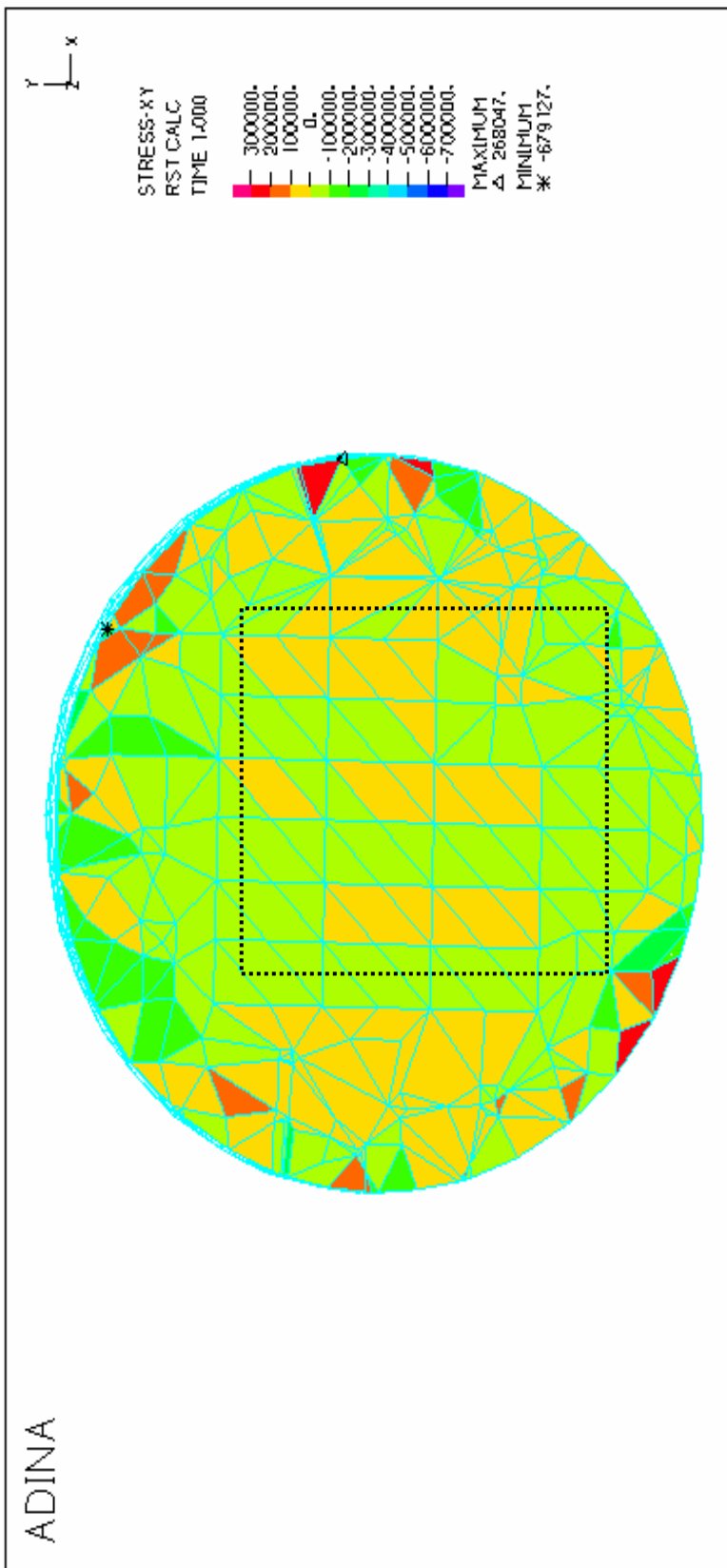
**Figure 4.15**. Shear Stress Calculating Area in the 3-D Model
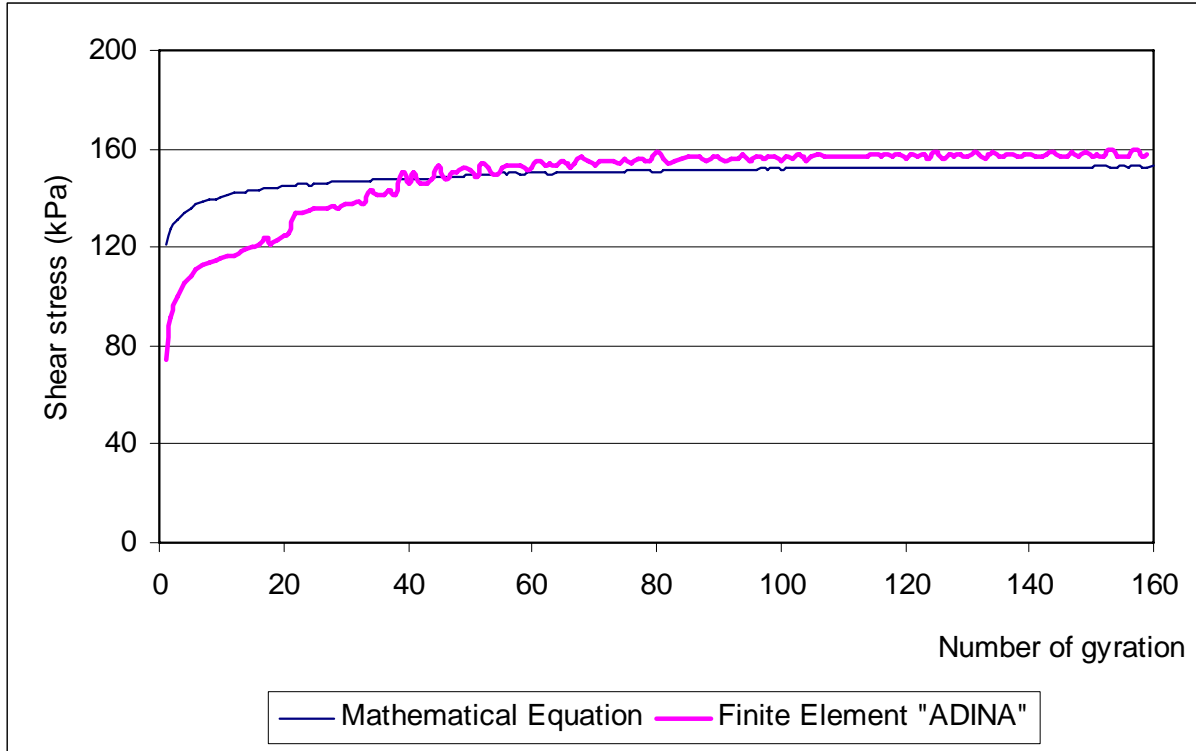
**Figure 4.16a**. Mix "C" under 600 kPa and 1.50° Angle of Gyration
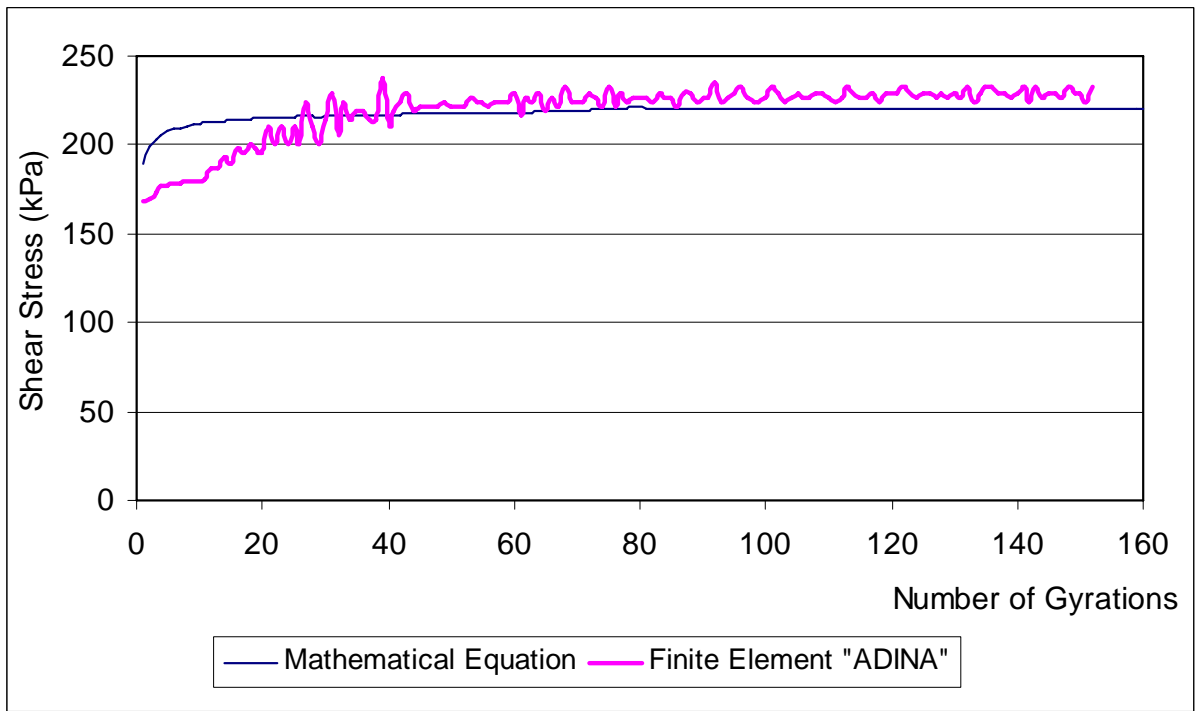


**Figure 4.16b**. Mix "D" under 600 kPa and 2.25° Angle of Gyration

102
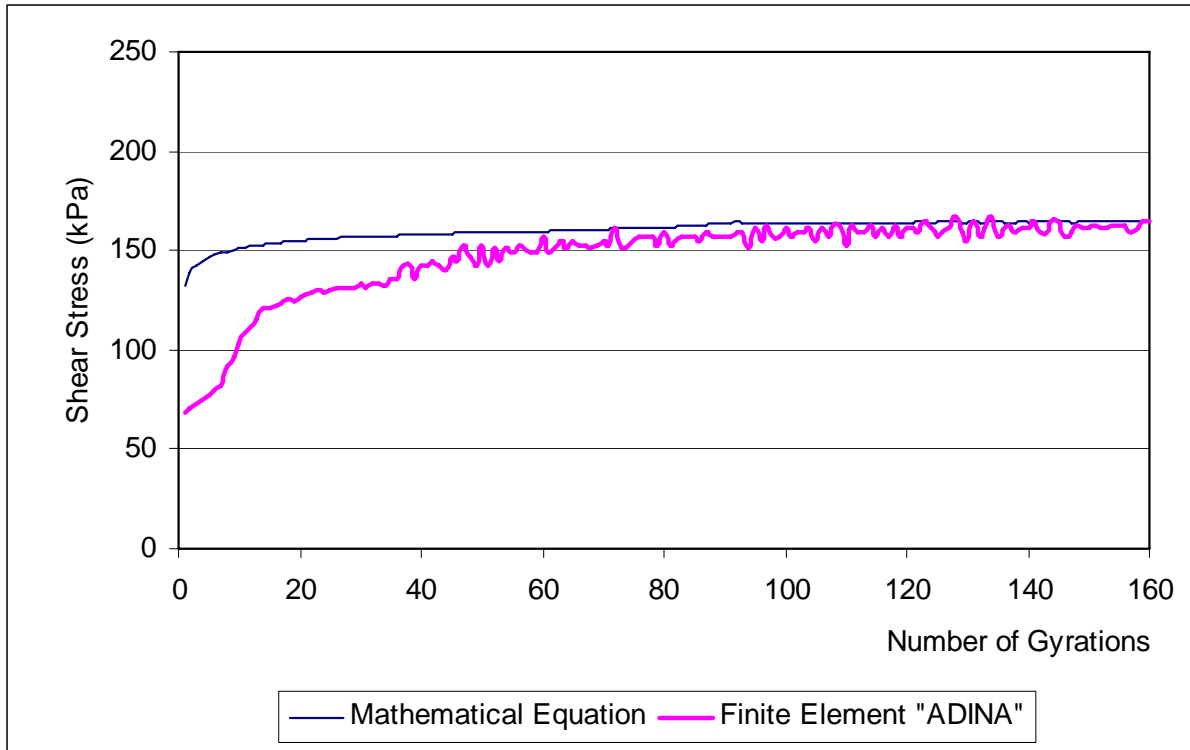
**Figure 4.16c**. Mix "C" under 450 kPa and 2.25° Angle of Gyration

**Figure 4.16 (a-c): Mixes "C" and "D' under different pressures and Angle of Gyration**

**Table 4.2** Energy Indices Values Derived From the Mathematical
Equation and the Finite Element

|  | Math. Equ. | Finite Element | Math. Equ. | Finite Element |
|---|---|---|---|---|
|  | TEI | TEI | CEI | CEI |
| C150-600 | 1458.568 | 1481.533 | 24.588 | 25.657 |
| D225-600 | 2943.882 | 3021.562 | 12.798 | 13.064 |
| C225-450 | 2495.676 | 2353.072 | 31.073 | 27.54 |

## 4.6  SUMMARY

A finite element model was introduced to model an asphalt specimen under compaction process

in the gyratory compaction. Two and three-dimensional models were developed to express the

shear stress distribution and compare it with the mathematical formula. The 2-D model showed

close results with the shear stress equation only at the early gyrations. However, the 3-D model

showed better correlations with measurements of the shear stress and energy indices at all

gyration.
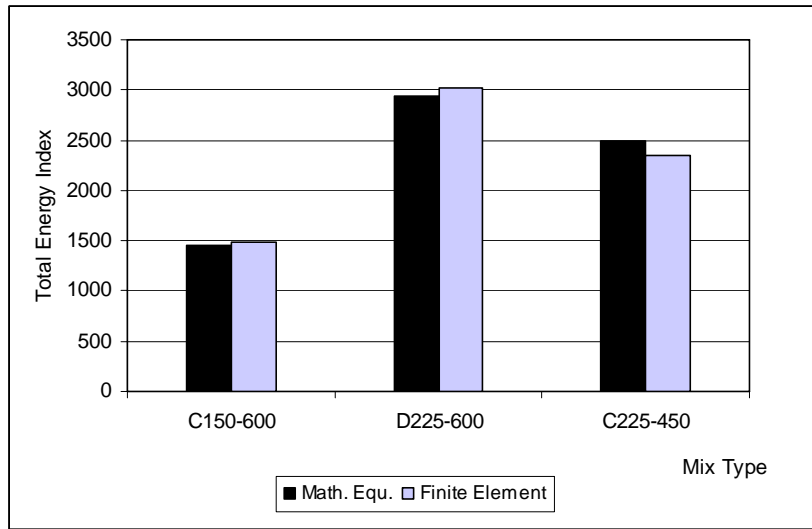


**Figure 4.17a**. Determination of the Total Energy Index in the Finite Element
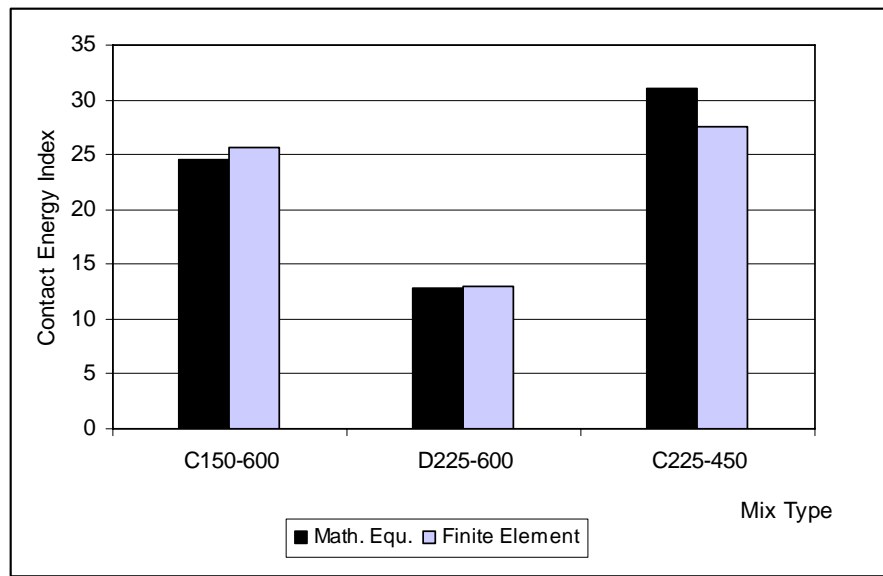


**Figure 4.17b**. Determination of the Contact Energy Index in the Finite Element

Figure 4.17(a& b): Determination of the Total & Contact Energy Indices in the Finite Element

# 5. THE ROLE OF INTERNAL STRUCTURE IN ASPHALT MIX STABILITY

## 5.1 INTRODUCTION

This chapter presents the results of analyzing the internal structure of asphalt mixes using image analysis techniques. The main objective is to demonstrate the influence of the aggregate orientation and contacts on the mix stability and shear strength. The mixes are similar to the ones analyzed in chapters 3 and 4. The image analysis results are compared with the shear stress measurements and energy indices developed in chapter 3.

## 5.2 IMAGE ANALYSIS METHODOLOGY

### 5.2.1 Image Analysis System

The image analysis system used in this study to characterize the internal structure of asphalt concrete consisted of the following devices and software: (1) An image processing and analysis program (Image Pro Plus 4.1, 1998), developed by Media Cybernetics founded in 1981. Image Pro Plus software was used to develop automated procedures for quantifying the internal structure of asphalt concrete. "Image Pro Plus has a built in language, IPBasic, which is a sub-programming language of Visual Basic, IPBasic language facilitates writing macros to automate the procedures and make it user friendly" noted by *Tashman (2001)*. (2) Pixera Visual Communication Suite, which consists of a digital camera and a program which displays a live image of the camera's field of view (Pixera, 1997). The program controls the camera with resolution selection, image manipulation, and capture capability. (3) A Windows NT based computer system with 128 MB RAM.

### 5.2.2  Image Analysis Techniques

Image analysis technique is the process of converting an image into a digital form and applying various mathematical procedures to extract significant information from the image. Recently *Masad et al. (1998, 1999a and b, Tashman 2001)* have developed computer automated image analysis techniques to analyze the internal structure of asphalt concrete. The techniques were successfully implemented to evaluate different laboratory compaction procedures. Image analysis technique involves three major steps: image acquisition, image processing, and image analysis illustrated as following. (*Tashman 2001)*:

**1- Image acquisition:** All the mixes were cut vertically with a diamond saw. A specimen was fastened between two clamps as it was advanced toward a rotating saw. The cutting speed was kept at a slow rate to improve the smoothness of the surface to acquire quality images. Each specimen was cut into two vertical sections as shown in Figure 5.1. Then two images were captured from the two faces of each cut- that is a total of four images per specimen. This is the most important step. A good image will produce accurate results with limited image processing and enhancement techniques.

**2- Image processing:** Each vertical section was placed under a live digital camera from which the image was captured by the computer. The live image appearing in the computer screen was used to visually aid in positioning and focusing the image and optimizing the light conditions to produce quality image. The camera lens was adjusted for focus and sensitivity before the final image was retained for analysis. Image processing is used for two different reasons, improving the visual appearance of images to human viewer, and preparing images for measurements of the features and structures present. Good Image processing does not reduce the amount of data
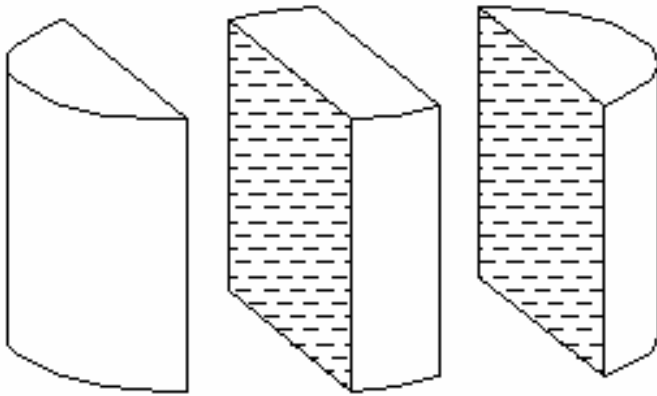
**Figure 5.1** An Asphalt Specimen After Cutting in Two Vertical Sections

presented but simply rearranges it. Some arrangements may be more appealing to the senses, while others may preserve more quantitative information. (*Russ, 1999)*

**3- Image analysis:** this step involves analyzing the processed image to get the required measurements. The measurement of images generally requires that features be well defined. Defining the features to be measured frequently requires image processing to correct acquisition defects, enhance the visibility of particular structures, threshold them from the background, and perform further steps to separate touching objects or select those to be measures. The types of measurements that will be performed on entire scenes or individual features are important in determining the appropriate processing steps. An image of a gyratory cut section was first captured under the digital camera (Pixera, 1997). The digital image was then saved in TIF format. The saved digital image is a true color image that has "RGB 24" class. RGB 24 class stands for Red Green Blue image with 24-bits size of each pixel. The true color RGB 24 image was converted to a "Gray Scale 8" image. Gray Scale 8 image is the most common for two

reasons: 1) its 1-byte-per pixel size (1 byte=8bits) makes it easy to manipulate with a computer which speeds up the processing, 2) it can faithfully represent any gray scale image because it provides 256 distinct levels of gray (the human eye can distinguish less than 200 gray levels). Gray Scale pixel values represent a level of grayness or brightness, ranging from completely black to completely white. In an 8-bit Gray Scale image, a pixel with a value of 0 is completely black, and a pixel with a value of 255 is completely white. After the image has been converted to a "Gray Scale 8", the intensities were equalized using the "Best Fit" equalizer. This will optimize the values of the image by stretching the intensity histogram to achieve the best possible contrast distribution of pixels values in the image. Best Fit assigns the bottom 3% of values to the shadow point (0), and the top 3% of the values to the highlight point (255). The rest of the values are distributed evenly across the scale. This makes the objects (aggregates) more distinguishable and easier to capture. "Watershed" filter was applied to separate the aggregates. The Watershed filter erodes the aggregates until they disappear, then dilates them again, but will not allow them to touch. At this point, the aggregates in the image were separated and ready to be analyzed. Figure 5.2.

**Figure 5.2**: Bilevel Image Obtained by Thresholding Gray Scale 8 Image

## 5.3   INTERNAL STRUCTURE PARAMETERS

The effects of aggregate contacts and orientation on their shear strength properties have been established by many studies in the past (e.g. *Oda 1972 and 1977, Tashman 2001*). Consequently, it would be of interest to measure aggregate orientation and contacts using image analysis techniques. This section discusses the parameters used in this study to represent the internal structure of gyratory compacted specimens and their relationship with the shear strength. More details about these parameters are given by *Tashman (2001)*.

### 5.3.1 Aggregate Orientation

The orientation of an aggregate is measured by the angle between its major axis and a horizontal line on the scanned image. The major axis length is defined by the greatest distance between two pixels of the boundary contour. Using the orientation of individual aggregates, the vector magnitude, $\Delta$ can be calculated to quantify the directional distribution of aggregates:

$$\text{Vector Magnitude}\,(\Delta) = \frac{100}{N}\sqrt{\left(\sum \sin 2\theta_k\right)^2 + \left(\sum \cos 2\theta_k\right)^2} \quad (\%) \qquad (5.1)$$

where $\theta_k$ is the orientation of an individual aggregate on an image from -90o to +90o measured from the horizontal direction, the positive sign indicates that the angle is measured counterclockwise from the horizontal direction. N is the number of aggregates on that image. The value of $\Delta$ varies from zero percent to 100 percent. Complete random distribution of the orientation will give a vector magnitude of zero percent. On the other hand, 100 percent of vector magnitude value means that all observed orientations have exactly the same direction.

*5.3.2 Aggregate Contacts*

To obtain the number of contacts, the image is first converted to a bi-level image, i.e.
black and white image using an automatic threshold value (T). The second step is separating the
aggregates in contact using a "Watershed Filter". The Watershed filter erodes the aggregates
until they disappear then dilates them again. The image is then inverted and a "Thinning Filter"
is applied to the inverted image, which reduces the image to its skeleton.  The resultant image
consists of segments of lines representing the regions of contacts of aggregates**.** These lines are
counted as the number of contacts. **(**Figure 5.3**)**

## 5.4   ANALYSIS AND RESULTS

Specimens from nine mixes A, C, D, E, G, I, K, L and O were compacted to 160 gyrations using
an angle $1.5^o$ and a pressure of 600 kPa.  The vector magnitude and number of contacts were
measured on these specimens and recorded in **Table 5.1**.

Table 5.1 The Values of the Quantifying Parameters of Aggregate Structure and Energy Indices**.**

| Mix | Vector Magnitude | Contacts/m$^2$ | TEI | CEI |
|:---:|:---:|:---:|:---:|:---:|
| C | 28.20 | 48782.35 | 1315.44 | 24.2 |
| D | 25.83 | 20373.76 | 1306.94 | 9.82 |
| K | 22.88 | 78746.01 | 1432.65 | 29.03 |
| L | 24.14 | 32180.49 | 1283.52 | 10.45 |
| A | 29.50 | 72429.41 | 1402.89 | 25.8 |
| G | 32.11 | 73383.30 | 1238.65 | 28.2 |
| I | 27.55 | 75322.26 | 1348.73 | 24.49 |
| O | 29.30 | 76300.46 | 1428.27 | 20.58 |

*(a)* Original Bilevel image

*(b)* Separating the aggregates by "Watershed Filter".

*(c)* Applying "Thinning Filter" reduces the image to its skeleton.

*(d)* Lines of contacts.
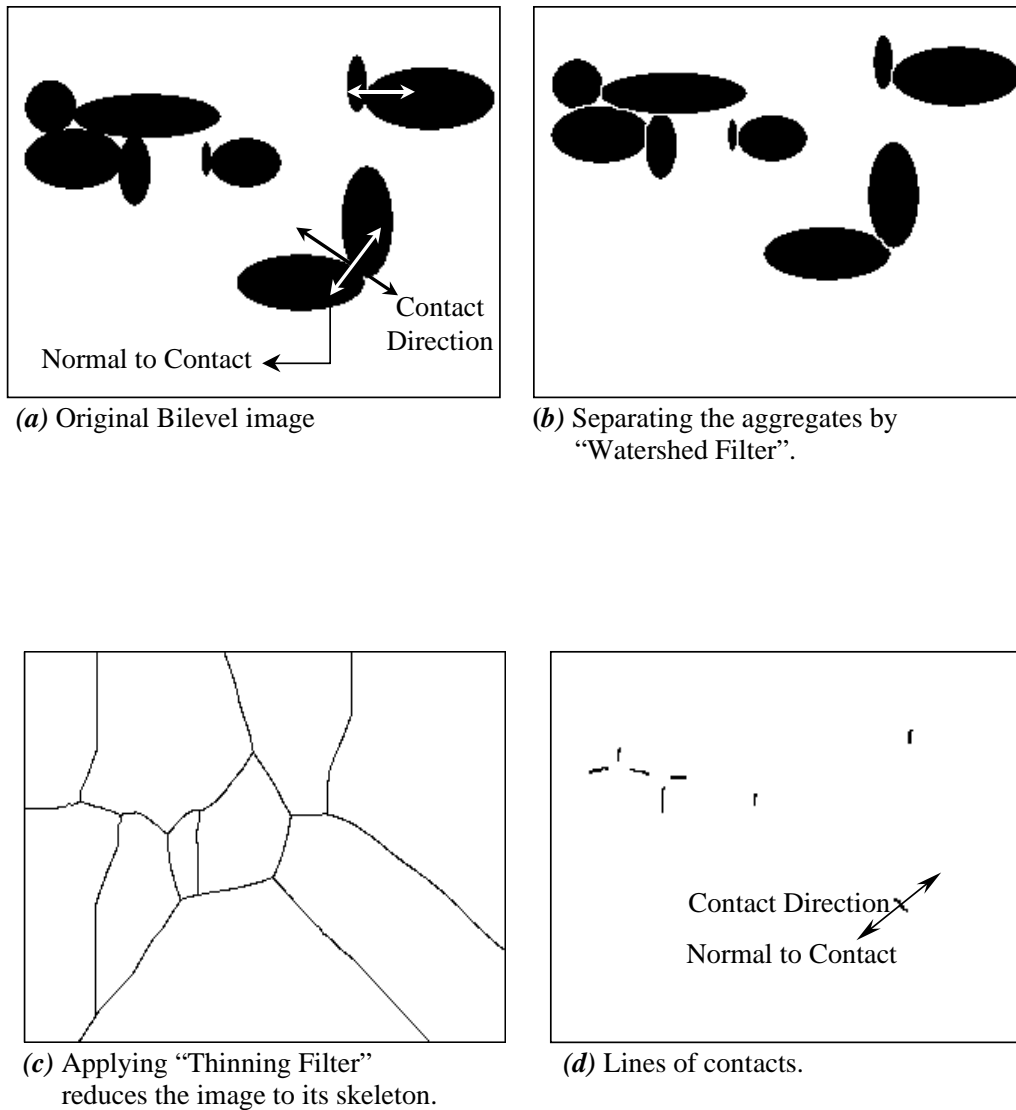
**Figure 5.3**: Illustration of the Image Analysis Procedure for Measuring Aggregate Contacts. *(Tashman 2001)*

Examples of images from some of these mixes are shown in

Figure 5.4. These values are compared with the contact energy index and total energy index as

shown in **Figure 5.5 –5.8**. The relationship between the contact energy index and vector

magnitude is shown in **Figure 5.5**. Except for mix K, there is a very good relationship between the vector magnitude and the contact energy index. **Figure 5.5**b shows that the correlation improved from $R^2$ of 0.17 to 0.77 when mix K is excluded from the analysis. **Figure 5.6** shows that very small correlation, if any, exists between the vector magnitude and the total energy index. These results are consistent with the findings in chapter 3 that the contact energy index is better than the total energy index in capturing the performance of asphalt mixes. The relationship in **Figure 5.7** shows very good correlation between the number of contacts and the contact energy index. However, poor correlation exists between the total energy index and number of contacts as shown in Figure 5.8.

The influence of binder content was studies using mixes A, C, G, L and I. The results are shown in Figure 5.9. As it can be seen that all mixes except mix G, an increase in the binder content caused an increase in the vector magnitude. This is can be attributed to the fact that the excess binder content works as a lubricant that facilitates aggregate orientation and yields higher vector magnitude. The influence of the aggregate type on the internal structure is investigated using specimens from mixes C, D, K, and L. Some specimens were compacted up to the maximum shear stress, while the others were compacted to 160 gyrations. Examples of images captured from these specimens are shown in

Figure 5.4. The vector magnitudes at the two levels of compactions are shown in Figure 5.10. It is evident from this figure that the mixes with limestone had higher vector magnitude at 160 gyrations compared with the gravel mixes (C vs. K, and D vs. L). Also, the difference in vector magnitude between the maximum shear stress and 160 gyrations dropped more for the gravel mixes than for the limestone mixes. In addition,
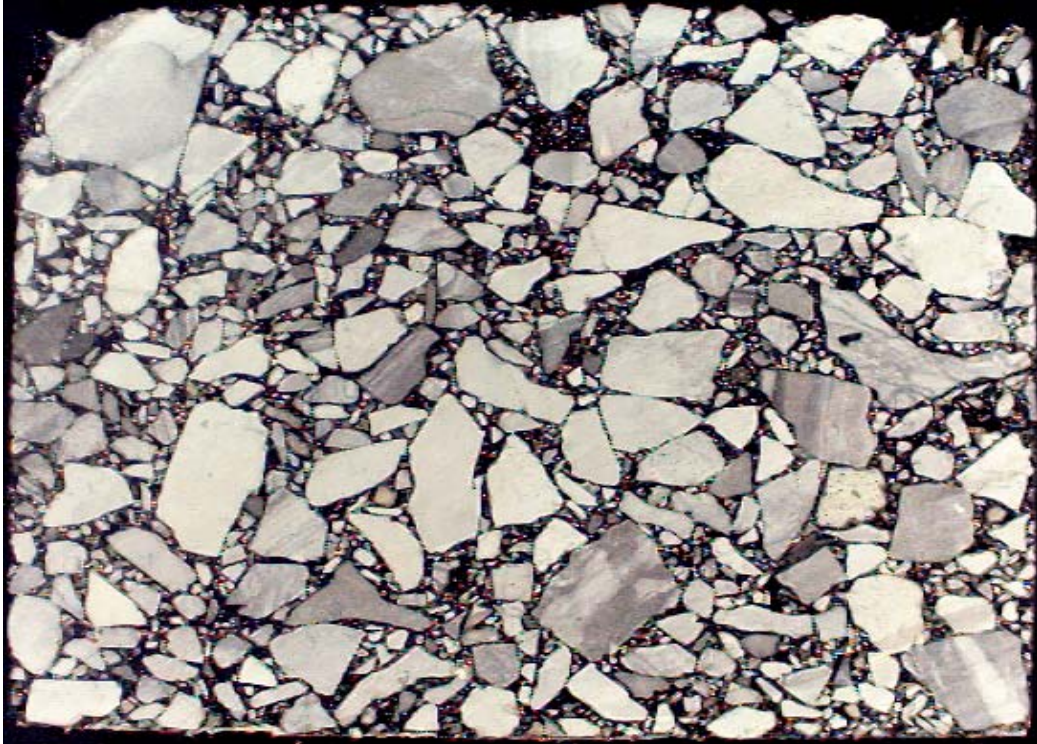
**Figure 5.4a**. A Typical Image of Mix C.
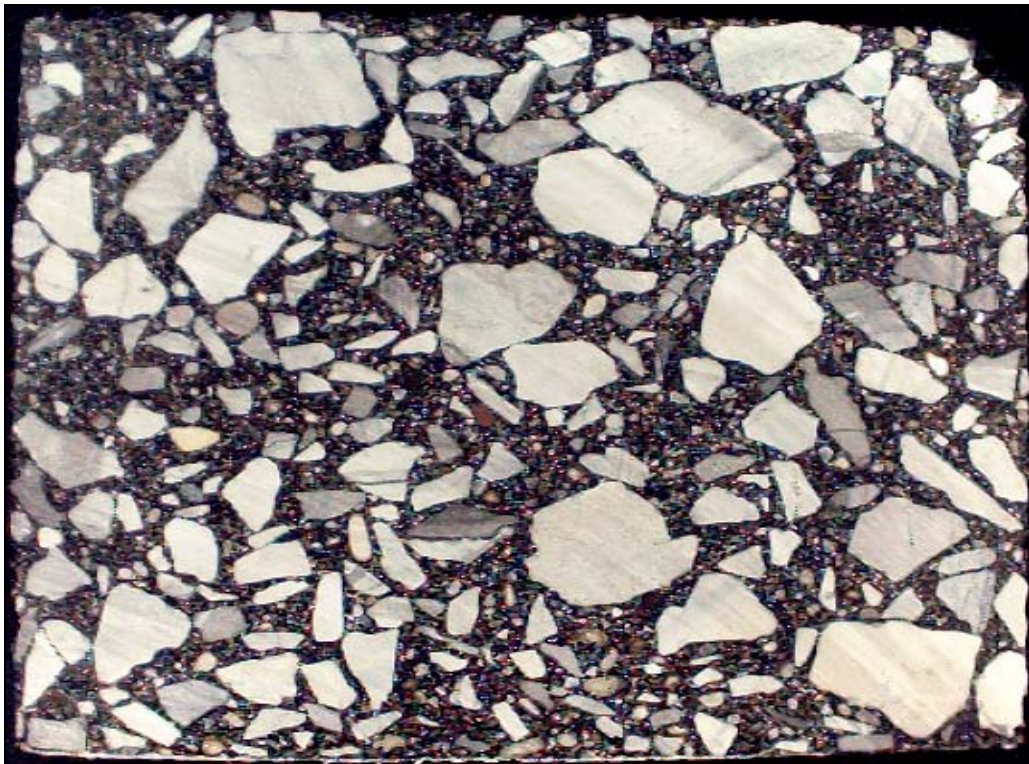


**Figure 5.4b**. A Typical Image of Mix D.

**Figure 5.4c**. A Typical Image of Mix K.
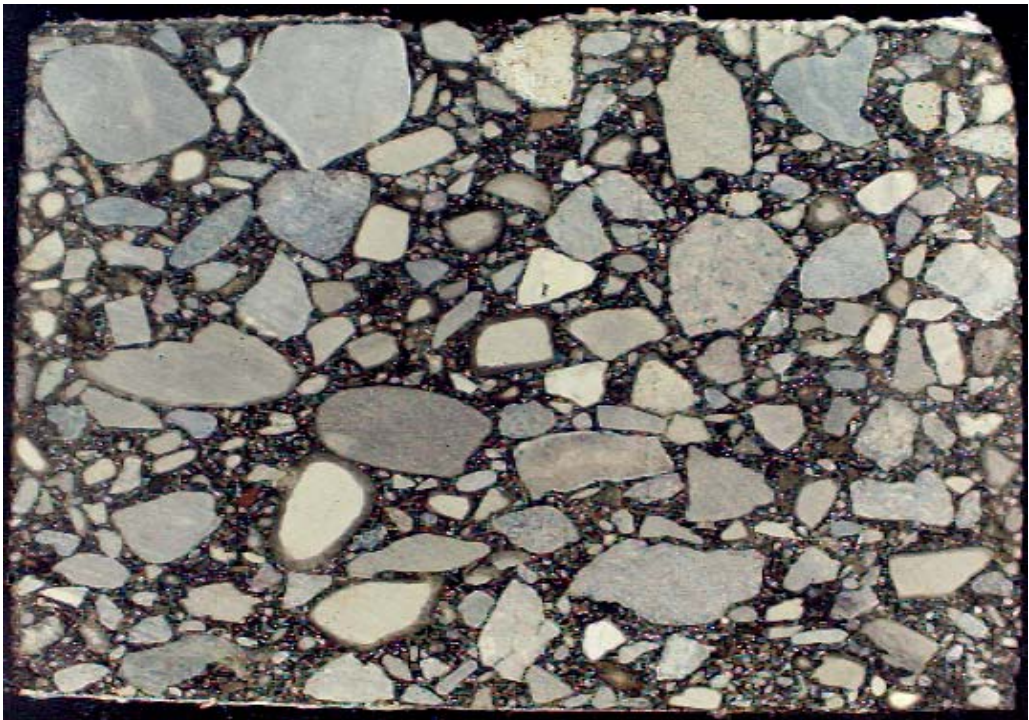


**Figure 5.4d**. A Typical Image of Mix L.

Figure 5.4(a-d): **Typical Images of Mixes C, D, K & L**
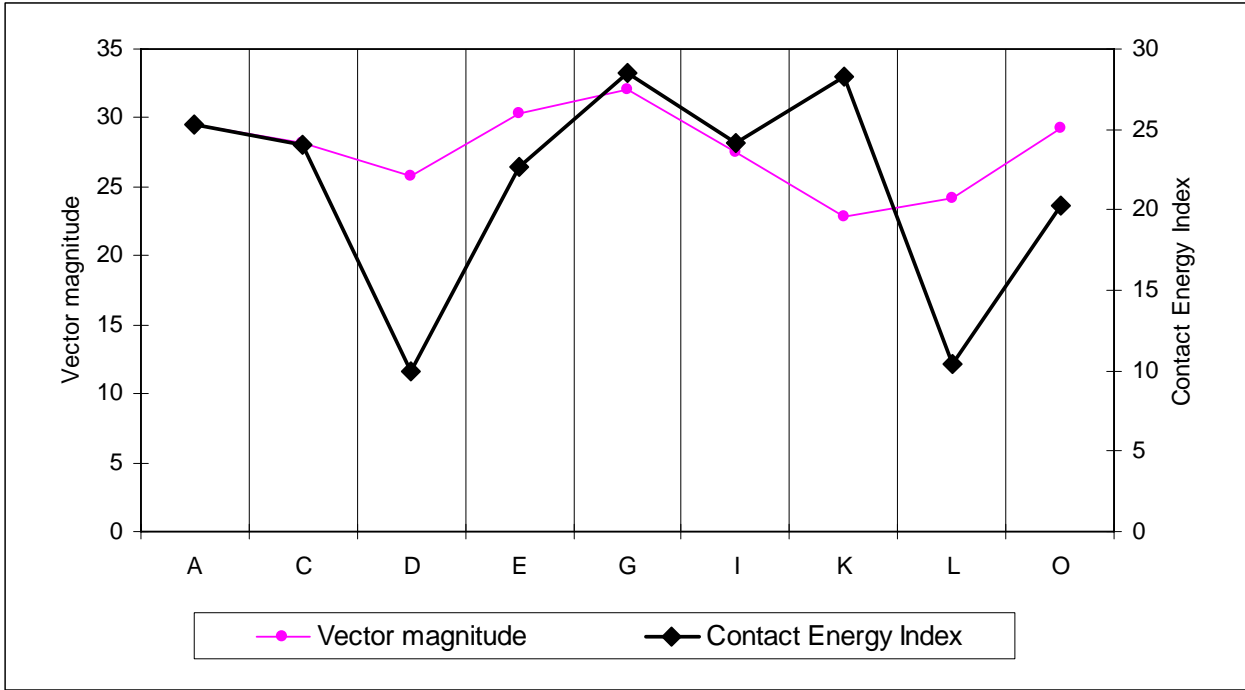
**A:** The Relation Between Contact Energy Index and the Vector Magnitude for Different Mixes.
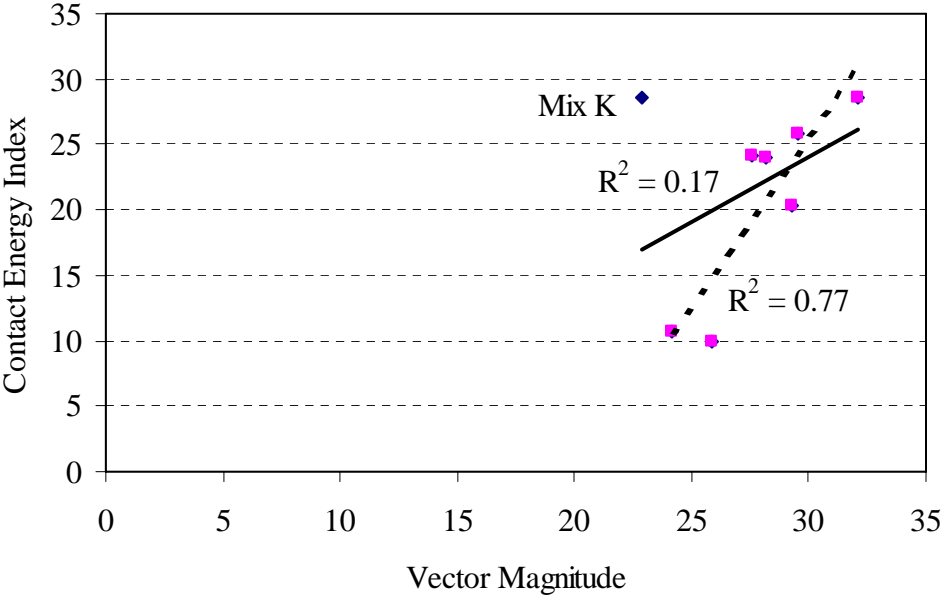


**B:**. Statistical Correlation Between the Contact Energy Index And the Vector Magnitude.

**Figure 5.5(a &b)** The Relation and Statistical Correlation Between Contact Energy Index and

the Vector Magnitude for Different Mixes.
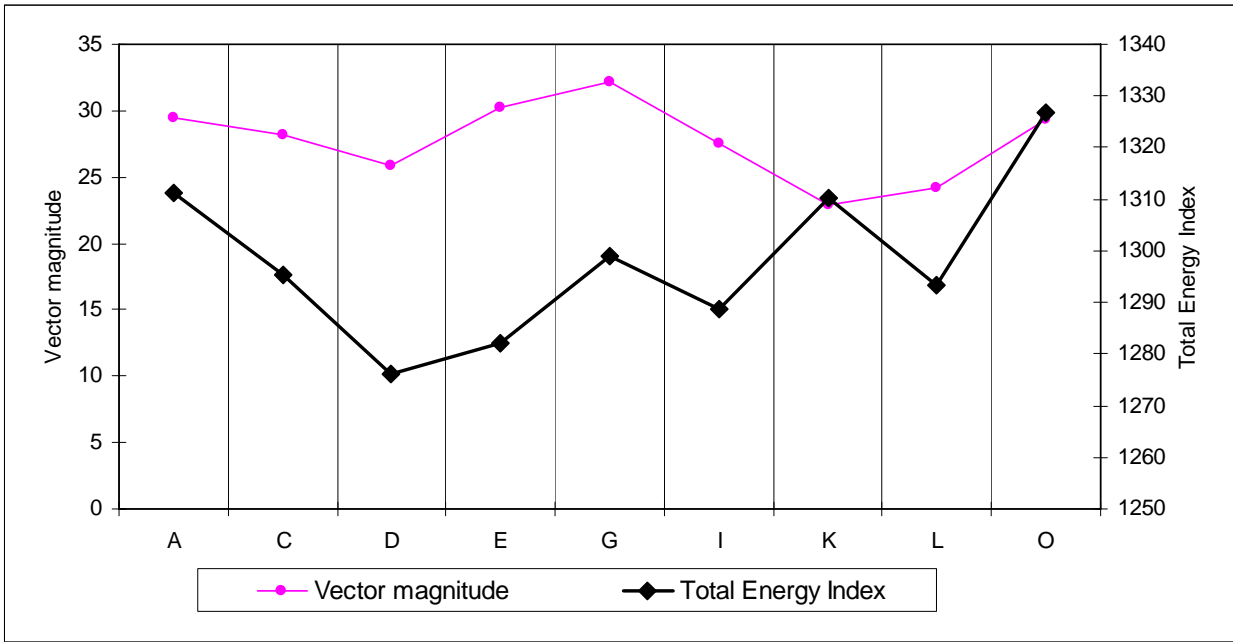
**A:** The Relation Between the Total Energy Index and the Vector Magnitude
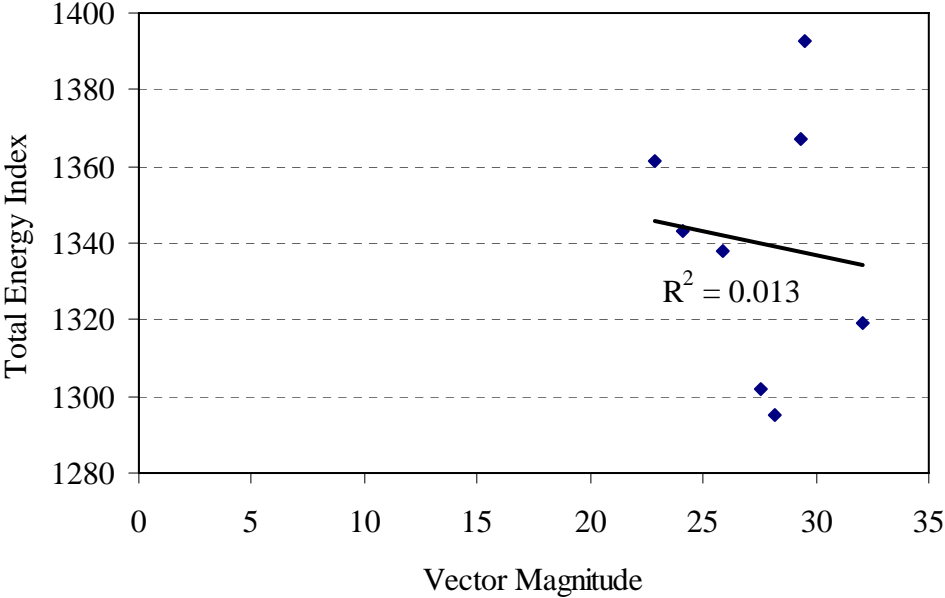


**B:**. Statistical Correlation

**Figure 5.6(a &b)** The Relation and Statistical Correlation Between Total Energy Index and the Vector Magnitude for Different Mixes.

**A**. The Relation Between Contact Energy Index and Number of Contacts for Different Mixes.



$R^2 = 0.7701$
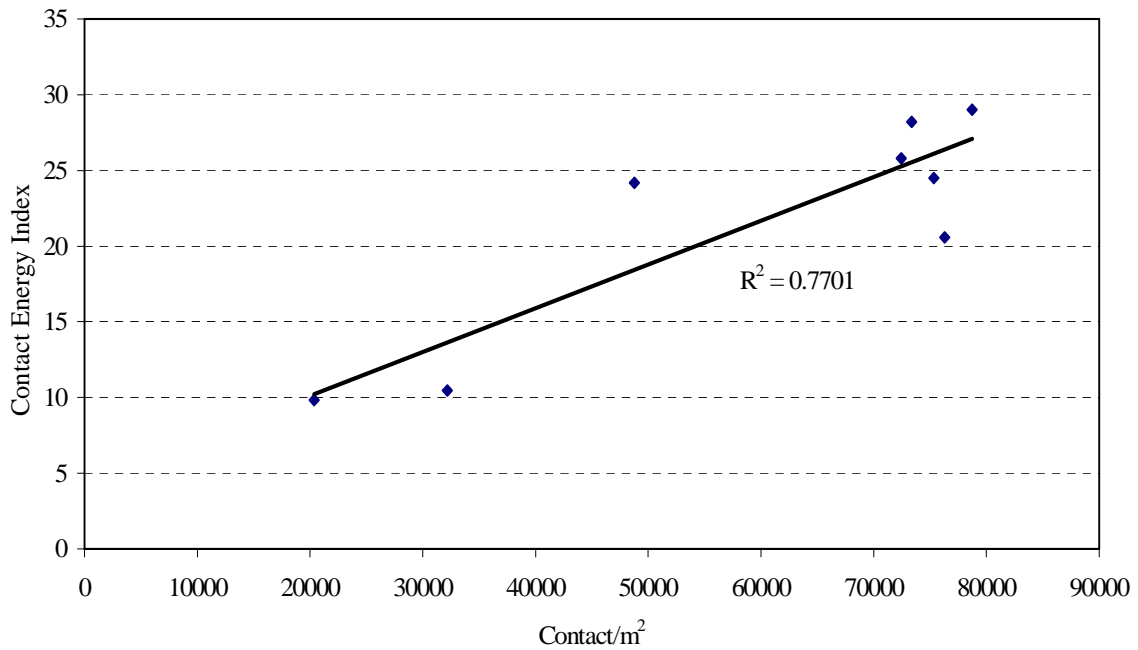
**B**. Statistical Correlation Between the Contact Energy Index and Number of Contacts.

**Figure 5.7 (a &b)** The Relation and Statistical Correlation Between Contact Energy Index and

the number of contacts for Different Mixes.
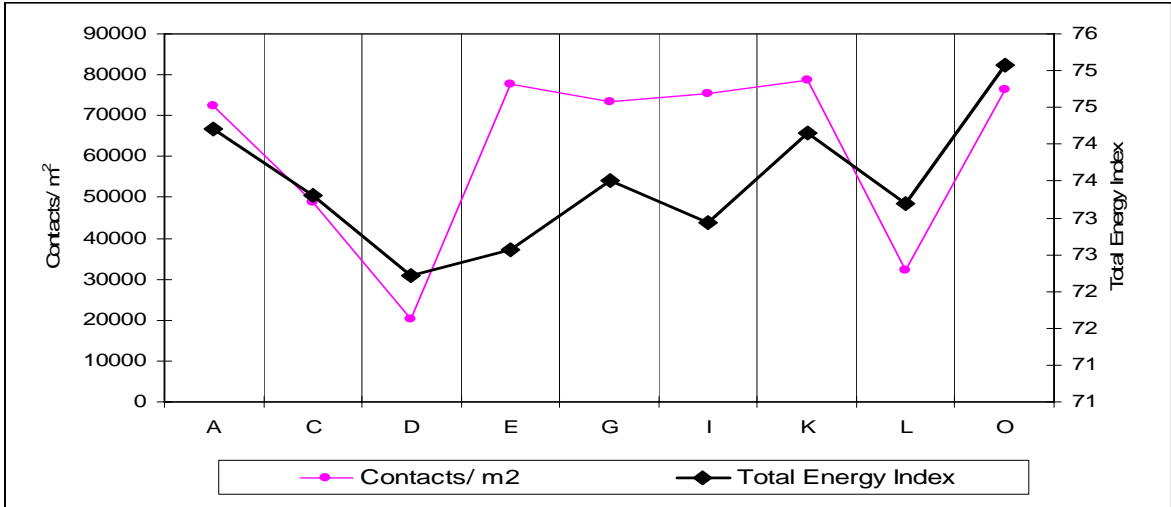
**B**. The Relation Between Total Energy Index and Number of Contacts for Different Mixes.



$$R^2 = 0.2694$$
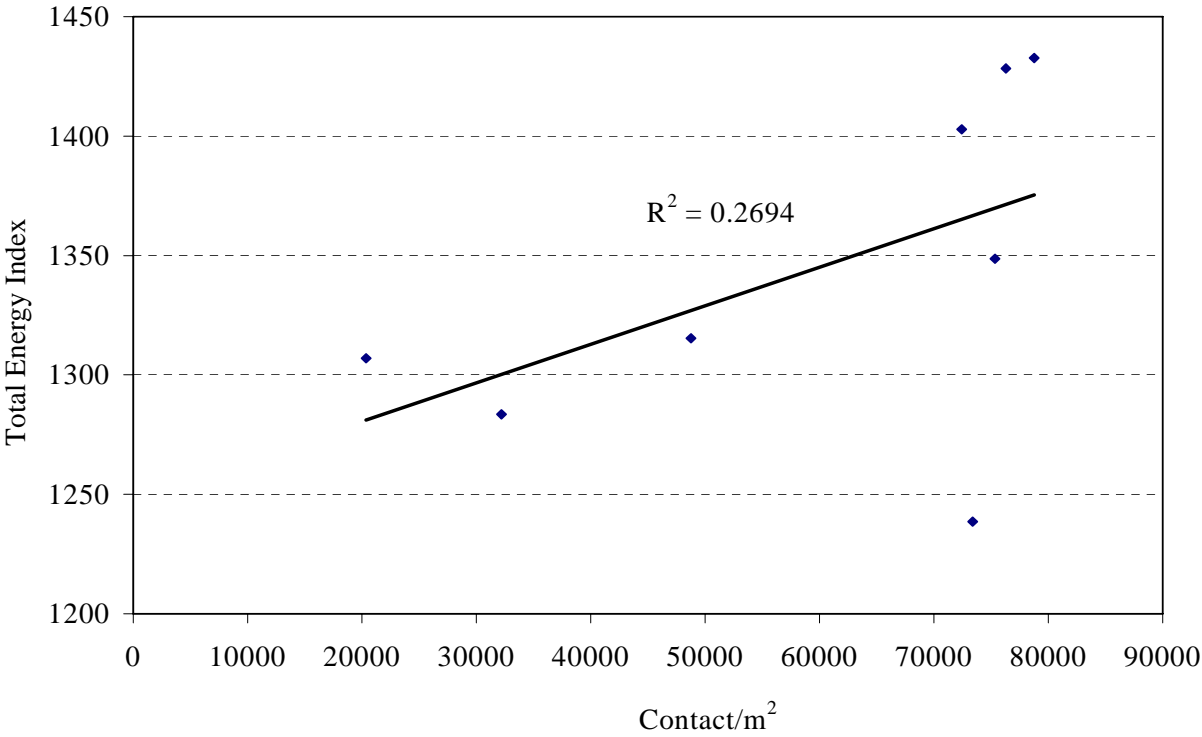
**B**. Statistical Correlation Between the Total Energy Index and Number of Contacts.

Figure 5.8(**a &b**): The Relation and Statistical Correlation Between Total Energy Index and the

number of contacts for Different Mixes.
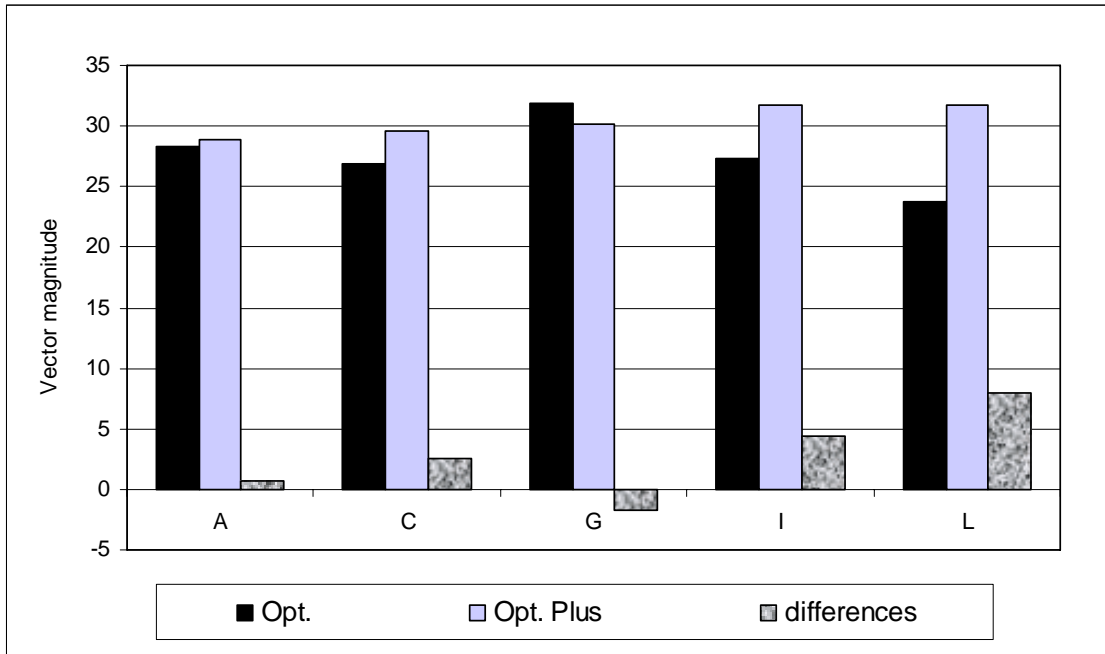
**Figure 5.9:** The Effect of Binder Content on Vector Magnitude.
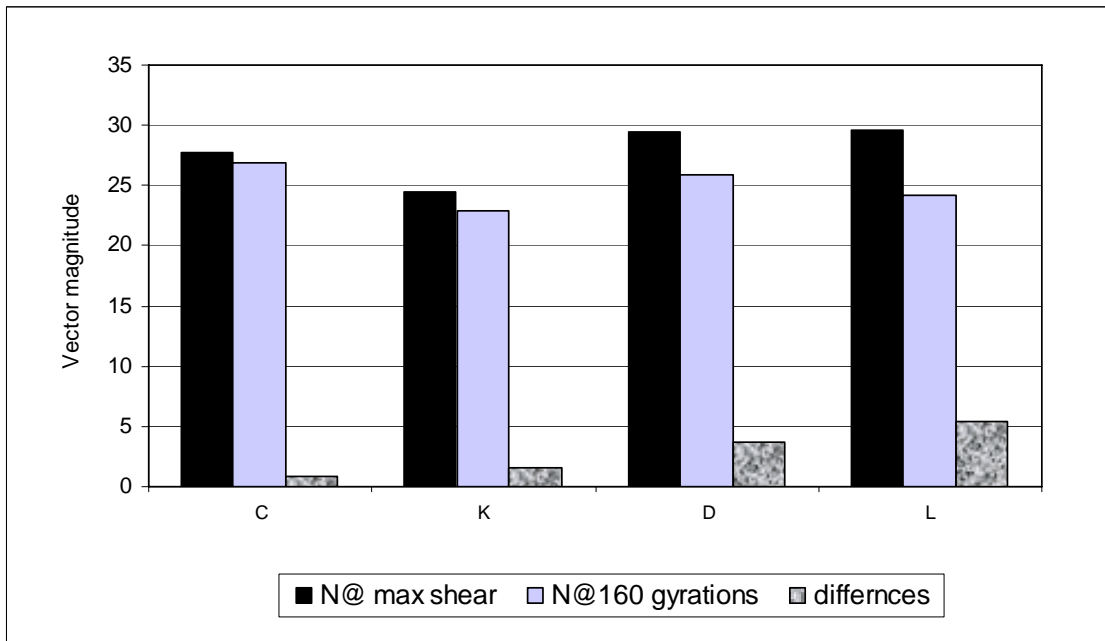


**Figure 5.10**: The Influence of Aggregate Type and Percent Natural Sand on Aggregate Orientation.

the effect of the natural sand is clear on the vector magnitude. An increase in the natural sand causes a decrease in the vector magnitude at 160 gyrations and an increase in the difference in the vector magnitude between the point at which the maximum shear stress is achieved and the end of compaction (C vs. D and K vs. L).

As shown in Figure 5.11 the number of contacts for mixes C and K was higher than for mixes D and L, respectively. The loss in number of contacts was higher for mixes D and L compared with mixes C and K, respectively as presented in Table 5.2. This loss was caused by the weak aggregate structure which caused aggregate reorientation and sliding.
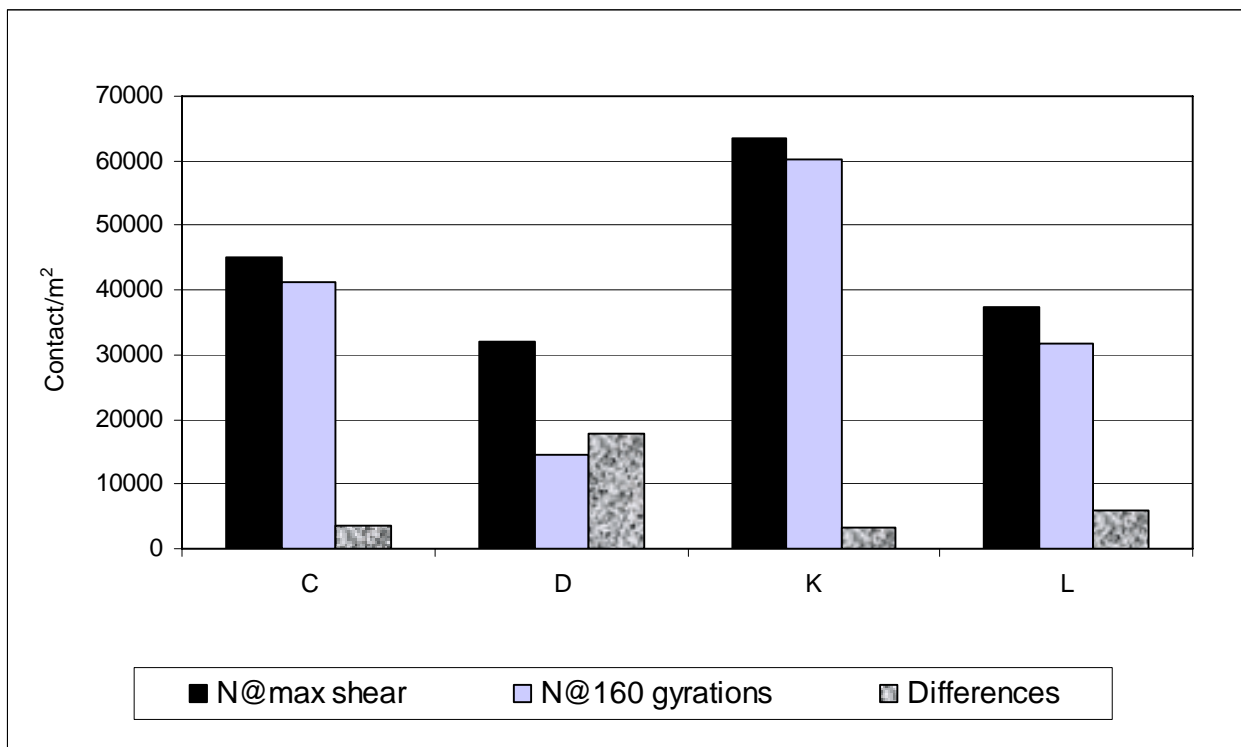


**Figure 5.11:** The Influence of Aggregate Type and Percent Natural Sand on Aggregate Contact.

**Table 5.2** The Values of the Contact Density at Different Compaction Gyrations.

| | Contact/m$^2$ | | |
| --- | --- | --- | --- |
| | N@max shear | N@160 gyrations | Differences |
| C | 44981.33 | 41363.91 | 3617.42 |
| D | 32070.17 | 14417.68 | 17652.49 |
| K | 63570.29 | 60282.78 | 3287.51 |
| L | 37518.59 | 31723.02 | 5795.57 |

## 5.5  SUMMARY

The internal structure was analyzed in terms of the vector magnitude (aggregate orientation) and aggregate contacts. In general, both the vector magnitude and number of contacts were found to increase with an increase in the contact energy index.  In addition, the total energy index had no correlation with the internal structure parameters. The binder content, aggregate type and percent of natural sand were also found to influence the aggregate orientation.  Limestone mixes and those without natural sand had higher vector magnitude and number of contacts. They also resisted the change in orientation and contacts beyond the point of maximum shear stresses more than the other mixes.

This is a blank Page

# 6. DEVELOPMENT AND EVALUATION OF ITD MIXES

## 6.1 DESCRIPTION OF SELECTED ITD MIXES

There are three mixes that have been identified by ITD research team from the three districts, D1, D2 and D3. The three mixes were developed using the Hveem design method, which was still adopted by ITD. The three mixes represented three different PG binder grades and three different gradations. Mix D1 with PG 58-28, Mix D2 with PG 64-34, and Mix D3 with PG 76-28. The mixes were evaluated to determine their acceptance in accordance to the Superpave mix design criteria. It was found that, the asphalt mix from district 1 that was designed using Hveem method (designated as D1-H), satisfies the Superpave criteria. Thus, the Superpave design of district 1 mix (designated as D1-S) is the same as D1-H, with no changes needed. Mix D2-H was slightly modified by changing the asphalt content. However, mix D3-H did not satisfy the Superpave criteria. Both changes in binder content and gradation are needed. The work is still in progress to optimize the D3 mix to satisfy the Superpave design criteria. Details of the mix design of these mixes are presented in Appendix C.

## 6.2 ITD MIXES EVALUATION USING SUPERPAVE GYRATORY COMPACTOR

Two experiments have been conducted to evaluate the ability of the developed shear stress and energy index to discern among different mixes. The experiment evaluated the influence of changes in the mix constituents including asphalt binder content, aggregate source, and type of gradation on the energy indices. Mixes were prepared and compacted using the Servopac compactor at University of Idaho.

Based on the discussions in the previous chapters, a typical compaction curve from the gyratory compaction is shown in **Figure 6.1.** The compaction curve is divided into two parts; the first one

has a steep change in percent air voids with an increase in number of gyrations. In part A, most of the applied energy is used in inducing volumetric permanent deformation (reduction in percent air voids), where the aggregates do not experience significant amount of shearing force. In part B, however, most of the energy applied by the induced angle does not cause significant volumetric change (small change in percent air voids). The energy is consumed in overcoming the shear resistance among the mix particles. Therefore, the energy calculations for assessing the mix stability under shear loading should focus on the second part of the compaction curve. The applied energy in "Part B" is either used in developing more contacts among the aggregates and cause reduction in percent air voids, or is dissipated by aggregate sliding as the aggregate structure fails to develop more contacts.

The details of calculation of the Contact energy index (CEI) and the Total energy index (TEI) are presented in Appendix D.
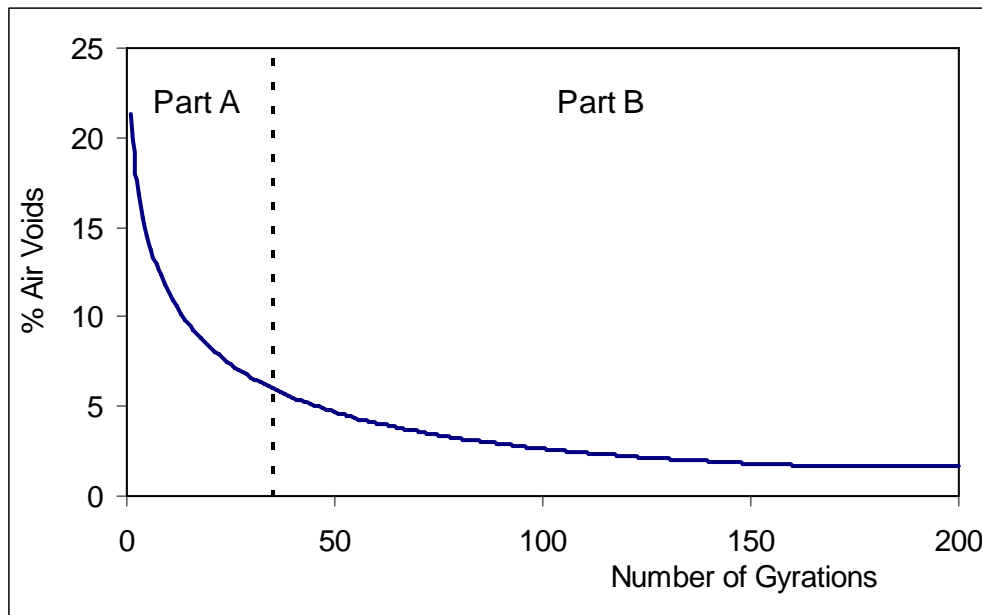


**Figure 6.1** Schematic Diagram Shows the Two Zones of the Compaction Curve

Prior to the analysis of the compaction energy, the repeatability of the compaction procedure should be evaluated in order to determine the number of specimens needed to represent each mix. Two specimens from each of the D1, D2, and D3 mixes were compacted using the same vertical pressure (600 kPa), angle (1.25°), and the rate of gyration (30 gyrations/minute). The compaction result shows that the maximum difference in percent air voids was about 0.4%, which is within the experimental error that is usually experienced in the laboratory. Consequently, it was decided to use only one specimen to represent each mix at a given set of variables.

### 6.2.1  Effect of percent of binder content on Total and Contact Energy Indices

Three different binder contents were used in each group from mix D1, D2 and D3 to investigate the effect of the binder content on the energy index. The first one was the optimum value determined from the Superpave mix design procedure. The second one was 1% higher than the optimum value, which is referred to herein as optimum plus. The third one was 1% lower than the optimum value, which is referred to herein as optimum minus. It was noticed that both the optimum plus and the optimum minus mixes reached a peak value at which it started to decrease with further compaction. However, most of the mixes with optimum asphalt content reached a maximum shear stress and stabilized at that value with further compaction. A comparison among the shear indices is presented in **Figure 6.2a - 6.2b** and **Table 6.1**. It is clear that the total energy index did not show a certain pattern in comparing the optimum, optimum plus, and optimum minus mixes. However, the contact energy index was always higher for mixes with optimum asphalt content. This indicates that the applied energy was used to develop contacts in the optimum mixes, while it was dissipated in aggregate sliding in the optimum plus and optimum minus mixes.
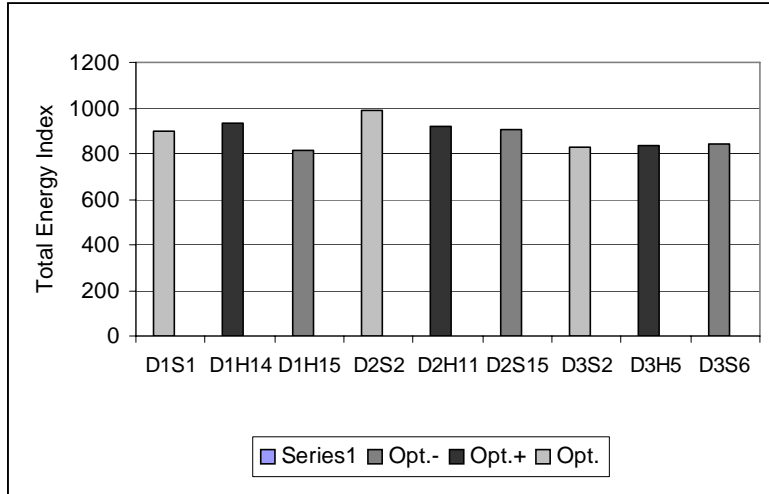
**Figure 6.2a** Comparisons among Mixes with Different Asphalt Content in Terms of the Total Energy Index
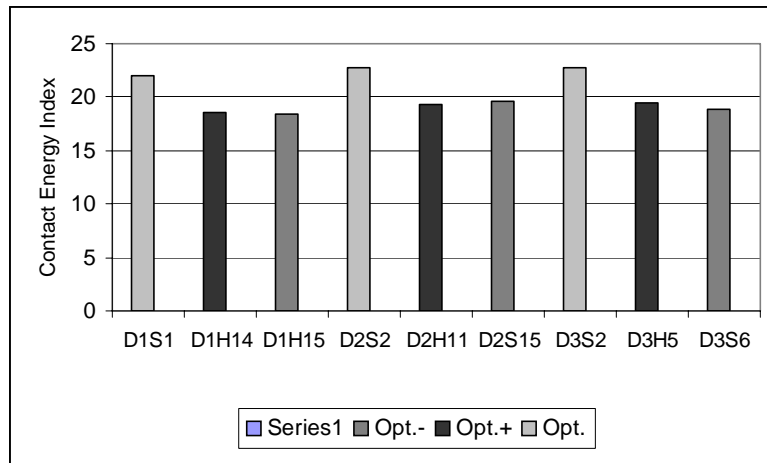


**Figure 6.2b** Comparisons among Mixes with Different Asphalt Content in Terms of the Contact Energy Index

**Table 6.1 Energy Indices of Mixes with different asphalt content**

| Mix | $P_b$ content | Total E.I | Contact E.I |
|------|------|------|------|
| D1S1 | Opt. | 901 | 22.053 |
| D1H14 | Opt.+ | 931.882 | 18.586 |
| D1H15 | Opt.- | 810.527 | 18.441 |
| D2S2 | Opt. | 989.84 | 22.783 |
| D2H11 | Opt.+ | 916.017 | 19.322 |
| D2H15 | Opt.- | 907.030 | 19.677 |
| D3S2 | Opt. | 824.894 | 22.788 |
| D3H5 | Opt.+ | 835.289 | 19.463 |
| D3S6 | Opt.- | 840.14 | 18.872 |

## 6.2.2  Effect of Aggregate Type

Three types of aggregates were used in this evaluation: D1, D2, and D3. A comparison among

the energy indices of the three mixes is shown **in Figures 6.3a - 6.3b** and **Table 6.2.** It is evident

that contact energy indices were highest for the D1 mix than for the D3 and D2 mixes.  This

indicates that the energy was used to developing more aggregate contacts was highest for the D1

mixes, and was lowest for the D2 mixes. It is known that D1 aggregate has more texture and

angularity than D3 and D2, which shows the highest stability as indicated by the energy indices.

Table 6.2 Energy Indices of Mixes with different aggregate type

| Mix | Total E.I | Contact E.I | Mix | Total E.I | Contact E.I |
|------|------|------|------|------|------|
| D1S1 | 901 | 22.053 | D2H2 | 924.27 | 17.815 |
| D1H2 | 970.54 | 21.839 | D3S2 | 824.894 | 22.788 |
| D2S2 | 989.84 | 22.783 | D3H5 | 834.918 | 12.41 |
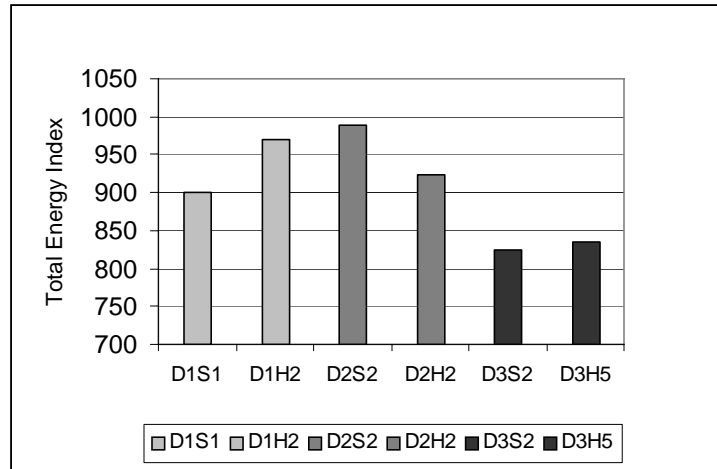
**Figure 6.3a** Comparisons among Mixes with Different Aggregate

Type in Terms of the Total Energy Index
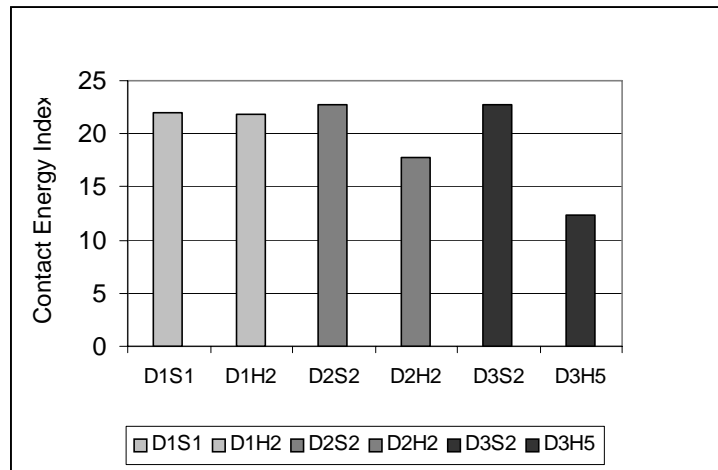


**Figure 6.3b** Comparisons among Mixes with Different Aggregate

Type in Terms of the Contact Energy Index

## 6.2.3  *Effect of Aggregate Gradation*

Two different gradations were used in this study from each group mix D1, D2 and D3. below the

restricted zone (BRZ) and above the restricted zone (ARZ). The BRZ gradation is usually

referred to as coarse gradation, while the ARZ gradation is referred to as fine aggregate. The

energy indices result shown in **Figure 6.4a - 6.4b** and **Table 6.3** are indicated that there are no

trend between the mix stability and location of the gradation shape, which is below or above the restricted zone.
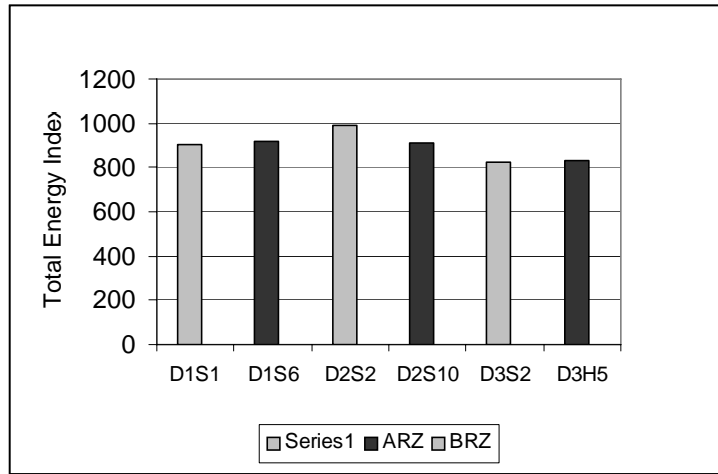


**Figure 6.4a** Comparisons among Mixes with Different Aggregate
Gradation Shape in Terms of the Total Energy Index
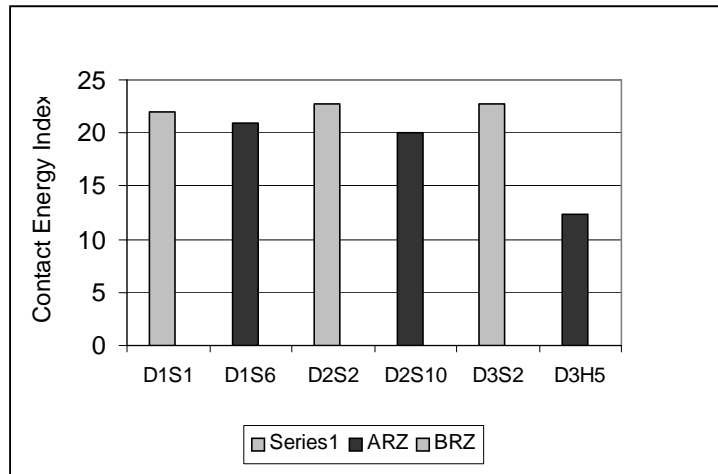


**Figure 6.4b** Comparisons among Mixes with Different Aggregate
Gradation Shape in Terms of the Contact Energy Index

**Table 6.3 Energy Indices of Mixes with different aggregate gradations**

| Mix | Total E.I | Contact E.I | Mix | Total E.I | Contact E.I |
|------|-----------|-------------|-------|-----------|-------------|
| D1S1 | 901 | 22.053 | D2S10 | 913.743 | 20.038 |
| D1S6 | 918.387 | 20.875 | D3S2 | 824.894 | 22.788 |
| D2S2 | 989.84 | 22.783 | D3H5 | 834.918 | 12.41 |

### 6.2.4 Summary of Effect of Mix Constituents on Energy Indices

Results of ITD Mixes revealed that the Total Energy Index did not correlate well with various mix design parameters. On the hand, the Contact Energy Index (CEI) was found to capture the influence of binder content, aggregate type on mix stability. However, there are no clear correlation found between CEI and aggregate the gradation.

## 6.3  ITD MIXES EVALUATION USING ASPAHLT PAVEMENT ANALYZER (APA)

Two compacted specimens from each of D1, D2, and D3 mix groups were sent to ITD for evaluation permanent deformation (rutting) used Asphalt Pavement Analyzer, APA rut test. The specimens were prepared at air voids of 7% percent and height of 150mm. The details of the APA rut test are shown in **Appendix E.** The relationship between the rut depth and the energy indices are shown in **Figure 6.5a, 6.5b** and **Table 6.4**. In general, the result shows that there is a trend between the mix stability as represented by the Contact Energy Index (CEI) and the rut depth measured at the APA test. In general, CEI index increased with a decrease in rut depth. Thus, mixes with high CEI values tend to resist rutting more than those with low CEI values.
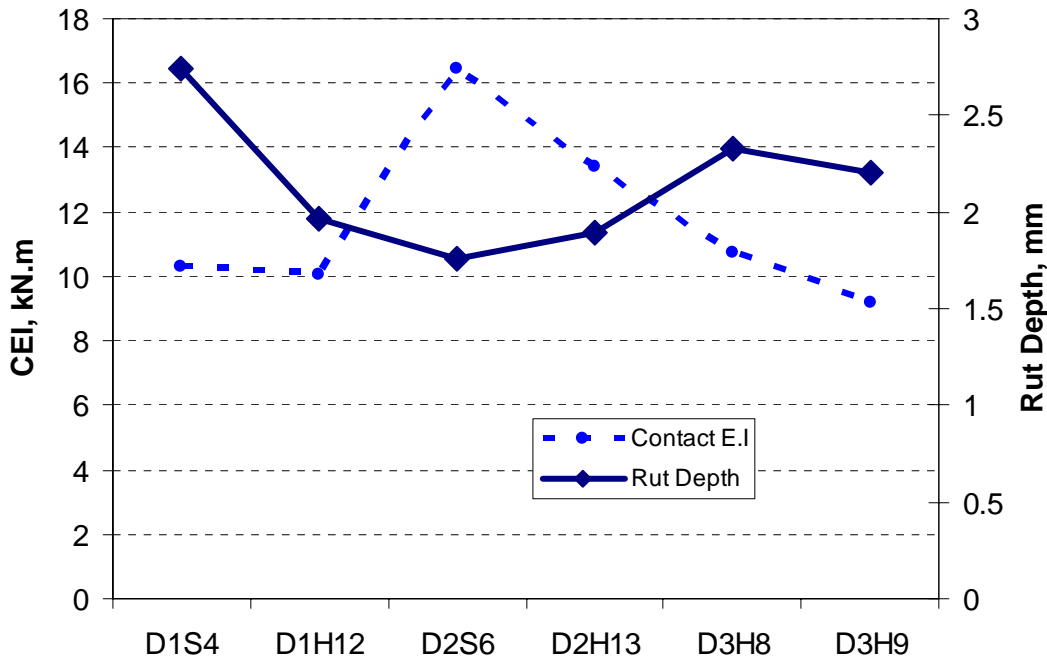
Figure 6.5 Variation of Rut Depth with CEI for ITD Mixes

**Table 6.4 Comparisons between the Rut Depth and Contact Energy Index**

| Mix | Rut Depth | Total E.I | Contact E.I | Mix | Rut Depth | Total E.I | Contact E.I |
|------|-----------|-----------|-------------|-------|-----------|-----------|-------------|
| D1S4 | 2.744 | 130.575 | 10.279 | D2H13 | 1.898 | 254.430 | 13.412 |
| D1H12 | 1.965 | 137.434 | 10.061 | D3H8 | 2.324 | 147.44 | 10.755 |
| D2S6 | 1.756 | 234.528 | 16.432 | D3H9 | 2.208 | 128.612 | 9.215 |

## 6.4   ITD MIXES EVALUATION USING IMAGE ANALYSIS

The objective of using imaging analysis is to capture the influence of the aggregate orientation and contacts on the mix stability and shear strength. The mixes used in this study are selected from total mixes from three different districts developed using Hveem and Superpave mix design method. Total mixes used in image analysis is 30. Twenty two specimens from each mix group were compacted to 160 gyration using an angle 1.25 and pressure of 600 kPa.  The vector

magnitude and number of contacts were measured on these specimens and recorded in **Table 6.5**. These values are compared with the contact energy index CEI and total energy index TEI as shown in **Figure 6.6 and 6.7** Results show that there is a good correlation between number of contacts and the contact energy index (CEI).

These results are consistent with those obtained from the NCHRP 9-16 mixes. They are also consistent with APA results presented earlier.

**Table 6.5** Values of the Quantifying Parameters of
Aggregate Structure and Energy Indices.

| Mix | Vector Magnitude | Contacts/m$^2$ | TEI | CEI |
|---|---|---|---|---|
| D1H4 | 27.90 | 72568.05 | 946.99 | 21.31 |
| D1S1 | 28.53 | 72685.12 | 901 | 22.05 |
| D2H2 | 27.94 | 48673.54 | 937.61 | 17.82 |
| D2S2 | 23.59 | 72935.81 | 920.56 | 22.87 |
| D3H4 | 22.84 | 38974.33 | 837.87 | 10.05 |
| D3S2 | 22.33 | 78736.06 | 824.89 | 22.79 |

In summary, the internal structure was analyzed in terms of the vector magnitude (aggregate orientation) and aggregate contacts. In general, both the vector magnitude and number of contacts were found to increase with an increase in the contact energy index. The total energy index did not show to correlate well with the internal structure parameters as measured by the number of contacts or vector magnitude.
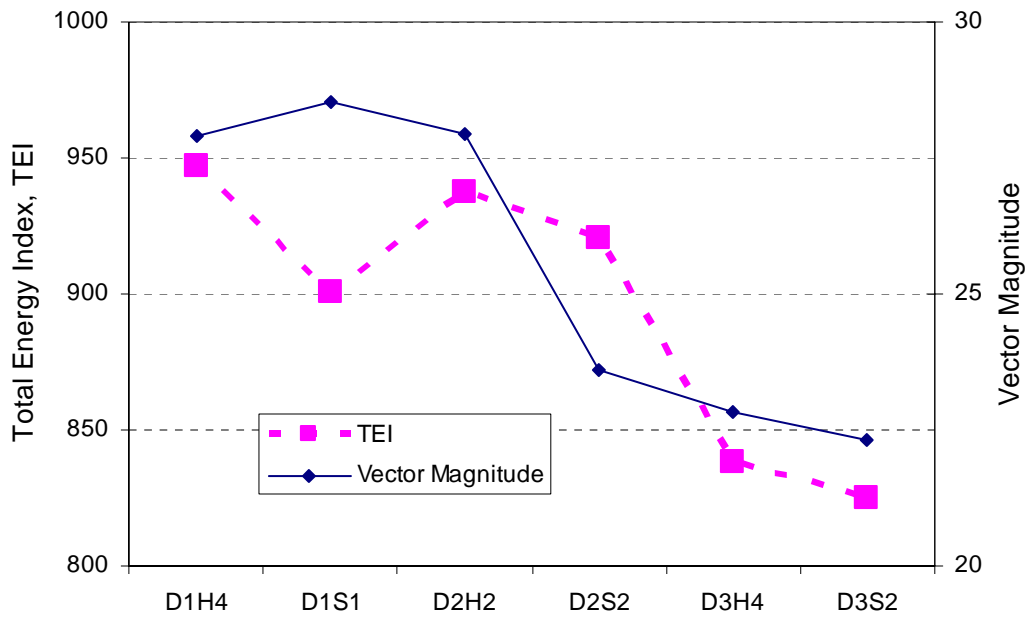
**Figure 6.6a Variation of the Vector Magnitude with TEI**
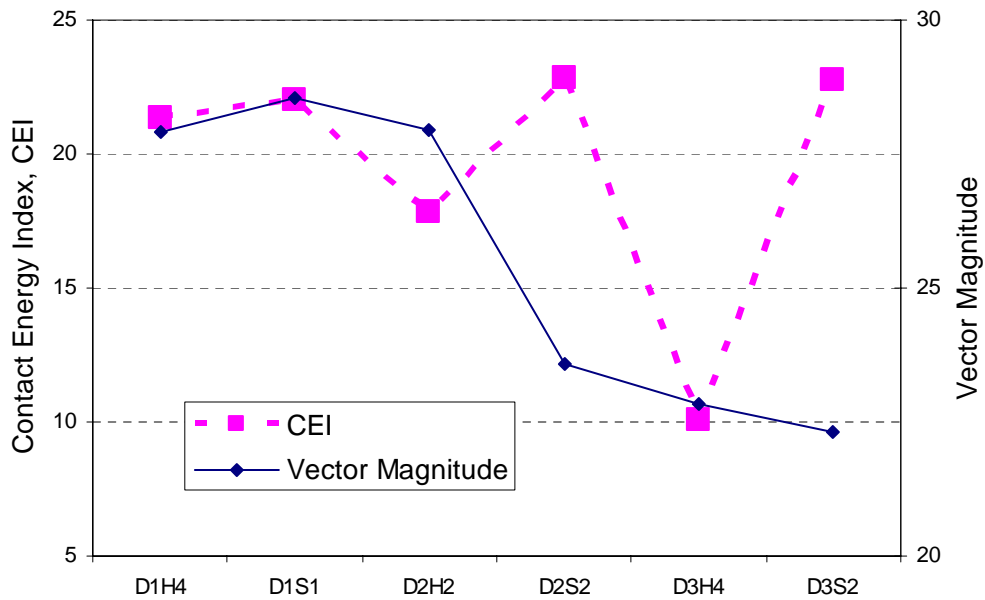


**Figure 6.6b Variation of the Vector Magnitude with CEI**
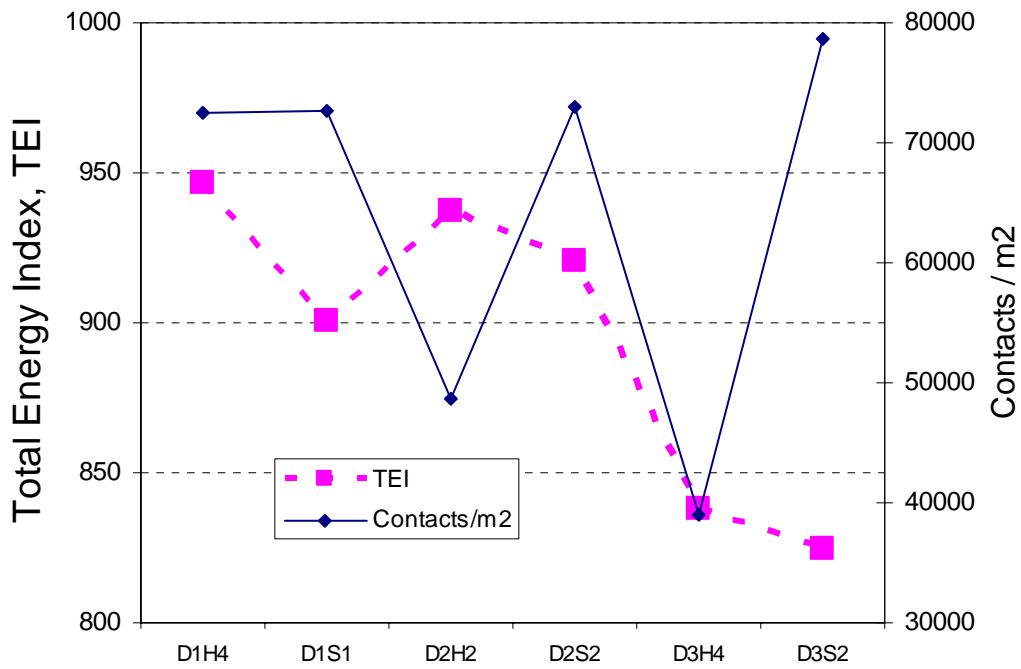
**Figure 6.7a Variation of the Number of Contacts with TEI**
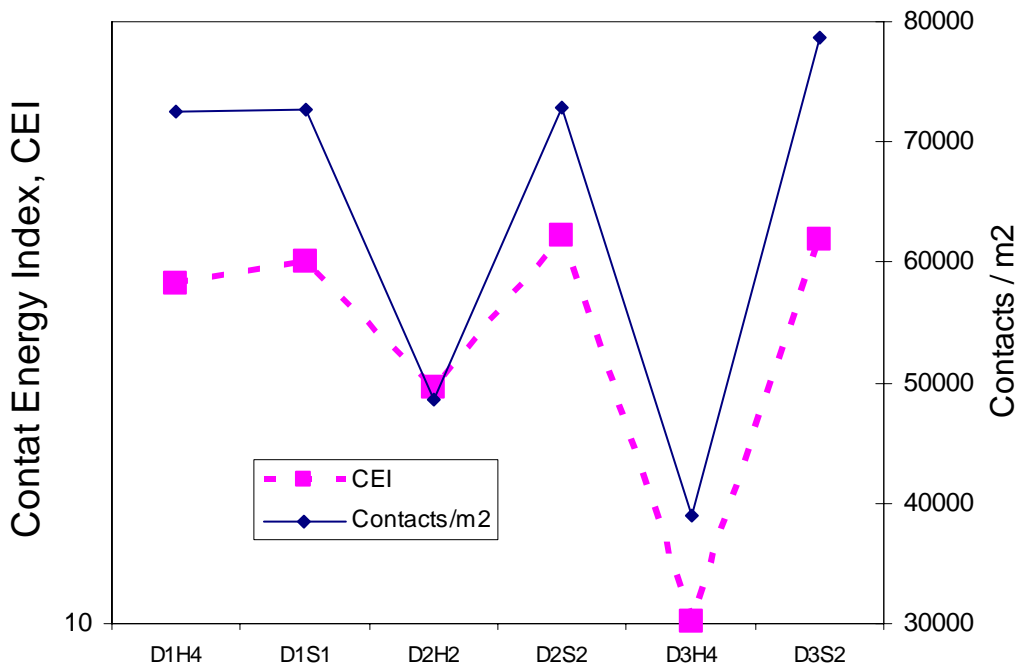


**Figure 6.7b Variation of the Number of Contacts with CEI**

133

# 7.   SUMMARY, CONCLUSIONS AND RECOMMENDATIONS

## 7.1   SUMMARY AND CONCLUSIONS

The new Superpave™ asphalt mix design system developed by the Strategic Highway Research Program (SHRP), considers the mix volumetrics in the design of hot-mix asphalt (HMA).  The absence of a performance test in the Superpave volumetric mix design procedure led many agencies to delay its implementation. Therefore, there is a need to develop methods for the assessment of HMA performance.  This report presents a new method to evaluate the mix shear strength during the design stage.  The shear strength is considered a measure of the mix resistance to permanent deformation.  The new method relies on the analysis of the mix response to the shear and normal forces applied on the mix during compaction in the Superpave Gyratory Compactor (SGC).

The report presents detailed analysis of the HMA compaction in the Servopac gyratory compactor.   The compaction forces are analyzed and a mathematical expression of the shear stress inside the mix is derived.   The shear stress value is used to calculate the compaction energy, which is divided into two regions according to the type of dominating strain.  The volumetric strain dominates the first region, while the shear strain dominates the second region. Analytical procedure is developed to identify these two regions.  An index termed as the "contact energy index, CEI" that reflects the compaction energy in the second region has been developed. The CEI showed to be an objective indicator of the mix stability as represented by its shear strength.  In this study, the contact energy index was used to analyze mixes with different constituents such as percent of binder, percent of natural sand, type of aggregate, gradation, and nominal maximum aggregate size.  The effect of the gyratory compaction variables such as the

angle of gyration, and vertical pressure on the contact energy index have also been investigated in order to determine the variables that would best discern among mixes with different constituents.

Based on the results of this research study, the contact energy index was lower for mixes with higher asphalt content over its optimum. Results also showed lower CEI values for mixes with high content of natural sand as compared to mixes without natural sand. Mixes made with gravel materials showed lower CEI values as compared to those with crushed limestone aggregates.

The Superpave shear test was used to measure G*, G*/sinδ and maximum shear strain of three mixes at two different temperatures. In general, the contact energy index has good correlation with these mechanical properties. The results show that the contact energy index increases with an increase in $G^*$ and $G^*$/sinδ, and a decrease in maximum shear strain. This shows the potential of the CEI in reflecting the mix stability and shear strength.

These results coincide with the intuitive expected performance of these mixes, which confirm that the CEI can be used as objective indicator of mix stability.

In order to make sure that the CEI trends were independent of mix compaction parameters (e.g. angle of gyration and compaction pressure), several comparison were made at varied angle of gyrations and varied compaction pressures. The results conformed same trends. This concludes that the CEI can still work as a stability indicator to discern mixes for any given compaction specifications.

Two and three dimensional finite element models are developed to simulate the compaction in the Servopac gyratory compactor. The two dimensional model is able to predict the measured shear stresses at small number of gyrations, and fails to predict shear stresses at number of

gyrations more than 19. However, the results from the three dimensional model compares very well with the shear stress and contact energy index calculated from experimental data. The three dimensional model includes the friction between the mix and the mold, and simulates most of the details of the loading mechanisms used in the Servopac gyratory compactor. The three dimensional model along with vertical deformation during compaction can be used to calculate the contact energy index and predict mix stability.

Analysis of the internal structure using imaging techniques is utilized in order to demonstrate the influence of the aggregate orientation and contacts on the mix stability and shear strength. In general, both the vector magnitude and number of contacts are found to increase with an increase in the contact energy index. In addition, the total energy index has no correlation with the internal structure parameters. The aggregate type and percent of natural sand are also found to influence the aggregate orientation. Limestone mixes and those without natural sand have higher vector magnitude and resist the change in orientation beyond the point of maximum shear stresses more than the other mixes.

## 7.2 RECOMMENDATIONS

Most of the available gyratory compactors are not equipped with a mechanism to measure the reaction forces such as $P_1$, $P_2$, and $P_3$ as done in the Servopac gyratory compactor. Therefore, it is recommended to develop an experimental setup to measure the reaction forces in order for the analysis methods developed in this study to be used in the evaluation of mixes compacted using gyratory compactors different than Servopac.

This report shows the potential of the contact energy index in differentiating mixes with different constituents. In addition, it shows that the contact energy index correlates with some of the mix mechanical properties. Consequently, the second recommendation is to use the developed

analysis methods to evaluate the stability of mixes with known resistance to rutting in the field. This would allow developing specifications for mix stability based on the results of the value of the contact energy index.

The third recommendation is related to the 3-D finite element model. Currently, the material properties are selected such that the vertical deformation in the model is similar to experimental measurements at different compaction levels. It is recommended to use a constitutive model to represent the change in the HMA properties during compaction.

# REFERENCES

1. AASHTO (1996). "Standard Specifications for Transportation Materials and Methods of Sampling and Testing." AASHTO Provisional Standards, MP2-95. Specifications for Superpave Volumetric Mix Design.

2. AASHTO. (2001). "Specifications for Superpave Volumetric Mix Design." Standard Specifications for Transportation Materials and Methods of Sampling and Testing, AASHTO Provisional Standards, Washington, D. C.

3. Abou-Chakra, H., Tuzun, U., (1999). "Coefficient of friction of binary granular mixtures in contact with a smooth wall. Part I: Direct shear box measurements of the effects of particle size ratio and particle surface roughness" Chemical Engineering Science, Vol. 54, Issue 24. pp. 5901-5912

4. ADINA, "Theory and Modeling Guide" Report ARD 00-7, August 2000, Volume I.

5. ADINA version 7.4 (2000). "ADINA R & D, Inc" Watertown, MA

6. Anderson, R, M, Huber, G, A, Walker D, E, and Zhang X. (2000). "Mixture Testing, Analysis and Field Performance of the Pilot Superpave Projects: The 1992 SPS-9 Mixtures" *Journal of the Association of Asphalt Paving Technologists*. Vol. 69.

7. Australian Standards (1995) - AS/NZS 2891.2.2 "Methods of Sampling and Testing Asphalt. Method 2.2 Sample Preparation" - *Compaction of Asphalt Test Specimens Using a Gyratory Compactor*.

8. *Bahia, H, Friemel, T, Peterson, P, and Russell, J. (1998). "Optimization of Constructability and Resistance to Traffic: A New Design Approach for HMA Using the Superpave Compactor." Journal of the Association of Asphalt Paving Technologists V.67-98, p.189.*

9. Butcher, M, (1998) "Determining Gyratory Compaction Characteristics Using Servopac Gyratory Compactor" *Transportation Research Record,* 1630

10. Chowdry, A., Gray, J., Button, J., and Little, D. (2001). "Effect of Aggregate Gradation on Permanent Deformation of Superpave HMA." A Paper Presented at the 80th Annual Meeting of the Transportation Research Board, Washington DC.

11. Cominsky, R, Harrigan, E, Leahy, R., (1994) "Level One Mix Design: Materials Selection, Compaction, and Conditioning" *SHRP-A-408*, 121.

12. Consugera, A., Little, D. N., Quintus, H.V., and Burati, J. (1989). "Comparative evaluation of laboratory compaction devices based on their ability to produce mixtures with engineering properties similar to those produced in the field." *TRR 1228*, Transportation Research Board, National Research Council, Washington D.C., 80-87

13. Crawley, A. B. (1993) "Gyratory Testing Machine Usage in Monitoring HMA Quality" United State Federal Highway Administration, Pupl. By ASCE, New York, USA, p 270-276

14. DeSombre, R, Chadbourn, B, Newcomb, DE, Voller, V, (1998) "Parameters to Define The Laboratory Compaction Temperature Range of Hot-Mix Asphalt" *Journal of the Association of Asphalt Paving Technologists* 67.

15. Eriksen, K. and V. Wegan. (1993). "Optical Methods for evaluation of Asphalt Concrete and Polymer-Modified Bituminous Binders." *Danish Road Institute*, Note 244.

16. Gauer, M. (1996). "Compaction of Asphalt in the Darmstadt Gyratory Compactor." International Workshop on the Use of the Gyratory Shear Compactor, LCPC, Nantes, France.

17. Guler, M., Bahia, H. U., Bosscher, P. J., Plesha, M. E. (2000). "Device for Measuring Shear Resistance of Hot-Mix Asphalt in the Gyratory Compactor." Transportation Research Record, Journal of the Transportation Research Board 1723, pp. 116-124.

18. Hand, A., and Epps, A. (2001). "Impact of Gradation Relative to the Superpave Restricted Zone on HMA Performance." A Paper Presented at the 80<sup>th</sup> Annual Meeting of the Transportation Research Board, Washington DC.

19. Huber G A, (1996) "Development of the Superpave Gyratory Compactor" *The Superpave Asphalt Research Program, The University of Texas at Austin*, web site (http://www.utexas.edu/research/superpave/articles/gyr_hist.html)

20. Image- Pro Plus Version 4.1. (1998). Media Cybernetics, L.P, Georgia, MD

*21.* IPC PTY LTD (1996) - *Servopac (Servo-Controlled Gyratory Compactor) Operating and Maintenance Manual.*

22. Kumar, A, Goetz W, (1974) "The Gyratory Testing Machine as a Design Tool and Instrument for Bituminous Mixture Evaluation" *Asphalt Paving Technology,* 43, 351-371.

23. Mallick, RB. (1999). "Use Of Superpave Gyratory Compactor To Characterize Hot-Mix Asphalt." Transportation Research Record - Journal of the Transportation Research Board 1681

24. Masad, E, Harman, T, Muhunthan, B, Shashidhar, N, (1998) "Aggregate Orientation and Segregation in Asphalt Concrete, Application of Geotechnical Principles In Pavement Engineering" *Proceedings of Sessions of Geo-Congress* 98, 69-80.

25. Masad, E., Muhunthan, B., Shashidhar, N., and Harman T. (1998). "Quantifying Labora-tory Compaction Effects on the Internal Structure of Asphalt Concrete." Paper submitted for Publication in Transportation Research Board.

26. Masad, E, Muhunthan, B, Shashidhar, N, Harman, T, (1999a). "Internal Structure Characterization of Asphalt Concrete Using Image Analysis*." Journal of Computing in Civil Engineering*, 13(2), 88-95.

27. Masad, E, Muhunthan, B, Shashidhar, N, Harman, T, (1999b). "Effect of Compaction Procedure on the Aggregate Structure in Asphalt Concrete*." Transportation Research Board,* No. 1681, 179-185

28. Masad, E. A., Tashman, L.S., Niranjanan, S., Little, D. (2001). "Micromechanics Based Analysis of Stiffness Anisotropy in Asphalt Mixes" Paper Number 01-2052 Submitted for publication in Transportation Research Board, 80th annual Meeting, January 9-13, 2001, Washington, D.C.

29. McRea J. L., (1962). "Gyratory Compaction Method for Determining Density Requirements For Subgrade and Base of Flexible Pavements." Miscellaneous paper No. 4-494, U.S. Army Engineering Waterways Experiment Station, Corps of Engineering, Vicksburg, MS, 2.

30. McRea, J. L., (1965). "Gyratory Testing Machine Technical Manual" Engineering Developments Company, Inc. Vicksburg, MS, 2.

31. Monismith, C. L. (1992). "Analytically based asphalt pavement design and rehabilita-tion." Transportation Research Record 1354, TRB, National Research Council, Washington, D. C., 5 – 26.

32. Moutier, F. (1996). "G.S.P. Result Modeling - Comments on the Compaction Ultimate Threshold, Eurasphalt & Eurobitume Congress. Strasbourg.

33. Moutier, F. (1997). "Gyratory Compactor (GC or PCG) Justification of its Use in the French Mix Design." Paper presented in the Superpave Asphalt Mixture Expert Task Group.

34. Moutier, F, Bonnot, J, Corte, JF, (1997) "Comparison of The Use of The Gyratory Compactor in The French Mix Design Method and in Superpave Level 1" *Proceedings of the Conference: Road Safety in Europe and Strategic Highway Research Program (SHRP).*

35. Murfee, J; Manzione, CW., (1992)."Construction Of Rut-Resistant Asphalt Mixtures" Transportation Research Record 1337

36. Oda, M, (1972a) "Initial Fabric and Their Relations to Mechanical Properties of Granular Material." *Soils and foundations,* 12(1), 17-36.

37. Oda, M, (1972b) "The Mechanism of Fabric Changes During Compressional Deformation of Sands" *Soils and foundations,* 12(2), 1-8.

38. Oda, M, (1977) "Co-Ordination Number and its Relation to Shear Strength of Granular Material" *Soils and Foundations,* 17(2), 29-42

39. Pixera. (1997). "Pixera visual Communication Suite for Windows 95" Pixera Corporation, California

40. Rand, D. A. (1997). "Comparative Analysis of Superpave Gyratory Compactors and TxDOT Gyratory Compactors." Master Thesis, University of Texas, Austin, TX.

*41.* Robert Cook, David Malkus, Michael Plesha (1989) "Concepts and Applications of Finite Element Analysis" *Third Edition*

Roberts, F L, Kandhal, P S, Brown, E R. Lee D, Kennedy, T W, (1996) "Hot Mix Asphalt Materials Mixture Design and Construction" *NAPA Education Foundation Lanham, Maryland, Second Edition*.

42. Romero, P. and Mogawer, W. (1998a). "Evaluation of the Superpave Shear Tester using 19-mm Mixtures from the Federal Highway Administration's Accelerated Loading Facility." *Journal of the Association of Asphalt Paving Technologist*, 67, 573-601.

43. Romero, P. and Mogawer, W. (1998b). "Evaluation of the Superpave Shear Tester's Ability to Discern Two Mixtures with Different Size Aggregates Using the FHWA's Accelerated Loading Facility." *In Transportation Research Record 1630, TRB*, National Research Council, Washington D.C., 69-76.

44. Russ, J., C. (1999). "The image Processing Handbook" third edition, CRC, Boca Raton, Fla.

45. Ruth, B. E., Shen, X. and Wang, L. H. (1991). "Gyratory Evaluation of Aggregate Blends to Determine Their Effects on Shear Resistance and Sensitivity to Asphalt Content." STP 1147, American Society for Testing Materials.

46. Ruth, B. E., and Schaub J.H. (1996). "Gyratory Testing Machine Simulation of Field Compaction of Asphalt Concrete." *Proceedings, Association of Asphalt Paving Technologists*, 35.

*47.* Ruth, B.E, (1996) "Evaluation of Pavement Materials for Design, Compaction, and Quality Control by Gyratory Testing Methods" *International Workshop on the Use of the Gyratory Shear Compactor, LCPC, Nantes, France.*

48. Servopac Monitor version 1.24 (2000). Australia

49. SHRP (1994), "Level One Mix Design: Material Selection, Compaction, and Conditioning" SHRP-A-408, Strategic Highway Research Program, National Research Council, DC.

50. Sigurjonsson, S, Ruth, BE (1990). "Use Of Gyratory Testing Machine To Evaluate Shear Resistance Of Asphalt Paving Mixture" Transportation Research Record 1259

51. Standard Test Method for Theoretical Maximum Specific Gravity and Density of Bituminous Paving Mixtures, (1999). Annual Book of ASTM Standards, Designation: D2041-95, Vol. 04.03, American Society for Testing and Material

52. Sousa, J. B., Harvey, J., Painter, L., Deacon, J. A. and Monismith, C.L. (1991). "Evaluation of Laboratory Procedures for Compacting Asphalt-Aggregate Mixtures" *Report No. SHRP-A-UWP=91-523*, Strategic Highway Research Program, National Research Council, Washington D.C.

53. Stuart, K, Davis, F, Parobeck, S, Sylor, T M, (1996) "Evaluation of the U.S. Corps of Engineers Gyratory Testing Machine Model 8A-6B-4C" *U.S. Department of Transportation, Federal Highway Administration,* FHWA-RD-95-205.

54. Tashman L., Masad E., Peterson B., and Saleh H. (2001). "Internal Structure Analysis of Asphalt Mixes to Improve The Simulation of Superpave Gyratory Compaction to Field Conditions" *Journal of the Association of Asphalt Paving Technologist*.

55. Tobita, Y. (1998) "Fabric Tensors in Constitutive Equations for Granular Materials." *Soils and Foundations*, Vol. 29(4), pp. 99-104

56. Yue, Z. Q., Bekking, and I. Morin. (1995). "Application of Digital Image Processing to quantitative study of Asphalt Concrete Microstructure." *Transp. Res. Rec. 1492*, Transportation Research Board, National Research Council, Washington D.C., 53-60

This is a blank Page

# List of Appendices

This is a blank Page

# APPENDIX A

**MIX PROPERTIES AND GRADATIONS –**

**MIXES OBTAINED FROM THE NCHRP 9-16 PROJECT**

## Mix A

| 9.5mm Limestone Coarse, 0% Sand | | |
|---|---|---|
| Limestone 8's | | 43% |
| Limestone Sand | | 13% |
| Washed LSS | | 44% |
| | | |
| Sieve | | Mass, g |
| 1 - 3/4 | (25 - 19 mm) | 0 |
| 3/4 - 1/2 | (19 - 12.5 mm) | 0 |
| 1/2 - 3/8 | (12.5 - 9.5 mm) | 441 |
| 3/8 - #4 | (9.5 - 4.75 mm) | 1652 |
| #4 - #8 | (4.75 - 2.36 mm) | 774 |
| #8 - #16 | (2.36 - 1.18 mm) | 612 |
| #16 - #30 | (1.18 - 0.6 mm) | 437 |
| #30 - #50 | (0.6 - 0.3 mm) | 266 |
| #50 - #100 | (0.3 - 0.15 mm) | 122 |
| #100 - #200 | (0.15 - 0.075 mm) | 50 |
| - #200 | ( - 0.075 mm) | 149 |
| TOTAL | | 4500 |
| PG 64-22 | | 5.30% |

## Mix B

| 9.5mm Limestone Coarse, 40% Sand | | |
|---|---|---|
| Limestone 8's | | 40% |
| Washed LSS | | 10% |
| Limestone Sand | | 10% |
| Natural Sand | | 40% |
| Sieve | | Mass, g |
| 1 - 3/4 | (25 - 19 mm) | 0 |
| 3/4 - 1/2 | (19 - 12.5 mm) | 0 |
| 1/2 - 3/8 | (12.5 - 9.5 mm) | 410 |
| 3/8 - #4 | (9.5 - 4.75 mm) | 1431 |
| #4 - #8 | (4.75 - 2.36 mm) | 436 |
| #8 - #16 | (2.36 - 1.18 mm) | 410 |
| #16 - #30 | (1.18 - 0.6 mm) | 594 |
| #30 - #50 | (0.6 - 0.3 mm) | 886 |
| #50 - #100 | (0.3 - 0.15 mm) | 189 |
| #100 - #200 | (0.15 - 0.075 mm) | 31 |
| - #200 | ( - 0.075 mm) | 113 |
| TOTAL | | 4500 |
| PG 76-22 | | 6.50% |

## Mix C

| 19mm Limestone Coarse, 0% Sand | | |
|---|---|---|
| Limestone 57's | | 42% |
| Limestone 8's | | 26% |
| Limestone Sand | | 20% |
| Washed LSS | | 12% |
| Sieve | | Mass, g |
| 1 - 3/4 | (25 - 19 mm) | 360 |
| 3/4 - 1/2 | (19 - 12.5 mm) | 756 |
| 1/2 - 3/8 | (12.5 - 9.5 mm) | 626 |
| 3/8 - #4 | (9.5 - 4.75 mm) | 1305 |
| #4 - #8 | (4.75 - 2.36 mm) | 410 |
| #8 - #16 | (2.36 - 1.18 mm) | 351 |
| #16 - #30 | (1.18 - 0.6 mm) | 243 |
| #30 - #50 | (0.6 - 0.3 mm) | 162 |
| #50 - #100 | (0.3 - 0.15 mm) | 81 |
| #100 - #200 | (0.15 - 0.075 mm) | 36 |
| - #200 | ( - 0.075 mm) | 171 |
| TOTAL | | 4500 |
| PG 76-22 | | 5.20% |

## Mix D

| 19mm Limestone Coarse, 40% Sand | | |
|---|---|---|
| Limestone 57's | | 48% |
| Limestone 8's | | 12% |
| Natural Sand | | 40% |
| | | |
| Sieve | | Mass, g |
| 1 - 3/4 | (25 - 19 mm) | 410 |
| 3/4 - 1/2 | (19 - 12.5 mm) | 864 |
| 1/2 - 3/8 | (12.5 - 9.5 mm) | 536 |
| 3/8 - #4 | (9.5 - 4.75 mm) | 824 |
| #4 - #8 | (4.75 - 2.36 mm) | 194 |
| #8 - #16 | (2.36 - 1.18 mm) | 221 |
| #16 - #30 | (1.18 - 0.6 mm) | 441 |
| #30 - #50 | (0.6 - 0.3 mm) | 792 |
| #50 - #100 | (0.3 - 0.15 mm) | 140 |
| #100 - #200 | (0.15 - 0.075 mm) | 9 |
| - #200 | ( - 0.075 mm) | 72 |
| TOTAL | | 4500 |
| PG 64-22 | | 4.70% |

## Mix E

| 9.5mm Limestone Fine, 0% Sand | | |
|---|---|---|
| Limestone 8's | | 12% |
| Washed LSS | | 44% |
| Limestone Sand | | 44% |
| | | |
| Sieve | | Mass, g |
| 1 - 3/4 | (25 - 19 mm) | 0 |
| 3/4 - 1/2 | (19 - 12.5 mm) | 0 |
| 1/2 - 3/8 | (12.5 - 9.5 mm) | 122 |
| 3/8 - #4 | (9.5 - 4.75 mm) | 716 |
| #4 - #8 | (4.75 - 2.36 mm) | 1062 |
| #8 - #16 | (2.36 - 1.18 mm) | 963 |
| #16 - #30 | (1.18 - 0.6 mm) | 675 |
| #30 - #50 | (0.6 - 0.3 mm) | 477 |
| #50 - #100 | (0.3 - 0.15 mm) | 212 |
| #100 - #200 | (0.15 - 0.075 mm) | 117 |
| - #200 | ( - 0.075 mm) | 158 |
| TOTAL | | 4502 |
| PG 76-22 | | 6.20% |

## Mix F

| 9.5mm Limestone Fine, 40% Sand | | |
|---|---|---|
| Limestone 8's | | 30% |
| Limestone Sand | | 30% |
| Natural Sand | | 40% |
| | | |
| Sieve | | Mass, g |
| 1 - 3/4 | (25 - 19 mm) | 0 |
| 3/4 - 1/2 | (19 - 12.5 mm) | 0 |
| 1/2 - 3/8 | (12.5 - 9.5 mm) | 306 |
| 3/8 - #4 | (9.5 - 4.75 mm) | 1112 |
| #4 - #8 | (4.75 - 2.36 mm) | 540 |
| #8 - #16 | (2.36 - 1.18 mm) | 500 |
| #16 - #30 | (1.18 - 0.6 mm) | 716 |
| #30 - #50 | (0.6 - 0.3 mm) | 950 |
| #50 - #100 | (0.3 - 0.15 mm) | 225 |
| #100 - #200 | (0.15 - 0.075 mm) | 77 |
| - #200 | ( - 0.075 mm) | 77 |
| TOTAL | | 4500 |
| PG 64-22 | | 7.10% |

## Mix G

| 19mm Limestone Fine, 0% Sand | | |
|---|---|---|
| Limestone 57's | | 18% |
| Limestone 8's | | 17% |
| Washed LSS | | 20% |
| Limestone Sand | | 45% |
| Sieve | | Mass, g |
| 1 - 3/4 | (25 - 19 mm) | 153 |
| 3/4 - 1/2 | (19 - 12.5 mm) | 324 |
| 1/2 - 3/8 | (12.5 - 9.5 mm) | 329 |
| 3/8 - #4 | (9.5 - 4.75 mm) | 923 |
| #4 - #8 | (4.75 - 2.36 mm) | 752 |
| #8 - #16 | (2.36 - 1.18 mm) | 720 |
| #16 - #30 | (1.18 - 0.6 mm) | 500 |
| #30 - #50 | (0.6 - 0.3 mm) | 374 |
| #50 - #100 | (0.3 - 0.15 mm) | 171 |
| #100 - #200 | (0.15 - 0.075 mm) | 104 |
| - #200 | ( - 0.075 mm) | 153 |
| TOTAL | | 4503 |
| PG 64-22 | | 5.50% |

## Mix H

| 19mm Limestone Fine, 40% Sand | | |
|---|---|---|
| Limestone 57's | | 20% |
| Limestone 8's | | 32% |
| Limestone Sand | | 8% |
| Natural Sand | | 40% |
| Sieve | | Mass, g |
| 1 - 3/4 | (25 - 19 mm) | 171 |
| 3/4 - 1/2 | (19 - 12.5 mm) | 360 |
| 1/2 - 3/8 | (12.5 - 9.5 mm) | 500 |
| 3/8 - #4 | (9.5 - 4.75 mm) | 1278 |
| #4 - #8 | (4.75 - 2.36 mm) | 329 |
| #8 - #16 | (2.36 - 1.18 mm) | 284 |
| #16 - #30 | (1.18 - 0.6 mm) | 504 |
| #30 - #50 | (0.6 - 0.3 mm) | 855 |
| #50 - #100 | (0.3 - 0.15 mm) | 162 |
| #100 - #200 | (0.15 - 0.075 mm) | 23 |
| - #200 | ( - 0.075 mm) | 36 |
| TOTAL | | 4500 |
| PG 76-22 | | 5.20% |

## Mix I

| 9.5mm Gravel Coarse, 0% Sand | | |
|---|---|---|
| | | |
| Gravel 8's | | 50% |
| Washed LSS | | 25% |
| Limestone Sand | | 25% |
| Sieve | | Mass, g |
| 1 - 3/4 | (25 - 19 mm) | 0 |
| 3/4 - 1/2 | (19 - 12.5 mm) | 0 |
| 1/2 - 3/8 | (12.5 - 9.5 mm) | 297 |
| 3/8 - #4 | (9.5 - 4.75 mm) | 1787 |
| #4 - #8 | (4.75 - 2.36 mm) | 923 |
| #8 - #16 | (2.36 - 1.18 mm) | 567 |
| #16 - #30 | (1.18 - 0.6 mm) | 383 |
| #30 - #50 | (0.6 - 0.3 mm) | 248 |
| #50 - #100 | (0.3 - 0.15 mm) | 117 |
| #100 - #200 | (0.15 - 0.075 mm) | 77 |
| - #200 | ( - 0.075 mm) | 104 |
| TOTAL | | 4503 |
| PG 64-22 | | 7.10% |

## Mix J

| 9.5mm Gravel Coarse, 40% Sand | | |
|---|---|---|
| Gravel 8's | | 50% |
| Limestone Sand | | 10% |
| Natural Sand | | 40% |
| | | |
| Sieve | | Mass, g |
| 1 - 3/4 | (25 - 19 mm) | 0 |
| 3/4 - 1/2 | (19 - 12.5 mm) | 0 |
| 1/2 - 3/8 | (12.5 - 9.5 mm) | 297 |
| 3/8 - #4 | (9.5 - 4.75 mm) | 1670 |
| #4 - #8 | (4.75 - 2.36 mm) | 594 |
| #8 - #16 | (2.36 - 1.18 mm) | 342 |
| #16 - #30 | (1.18 - 0.6 mm) | 518 |
| #30 - #50 | (0.6 - 0.3 mm) | 842 |
| #50 - #100 | (0.3 - 0.15 mm) | 171 |
| #100 - #200 | (0.15 - 0.075 mm) | 23 |
| - #200 | ( - 0.075 mm) | 45 |
| TOTAL | | 4500 |
| PG 76-22 | | 5.90% |

## Mix K

| 19mm Gravel Coarse, 0% Sand | | |
|---|---|---|
| Gravel 57's | | 30% |
| Gravel 8's | | 25% |
| Washed LSS | | 25% |
| Limestone Sand | | 20% |
| Sieve | | Mass, g |
| 1 - 3/4 | (25 - 19 mm) | 270 |
| 3/4 - 1/2 | (19 - 12.5 mm) | 500 |
| 1/2 - 3/8 | (12.5 - 9.5 mm) | 405 |
| 3/8 - #4 | (9.5 - 4.75 mm) | 1238 |
| #4 - #8 | (4.75 - 2.36 mm) | 752 |
| #8 - #16 | (2.36 - 1.18 mm) | 518 |
| #16 - #30 | (1.18 - 0.6 mm) | 347 |
| #30 - #50 | (0.6 - 0.3 mm) | 216 |
| #50 - #100 | (0.3 - 0.15 mm) | 131 |
| #100 - #200 | (0.15 - 0.075 mm) | 68 |
| - #200 | ( - 0.075 mm) | 59 |
| TOTAL | | 4504 |
| PG 76-22 | | 5.40% |

## Mix L

| 19mm Gravel Coarse, 40% Sand | | |
|---|---|---|
| Gravel 57's | | 35% |
| Gravel 8's | | 25% |
| Limestone Sand | | 0% |
| Natural Sand | | 40% |
| Sieve | | Mass, g |
| 1 - 3/4 | (25 - 19 mm) | 315 |
| 3/4 - 1/2 | (19 - 12.5 mm) | 581 |
| 1/2 - 3/8 | (12.5 - 9.5 mm) | 450 |
| 3/8 - #4 | (9.5 - 4.75 mm) | 1157 |
| #4 - #8 | (4.75 - 2.36 mm) | 374 |
| #8 - #16 | (2.36 - 1.18 mm) | 243 |
| #16 - #30 | (1.18 - 0.6 mm) | 441 |
| #30 - #50 | (0.6 - 0.3 mm) | 792 |
| #50 - #100 | (0.3 - 0.15 mm) | 95 |
| #100 - #200 | (0.15 - 0.075 mm) | 9 |
| - #200 | ( - 0.075 mm) | 45 |
| TOTAL | | 4500 |
| PG 64-22 | | 5.60% |

## Mix M

| 9.5mm Gravel Fine, 0% Sand | | |
|---|---|---|
| Gravel 8's | | 5% |
| Limestone Sand | | 65% |
| Washed LSS | | 30% |
| | | |
| Sieve | | Mass, g |
| 1 - 3/4 | (25 - 19 mm) | 0 |
| 3/4 - 1/2 | (19 - 12.5 mm) | 0 |
| 1/2 - 3/8 | (12.5 - 9.5 mm) | 32 |
| 3/8 - #4 | (9.5 - 4.75 mm) | 473 |
| #4 - #8 | (4.75 - 2.36 mm) | 1152 |
| #8 - #16 | (2.36 - 1.18 mm) | 1017 |
| #16 - #30 | (1.18 - 0.6 mm) | 729 |
| #30 - #50 | (0.6 - 0.3 mm) | 504 |
| #50 - #100 | (0.3 - 0.15 mm) | 266 |
| #100 - #200 | (0.15 - 0.075 mm) | 144 |
| - #200 | ( - 0.075 mm) | 185 |
| TOTAL | | 4500 |
| PG 76-22 | | 7.50% |

## Mix N

| 9.5mm Gravel Fine, 40% Sand | | |
|---|---|---|
| Gravel 8's | | 16% |
| Limestone Sand | | 44% |
| Natural Sand | | 40% |
| | | |
| Sieve | | Mass, g |
| 1 - 3/4 | (25 - 19 mm) | 0 |
| 3/4 - 1/2 | (19 - 12.5 mm) | 0 |
| 1/2 - 3/8 | (12.5 - 9.5 mm) | 94 |
| 3/8 - #4 | (9.5 - 4.75 mm) | 675 |
| #4 - #8 | (4.75 - 2.36 mm) | 716 |
| #8 - #16 | (2.36 - 1.18 mm) | 635 |
| #16 - #30 | (1.18 - 0.6 mm) | 779 |
| #30 - #50 | (0.6 - 0.3 mm) | 1022 |
| #50 - #100 | (0.3 - 0.15 mm) | 270 |
| #100 - #200 | (0.15 - 0.075 mm) | 77 |
| - #200 | ( - 0.075 mm) | 234 |
| TOTAL | | 4500 |
| PG 64-22 | | 6.30% |

## Mix O

| 19mm Gravel Fine, 0% Sand | | |
|---|---|---|
| Gravel 57's | | 18% |
| Gravel 8's | | 17% |
| Limestone Sand | | 50% |
| Washed LSS | | 15% |
| Sieve | | Mass, g |
| 1 - 3/4 | (25 - 19 mm) | 162 |
| 3/4 - 1/2 | (19 - 12.5 mm) | 302 |
| 1/2 - 3/8 | (12.5 - 9.5 mm) | 252 |
| 3/8 - #4 | (9.5 - 4.75 mm) | 914 |
| #4 - #8 | (4.75 - 2.36 mm) | 896 |
| #8 - #16 | (2.36 - 1.18 mm) | 662 |
| #16 - #30 | (1.18 - 0.6 mm) | 522 |
| #30 - #50 | (0.6 - 0.3 mm) | 351 |
| #50 - #100 | (0.3 - 0.15 mm) | 176 |
| #100 - #200 | (0.15 - 0.075 mm) | 131 |
| - #200 | ( - 0.075 mm) | 135 |
| TOTAL | | 4500 |
| PG 64-22 | | 5.00% |

## Mix P

| 19mm Gravel Fine, 40% Sand | | |
|---|---|---|
| Gravel 57's | | 29% |
| Gravel 8's | | 13% |
| Limestone Sand | | 18% |
| Natural Sand | | 40% |
| Sieve | | Mass, g |
| 1 - 3/4 | (25 - 19 mm) | 261 |
| 3/4 - 1/2 | (19 - 12.5 mm) | 481 |
| 1/2 - 3/8 | (12.5 - 9.5 mm) | 329 |
| 3/8 - #4 | (9.5 - 4.75 mm) | 765 |
| #4 - #8 | (4.75 - 2.36 mm) | 473 |
| #8 - #16 | (2.36 - 1.18 mm) | 374 |
| #16 - #30 | (1.18 - 0.6 mm) | 580 |
| #30 - #50 | (0.6 - 0.3 mm) | 886 |
| #50 - #100 | (0.3 - 0.15 mm) | 194 |
| #100 - #200 | (0.15 - 0.075 mm) | 36 |
| - #200 | ( - 0.075 mm) | 121 |
| TOTAL | | 4500 |
| PG 76-22 | | 6.20% |

This is a blank Page

# APPENDIX B

## WORKSHEET FOR CALCULATING SHEAR STRESS AND

## CONTACT ENERGY INDEX, CEI

# Recommended Procedure for Calculating the Shear Force and Contact Energy Index (CEI)

1. Prepare gyratory specimens and compact them up to 200 gyrations
2. Fit a polynomial function to the compaction curve (Air voids, % versus Number of Gyrations, N)
3. Use the polynomial function to determine the number of gyration ($N_{G1}$) at which the change in the slope is equal to 0.001%.
4. Use the equation:

$$S = \frac{2 * W * L}{A * h}$$

   with S, A, and h values to calculate W (the actuator force value $P_1$) at every gyration, where:
   S: is the shear stress,
   A and h: are the sectional area and the height respectively,
   W: is the applied forced to proceed the angle, and
   L: is the moment arm (165 mm)
5. Use the equation (3.11, Chapter 3) to determine the shear force, $S_\theta$

$$S_\theta = (N_2 - N_1)\cos\theta + \frac{1}{2}\left(\sum P - W_d\right)\tan\theta$$

   where: $N_2$-$N_1$ is derived from equation (3.8), (the parameters in this equation can be found in the next table,
   $\Sigma P$: is calculated from equations (3.7), and (3.1),
   $W_d$ : is the weight of the mold (For Servopac Gyratory at UI, 15960 gm) and
   θ: is the angle of gyration
6. Use equation (3.16) to calculate the contact energy index

$$\text{Contact Energy index} = \sum_{N_{G1}}^{N_{G2}} S_\theta \cdot d_e$$

   where : $S_\theta$ is the shear force derived from step 5
   $d_e$ is the change in height at each consecutive gyrations
   $N_{G1}$: is derived from step 3
   $N_{G2}$ : is the termination number of gyration ( i.e. 200)

Measurements and Data required for Mix A at Pressure of 600 kPa and Angle of 1.5°

| mix ID | A | |
|---|---|---|
| diameter (D) | 150 | mm |
| vertical stress (A) | 600 | kPa |
| angle ($\theta$) | 1.5 | degree |
| mix weight ($W_m$) | 4.69 | kg |
| max specific gravity ($G_{mm}$) | 2506 | kg/m3 |
| max No. of gyrations | 160 | |
| mold weight ($W_d$) | 15.96 | kg |
| moment arm (L) | 165 | mm |
| friction factor ($\mu$) | 0.28 | |
| $x_\theta$ | 12.5 | mm |
| $N_{G1}$ | 14 | |
| $d_1$ (=$d_2$) | 142.89 | mm |

| N | Pres. | Servopac output | | | P1 (N) | P2,P3 (N) | Determination of $N_{G1}$ | | | N2-N1 | N1+N2 | $S_0$ (kPa) | Contact E.I. | Total E.I. |
|---|---|---|---|---|---|---|---|---|---|---|---|---|---|---|
| | | height | angle | shear | | | % Av | slope | Δ slope | | | | | |
| 1 | 580 | 137.72 | 1.39 | 162 | 1194.73 | 1402.78 | 23.089 | -8.618 | 0.920 | 2108.396 | -2974.281 | 118.13 | | 7.60 |
| 2 | 599 | 133.02 | 1.54 | 278 | 1980.25 | 2210.17 | 20.372 | -9.539 | 0.635 | 2229.016 | -4424.546 | 124.21 | 9.81 | 8.85 |
| 3 | 600 | 130.17 | 1.52 | 319 | 2223.62 | 2446.06 | 18.635 | -10.174 | 0.364 | 2288.11 | -4829.697 | 127.41 | 6.26 | 8.96 |
| 4 | 600 | 128.14 | 1.5 | 342 | 2346.76 | 2562.85 | 17.341 | -10.537 | 0.206 | 2328.024 | -5026.059 | 129.61 | 4.57 | 9.00 |
| 5 | 600 | 126.57 | 1.5 | 357 | 2419.68 | 2633.12 | 16.309 | -10.743 | 0.111 | 2353.146 | -5144.499 | 130.98 | 3.60 | 9.09 |
| 6 | 600 | 125.29 | 1.49 | 368 | 2469.01 | 2678.88 | 15.453 | -10.855 | 0.052 | 2376.714 | -5219.129 | 132.30 | 2.96 | 9.12 |
| 7 | 600 | 124.23 | 1.49 | 378 | 2514.65 | 2722.74 | 14.725 | -10.907 | 0.014 | 2393.926 | -5292.708 | 133.24 | 2.48 | 9.19 |
| 8 | 600 | 123.3 | 1.49 | 386 | 2548.64 | 2755.18 | 14.092 | -10.921 | -0.011 | 2408.849 | -5346.485 | 134.06 | 2.19 | 9.24 |
| 9 | 600 | 122.51 | 1.49 | 393 | 2578.24 | 2783.45 | 13.533 | -10.910 | -0.029 | 2421.67 | -5393.429 | 134.77 | 1.87 | 9.29 |
| 10 | 600 | 121.8 | 1.49 | 398 | 2595.91 | 2799.93 | 13.035 | -10.881 | -0.040 | 2432.795 | -5419.71 | 135.39 | 1.69 | 9.33 |
| 11 | 600 | 121.16 | 1.49 | 403 | 2614.71 | 2817.66 | 12.585 | -10.841 | -0.049 | 2443.045 | -5448.511 | 135.96 | 1.53 | 9.37 |
| 12 | 600 | 120.59 | 1.49 | 407 | 2628.23 | 2830.24 | 12.176 | -10.792 | -0.054 | 2452.054 | -5468.431 | 136.46 | 1.37 | 9.41 |
| 13 | 600 | 120.09 | 1.49 | 410 | 2636.63 | 2837.79 | 11.802 | -10.738 | -0.058 | 2459.809 | -5479.714 | 136.89 | 1.21 | 9.44 |
| 14 | 600 | 119.63 | 1.49 | 413 | 2645.75 | 2846.14 | 11.457 | -10.680 | -0.061 | 2467.053 | -5492.578 | 137.30 | 1.11 | 9.47 |
| 15 | 600 | 119.19 | 1.49 | 416 | 2655.17 | 2854.82 | 11.138 | -10.619 | -0.062 | 2474.052 | -5506.116 | 137.69 | 1.07 | 9.49 |
| 16 | 601 | 118.78 | 1.49 | 419 | 2665.11 | 2864.41 | 10.841 | -10.557 | -0.063 | 2484.533 | -5521.642 | 138.27 | 1.00 | 9.53 |
| 17 | 601 | 118.44 | 1.49 | 421 | 2670.17 | 2868.90 | 10.564 | -10.493 | -0.064 | 2489.87 | -5528.14 | 138.57 | 0.83 | 9.55 |
| 18 | 601 | 118.1 | 1.49 | 422 | 2668.83 | 2866.99 | 10.305 | -10.430 | -0.064 | 2494.873 | -5523.242 | 138.86 | 0.83 | 9.57 |
| 19 | 601 | 117.76 | 1.5 | 424 | 2673.76 | 2872.67 | 10.060 | -10.366 | -0.064 | 2496.824 | -5533.035 | 138.95 | 0.83 | 9.64 |
| 20 | 601 | 117.45 | 1.5 | 426 | 2679.30 | 2877.69 | 9.830 | -10.302 | -0.063 | 2501.788 | -5540.597 | 139.23 | 0.76 | 9.66 |
| 21 | 601 | 117.18 | 1.5 | 427 | 2679.41 | 2877.35 | 9.613 | -10.239 | -0.063 | 2505.866 | -5538.793 | 139.46 | 0.66 | 9.68 |
| 22 | 601 | 116.91 | 1.5 | 429 | 2685.76 | 2883.24 | 9.406 | -10.176 | -0.062 | 2510.297 | -5548.087 | 139.70 | 0.67 | 9.70 |
| 23 | 601 | 116.66 | 1.5 | 430 | 2686.27 | 2883.32 | 9.210 | -10.114 | -0.061 | 2514.115 | -5547.122 | 139.92 | 0.62 | 9.71 |
| 24 | 601 | 116.44 | 1.5 | 431 | 2687.43 | 2884.12 | 9.024 | -10.053 | -0.060 | 2517.523 | -5547.565 | 140.11 | 0.54 | 9.73 |
| 25 | 601 | 116.2 | 1.49 | 431 | 2681.90 | 2876.87 | 8.846 | -9.993 | -0.060 | 2524.289 | -5532.46 | 140.52 | 0.59 | 9.69 |
| 26 | 601 | 115.98 | 1.49 | 433 | 2689.24 | 2883.84 | 8.677 | -9.933 | -0.059 | 2528.055 | -5543.91 | 140.73 | 0.55 | 9.70 |
| 27 | 601 | 115.78 | 1.5 | 434 | 2690.80 | 2886.37 | 8.514 | -9.874 | -0.058 | 2527.784 | -5548.637 | 140.69 | 0.50 | 9.77 |
| 28 | 601 | 115.59 | 1.5 | 434 | 2686.39 | 2881.64 | 8.359 | -9.816 | -0.057 | 2530.453 | -5539.353 | 140.85 | 0.47 | 9.78 |
| 29 | 601 | 115.39 | 1.5 | 435 | 2687.92 | 2882.83 | 8.210 | -9.759 | -0.056 | 2533.61 | -5540.585 | 141.03 | 0.50 | 9.79 |
| 30 | 601 | 115.22 | 1.49 | 435 | 2683.96 | 2877.28 | 8.066 | -9.703 | -0.055 | 2539.42 | -5528.862 | 141.38 | 0.42 | 9.75 |
| 31 | 601 | 115.06 | 1.5 | 436 | 2686.39 | 2880.75 | 7.929 | -9.648 | -0.054 | 2538.608 | -5535.401 | 141.31 | 0.40 | 9.81 |
| 32 | 601 | 114.86 | 1.49 | 437 | 2687.87 | 2880.60 | 7.796 | -9.593 | -0.054 | 2545.193 | -5533.163 | 141.70 | 0.50 | 9.77 |
| 33 | 601 | 114.72 | 1.49 | 437 | 2684.60 | 2877.08 | 7.668 | -9.540 | -0.053 | 2547.175 | -5526.287 | 141.82 | 0.35 | 9.78 |
| 34 | 601 | 114.56 | 1.5 | 437 | 2680.85 | 2874.36 | 7.545 | -9.487 | -0.052 | 2546.034 | -5521.795 | 141.74 | 0.40 | 9.84 |

**B - 3**

| N | Pres. | Servopac output height | angle | shear | P1 (N) | P2,P3 (N) | Determination of $N_{G1}$ % Av | slope | Δ slope | N2-N1 | N1+N2 | $S_θ$ (kPa) | Contact E.I. | Total E.I. |
|---|---|---|---|---|---|---|---|---|---|---|---|---|---|---|
| 35 | 601 | 114.41 | 1.49 | 438 | 2683.47 | 2875.44 | 7.426 | -9.435 | -0.051 | 2551.917 | -5521.974 | 142.09 | 0.38 | 9.80 |
| 36 | 601 | 114.28 | 1.5 | 439 | 2686.54 | 2879.58 | 7.311 | -9.384 | -0.050 | 2550.698 | -5529.828 | 142.00 | 0.33 | 9.86 |
| 37 | 601 | 114.14 | 1.5 | 439 | 2683.25 | 2876.05 | 7.199 | -9.333 | -0.050 | 2552.693 | -5522.917 | 142.11 | 0.35 | 9.86 |
| 38 | 601 | 114.03 | 1.49 | 439 | 2680.66 | 2871.99 | 7.091 | -9.283 | -0.049 | 2557.671 | -5514.148 | 142.41 | 0.28 | 9.82 |
| 39 | 601 | 113.88 | 1.5 | 439 | 2677.14 | 2869.50 | 6.987 | -9.234 | -0.048 | 2556.407 | -5510.082 | 142.33 | 0.38 | 9.88 |
| 40 | 601 | 113.77 | 1.5 | 439 | 2674.55 | 2865.44 | 6.886 | -9.186 | -0.048 | 2561.385 | -5501.326 | 142.63 | 0.28 | 9.83 |
| 41 | 601 | 113.65 | 1.49 | 440 | 2677.82 | 2869.79 | 6.787 | -9.138 | -0.047 | 2560.039 | -5509.568 | 142.53 | 0.30 | 9.89 |
| 42 | 601 | 113.53 | 1.49 | 439 | 2668.91 | 2859.40 | 6.692 | -9.091 | -0.046 | 2564.822 | -5489.489 | 142.83 | 0.30 | 9.85 |
| 43 | 601 | 113.41 | 1.5 | 441 | 2678.23 | 2869.80 | 6.599 | -9.045 | -0.046 | 2563.822 | -5508.512 | 142.75 | 0.30 | 9.91 |
| 44 | 601 | 113.31 | 1.49 | 441 | 2675.87 | 2865.99 | 6.509 | -8.999 | -0.045 | 2568.663 | -5500.253 | 143.04 | 0.25 | 9.86 |
| 45 | 601 | 113.2 | 1.5 | 441 | 2673.27 | 2864.49 | 6.422 | -8.954 | -0.045 | 2566.843 | -5498.104 | 142.92 | 0.28 | 9.92 |
| 46 | 601 | 113.1 | 1.49 | 441 | 2670.91 | 2860.68 | 6.336 | -8.909 | -0.044 | 2571.684 | -5489.855 | 143.22 | 0.25 | 9.87 |
| 47 | 602 | 113.02 | 1.5 | 441 | 2669.02 | 2860.25 | 6.253 | -8.865 | -0.044 | 2573.441 | -5489.94 | 143.30 | 0.20 | 9.95 |
| 48 | 602 | 112.91 | 1.49 | 441 | 2666.43 | 2856.19 | 6.173 | -8.821 | -0.043 | 2578.433 | -5481.198 | 143.60 | 0.28 | 9.90 |
| 49 | 602 | 112.83 | 1.5 | 441 | 2664.54 | 2855.44 | 6.094 | -8.778 | -0.043 | 2576.189 | -5480.519 | 143.46 | 0.20 | 9.96 |
| 50 | 601 | 112.71 | 1.49 | 441 | 2661.70 | 2850.82 | 6.017 | -8.736 | -0.042 | 2577.311 | -5470.542 | 143.54 | 0.30 | 9.90 |
| 51 | 601 | 112.62 | 1.5 | 441 | 2659.58 | 2849.81 | 5.942 | -8.694 | -0.042 | 2575.219 | -5469.353 | 143.41 | 0.23 | 9.95 |
| 52 | 602 | 112.54 | 1.49 | 441 | 2657.69 | 2846.83 | 5.869 | -8.652 | -0.041 | 2583.79 | -5462.87 | 143.91 | 0.20 | 9.92 |
| 53 | 602 | 112.42 | 1.5 | 442 | 2660.87 | 2851.08 | 5.797 | -8.611 | -0.041 | 2582.475 | -5470.911 | 143.82 | 0.31 | 9.98 |
| 54 | 602 | 112.34 | 1.5 | 442 | 2658.98 | 2849.06 | 5.728 | -8.570 | -0.040 | 2583.638 | -5466.936 | 143.89 | 0.20 | 9.99 |
| 55 | 602 | 112.25 | 1.49 | 442 | 2656.85 | 2845.51 | 5.660 | -8.530 | -0.040 | 2588.343 | -5459.209 | 144.17 | 0.23 | 9.94 |
| 56 | 602 | 112.17 | 1.5 | 443 | 2660.96 | 2850.75 | 5.593 | -8.490 | -0.040 | 2586.451 | -5469.187 | 144.04 | 0.20 | 10.00 |
| 57 | 602 | 112.12 | 1.5 | 442 | 2653.77 | 2843.48 | 5.528 | -8.450 | -0.039 | 2586.843 | -5456.005 | 144.07 | 0.13 | 10.00 |
| 58 | 602 | 112.03 | 1.49 | 443 | 2657.64 | 2845.93 | 5.464 | -8.411 | -0.039 | 2591.887 | -5458.974 | 144.37 | 0.23 | 9.95 |
| 59 | 602 | 111.97 | 1.49 | 443 | 2656.22 | 2844.40 | 5.402 | -8.372 | -0.038 | 2592.762 | -5455.99 | 144.42 | 0.15 | 9.96 |
| 60 | 602 | 111.88 | 1.49 | 443 | 2654.08 | 2842.12 | 5.341 | -8.334 | -0.038 | 2594.076 | -5451.514 | 144.50 | 0.23 | 9.96 |
| 61 | 602 | 111.82 | 1.5 | 442 | 2646.67 | 2835.87 | 5.281 | -8.296 | -0.038 | 2591.224 | -5441.097 | 144.33 | 0.15 | 10.02 |
| 62 | 602 | 111.75 | 1.5 | 443 | 2651.00 | 2840.08 | 5.223 | -8.258 | -0.037 | 2592.585 | -5448.277 | 144.40 | 0.18 | 10.02 |
| 63 | 602 | 111.68 | 1.49 | 443 | 2649.34 | 2837.04 | 5.166 | -8.221 | -0.037 | 2597 | -5441.566 | 144.67 | 0.18 | 9.97 |
| 64 | 602 | 111.61 | 1.5 | 443 | 2647.68 | 2836.52 | 5.109 | -8.184 | -0.037 | 2594.635 | -5441.306 | 144.52 | 0.18 | 10.03 |
| 65 | 602 | 111.55 | 1.49 | 443 | 2646.26 | 2833.74 | 5.054 | -8.147 | -0.036 | 2598.903 | -5435.1 | 144.78 | 0.15 | 9.98 |
| 66 | 602 | 111.51 | 1.5 | 443 | 2645.31 | 2833.98 | 5.001 | -8.111 | -0.036 | 2596.102 | -5436.327 | 144.60 | 0.10 | 10.04 |
| 67 | 602 | 111.41 | 1.49 | 443 | 2642.93 | 2830.18 | 4.948 | -8.075 | -0.036 | 2600.956 | -5428.136 | 144.90 | 0.26 | 9.99 |
| 68 | 602 | 111.38 | 1.49 | 443 | 2642.22 | 2829.42 | 4.896 | -8.039 | -0.036 | 2601.396 | -5426.643 | 144.92 | 0.08 | 9.99 |

| N | Pres. | Servopac output height | angle | shear | P1 (N) | P2,P3 (N) | Determination of $N_{G1}$ % Av | slope | Δ slope | N2-N1 | N1+N2 | $S_\theta$ (kPa) | Contact E.I. | Total E.I. |
|----|-----|--------|------|-----|---------|----------|-------|--------|--------|-----------|-----------|--------|------|-------|
| 69 | 602 | 111.32 | 1.49 | 443 | 2640.80 | 2827.89 | 4.845 | -8.003 | -0.035 | 2602.277 | -5423.659 | 144.97 | 0.15 | 10.00 |
| 70 | 602 | 111.25 | 1.5  | 443 | 2639.14 | 2827.37 | 4.795 | -7.968 | -0.035 | 2599.922 | -5423.38  | 144.83 | 0.18 | 10.05 |
| 71 | 602 | 111.2  | 1.5  | 443 | 2637.95 | 2826.10 | 4.746 | -7.933 | -0.035 | 2600.657 | -5420.89  | 144.87 | 0.13 | 10.06 |
| 72 | 602 | 111.13 | 1.49 | 443 | 2636.29 | 2823.07 | 4.698 | -7.898 | -0.035 | 2605.07  | -5414.207 | 145.14 | 0.18 | 10.01 |
| 73 | 602 | 111.1  | 1.49 | 443 | 2635.58 | 2822.30 | 4.651 | -7.864 | -0.034 | 2605.512 | -5412.714 | 145.16 | 0.08 | 10.01 |
| 74 | 602 | 111.02 | 1.5  | 443 | 2633.68 | 2821.52 | 4.604 | -7.829 | -0.034 | 2603.309 | -5411.926 | 145.02 | 0.21 | 10.07 |
| 75 | 602 | 110.98 | 1.5  | 443 | 2632.73 | 2820.51 | 4.559 | -7.795 | -0.034 | 2603.899 | -5409.934 | 145.06 | 0.10 | 10.07 |
| 76 | 602 | 110.91 | 1.5  | 443 | 2631.07 | 2818.73 | 4.514 | -7.761 | -0.034 | 2604.932 | -5406.448 | 145.12 | 0.18 | 10.07 |
| 77 | 602 | 110.86 | 1.5  | 443 | 2629.89 | 2817.46 | 4.470 | -7.728 | -0.033 | 2605.671 | -5403.958 | 145.16 | 0.13 | 10.08 |
| 78 | 602 | 110.82 | 1.49 | 443 | 2628.94 | 2815.19 | 4.427 | -7.694 | -0.033 | 2609.639 | -5398.784 | 145.40 | 0.10 | 10.03 |
| 79 | 602 | 110.78 | 1.49 | 443 | 2627.99 | 2814.17 | 4.385 | -7.661 | -0.033 | 2610.23  | -5396.794 | 145.44 | 0.10 | 10.03 |
| 80 | 602 | 110.73 | 1.5  | 443 | 2626.80 | 2814.15 | 4.343 | -7.628 | -0.033 | 2607.592 | -5397.484 | 145.27 | 0.13 | 10.08 |
| 81 | 602 | 110.72 | 1.5  | 443 | 2626.57 | 2813.90 | 4.302 | -7.595 | -0.033 | 2607.74  | -5396.986 | 145.28 | 0.03 | 10.08 |
| 82 | 602 | 110.64 | 1.5  | 443 | 2624.67 | 2811.87 | 4.261 | -7.563 | -0.032 | 2608.924 | -5393.001 | 145.35 | 0.21 | 10.09 |
| 83 | 602 | 110.58 | 1.5  | 443 | 2623.24 | 2810.34 | 4.222 | -7.530 | -0.032 | 2609.812 | -5390.013 | 145.40 | 0.15 | 10.09 |
| 84 | 602 | 110.55 | 1.49 | 442 | 2616.61 | 2802.41 | 4.183 | -7.498 | -0.032 | 2613.293 | -5374.807 | 145.62 | 0.08 | 10.04 |
| 85 | 602 | 110.5  | 1.49 | 443 | 2621.35 | 2807.06 | 4.144 | -7.466 | -0.032 | 2614.371 | -5382.863 | 145.68 | 0.13 | 10.04 |
| 86 | 602 | 110.45 | 1.5  | 442 | 2614.25 | 2801.12 | 4.106 | -7.434 | -0.032 | 2611.405 | -5373.004 | 145.50 | 0.13 | 10.10 |
| 87 | 602 | 110.41 | 1.5  | 442 | 2613.30 | 2800.11 | 4.069 | -7.403 | -0.032 | 2611.998 | -5371.016 | 145.53 | 0.10 | 10.10 |
| 88 | 602 | 110.39 | 1.49 | 441 | 2606.91 | 2792.44 | 4.032 | -7.371 | -0.031 | 2615.326 | -5356.333 | 145.74 | 0.05 | 10.05 |
| 89 | 602 | 110.32 | 1.5  | 441 | 2605.26 | 2791.92 | 3.996 | -7.340 | -0.031 | 2613     | -5356.02  | 145.59 | 0.18 | 10.11 |
| 90 | 602 | 110.28 | 1.49 | 441 | 2604.32 | 2789.66 | 3.961 | -7.308 | -0.031 | 2616.958 | -5350.881 | 145.83 | 0.10 | 10.06 |
| 91 | 602 | 110.25 | 1.5  | 441 | 2603.61 | 2790.15 | 3.926 | -7.277 | -0.031 | 2614.04  | -5352.546 | 145.65 | 0.08 | 10.11 |
| 92 | 602 | 110.21 | 1.49 | 441 | 2602.66 | 2787.89 | 3.891 | -7.246 | -0.031 | 2617.998 | -5347.411 | 145.90 | 0.10 | 10.06 |
| 93 | 602 | 110.18 | 1.5  | 441 | 2601.96 | 2788.38 | 3.857 | -7.216 | -0.031 | 2615.081 | -5349.073 | 145.71 | 0.08 | 10.11 |
| 94 | 602 | 110.12 | 1.49 | 441 | 2600.54 | 2785.61 | 3.824 | -7.185 | -0.031 | 2619.336 | -5342.95  | 145.97 | 0.15 | 10.06 |
| 95 | 602 | 110.1  | 1.5  | 441 | 2600.07 | 2786.35 | 3.791 | -7.154 | -0.030 | 2616.272 | -5345.103 | 145.78 | 0.05 | 10.12 |
| 96 | 602 | 110.05 | 1.49 | 441 | 2598.89 | 2783.84 | 3.758 | -7.124 | -0.030 | 2620.377 | -5339.48  | 146.03 | 0.13 | 10.07 |
| 97 | 602 | 110.02 | 1.5  | 441 | 2598.18 | 2784.33 | 3.726 | -7.094 | -0.030 | 2617.463 | -5341.133 | 145.85 | 0.08 | 10.12 |
| 98 | 602 | 109.98 | 1.5  | 440 | 2591.34 | 2777.42 | 3.695 | -7.064 | -0.030 | 2617.725 | -5328.659 | 145.87 | 0.10 | 10.13 |
| 99 | 602 | 109.95 | 1.5  | 440 | 2590.64 | 2776.67 | 3.664 | -7.034 | -0.030 | 2618.172 | -5327.173 | 145.90 | 0.08 | 10.13 |
| 100 | 602 | 109.91 | 1.49 | 440 | 2589.69 | 2774.42 | 3.633 | -7.004 | -0.030 | 2622.125 | -5322.057 | 146.14 | 0.10 | 10.08 |
| 101 | 602 | 109.88 | 1.49 | 439 | 2583.10 | 2767.78 | 3.603 | -6.974 | -0.030 | 2622.235 | -5310.093 | 146.15 | 0.08 | 10.08 |
| 102 | 602 | 109.84 | 1.5  | 439 | 2582.16 | 2768.01 | 3.573 | -6.944 | -0.030 | 2619.48  | -5311.249 | 145.98 | 0.10 | 10.13 |

| N | Pres. | Servopac output | | | P1 (N) | P2,P3 (N) | Determination of $N_{G1}$ | | | N2-N1 | N1+N2 | $S_\theta$ (kPa) | Contact E.I. | Total E.I. |
|---|---|---|---|---|---|---|---|---|---|---|---|---|---|---|
| | | height | angle | shear | | | % Av | slope | Δ slope | | | | | |
| 103 | 602 | 109.82 | 1.5 | 439 | 2581.69 | 2767.50 | 3.544 | -6.915 | -0.029 | 2619.778 | -5310.261 | 146.00 | 0.05 | 10.13 |
| 104 | 602 | 109.78 | 1.5 | 439 | 2580.75 | 2766.50 | 3.515 | -6.886 | -0.029 | 2620.376 | -5308.283 | 146.03 | 0.10 | 10.14 |
| 105 | 602 | 109.77 | 1.49 | 439 | 2580.52 | 2765.00 | 3.486 | -6.856 | -0.029 | 2623.876 | -5304.661 | 146.25 | 0.03 | 10.08 |
| 106 | 602 | 109.71 | 1.49 | 439 | 2579.11 | 2763.49 | 3.458 | -6.827 | -0.029 | 2624.772 | -5301.698 | 146.30 | 0.16 | 10.09 |
| 107 | 602 | 109.67 | 1.49 | 439 | 2578.17 | 2762.49 | 3.430 | -6.798 | -0.029 | 2625.37 | -5299.723 | 146.33 | 0.10 | 10.09 |
| 108 | 602 | 109.65 | 1.5 | 438 | 2571.82 | 2757.35 | 3.403 | -6.769 | -0.029 | 2621.986 | -5291.399 | 146.13 | 0.05 | 10.14 |
| 109 | 602 | 109.62 | 1.49 | 438 | 2571.12 | 2755.36 | 3.376 | -6.740 | -0.029 | 2625.781 | -5286.799 | 146.36 | 0.08 | 10.09 |
| 110 | 602 | 109.6 | 1.49 | 438 | 2570.65 | 2754.85 | 3.349 | -6.711 | -0.029 | 2626.08 | -5285.813 | 146.38 | 0.05 | 10.09 |
| 111 | 602 | 109.56 | 1.49 | 438 | 2569.71 | 2753.85 | 3.323 | -6.683 | -0.029 | 2626.678 | -5283.841 | 146.41 | 0.10 | 10.09 |
| 112 | 602 | 109.53 | 1.49 | 438 | 2569.01 | 2753.09 | 3.297 | -6.654 | -0.029 | 2627.127 | -5282.362 | 146.44 | 0.08 | 10.10 |
| 113 | 602 | 109.52 | 1.5 | 437 | 2562.91 | 2748.21 | 3.271 | -6.626 | -0.028 | 2623.598 | -5274.539 | 146.23 | 0.03 | 10.15 |
| 114 | 602 | 109.48 | 1.49 | 437 | 2561.97 | 2745.97 | 3.246 | -6.597 | -0.028 | 2627.539 | -5269.456 | 146.47 | 0.10 | 10.10 |
| 115 | 602 | 109.45 | 1.49 | 436 | 2555.41 | 2739.36 | 3.221 | -6.569 | -0.028 | 2627.652 | -5257.542 | 146.48 | 0.08 | 10.10 |
| 116 | 602 | 109.43 | 1.5 | 436 | 2554.94 | 2740.10 | 3.196 | -6.541 | -0.028 | 2624.614 | -5259.67 | 146.29 | 0.05 | 10.15 |
| 117 | 602 | 109.39 | 1.49 | 436 | 2554.01 | 2737.86 | 3.172 | -6.512 | -0.028 | 2628.551 | -5254.596 | 146.53 | 0.10 | 10.10 |
| 118 | 602 | 109.37 | 1.5 | 437 | 2559.40 | 2744.45 | 3.148 | -6.484 | -0.028 | 2625.848 | -5267.151 | 146.36 | 0.05 | 10.16 |
| 119 | 602 | 109.33 | 1.5 | 435 | 2546.75 | 2731.74 | 3.124 | -6.456 | -0.028 | 2625.781 | -5244.327 | 146.36 | 0.10 | 10.16 |
| 120 | 602 | 109.31 | 1.49 | 435 | 2546.29 | 2730.00 | 3.101 | -6.428 | -0.028 | 2629.415 | -5240.242 | 146.59 | 0.05 | 10.11 |
| 121 | 602 | 109.3 | 1.49 | 435 | 2546.06 | 2729.75 | 3.078 | -6.401 | -0.028 | 2629.565 | -5239.752 | 146.59 | 0.03 | 10.11 |
| 122 | 602 | 109.25 | 1.49 | 435 | 2544.89 | 2728.51 | 3.055 | -6.373 | -0.028 | 2630.315 | -5237.302 | 146.64 | 0.13 | 10.11 |
| 123 | 602 | 109.23 | 1.5 | 434 | 2538.58 | 2723.39 | 3.032 | -6.345 | -0.028 | 2626.95 | -5229.004 | 146.44 | 0.05 | 10.16 |
| 124 | 602 | 109.2 | 1.49 | 433 | 2532.03 | 2715.56 | 3.010 | -6.317 | -0.028 | 2630.394 | -5214.022 | 146.65 | 0.08 | 10.11 |
| 125 | 602 | 109.18 | 1.5 | 433 | 2531.57 | 2716.30 | 2.988 | -6.290 | -0.027 | 2627.369 | -5216.143 | 146.46 | 0.05 | 10.17 |
| 126 | 602 | 109.16 | 1.5 | 433 | 2531.10 | 2715.80 | 2.966 | -6.262 | -0.027 | 2627.67 | -5215.165 | 146.48 | 0.05 | 10.17 |
| 127 | 602 | 109.13 | 1.5 | 433 | 2530.41 | 2715.05 | 2.945 | -6.235 | -0.027 | 2628.121 | -5213.699 | 146.51 | 0.08 | 10.17 |
| 128 | 602 | 109.11 | 1.5 | 433 | 2529.94 | 2714.55 | 2.924 | -6.208 | -0.027 | 2628.422 | -5212.722 | 146.53 | 0.05 | 10.17 |
| 129 | 602 | 109.09 | 1.49 | 433 | 2529.48 | 2712.83 | 2.903 | -6.180 | -0.027 | 2632.048 | -5208.652 | 146.75 | 0.05 | 10.12 |
| 130 | 602 | 109.08 | 1.5 | 433 | 2529.25 | 2713.81 | 2.882 | -6.153 | -0.027 | 2628.874 | -5211.255 | 146.55 | 0.03 | 10.17 |
| 131 | 602 | 109.05 | 1.5 | 433 | 2528.55 | 2713.06 | 2.862 | -6.126 | -0.027 | 2629.326 | -5209.789 | 146.58 | 0.08 | 10.17 |
| 132 | 602 | 109.03 | 1.5 | 431 | 2516.41 | 2700.89 | 2.842 | -6.099 | -0.027 | 2628.961 | -5188.015 | 146.57 | 0.05 | 10.17 |
| 133 | 602 | 109.01 | 1.49 | 431 | 2515.95 | 2699.16 | 2.822 | -6.072 | -0.027 | 2632.58 | -5183.954 | 146.79 | 0.05 | 10.12 |
| 134 | 602 | 108.98 | 1.5 | 431 | 2515.26 | 2699.65 | 2.802 | -6.045 | -0.027 | 2629.715 | -5185.581 | 146.61 | 0.08 | 10.18 |
| 135 | 602 | 108.95 | 1.49 | 431 | 2514.57 | 2697.68 | 2.782 | -6.018 | -0.027 | 2633.484 | -5181.036 | 146.84 | 0.08 | 10.12 |
| 136 | 602 | 108.94 | 1.5 | 431 | 2514.33 | 2698.66 | 2.763 | -5.991 | -0.027 | 2630.318 | -5183.634 | 146.64 | 0.03 | 10.18 |

**B - 6**

This is a blank Page

# APPENDIX C

**JOB MIX FORMULA FOR ITD MIXES (D1, D2 and D3)**

Job Mix Formula for Mix D1

# IDAHO TRANSPORTATION DEPARTMENT
## Department Memorandum

**DATE:** AUGUST 23, 2000

RECEIVED

AUG 2 5 2000

I.T.D. DIV OF HIGHWAYS
COEUR D'ALENE, IDAHO

**PROJECT NO.(S):** IM-90-1(190)10
**AND STP-7236(102)**

**TO:** DAVE FIELDS, P. E.
DIST. 1 CD'A RES. ENGR

**KEY NO.(S): 0519 AND 7584**

**FROM:** TOM BAKER, P.E
MATERIALS ENGINEER

**PROJECT ID, CNTY, ETC.:**
KOOTENAI COUNTY
I90, N.W. BLVD/RAMSEY RD
AND N.W. BLVD IC GATEWAY

**RE:** **PLANT MIX PAVEMENT CLASS I**
SOURCE KT-215
STRATA REPORT NO. S990037-3
ITD LAB REPORT NO. 00 A0125
ASPHALT PG 58 -28

The Job Mix Formula submitted by the Contractor is **CONFIRMED** at the Contractor's selected asphalt content of 4.8% by weight of mix.

Based on source file history the Immersion Compression results are **CONFIRMED** at 0.5% anti-stripping additive.

If you have any questions or comments please call Mike Santi, Pavement Engr., at 334-8450 or Barry Tyler, Aggregate-Asphalt Mix Supv., at 334-8456.

Testing start date = 6/22/00
Testing due date = 7/6/00
Testing completed = 6/28/00
District notified 7/25/00     Renotified 8/23/00
                              Previously confirmed for project STR-5733(603)

cc:     Dave Fields, CD'A Res.
        Dist. 1 Engr.
        Dist. 1 Matls Engr.
        Construction
        Mike Santi
        Asphalt Mix Lab
        File

**C - 3**

# REPORT OF TEST ON AGGREGATE

Lab No. __00 A0163__

Sample of __Plant Mix Design Class I__      Job Order No. __0A-160__

Key No. __0519__    Project No. __IM-90-1(190)10__     Source No. __Kt-215__

Ident No. __ICA / I951510   - A - CE / 101-CX__     Contract Item No. __405-A-1__

Date Sampled __7/26/00__    By __Ron Shippy__     For __Dave Fields__

Test Hole No. _____ Depth _____ County __Kootenai__

Sampled From __stockpiles__     Quantity Represented _____

Location __I90, N.W. Blvd/Ramsey Rd & N.W. Blvd IC Gateway__

Remarks __Also for STP-7235(102) Key 7584__

Test For __Commercial Confirmation Class I__     Date Received __7/28/00__

## Test Results

### Gradation-Percent Passing

| | Stkp | Stkp | Stkp | Stkp | Stkp | | Trial | Com | | |
|---|---|---|---|---|---|---|---|---|---|---|
| Column No. | 1 | 2 | 3 | 4 | 5 | 6 | 7 | 8 | 9 | 10 |
| | A | B | C | FS* | CS* | | 1 | JMF | | |
| 75 mm (3 In.) | | | | | | | | | | |
| 50 mm (2 In.) | | | | | | | | | | |
| 37.5 mm (1½ In.) | | | | | | | | | | |
| 25 mm (1 In.) | 100 | | | | | | 100 | 100 | | |
| 19 mm (3/4 In.) | 92 | 100 | | | | | 99 | 99 | | |
| 12.5 mm (1/2 In.) | 20 | 93 | | | | | 88 | 87 | | |
| 9.5 mm (3/8 In.) | 4 | 62 | 100 | 100 | | | 76 | 75 | | |
| 4.75 mm (No.4) | 2 | 6 | 89 | 98 | 100 | | 53 | 51 | | |
| 2.36 mm (No.8) | 2 | 2 | 55 | 87 | 84 | | 36 | 34 | | |
| 1.18 mm (No.16) | 2 | 1 | 34 | 69 | 45 | | 23 | 22 | | |
| 600 μm (No.30) | 1 | 1 | 23 | 46 | 14 | | 15 | 15 | | |
| 300 μm (No.50) | 1 | 1 | 16 | 21 | 5 | | 9 | 10 | | |
| 150 μm (No. 100) | 1 | 1 | 12 | 6 | 3 | | 5 | 7 | | |
| 75 μm (No.200) | 1.1 | 1.1 | 9.3 | 2.2 | 2.3 | | 4.8 | 5.8 | | |
| Sand Equiv. | | | 69 | 78 | 90 | | | | | |
| T-304 Voids | | | | | | | | | | |
| Liquid Limit | | | | | | | | | | |
| Plastic Index | | | | | | | | | | |

| Resistance Value | |
|---|---|
| Dry (Kg/M³) Max. | |
| Ethylene Glycol % Ret. | |

| SP.GR. | +4.75 mm | -4.75 mm | Ave. |
|---|---|---|---|
| Bulk | | | |
| Apparent | | | |
| Absorption | | | |

| Los Angeles Abrasion | |
|---|---|
| Grading | |
| 500 Rev. | % |

| Crushed Particles Retained | |
|---|---|
| 90% One Face +4.75 mm | % |
| 60% Two Faces +4.75 mm | % |
| Wt. Kg/M³ Loose. | |
| Cleaness Value | |

**For Further Tests, See Lab No's**

STRATA Report No. S000037-3

Date Aggregate Delivered   7/28/00    Date Started   8/15/00

Date Asphalt Delivered   8/15/00    Date Due   8/29/00

Date Commericial Report Received   8/10/00    Date Completed   8/17/00

Remarks:

*FS = Fine Sand (Washed Dover) and CS= Coarse Sand. All stockpiles have been adjusted to match STRATA's gradations.

Material as Represented is:   ☐ Acceptable   ☐ Subject to Rejection   ☒ For Information Only

Recommendations For Mix Design:    Sheet __3__ of __5__

Date Mailed __AUG 24 2000__

**THOMAS S. BAKER**

_____ ,P.E.

Materials Engineer

C - 4

# GRADATION OF INDIVIDUAL STOCKPILES

KEY NO. 0519    PROJECT NO. IM-90-1(190)10    SOURCE NO. Kt-215

DESCRIPTION 00 A0163    TRIAL NO. 1

ITEM NO. 405-A-1    ITEM _____

## PERCENT PASSING

| STOCKPILE | 37.5mm (1½In.) | 31.5mm (1¼In.) | 25mm (1In.) | 19mm (3/4In.) | 12.5mm (1/2In.) | 9.5mm (3/8In.) | 4.75mm (No.4) | 2.36mm (No.8) | 1.18mm (No.16) | 0.6mm (No.30) | 0.3mm (No.50) | 0.15mm (No.100) | 0.075mm (No.200) |
|---|---|---|---|---|---|---|---|---|---|---|---|---|---|
| A | 100 | 100 | 100 | 92 | 20 | 4 | 2 | 2 | 2 | 1 | 1 | 1 | 1.1 |
| B | 100 | 100 | 100 | 100 | 93 | 62 | 6 | 2 | 1 | 1 | 1 | 1 | 1.1 |
| C | 100 | 100 | 100 | 100 | 100 | 100 | 89 | 55 | 34 | 23 | 16 | 12 | 9.3 |
| F.S. | 100 | 100 | 100 | 100 | 100 | 100 | 98 | 87 | 69 | 46 | 21 | 6 | 2.2 |
| C.S. | 100 | 100 | 100 | 100 | 100 | 100 | 100 | 84 | 45 | 14 | 5 | 3 | 2.3 |

## STOCKPILE RATIOS AND BLEND OF AGGREGATE

### PERCENT PASSING

| STOCKPILE | BLEND % | 37.5mm (1½In.) | 31.5mm (1¼In.) | 25mm (1In.) | 19mm (3/4In.) | 12.5mm (1/2In.) | 9.5mm (3/8In.) | 4.75mm (No.4) | 2.36mm (No.8) | 1.18mm (No.16) | 0.6mm (No.30) | 0.3mm (No.50) | 0.15mm (No.100) | 0.075mm (No.200) |
|---|---|---|---|---|---|---|---|---|---|---|---|---|---|---|
| A | 12% | 12 | 12 | 12 | 11 | 2 | 0 | 0 | 0 | 0 | 0 | 0 | 0 | 0.1 |
| B | 32% | 32 | 32 | 32 | 32 | 30 | 20 | 2 | 1 | 0 | 0 | 0 | 0 | 0.4 |
| C | 43% | 43 | 43 | 43 | 43 | 43 | 43 | 38 | 24 | 15 | 10 | 7 | 5 | 4.0 |
| F.S. | 8% | 8 | 8 | 8 | 8 | 8 | 8 | 8 | 7 | 6 | 4 | 2 | 0 | 0.2 |
| C.S. | 5% | 5 | 5 | 5 | 5 | 5 | 5 | 5 | 4 | 2 | 1 | 0 | 0 | 0.1 |
| BLEND | | 100 | 100 | 100 | 99 | 88 | 76 | 53 | 36 | 23 | 15 | 9 | 5 | 4.8 |
| TARGET | | 100 | 100 | 100 | 99 | 87 | 75 | 51 | 34 | 22 | 15 | 10 | 7 | 5.8 |

THOMAS S. BAKER _____ ,P.E. MATERIALS ENGINEER

DATE MAILED AUG 24 2000

# REPORT OF ASPHALT MIX DESIGN TEST RESULTS
## (COMMERCIAL CONFIRMATION)

Key No. __0519__    Project No. __IM-90-1(190)10__     Lab No. __00 A0163__

Test For __Commercial Confirmation Class I__    Source No. __Kt-215__    Trial No. __1__

Comments   Stkp. "A"=12%; "B"=32%; "C"=43%; "F.S."=8%; "C.S."=5%

## HVEEM MIX DESIGN RESULTS  58-28

| Type of Asphalt Used | | PG 64-34 | | |
|---|---|---|---|---|
| % Asphalt by Wt. of Mix | 5.0 | Mix Temp F° | 317.0 | |
| % Asphalt by Wt. of Agg. | 5.3 | Comp. Temp F° | 273.0 | |
| | COM. | ITD | DIFF. | TOLER. |
| MAX. THEO. DEN. | 155.6 | 153.6 | 2.0 | *1 |
| WT./C.F. ASPH. MIX | 149.4 | 149.2 | 0.2 | *1 |
| WT./C.F. AGGREGATE | 141.9 | 141.7 | 0.2 | |
| STABILITY NUMBER | 37 | 38 | 1 | *2 |
| % V.M.A. | 14.4 | 14.6 | 0.2 | *3 |
| % AIR VOIDS | 4.0 | 2.9 | 1.1 | *4 |
| E.A.C. | 4.7 | 5.3 | 0.6 | |
| A. F. T. (MICRONS) | 9 | 12 | 3 | *5 |
| SURFACE AREA | 24.72 | 21.82 | 2.90 | ± 3.0 |

## TRIAL AND JMF GRADATION

| % Passing | JMF | TRIAL | DIFF. | TOLER. |
|---|---|---|---|---|
| 37.5 mm | 100.0 | 100.0 | 0 | ± 3.0 |
| 25 mm | 100.0 | 100.0 | 0 | ± 3.0 |
| 19 mm | 99.0 | 99.0 | 0 | ± 3.0 |
| 12.5 mm | 87.0 | 88.0 | 1 | ± 3.0 |
| 9.5 mm | 75.0 | 76.0 | 1 | ± 3.0 |
| 4.75 mm | 51.0 | 53.0 | 2 | ± 3.0 |
| 2.36 mm | 34.0 | 36.0 | 2 | ± 3.0 |
| 1.18 mm | 22.0 | 23.0 | 1 | ± 2.0 |
| 600 µm | 15.0 | 15.0 | 0 | ± 2.0 |
| 300 µm | 10.0 | 9.0 | 1 | ± 2.0 |
| 150 µm | 7.0 | 5.0 | 2 | ± 2.0 |
| 75 µm | 5.8 | 4.8 | 1.0 | ± 1.0 |

## IMMERSION COMPRESSION RESULTS

| ASPHALT ADDITIVE | | Ad-here 65-50 | | |
|---|---|---|---|---|
| | | I.R.S. % | | |
| % ANTI-STRIP | COM. | ITD | DIFF. | SPECS. |
| 0.5 | 92.0 | | | *6 |

| NCAT CORRECTION | 0.2 |
|---|---|
| Commercial Lab. | STRATA, Spokane |
| Commercial Lab. No. | S000037-3 |
| ITD Testing by | FC/MT8-17-00 |

*1 Specs. The difference between any two labs cannot exceed 32 kg/m³ (2.0 pcf).

*2 Specs. Minimum Stability by Class of Mix. Class I (37), Class II (35), Class III (30). Tolerance. The stability on the contractor's mix design test report must equal or exceed specified stability, at the job mix asphalt content. If ITD's confirmation tests at the job mix asphalt content yeild stability results which also equals or exceeds specified stability, then the contractor's stability results are confirmed. If ITD's confirmation test results are below specified stability, then the contractor's stability results are considered to be confirmed only if the contractor's and ITD's stabilities (each recored to the nearest integer) do not differ by more the six (6) stability points and if the average of the two (rounded to the nearest integer) is not less then the specified stability.

*3 Specs. Minimum VMA by Nominal Maximun Aggregate Size. 9.5 mm (15.0), 12.5 mm (14.0), 19.0 mm (13.0), 25.0 mm (12.0), 37.5 mm (11.0). Tolerance. If the contractor's VMA meets the minimum specifications and ITD's VMA falls below the minimum specification by no more than 1.5%, the contractor's VMA is confirmed.

*4 Specs. 3.0%-5.0%. Tolerance. If the contractor's design results and ITD's results disagree not more than 1.5% and ITD'S results do not fall beyond the specification limits of 3.0% - 5.0% by more than 0.5%, the design air voids are considered comparable and the contractor's air voids are confirmed.

*5 Specs. Minimum Film Thickness is 6 microns. Tolerance. If ITD's AFT falls below the specification of 6 microns the confirmation will be based solely on the judgment of ITD.

*6 Specs. Minimum Immersion Compression IRS is 85%. Tolerance. If ITD's results fall below the minimum of 85%, confirmation will be based solely on the judgment of ITD. Past source file data, if any, should be utilized to make this judgment.

The Job Mix Formula submitted by the Contractor is __CONFIRMED__ at the Contractor's selected asphalt content o 5.0 %, by weight of mix. For use on the project(s) listed on this report only.

The Immersion Compression results are confirmed at 0.5 % anti-stripping additive.

REMARKS:

DATE MAILED   AUG 2 4 2000    MATERIALS ENGINEER    THOMAS S. BAKER   ,P.E.

C - 6

# GRADATION CHART

KEY NO. 0519　　　　PROJECT NO. IM-90-1(190)10　　　　SOURCE NO. Kt-215

DESCRIPTION 00 A0163

ITEM NO. 405-A-1　　　　ITEM　　　　TRIAL NO. 1

### HORIZONTAL SCALE REPRESENTS SIEVE SIZES RAISED TO THE 0.45 POWER

A = 12%
B = 32%
C = 43%
F.S. = 8%
C.S. = 5%

S.A. 4.47 (21.82)
SPG 2.66
ASPG 2.73

| Sieve | Percent |
|-------|---------|
| 37.5mm (1½In.) | 100 |
| 31.5mm (1¼In.) | 100 |
| 25mm (1In.) | 100 |
| 19mm (3/4In.) | 99 |
| 12.5mm (1/2In.) | 88 |
| 9.5mm (3/8In.) | 76 |
| 4.75mm (No.4) | 53 |
| 2.36mm (No.8) | 36 |
| 1.18mm (No.16) | 23 |
| 0.6mm (No.30) | 15 |
| 0.3mm (No.50) | 9 |
| 0.15mm (No.100) | 5 |
| 0.075mm (No.200) | 4.8 |

PERCENT PASSING

SIEVE SIZES (mm)
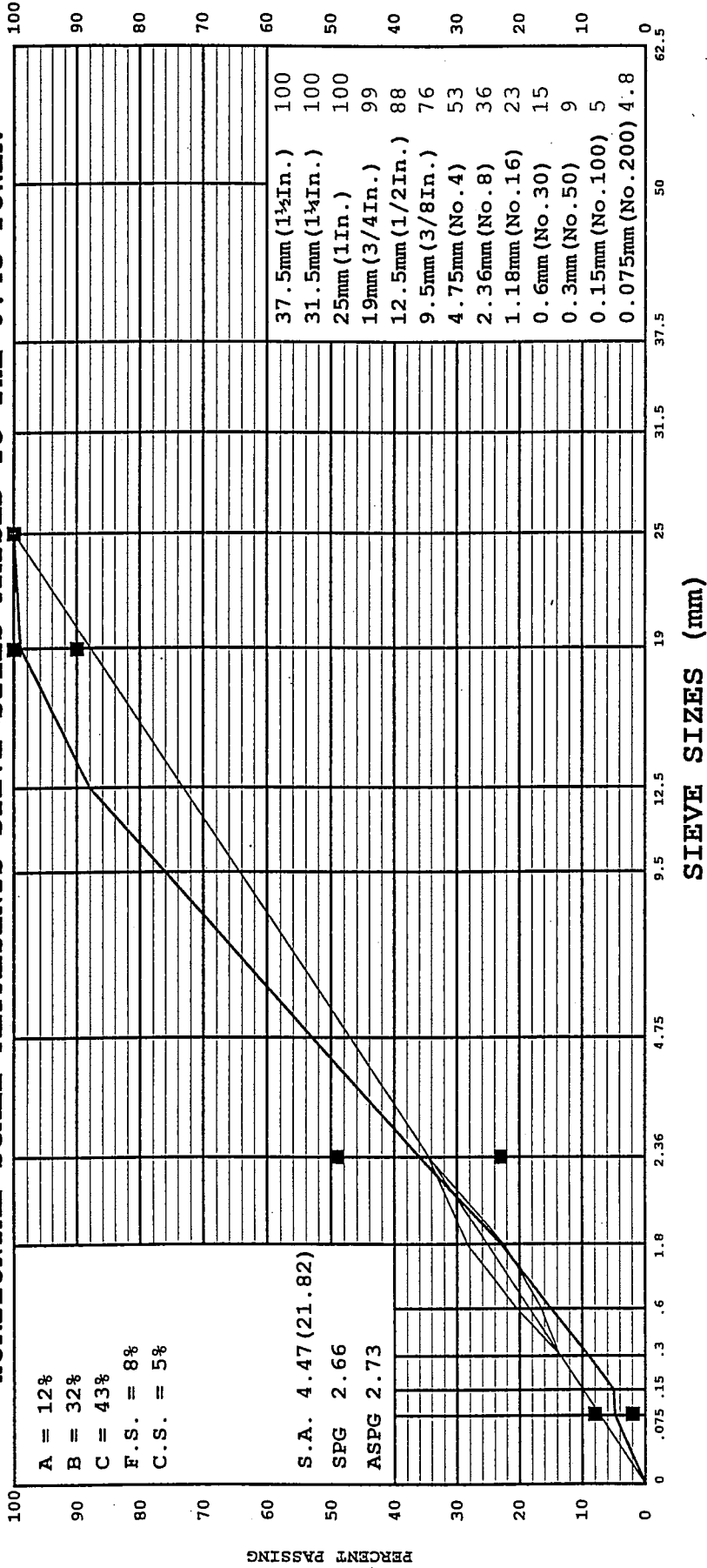
COMMENTS:

THOMAS S. BAKER

DATE MAILED　AUG 24 2000　　　　, P.E. MATERIALS ENGINEER

cc:    MTLS (W/A)
         CONST (W/A)
         RE SNDPT (W/A)
         DMTLS (W/A)
         DF

August 1, 2000

Mr. Scott A. Bernhard, Project Manager        RE: Project No. IM-90-1(190)10 & STP-7235(102)
Max J. Kuney Company                NW BLVD/RAMSEY RD IC &
P. O. Box 4008                      NW BLVD IC GATEWAY, CDA
Spokane, WA 99202-0008           Key No. 0519 & 7584
                                  Contract No.  6317
                                  Change of Source Request No. 1

Mr. Bernhard,

Your request to use Source Kt-215c (Interstate - Hayden), as a Contractor furnished source, has been approved for the following contract items:

| ITEM NUMBER | ITEM DESCRIPTION |
|---|---|
| 303-020A | 19 mm Agg for Base |
| 405-005A | Pl Mx Pav CL I |
| 412-010A | Pl Mx Seal Ty PMS-MG |

The approval for the quality of this material is based upon Laboratory Report No. SL06567 (Strata).

It is understood that the use of Kt-215c is granted upon the condition that the materials used are within the specifications of this contract. Only materials in existing stockpiles shall be used until the Archaeological report is returned.

You will assume full responsibility for any and all claims, liabilities, and/or damages by reason of the removal of material from Sources Kt-215c.

Any claim for additional payment cannot be allowed, and it is further understood that should the source prove inadequate in quantity or unsuitable in quality, any expense involved to produce material as contracted for will be borne by your company.

Sincerely,

## ORIGINAL SIGNED BY:

L. Scott Stokes, P.E.
District Engineer

LSS:JD:jd\Kt-215request1NWBlvd.doc

AUG 2 4 2000

**THOMAS S. BAKER**

**C - 8**

University of Idaho
KT-215 makeup

**5500 gram sample**

| | crush | cs | fs |
|---|---|---|---|
| 3/4 | 52.8 | 0.0 | 0.0 |
| 1/2 | 598.4 | 0.0 | 0.0 |
| 3/8 | 651.2 | 0.0 | 0.0 |
| 4 | 1259.0 | 8.8 | 0.0 |
| 8 | 874.5 | 48.4 | 44.0 |
| 16 | 507.2 | 79.2 | 107.3 |
| 30 | 265.9 | 101.2 | 85.3 |
| 50 | 168.0 | 110.0 | 24.8 |
| 100 | 97.0 | 66.0 | 5.5 |
| 200 | 64.5 | 16.7 | 1.9 |
| -200 | 246.6 | 9.7 | 6.3 |
| | 4785 | 440 | 275 | 5500 |

**20 samples**

| | crush | cs | fs |
|---|---|---|---|
| 3/4 | 1056.0 | 0.0 | 0.0 |
| 1/2 | 11968.0 | 0.0 | 0.0 |
| 3/8 | 13024.0 | 0.0 | 0.0 |
| 4 | 25179.0 | 176.0 | 0.0 |
| 8 | 17490.0 | 968.0 | 880.0 |
| 16 | 10144.2 | 1584.0 | 2145.0 |
| 30 | 5317.4 | 2024.0 | 1705.0 |
| 50 | 3359.4 | 2200.0 | 495.0 |
| 100 | 1940.4 | 1320.0 | 110.0 |
| 200 | 1290.3 | 334.4 | 38.5 |
| -200 | 4931.3 | 193.6 | 126.5 |
| | 95700.0 | 8800.0 | 5500.0 | 110000 |

# IDAHO ASPHALT SUPPLY
## Viscosity-Temperature Chart

| Temp (°C) | Viscosity (mPa-s) |
|-----------|-------------------|
| 110 | 1078 |
| 135 | 281 |
| 165 | 84 |

**PRODUCT: PG58-28**

Specific Gravity      1.028

| | °C | | °F | |
|---|---|---|---|---|
| *Mixing Temperature Range* | 144 | - 149 | 291 | - 300 |
| *Compaction Temperature Range* | 133 | - 137 | 271 | - 279 |
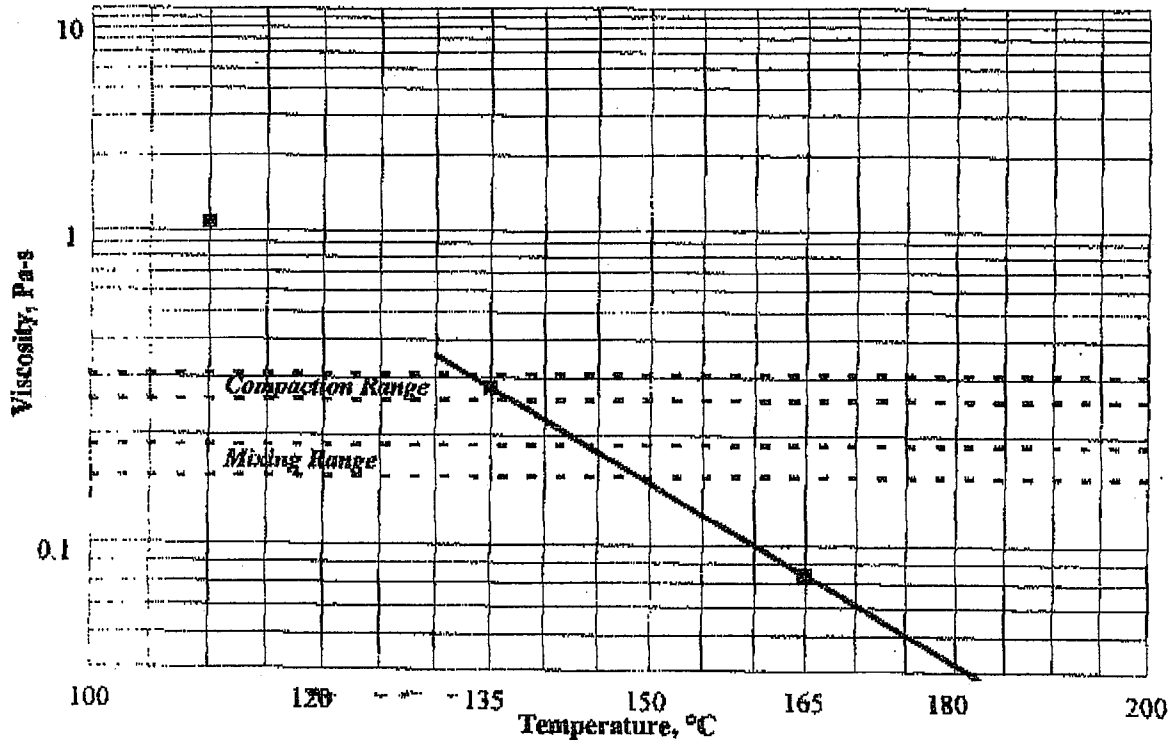


**Note:** Viscosity-Temperature charts for asphalts are obtained at a fixed shear rate (<100 sec-1) and do not correspond to actual shear rates in the field. In particular compaction temperatures are dependent upon type of compactor used and environmental conditions, and therefore should be established by a test strip.

SR# 390
WR# 1672

RA

5/26/00

Idaho Asphalt Supply, Inc.

# Job Mix Formula for Mix D2

# IDAHO TRANSPORTATION DEPARTMENT
### Department Memorandum

D2

**DATE:** APRIL 7, 2000

**PROJECT NO.(S):** NH-STP-4114(062)

**TO:** DORAL HOFF, P. E.
DISTRICT 2 RES. B ENGR.

**KEY NO.(S):** 2483

**FROM:** TOM BAKER, P.E.
MATERIALS ENGINEER

**PROJECT ID, CNTY, ETC.:**
LATAH COUNTY
MOSCOW COUPLET, SOUTH
CONNECTION

**RE:** PLANT MIX PAVEMENT CLASS I
SOURCE WCW-18
KLEINFELDER LAB. NO. 30-621411
ITD LAB NO. 00 A0032
ASPHALT PG 58 -34

The Job Mix Formula submitted by the contractor is **CONFIRMED** at the contractor's selected asphalt content of 6.1%, by weight of dry aggregate.

Based on contract recommendations we **CONFIRM** the Immersion Compression results at 0.5% anti-stripping additive.

If you have any questions or comments please call Mike Santi, Pavement Engr., at 334-8450 or Barry Tyler, Aggregate-Asphalt Mix Supv., at 334-8456.

Testing start date = 4/4/00
Testing due date = 4/18/00
Testing completed = 4/6/00
District notified = 4/7/00

| Post-It® Fax Note | 7671 | Date 4/7 | # of pages ▶ 3 |
|---|---|---|---|
| To Doral Hoff | | From Tyler | |
| Co./Dept. | | Co. | |
| Phone # | | Phone # | |
| Fax # | | Fax # | |

cc:     Doral Hoff, Dist. 2 Res. B Engr.
Dist. 2 Engr.
Dist. 2 Matls Engr.
Construction
Mike Santi
File

C - 12

# REPORT OF ASPHALT MIX DESIGN TEST RESULTS
## (COMMERCIAL CONFIRMATION)

Sheet ___ of ___

Key No. **2483**    Project No. **NH-STP-4114(062)**    Lab No. **00 A003**

Test For **Commercial Confirmation CI.I**    Source No. **WCW-18**    Trial No. **1**

Comments

## HVEEM MIX DESIGN RESULTS  64-34

ASPHALT USED          Pg 58-34

| MIX Temp F° | 310.0 | Comp. Temp F° | | 285.0 | |
|---|---|---|---|---|---|
| % ASPH. BY WT. OF AGGREGATE | | | | 6.1 | |
| | COM. | ITD | DIFF. | TOLER. | |
| MAX. THEO. DEN. | 160.4 | 159.9 | 0.5 | *1 | |
| WT./C.F. ASPH. MIX | 153.8 | 152.4 | 1.4 | *1 | |
| WT./C.F. AGGREGATE | 145.0 | 143.7 | 1.3 | | |
| STABILITY NUMBER | 40 | 38 | 2 | *2 | |
| % V.M.A. | 13.0 | 14.4 | 1.4 | *3 | |
| % AIR VOIDS | 4.1 | 4.7 | 0.6 | *4 | |
| E.A.C. | 3.9 | 4.3 | 0.4 | | |
| A. F. T. (MICRONS) | 7.8 | 8.6 | 0.8 | *5 | |
| SURFACE AREA | 24.12 | 24.12 | 0.00 | ± 3.0 | |

## TRIAL AND JMF GRADATION

| % Passing | JMF | TRIAL | DIFF. | TOLER |
|---|---|---|---|---|
| 37.5 mm | 100.0 | 100.0 | 0 | ± 3.0 |
| 25 mm | 100.0 | 100.0 | 0 | ± 3.0 |
| 19 mm | 99.0 | 99.0 | 0 | ± 3.0 |
| 12.5 mm | 80.0 | 80.0 | 0 | ± 3.0 |
| 9.5 mm | 69.0 | 69.0 | 0 | ± 3.0 |
| 4.75 mm | 50.0 | 51.0 | 1 | ± 3.0 |
| 2.36 mm | 31.0 | 33.0 | 2 | ± 3.0 |
| 1.18 mm | 20.0 | 22.0 | 2 | ± 2.0 |
| 600 μm | 13.0 | 14.0 | 1 | ± 2.0 |
| 300 μm | 10.0 | 10.0 | 0 | ± 2.0 |
| 150 μm | 8.0 | 7.0 | 1 | ± 2.0 |
| 75 μm | 5.9 | 5.7 | 0.2 | ± 1.0 |

## IMMERSION COMPRESSION RESULTS

ASPHALT ADDITIVE          Ad-here 65 50

| | I.R.S. % |
|---|---|

| % ANTI-STRIP | COM. | ITD | DIFF. | SPECS. |
|---|---|---|---|---|
| 0.5 | 91.0 | | | *6 |

| NCAT CORRECTION | 0.7 |
|---|---|
| Commercial Lab. | Kleinfelder |
| Commercial Lab. No. | 30-621411 |
| ITD Testing by | mt/fc 4-7-00 |

*1 Specs. The difference between any two labs cannot exceed 32 kg/m³ (2.0 pcf).

*2 Specs. Minimum Stability by Class of Mix. Class I (37), Class II (35), Class III (30). Tolerance. The stability on the contractor's mix design test report must equal or exceed specified stability, at the job mix asphalt content. If ITD's confirmation tests at the job mix asphalt content yield stability results which also equals or exceeds specified stability, then the contractor's stability results are confirmed. If ITD's confirmation test results are below specified stability, then the contractor's stability results are considered to be confirmed only if the contractor's and ITD's stabilities (each recored to the nearest integer) do not differ by more the six (6) stability points and if the average of the two (rounded to the nearest integer) is not less than the specified stability.

*3 Specs. Minimum VMA by Nominal Maximum Aggregate Size. 9.5 mm (15.0), 12.5 mm (14.0), 19.0 mm (13.0), 25.0 mm (12.0), 37.5 mm (11.0). Tolerance. If the contractor's VMA meets the minimum specifications and ITD's VMA falls below the minimum specification by no more than 1.5%, the contractor's VMA is confirmed.

*4 Specs. 3.0%-5.0%. Tolerance. If the contractor's design results and ITD's results disagree not more than 1.5% and ITD'S results do not fall beyond the specification limits of 3.0% - 5.0% by more than 0.5%, the design air voids are considered comparable and the contractor's air voids are confirmed.

*5 Specs. Minimum Film Thickness is 6 microns. Tolerance. If ITD's AFT falls below the specification of 6 microns the confirmation will be based solely on the judgment of ITD.

*6 Specs. Minimum Immersion Compression IRS is 85%. Tolerance. If ITD's results fall below the minimum of 85%, confirmation will be based solely on the judgment of ITD. Past source file data, if any, should be utilized to make this judgment.

The Job Mix Formula submitted by the contractor is **CONFIRMED** at the contractor's selected asphalt content of 6.1 %, by weight of dry aggregate. For use on the project(s) listed on this report only.

The Immersion Compression results are confirmed at 0.5 % anti-stripping additive.

REMARKS: _____

DATE MAILED _____    MATERIALS ENGINEER _____ P.E.

C - 13

# GRADATION OF INDIVIDUAL STOCKPILES

ITD-878 1-86

KEY NO. 2483   PROJECT NO. NH-STP-4114(062)   SOURCE NO. WCW-18

DESCRIPTION 00 A0032

ITEM NO. 405A   ITEM ____   TRIAL NO. 1

## PERCENT PASSING

| STOCKPILE | 37.5mm (1½in.) | 31.5mm (1¼in.) | 25mm (1in.) | 19mm (3/4in.) | 12.5mm (1/2in.) | 9.5mm (3/8in.) | 4.75mm (No.4) | 2.36mm (No.8) | 1.18mm (No.16) | 0.6mm (No.30) | 0.3mm (No.50) | 0.15mm (No.100) | 0.075mm (No.200) |
|---|---|---|---|---|---|---|---|---|---|---|---|---|---|
| A | 100 | 100 | 100 | 96 | 15 | 5 | 3 | 2 | 2 | 1 | 1 | 1 | 1.1 |
| B | 100 | 100 | 100 | 100 | 88 | 55 | 10 | 6 | 6 | 5 | 4 | 4 | 3.5 |
| C | 100 | 100 | 100 | 100 | 100 | 100 | 88 | 59 | 38 | 24 | 17 | 12 | 8.7 |

## STOCKPILE RATIOS AND BLEND OF AGGREGATE

## PERCENT PASSING

| STOCKPILE % | BLEND % | 37.5mm (1½in.) | 31.5mm (1¼in.) | 25mm (1in.) | 19mm (3/4in.) | 12.5mm (1/2in.) | 9.5mm (3/8in.) | 4.75mm (No.4) | 2.36mm (No.8) | 1.18mm (No.16) | 0.6mm (No.30) | 0.3mm (No.50) | 0.15mm (No.100) | 0.075mm (No.200) |
|---|---|---|---|---|---|---|---|---|---|---|---|---|---|---|
| A | 20% | 20 | 20 | 20 | 19 | 3 | 1 | 1 | 0 | 0 | 0 | 0 | 0.2 | |
| B | 27% | 27 | 27 | 27 | 27 | 24 | 15 | 3 | 2 | 1 | 1 | 1 | 0.9 | |
| C | 53% | 53 | 53 | 53 | 53 | 53 | 53 | 47 | 31 | 20 | 13 | 9 | 6 | 4.6 |
| BLEND | | 100 | 100 | 100 | 99 | 80 | 69 | 51 | 33 | 22 | 14 | 10 | 7 | 5.7 |
| TARGET | | 100 | 100 | 100 | 99 | 80 | 69 | 50 | 31 | 20 | 13 | 10 | 7 | 5.9 |

DATE MAILED _____

_____
P.E. MATERIALS ENGINEER

D2 Binder
PG 64-34

# KOCH Pavement Solutions™
...Longer Lasting Roads

**P.O. Box 6226**
**N. 4327 Thor St.**
**Spokane, WA 99217-0904**

TOTAL NUMBER OF PAGES __2__ (INCLUDING THIS COVER SHEET)

TO: _University of Idaho_
FAX #: _208-885-6608_
TELEPHONE #: _208-885-6784_
ATTENTION: _Dr. Fouad M. Bayomy_

FROM: _Stephen Van De Bogert_
FAX # 509/487-5170
SUBJECT: _Temp/Visc Curve PG 64-34 T_

Thanks

Steve

**If this transmission does not go through properly, please call: 509/487-4560**

# Temperature-Viscosity Graph

**KOCH Pavement Solutions™**
...Longer Lasting Roads

### Sample ID

| Material | PG64-34 |
|---|---|
| Sample # | |
| Date | |
| Specific Gravity, 15°C | 1.024 |

### Viscosity Data

| Temperature, C | Viscosity, cPs |
|---|---|
| 110 | 2378 |
| 135 | 583 |
| 163 | 171 |
| 180 | |

### Mixing and Compacting Recommendations

| Range | Temperature, F | Temperature, C |
|---|---|---|
| Mixing-Hi Temp | 330 | 166 |
| Mixing-Low Temp | 315 | 157 |
| Compaction-High Temp | 285 | 141 |
| Compaction-Low Temp | 275 | 135 |

PG64-34



| | | |
|---|---|---|
| Mixing Range | 315 to 330 °F |
| Compaction Range | 275 to 285 °F |

C - 16
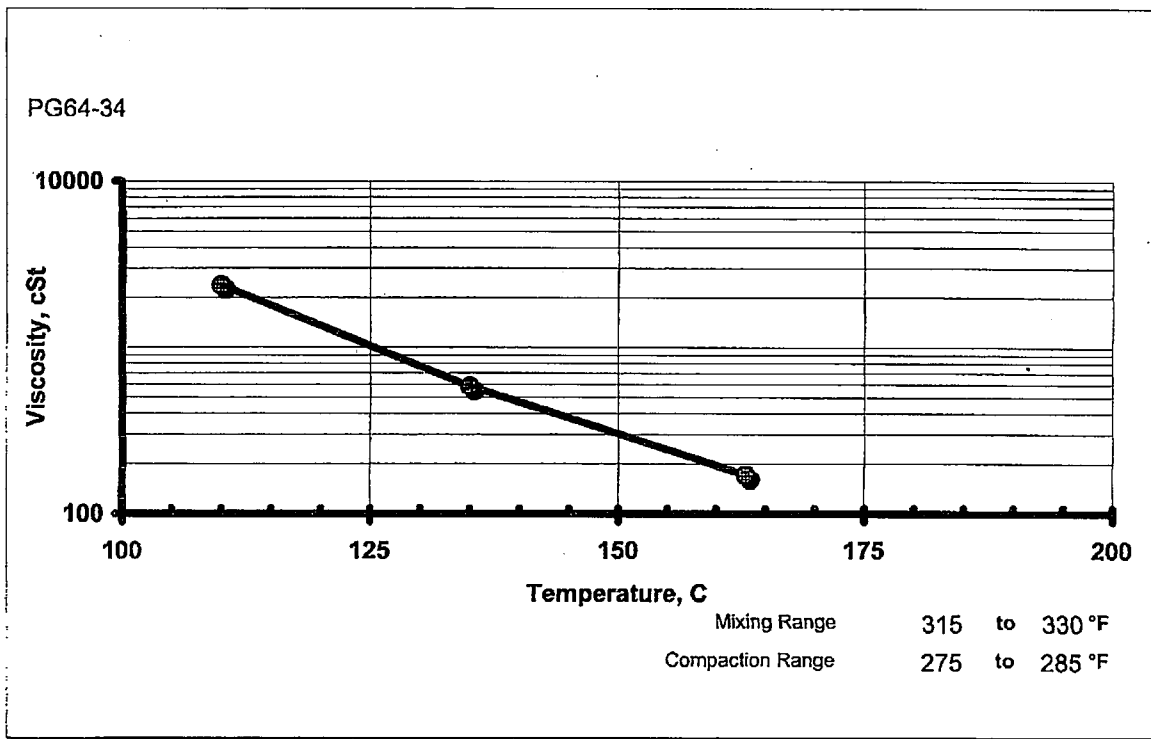
# Job Mix Formula for Mix D3

# KLEINFELDER
An employee owned company

# TECHNICAL REPORT
## MIX DESIGN
### Idaho Transportation Department
### Class I LS Plant Mix

| | | | |
|---|---|---|---|
| REPORT TO: | Idaho Sand and Gravel<br>PO Box 950<br>Nampa, Idaho 83653 | DATE:<br>JOB NUMBER:<br>REVISION DATE: | March 10, 2001<br>30-612417.341 |
| ATTENTION: | Mr. Pat Wood | LAB NUMBER:<br>SAMPLED BY: | 1576<br>L. Colberg |
| REPORT OF: | STP-3230(104)<br>44th St. to JCT I-184 | DATE SAMPLED:<br>DATE RECEIVED:<br>DATE TESTED: | February 23, 2001<br>February 22, 2001<br>March 5, 2001 |

## SAMPLE IDENTIFICATION

On February 23, 2001, our personnel received stockpile samples from the PY-65 and CN-67 Sources. Gradation averages were supplied by Idaho Sand and Gravel. The material was separated by sieve sizes and recombined to the target values of the Job Mix Formula (JMF) as representation of the stockpile averages.

## TESTS PERFORMED

Aggregate test results and the job mix formula are summarized in Table 1. The laboratory test procedures utilized in the mix design are indicated in Table 2. Tests performed include sieve analysis, specific gravity and absorption. Mixture tests included Hveem stability, unit weight, and maximum theoretical specific gravity. The mixture test results are shown in Table 3. Aggregates and mixture properties are presented in comparison with the Idaho Transportation Department Standard Specifications for Highway Construction and project specific special provisions. Graphical summaries of the effect of asphalt content on mix properties are provided on Plates 1, 2, and 3. The asphalt concrete mix design was performed in general accordance with the Hveem Test Method (AASHTO T-246 & T-247). The laboratory mixing temperature used was 330°F (165°C) and the compaction temperature used was 290°F (144°C). PG 76-28 Asphalt was supplied by Idaho Asphalt Supply Co.

Based upon the data in Tables 3 and 4 and Plates 1, 2, and 3 an asphalt content of 4.8% (by Total Weight of Mix) provides a laboratory mix with fully-coated aggregates and minimal free asphalt cement; and stability VMA. film thickness and air voids comply with the requirements of the standard specifications. A summary of calculated mixture properties at the recommended optimum asphalt content is provided in Table 4.

L: 2001\Projects\30612417.30GIR058.doc
Copyright 2001 Kleinfelder. Inc.

Page 1 of 4

March 13, 2001

C - 18
KLEINFELDER  10221 W. Emerald Street, Suite 180, Boise, ID 83704  (208) 376-9700  (208) 376-9703 fax
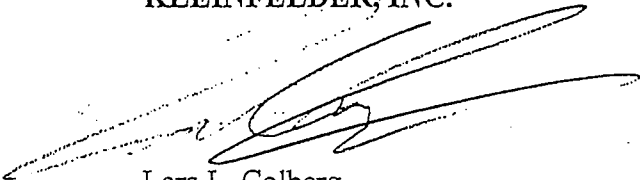
## LIMITATIONS

Our professional services have been performed using the care and skill ordinarily exercised, under similar circumstances, by reputable testing firms performing in this or similar localities. No warranty, express or implied, is made. This report has been prepared for Idaho Sand and Gravel to be used as an aid in design or construction of a Class I LS plant mix bituminous pavement. This is not a bidding document, and any contractor or client reviewing the test data must draw his own conclusions regarding specific construction techniques to be used with these materials. The data furnished represent only the results of tests performed on specific samples. The data has not been evaluated in terms of the engineering criteria or specific construction methods.

Kleinfelder personnel will provide technical assistance during the submittal, approval, and production usage of the JMF upon your request. If you have any questions or need additional information, please feel free to contact our Boise office.

Respectfully submitted,

**KLEINFELDER, INC.**

Lars L. Colberg
Supervisory Technician, Asphalt/Laboratory

Paul E. Wasser, P.E.
Project Manager

## TABLE 1
## SIEVE ANALYSIS (AASHTO T27)

| Description | A-Pile | F-Pile | C-Pile | | Combined Aggregates | Job Mix Formula |
|---|---|---|---|---|---|---|
| Bin Percentage | 40% | 10% | 50% | | | |
| Screen or Sieve Size | Percent Passing | | | | | |
| 1 1/2"        37.5 mm | | 100 | | | 100 | |
| 1"            25.0 mm | 100 | 70 | | | 97 | |
| 3/4"          19.0 mm | 93 | 7 | | | 88 | |
| 1/2"          12.5 mm | 25 | 1 | | | 60 | |
| 3/8"           9.5 mm | 7 | 1 | 100 | | 53 | |
| No. 4         4.75 mm | 2 | 1 | 92 | | 47 | |
| No. 8         2.36 mm | 1 | 1 | 62 | | 32 | |
| No. 16        1.18 mm | 1 | 1 | 42 | | 22 | |
| No. 30        600 um | 1 | 1 | 29 | | 15 | |
| No. 50        300 um | 1 | 1 | 19 | | 10 | |
| No. 100       150 um | 1 | 1 | 11 | | 6 | |
| No. 200        75 um | 1.1 | 0.5 | 7.0 | | 4.0 | |
| Surface Area    ft²/lb | | | | | 21.00 | |
| Surface Area    m²/kg | | | | | 4.30 | |

| Specific Gravities | | | | |
|---|---|---|---|---|
| Asphalt | | | | |
| Aggregate | Coarse | | Fine | Combined |
| Bulk Dry | 2.579 | | 2.512 | 2.547 |
| Bulk SSD | 2.607 | | 2.568 | 2.589 |
| Apparent | 2.654 | | 2.661 | 2.657 |
| Absorption | 1.1 | | 2.2 | 1.6 |
| Effective | | | | 2.598 |

## TABLE NO. 2
## LABORATORY TEST PROCEDURES

| Laboratory Test | ASTM Test Method | AASHTO Test Method |
|---|---|---|
| Uncompacted Void Ratio | *C-1252 | |
| Wash Gradation | C-117 | *T-11 |
| Sieve Analysis | C-136 | *T-27 |
| Specific Gravity of Fine Aggregate | C-128 | *T-84 |
| Specific Gravity of Coarse Aggregate | C-127 | *T-85 |
| Marshall Mix Design | D-1559 | T-245 |
| Hveem Mix Design | D-1561 | *T-247 |
| Specific Gravity | D-2041 | *T-209 |
| Bulk Specific Gravity of Compacted Samples | D-2726 | *T-166 |
| Percent Voids | D-3203 | *T-269 |
| Resistance to Moisture Procedure | D-1075 | *T-165 |
| Tensile Strength Ratio | D-4867 | T-283 |
| Lottman Stripping Test | | WSDOT 718 |

Note:     * = Test Methods Used in Design

## TABLE NO. 3.
## SUMMARY OF MIXTURE PROPERTIES AT THE ASPHALT
## CEMENT CONTENT INDICATED (BY DRY WEIGHT OF AGGREGATE)

| Mixture Properties | Test Method | Test Results | | | | |
|---|---|---|---|---|---|---|
| Asphalt Cement Content by Wt. of Agg. %. | --- | 4.0 | 4.5 | 5.0 | 5.5 | 6.0 |
| Unit Weight, lb/ft³ | AASHTO T-166 | 143.5 | 144.6 | 145.3 | 145.5 | 144.9 |
| Unit Weight, kg/m³ | AASHTO T-166 | 2300 | 2317 | 2328 | 2331 | 2322 |
| Air Voids Total Mix, %. | AASHTO T-269 | 6.3 | 5.0 | 3.9 | 3.1 | 2.9 |
| Relative HVEEM Stability, lbs. | AASHTO T-246/247 | 49 | 53 | 52 | 47 | 40 |
| Percent VMA | | 13 | 13 | 13 | 13 | 14 |
| Voids Filled with Asphalt, VFA, %. | MS-2 | 52 | 62 | 70 | 76 | 79 |
| Maximum Theoretical Unit Weight, lb/ft³ | AASHTO T-209 | 153.1 | 152.1 | 151.1 | 150.2 | 149.2 |
| Maximum Theoretical Unit Weight, kg/m³ | AASHTO T-209 | 2454 | 2438 | 2422 | 2406 | 2391 |
| Marshall Stability, lbs. | ASTM D1559 | -- | -- | -- | -- | -- |
| Flow 1/100 in. | | -- | -- | -- | -- | -- |

## TABLE NO. 4
## MIXTURE PROPERTIES AT RECOMMENDED OPTIMUM ASPHALT CONTENT

| Mixture Properties | Test Method | Mixture Properties at Optimum Asphalt Content | Mix Design Specifications |
|---|---|---|---|
| Actual Asphalt Content (% by total wt. of agg.) | | 5.0 | -- |
| Actual Asphalt Content (% by total wt. of mix) | | 4.8 | -- |
| Added Asphalt Content (% by total wt. of agg.) | | -- | |
| Added Asphalt Content (% by total wt. of mix) | | -- | -- |
| HVEEM Relative Stability, lbs | AASHTO T-246/T-247 | 51 | 37 minimum |
| Voids Total Mix, % | AASHTO T-269 | 3.9 | 3 - 5 |
| Percent VMA | | 13 | 12 minimum |
| Voids Filled with Asphalt, VFA, %. | MS-2 | 70 | -- |
| Bulk Mix Unit Weight, lb/ft³ | AASHTO T-166 | 145.3 | -- |
| Bulk Mix Unit Weight, kg/m³ | AASHTO T-166 | 2328 | -- |
| Maximum Theoretical Unit Weight, lb/ft³ | AASHTO T-209 | 151.1 | -- |
| Maximum Theoretical Unit Weight, kg/m³ | AASHTO T-209 | 2422 | -- |
| "Index of Retained Stability," % | AASHTO T-165/167 | 90% | 85 minimum |
| Marshall Stability, lbs. | ASTM D1559 | -- | -- |
| Flow 1/100 in. | | -- | -- |
| Uncompacted Void Ratio | ASTM C1252 | 47 | 45 minimum |
| Ignition Oven Correlation Factor | AASHTO T-30 | .29 | -- |
| Type Anti-strip used | | .5% Unichem 8161 | -- |
| Asphalt Film Thickness | | 9.5 | 6 micron |

L:\2001\Projects\30612417\3061R058.doc
Copyright 2001 Kleinfelder, Inc.

Page 4 of 4

March 13, 2001

KLEINFELDER   10221 W. Emerald Street, Suite 180, Boise, ID 83704   (208) 376-9700   (208) 376-9703 fax

C-21

Design Curves for Proposed Job Mix Formula (JMF)

Unit Weight



% ASPHALT CEMENT (AGG)

Max Theo Unit Weight



% ASPHALT CEMENT (AGG)

Plate #1
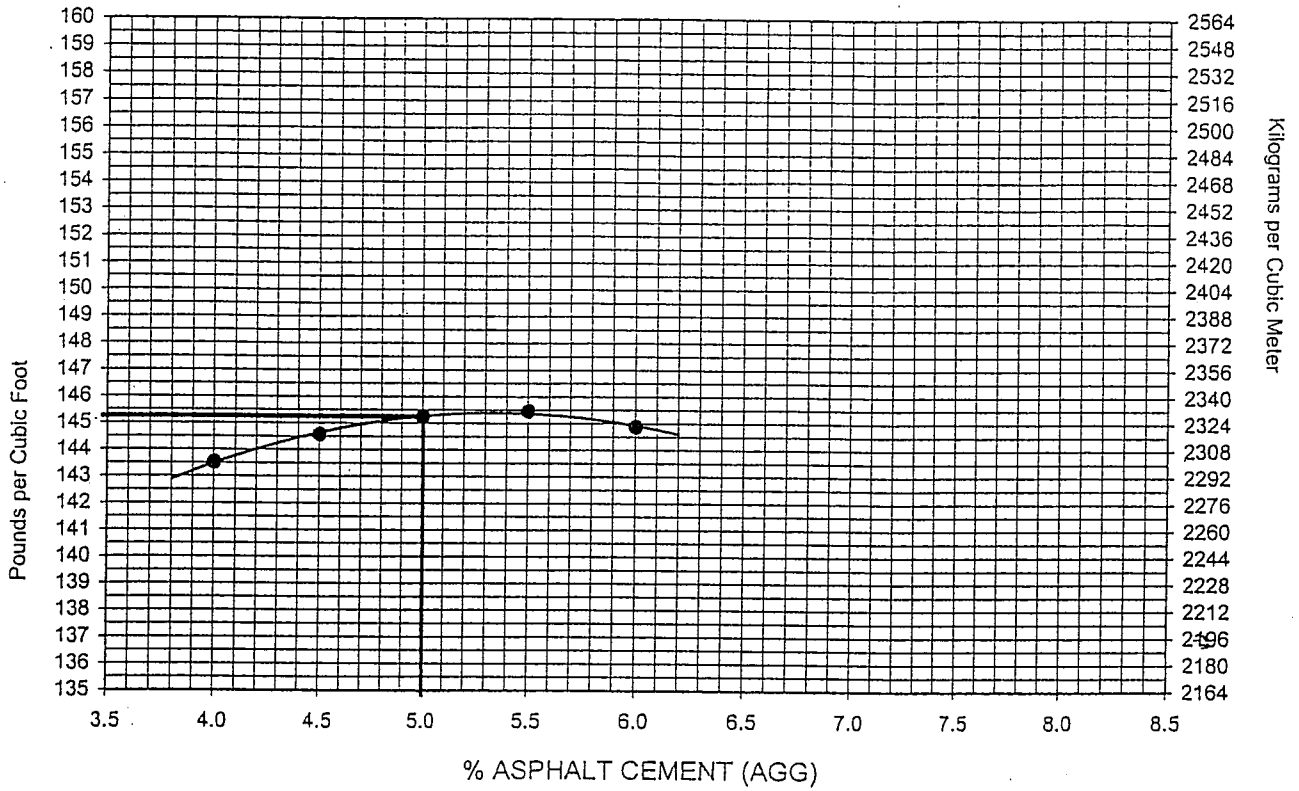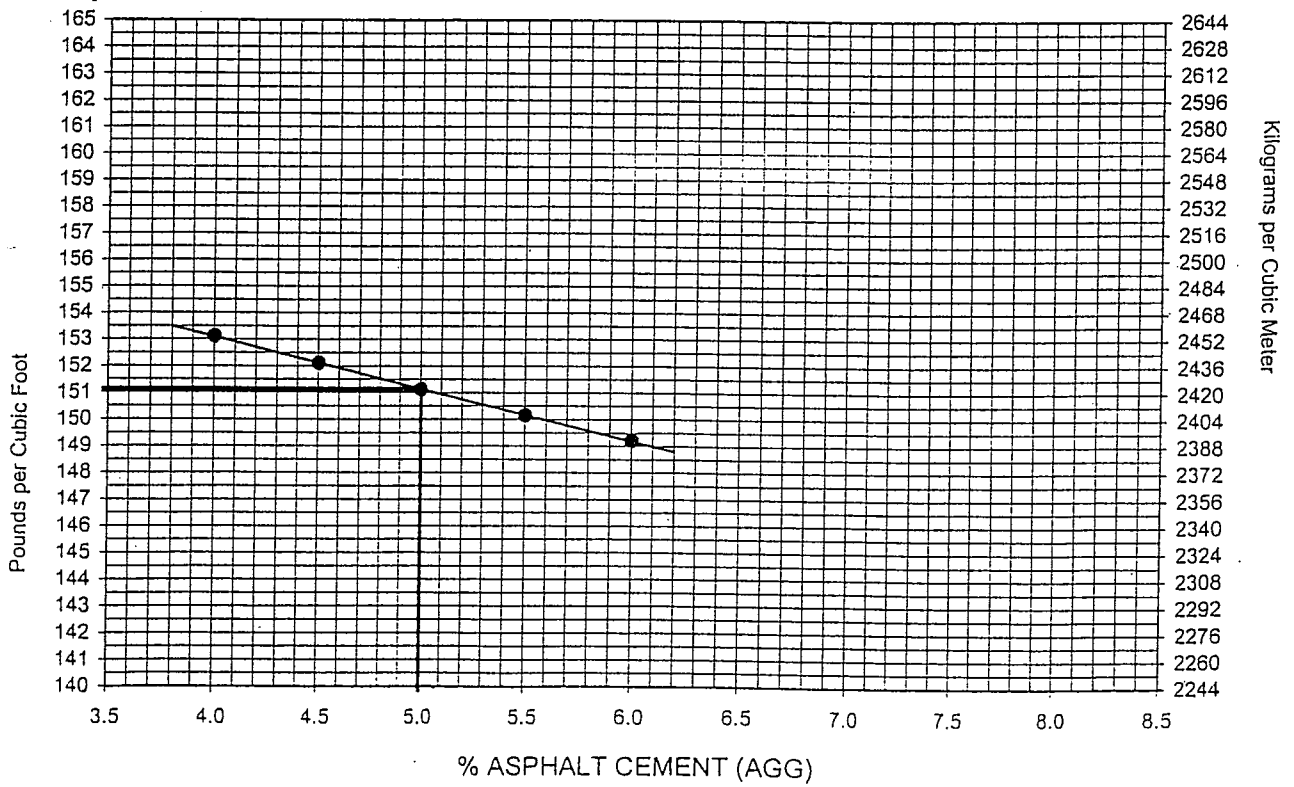
Design Curves for Proposed Job Mix Formula (JMF)

## % Air Voids



Y-axis: Percent Total Voids (0 to 20)
X-axis: %ASPHALT CEMENT (AGG) (3.5 to 8.5)

## VMA



Y-axis: Voids in Mineral Aggregate (10 to 20)
X-axis: % ASPHALT CEMENT (AGG) (3.5 to 8.5)

**C - 23**

Plate #2
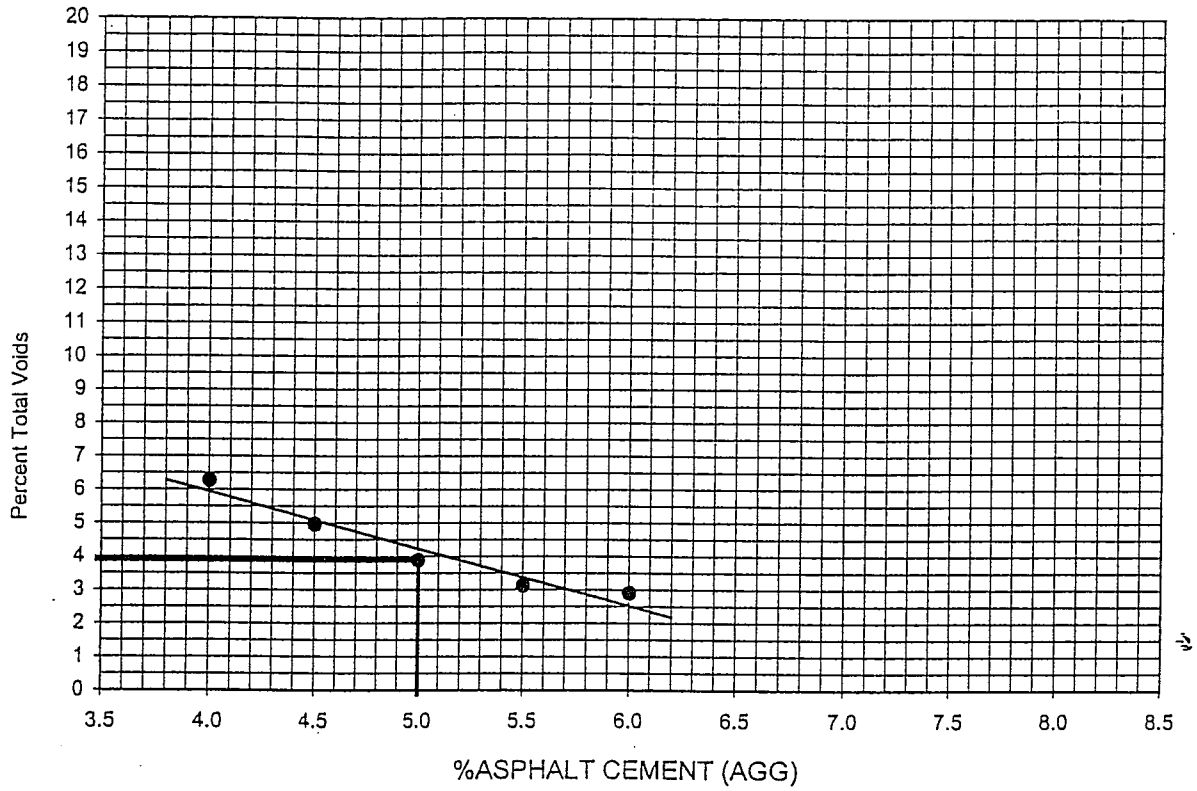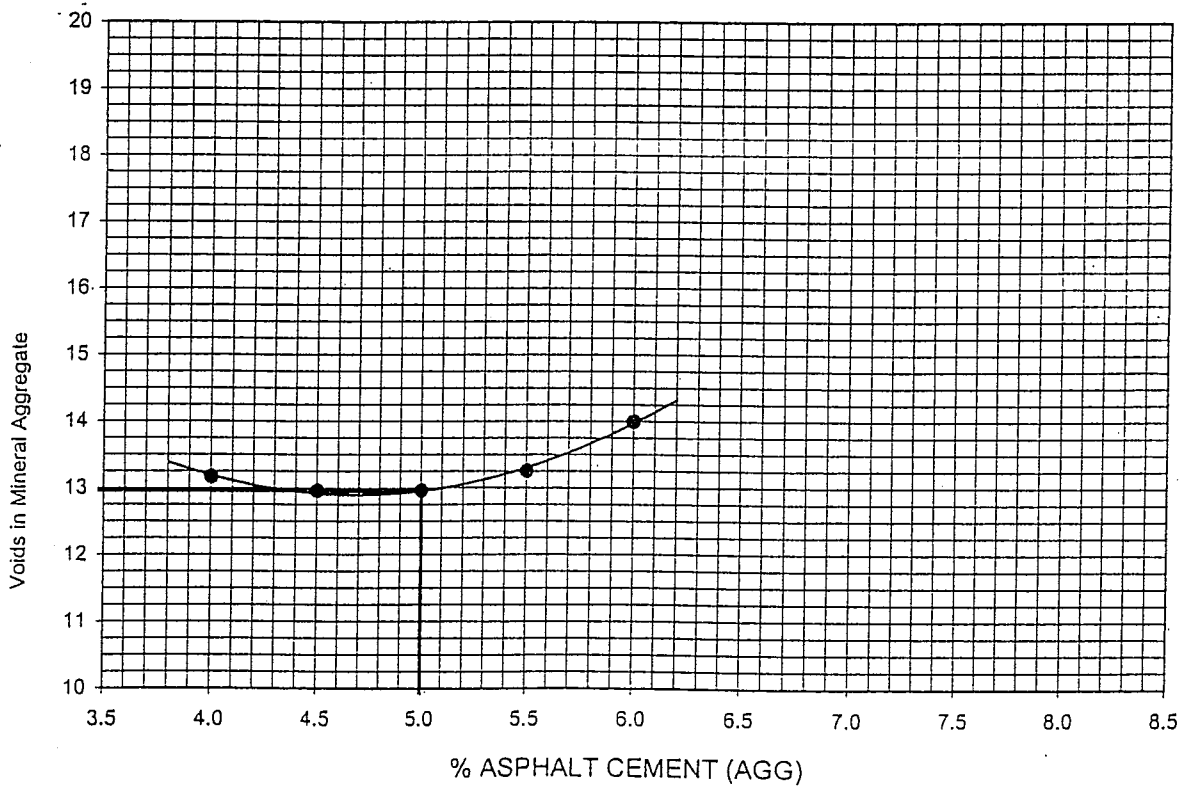
Design Curves for Proposed Job Mix Formula (JMF)

## Stabilometer



Stabilometer Values vs % ASPHALT CEMENT (AGG)

## Voids Filled



Voids Filled vs % ASPHALT CEMENT (AGG)

**C - 24**

Plate #3
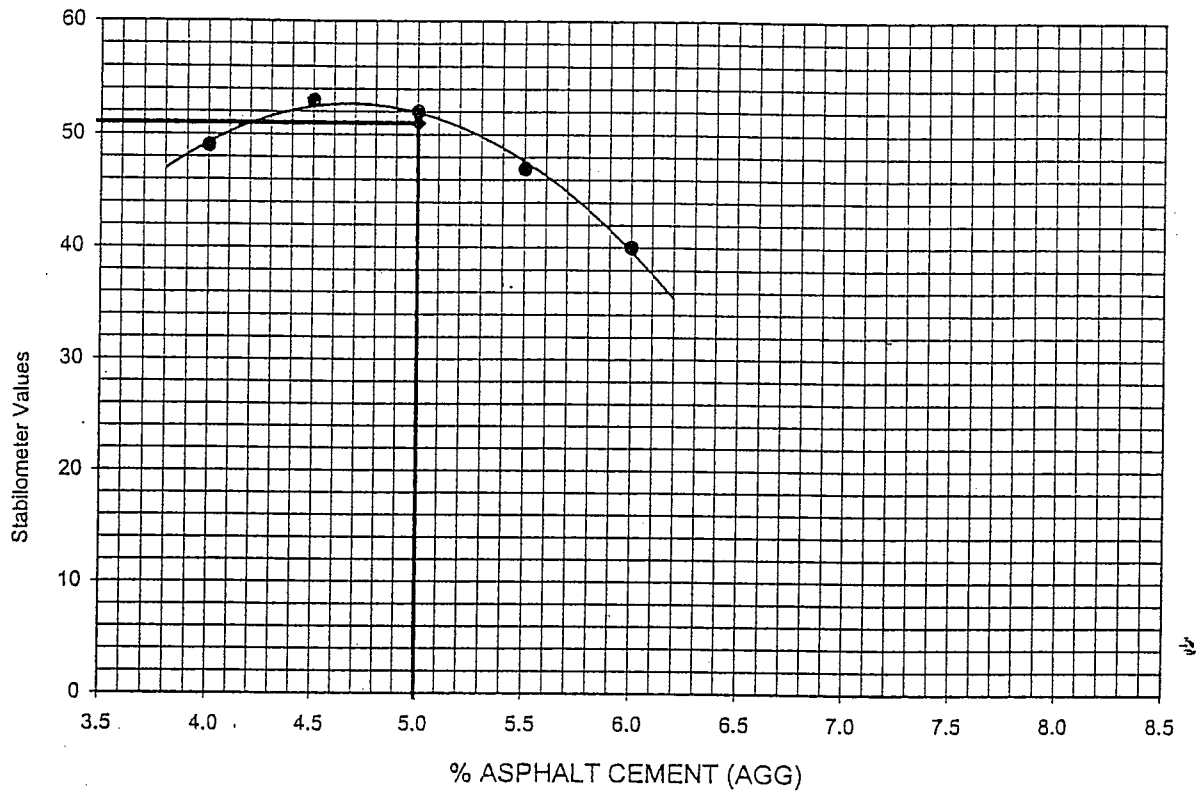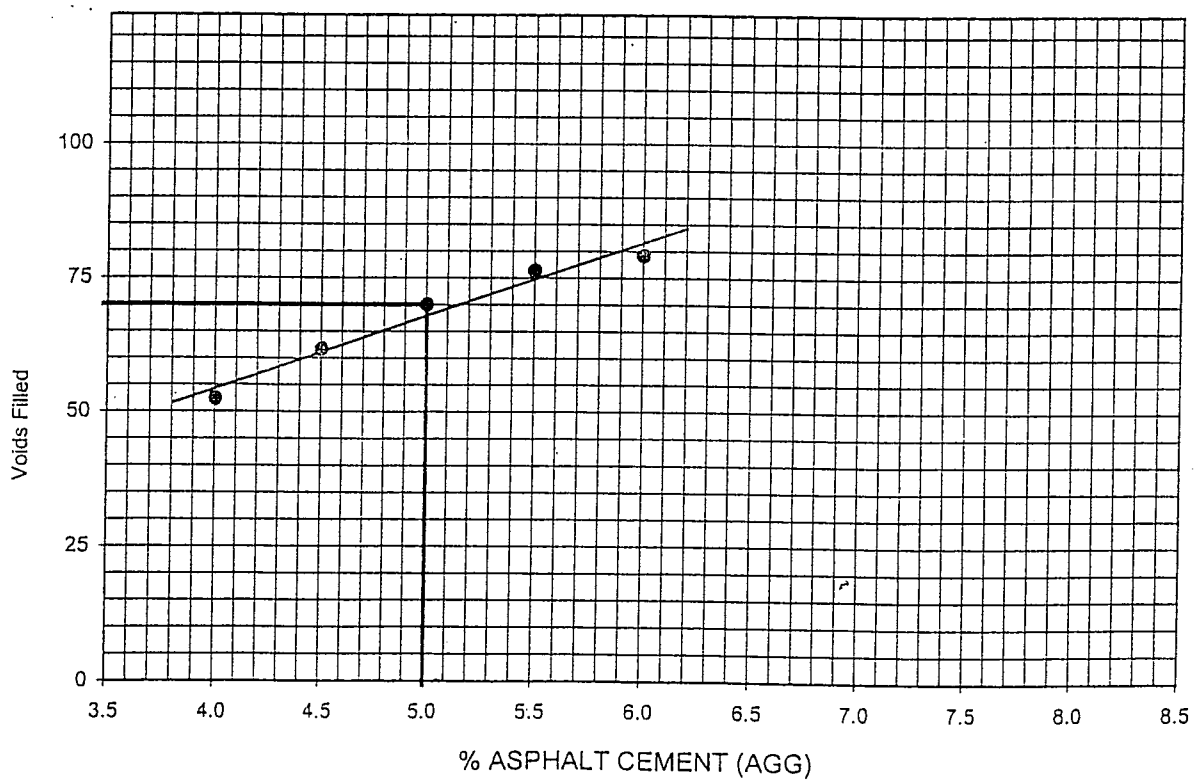
# KLEINFELDER

## AC Worksheet

PROJECT 44th to JCT. I-84 (STP-3230(104)    FILE NO.: _____

CLIENT Idaho Sand & Gravel    DATE: 2/28/01

SOURCE Cn-67c / Py-65c    DATE REC: 2/23/01

MIX TYPE Hveem    BY: BE

OIL TYPE PG 76-28    Supplier: Idaho    Anti-Strip: Uni-chem    APPROVAL: _____

| SIZE | 2.547 | | | SCREENS | % PASSING | % RET. | IND. WT. | CUM. WT. | I.C.s |
|---|---|---|---|---|---|---|---|---|---|
| PILE | A-pile | 40 % | | | | | | 6 1099 | 9 1747 |
| | | | | 3/4" | 93 | 7 | 31 | 31 | 49 |
| | | | | 1/2" | 25 | 68 | 299 | 330 | 524 |
| | | | | 3/8" | 7 | 18 | 79 | 409 | 650 |
| | | | | #4 | 2 | 5 | 22 | 431 | 685 |
| Moisture | 0.0 | | | -4 | 0 | 2 | 9 | 440 | 699 |
| | | | | | | | | | |
| TOTAL | 440 | | | | | | | | |
| PILE | F-pile | 10 % | | | | | | | |
| | | | 1" ~~1/2"~~ | 1 | 99 | 33 109 | ~~549~~ 473 ~~873~~ | 752 |
| | | | ~~3/4"~~ ~~3/8"~~ | 1 | 0 | 69 0 | ~~549~~ 542 ~~873~~ | 862 |
| | | | 1/2" ~~#4~~ | 1 | 0 | 8 0 | ~~549~~ 550 ~~873~~ | 875 |
| | | | ~~-4~~ | ~~0~~ | 1 | 1 | ~~550~~ | 875 |
| TOTAL | 110 | | | | | | | | |
| PILE | C-pile | 50 % | | | | | | | |
| | | | | #4 | 92 | 8 | 44 | 594 | 944 |
| Moisture | 2.0 | | | -4 | 0 | 92 | (505)516 | 1110 | 1765 |
| TOTAL | 549 | | | | | | | | |
| PILE | | 0 % | | | | | | | |
| | | | | #4 | | | | | |
| Moisture | 0.0 | | | -4 | | | | | |
| TOTAL | 0 | | | | | | | | |
| PILE | | 0 % | | | | | | | |
| | | | | 3/4" | | | | | |
| | | | | 1/2" | | | | | |
| | | | | 3/8" | | | | | |
| | | | | #4 | | | | | |
| Moisture | 0.0 | | | -4 | | | | | |
| TOTAL | 0 | | | | | | | | |

| SPEC. ID | 4.0 | 4.5 | 5.0 | 5.5 | 6.0 | | 5.5 |
|---|---|---|---|---|---|---|---|
| WT. AGG | 1095.2 | 1094.9 | 1095.3 | 1096.5 | 1096.2 | | 1095.1 |
| WT. OIL | 73.8 | 49.3 | 54.8 | 60.3 | 65.8 | | 60.2 |
| THEO. WT | | | | | | | |
| ACT WT | | | | | | | |

44th to JCT I-84.xls

**C - 25**

# IDAHO ASPHALT SUPPLY
## Viscosity-Temperature Chart

| Temp (°C) | Viscosity (mPa-s) |
|-----------|-------------------|
| 135 | 1695 |
| 166 | 456 |
| 185 | 235 |

**PRODUCT PG76-28**

Specific Gravity    1.030

| | °C | | | °F | | |
|---|---|---|---|---|---|---|
| Mixing Temperature Range | 160 | - | 171 | 320 | - | 340 |
| Compaction Temperature Range | 138 | - | 149 | 280 | - | 300 |



Compaction Range

Mixing Range

Viscosity, Pa-s
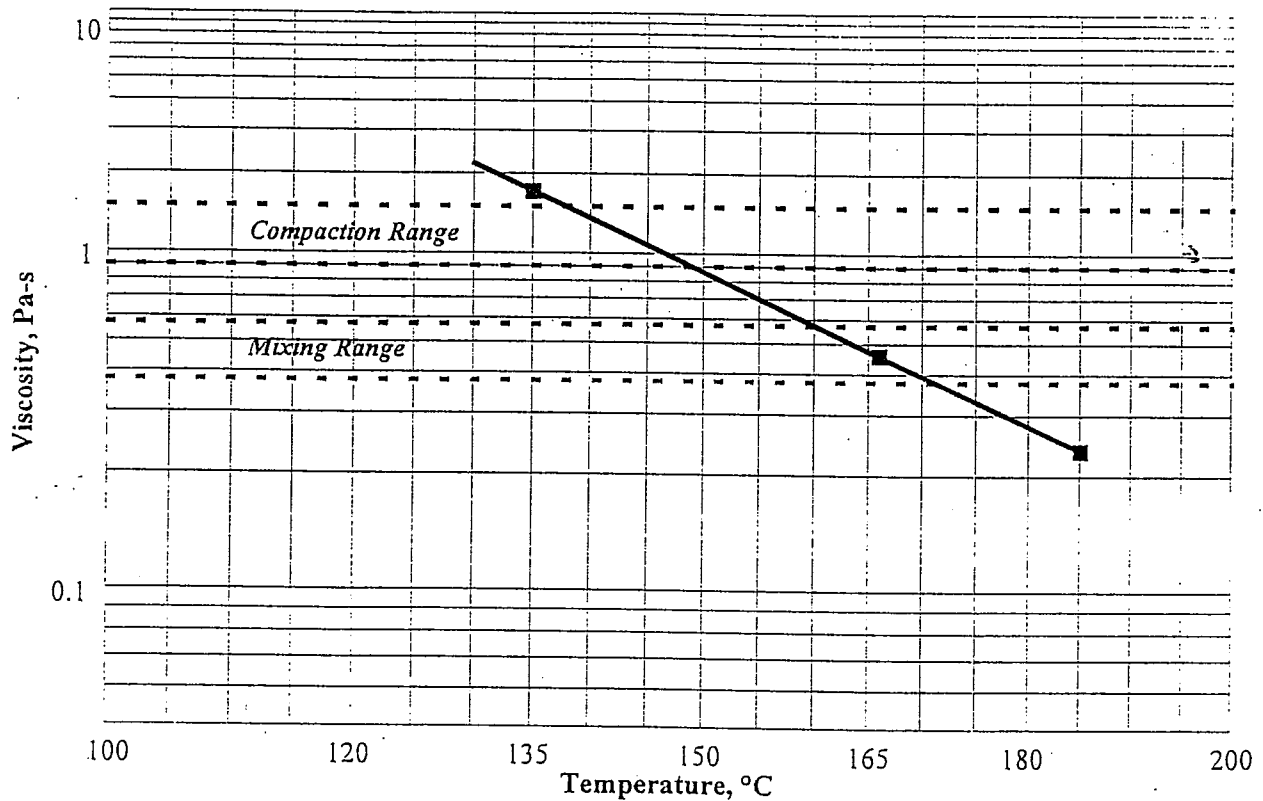
Temperature, °C

Note: Viscosity-Temperature charts for polymer modified asphalts are obtained at a fixed shear rate (<100 sec-1) and do not correspond to actual shear rates in the field. In particular compaction temperatures are dependent upon type of compactor used and environmental conditions, and therefore should be established by a test strip.

# APPENDIX D

**Data for ITD Mixes**

**Gradation, Volumetric Analysis and Calculation of**

**Energy Indices (CEI and TEI)**

# Gradation Analysis of ITD Mixes (Hveem and Superpave)

## Mix D1

**Mix D1 Gradation and wt.of aggr.(Hveem and SP)**

| Sieve Sizes | | Trial passing | Wt of agg. (4500g) | Wt of agg. (5500g) | Wt of agg. (5799g) hight 150 |
|---|---|---|---|---|---|
| 25mm | (1In) | 100% | | | |
| 19mm | (3/4 In) | 99% | 45 | 55 | 58 |
| 12.5mm | (1/2 In) | 88% | 495 | 605 | 638 |
| 9.5mm | (3/8 In) | 76% | 540 | 660 | 696 |
| 4.75mm | (N0.4) | 53% | 1035 | 1265 | 1334 |
| 2.36mm | (No.8) | 36% | 765 | 935 | 986 |
| 1.18mm | (No.30) | 23% | 585 | 715 | 754 |
| 600um | (No.50) | 15% | 360 | 440 | 464 |
| 300um | (No.16) | 9% | 270 | 330 | 348 |
| 150um | (No.100) | 5% | 180 | 220 | 232 |
| 75um | (No.200) | 4.8% | 9 | 11 | 12 |
| | -200 | | 216 | 264 | 278 |
| Total wt.of agg. | | | **4500** | **5500** | **5799** |
| Pb by wt.of agg. | Hv. | 5.3% | | | |
| | SP. | 5.3% | | | |
| Wt.of asphalt | Hv. | | **239** | **292** | **307** |
| | SP. | | **239** | **292** | **307** |

**Mix D1 - Changed Gradation of SP and wt.of aggr.**

| Sieve Sizes | | Trial passing | Wt of agg. (4500g) | Wt of agg. (5500g) | Wt of agg. (5799g) hight 150 |
|---|---|---|---|---|---|
| 25mm | (1In) | 100% | | | |
| 19mm | (3/4 In) | 93% | 315 | 385 | 406 |
| 12.5mm | (1/2 In) | 71% | 990 | 1210 | 1276 |
| 9.5mm | (3/8 In) | 53% | 810 | 990 | 1044 |
| 4.75mm | (N0.4) | 34% | 855 | 1045 | 1102 |
| 2.36mm | (No.8) | 26% | 360 | 440 | 464 |
| 1.18mm | (No.30) | 20% | 270 | 330 | 348 |
| 600um | (No.50) | 13% | 315 | 385 | 406 |
| 300um | (No.16) | 8% | 225 | 275 | 290 |
| 150um | (No.100) | 4% | 180 | 220 | 232 |
| 75um | (No.200) | 3.0% | 45 | 55 | 58 |
| | -200 | | 135 | 165 | 174 |
| Total wt.of agg. | | | **4500** | **5500** | **5799** |
| Pb by wt.of agg. | | | | | |
| | SP. | 5.3% | | | |
| Wt.of asphalt | | | | | |
| | SP. | | **239** | **292** | **307** |

# Gradation Analysis of ITD Mixes (Hveem and Superpave)

## Mix D2

**Mix D2 - Gradation and wt.of aggr.(Hveem and SP)**

| Sieve Sizes | | Trial passing | Wt of agg. (4500g) | Wt of agg. (5500g) | Wt of agg.for Hv. (5961g) hight 150 | Wt of agg.for SP. (5917g) hight 150 |
|---|---|---|---|---|---|---|
| 25mm | (1In) | 100% | | | | |
| 19mm | (3/4 In) | 99% | 45 | 55 | 60 | 59 |
| 12.5mm | (1/2 In) | 80% | 855 | 1045 | 1133 | 1124 |
| 9.5mm | (3/8 In) | 69% | 495 | 605 | 656 | 651 |
| 4.75mm | (N0.4) | 51% | 810 | 990 | 1073 | 1065 |
| 2.36mm | (No.8) | 33% | 810 | 990 | 1073 | 1065 |
| 1.18mm | (No.30) | 22% | 495 | 605 | 656 | 651 |
| 600um | (No.50) | 14% | 360 | 440 | 477 | 473 |
| 300um | (No.16) | 10% | 180 | 220 | 238 | 237 |
| 150um | (No.100) | 7% | 135 | 165 | 179 | 178 |
| 75um | (No.200) | 5.7% | 58.5 | 71.5 | 77 | 77 |
| | -200 | | 256.5 | 313.5 | 340 | 337 |
| Total wt.of agg. | | | **4500** | **5500** | **5961** | **5917** |
| Pb by wt.of agg. | Hv. | 6.1% | | | | |
| | SP. | 6.6% | | | | |
| Wt.of asphalt | Hv. | | **275** | **336** | **364** | **361** |
| | SP. | | **298** | **364** | **395** | **392** |

**Mix D2 - Changed Gradation of SP and wt.of aggr**

| Sieve Sizes | | Trial passing | Wt of agg. (4500g) | Wt of agg. (5500g) | Wt of agg.for Hv. (5961g) hight 150 | Wt of agg.for SP. (5917g) hight 150 |
|---|---|---|---|---|---|---|
| 25mm | (1In) | 100% | | | | |
| 19mm | (3/4 In) | 93% | 315 | 385 | 417 | 414 |
| 12.5mm | (1/2 In) | 70% | 1035 | 1265 | 1371 | 1361 |
| 9.5mm | (3/8 In) | 51% | 855 | 1045 | 1133 | 1124 |
| 4.75mm | (N0.4) | 34% | 765 | 935 | 1013 | 1006 |
| 2.36mm | (No.8) | 24% | 450 | 550 | 596 | 592 |
| 1.18mm | (No.30) | 20% | 180 | 220 | 238 | 237 |
| 600um | (No.50) | 13% | 315 | 385 | 417 | 414 |
| 300um | (No.16) | 9% | 180 | 220 | 238 | 237 |
| 150um | (No.100) | 7% | 90 | 110 | 119 | 118 |
| 75um | (No.200) | 4.5% | 112.5 | 137.5 | 149 | 148 |
| | -200 | | 202.5 | 247.5 | 268 | 266 |
| Total wt.of agg. | | | **4500** | **5500** | **5961** | **5917** |
| Pb by wt.of agg. | | | | | | |
| | SP. | 6.62% | | | | |
| Wt.of asphalt | | | | | | |
| | SP. | | **298** | **364** | **395** | **392** |

# Gradation Analysis of ITD Mixes (Hveem and Superpave)

## Mix D3

**Mix D3 - Gradation and wt.of aggr.(Hveem)**

| Sieve Sizes | | Trial passing | Wt of agg. (4500g) | Wt of agg. (5500g) | Wt of agg.for Hv. (5683g) hight 150 |
|---|---|---|---|---|---|
| 37.5mm | (11/2 In) | 100% | | | |
| 25mm | (1In) | 97% | 135 | 165 | 170.49 |
| 19mm | (3/4 In) | 88% | 405 | 495 | 511.47 |
| 12.5mm | (1/2 In) | 60% | 1260 | 1540 | 1591.24 |
| 9.5mm | (3/8 In) | 53% | 315 | 385 | 397.81 |
| 4.75mm | (N0.4) | 47% | 270 | 330 | 340.98 |
| 2.36mm | (No.8) | 32% | 675 | 825 | 852.45 |
| 1.18mm | (No.30) | 22% | 450 | 550 | 568.3 |
| 600um | (No.50) | 15% | 315 | 385 | 397.81 |
| 300um | (No.16) | 10% | 225 | 275 | 284.15 |
| 150um | (No.100) | 6% | 180 | 220 | 227.32 |
| 75um | (No.200) | 4.0% | 90 | 110 | 113.66 |
| | -200 | | 180 | 220 | 227.32 |
| Total wt.of agg. | | | **4500** | **5500** | **5683** |
| Pb by wt.of agg. | Hv. | 5.0% | | | |
| Wt.of asphalt | Hv. | | **225** | **275** | **284** |

**Mix D3 - Changed Gradation and wt.of aggr.**

| Sieve Sizes | | Trial passing | Wt of agg. (4500g) | Wt of agg. (5500g) | Wt of agg.for Hv. (5683g) hight 150 |
|---|---|---|---|---|---|
| 37.5mm | (11/2 In) | 100% | | | |
| 25mm | (1In) | 97% | 135 | 165 | 170.49 |
| 19mm | (3/4 In) | 88% | 405 | 495 | 511.47 |
| 12.5mm | (1/2 In) | 60% | 1260 | 1540 | 1591.24 |
| 9.5mm | (3/8 In) | 53% | 315 | 385 | 397.81 |
| 4.75mm | (N0.4) | 47% | 270 | 330 | 340.98 |
| 2.36mm | (No.8) | 32% | 675 | 825 | 852.45 |
| 1.18mm | (No.30) | 22% | 450 | 550 | 568.3 |
| 600um | (No.50) | 15% | 315 | 385 | 397.81 |
| 300um | (No.16) | 10% | 225 | 275 | 284.15 |
| 150um | (No.100) | 6% | 180 | 220 | 227.32 |
| 75um | (No.200) | 4.0% | 90 | 110 | 113.66 |
| | -200 | | 180 | 220 | 227.32 |
| Total wt.of agg. | | | **4500** | **5500** | **5683** |
| Pb by wt.of agg. | Hv. | 5.0% | | | |
| Wt.of asphalt | Hv. | | **225** | **275** | **284** |

Volumetric Analysis of Samples for ITD Mixes at N-initial

## Samples for Mix D1 at Ni

| Samples for D1 | D1S3 at N40 | D1S4 at N40 | D1H6 at N100 | D1H7 at N85 | D1H8 at N85 | D1h9 at N85 | D1H10 at N50 | D1H12 at N40 |
|---|---|---|---|---|---|---|---|---|
| Asphalt content Pb by aggr.WT | 5.25% | 5.25% | 5.30% | 5.3% | 5.30% | 5.30% | 5.3% | 5.3% |
| Asphalt content Pb by mix WT | 5.0% | 5.0% | 5.00% | 5.0% | 5.0% | 5.0% | 5.0% | 5.0% |
| Wdry: | 5989 | 6086.5 | 5772 | 5773 | 5777 | 5773 | 5765 | 5830 |
| Wsub: | 3433.3 | 3494.2 | 3369 | 3345 | 3378 | 3368 | 3325 | 3380 |
| Wssd: | 6023 | 6123.7 | 5794 | 5822.2 | 5796.4 | 5794.3 | 5808 | 5896.2 |
| Gmm: | 2.478 | 2.478 | 2.478 | 2.478 | 2.478 | 2.478 | 2.478 | 2.478 |
| Gsb: | 2.66 | 2.66 | 2.66 | 2.66 | 2.66 | 2.66 | 2.66 | 2.66 |
| Ps: | 95.0% | 95.0% | 95.0% | 95.0% | 95.0% | 95.0% | 95.0% | 95.0% |
| H | 148.61 | 151.15 | 139.5 | 140.42 | 138.84 | 139.16 | 141.23 | 141.83 |
| | | | | | | | | |
| Gmb=Wdry/Wssd-Wsub | | | | | | | | |
| Gmb(measured) | 2.313 | 2.315 | 2.380 | 2.330 | 2.389 | 2.379 | 2.322 | 2.317 |
| Gmb(estimated) | 2.282 | 2.280 | 2.343 | 2.328 | 2.356 | 2.349 | 2.311 | 2.327 |
| CF | 1.014 | 1.015 | 1.016 | 1.001 | 1.014 | 1.013 | 1.005 | 0.996 |
| Gmb(estimated)@Nmax: | 2.282 | 2.280 | 2.343 | 2.328 | 2.356 | 2.349 | 2.311 | 2.327 |
| Gmb(corrected)@Nmax: | 2.313 | 2.315 | 2.380 | 2.330 | 2.389 | 2.379 | 2.322 | 2.317 |
| %Va=1-Gmb/Gmm | | | | | | | | |
| %Va | 6.7% | 6.6% | 3.9% | 6.0% | 3.6% | 4.0% | 6.3% | 6.5% |
| %VMA=100-Gmb*Ps/Gsb | | | | | | | | |
| %VMA | 17.4% | 17.3% | 15.0% | 16.8% | 14.7% | 15.0% | 17.1% | 17.3% |
| %VFA=100*(VMA-Va)/VMA | | | | | | | | |
| %VFA | 61.7% | 62.0% | 73.7% | 64.5% | 75.5% | 73.5% | 63.1% | 62.3% |

# Volumetric Analysis of Samples for ITD Mixes at N-initial

## Samples for Mix D2 at Ni

| Samples for D2 | D2H7 at N90 | D2H8 at N95 | D2H9 at N70 | D2H13 at N70 | D2H14 at N70 | D2S3 at N70 | D2S4 at N70 | D2S5 at N40 | D2S6 at N60 | D2S8 at N60 |
|---|---|---|---|---|---|---|---|---|---|---|
| Asphalt content Pb by aggr.WT | 6.10% | 6.1% | 6.1% | 6.1% | 6.1% | 6.62% | 6.62% | 6.62% | 6.62% | 6.62% |
| Asphalt content Pb by mix WT | 5.75% | 5.75% | 5.75% | 5.75% | 5.75% | 6.20% | 6.20% | 6.20% | 6.20% | 6.20% |
| Wdry: | 5753.2 | 5832.8 | 5798.3 | 6276.5 | 6302.5 | 5824 | 5817 | 5806.6 | 6260.1 | 6275.3 |
| Wsub: | 3405 | 3448 | 3417.3 | 3687.5 | 3706 | 3437 | 3424 | 3388.6 | 3680.2 | 3674.6 |
| Wssd: | 5800.3 | 5865.2 | 5837 | 6308 | 6345.1 | 5869 | 5854 | 5853.2 | 6302.6 | 6334.9 |
| Gmm: | 2.567 | 2.567 | 2.567 | 2.567 | 2.567 | 2.548 | 2.548 | 2.548 | 2.548 | 2.548 |
| Gsb: | 2.68 | 2.68 | 2.68 | 2.68 | 2.68 | 2.68 | 2.68 | 2.68 | 2.68 | 2.68 |
| Ps: | 94.25% | 94.25% | 94.25% | 94.25% | 94.25% | 93.80% | 93.80% | 93.80% | 93.80% | 93.80% |
| H90: | 137.81 | 140.3 | 140.83 | 151.62 | 153.17 | 138.92 | 138.71 | 144.01 | 152.59 | 154.85 |
| | | | | | | | | | | |
| Gmb=Wdry/Wssd-Wsub | | | | | | | | | | |
| Gmb(measured) | 2.402 | 2.413 | 2.396 | 2.395 | 2.388 | 2.395 | 2.394 | 2.356 | 2.387 | 2.359 |
| Gmb(estimated) | 2.364 | 2.354 | 2.331 | 2.344 | 2.330 | 2.374 | 2.374 | 2.283 | 2.323 | 2.294 |
| CF | 1.016 | 1.025 | 1.028 | 1.022 | 1.025 | 1.009 | 1.008 | 1.032 | 1.028 | 1.028 |
| Gmb(estimated)@Nmax: | 2.364 | 2.354 | 2.331 | 2.344 | 2.330 | 2.374 | 2.374 | 2.283 | 2.323 | 2.294 |
| Gmb(corrected)@Nmax: | 2.402 | 2.413 | 2.396 | 2.395 | 2.388 | 2.395 | 2.394 | 2.356 | 2.387 | 2.359 |
| %Va=1-Gmb/Gmm | | | | | | | | | | |
| %Va@N90: | 6.4% | 6.0% | 6.7% | 6.7% | 7.0% | 6.02% | 6.05% | 7.5% | 6.3% | 7.42% |
| %VMA=100-Gmb*Ps/Gsb | | | | | | | | | | |
| %VMA | 15.53% | 15.1% | 15.7% | 15.8% | 16.0% | 16.2% | 16.2% | 17.5% | 16.4% | 17.4% |
| %VFA=100*(VMA-Va)/VMA | | | | | | | | | | |
| %VFA | 58.58% | 60.4% | 57.7% | 57.5% | 56.5% | 62.8% | 62.7% | 57.0% | 61.6% | 57.4% |

Volumetric Analysis of Samples for ITD Mixes at N-initial

## Sample for Mix D3 at Ni

| Samples for D3 | D3H6 at N40 | D3H7 at N40 | D3H8 at N40 | D3H9 at N50 |
|---|---|---|---|---|
| Asphalt content Pb by aggr.W | 5.0% | 5.0% | 5.0% | 5.0% |
| Asphalt content Pb by mix W | 4.8% | 4.8% | 4.8% | 4.8% |
| Wdry: | 5758.2 | 5757.5 | 5929.7 | 5937.1 |
| Wsub: | 3290 | 3302 | 3384 | 3394.1 |
| Wssd: | 5850 | 5844 | 5996.8 | 6018.6 |
| Gmm: | 2.422 | 2.422 | 2.422 | 2.422 |
| Gsb: | 2.547 | 2.547 | 2.547 | 2.547 |
| Ps: | 95.24% | 95.24% | 95.24% | 95.24% |
| H | 147.07 | 143.81 | 151.04 | 153.04 |
| | | | | |
| Gmb=Wdry/Wssd-Wsub | | | | |
| Gmb(measured) | 2.249 | 2.265 | 2.269 | 2.262 |
| Gmb(estimated) | 2.217 | 2.267 | 2.223 | 2.196 |
| CF | 1.015 | 0.999 | 1.021 | 1.030 |
| Gmb(estimated) @Nmax: | 2.217 | 2.267 | 2.223 | 2.196 |
| Gmb(corrected) @Nmax: | 2.249 | 2.265 | 2.269 | 2.262 |
| %Va=1-Gmb/Gmm | | | | |
| **%Va** | **7.1%** | **6.5%** | **6.3%** | **6.6%** |
| %VMA=100-Gmb*Ps/Gsb | | | | |
| **%VMA** | **15.9%** | **15.3%** | **15.1%** | **15.4%** |
| %VFA=100*(VMA-Va)/VMA | | | | |
| **%VFA** | **55.1%** | **57.6%** | **58.4%** | **57.2%** |

# Volumetric Analysis and CEI Calculations for Samples of Mix D1

Samples Compacted to N max = 160

| Sample for D1 | D1H1 | D1H2 | D1H3 | D1H4 | D1H5 | D1S1 | D1S2 | D1H13 | D1H14 | D1H15 | D1H16 | D1S5(ch.g) | D1S6(ch.g) |
|---|---|---|---|---|---|---|---|---|---|---|---|---|---|
| Asphalt content, Pb by aggregate weight | 5.3% | 5.3% | 5.3% | 5.3% | 5.3% | 5.3% | 5.3% | 6.3% | 6.3% | 4.3% | 4.3% | 5.3% | 5.3% |
| Asphalt content, Pb by mix weight | 5.0% | 5.0% | 5.0% | 5.0% | 5.0% | 5.0% | 5.0% | 5.93% | 5.93% | 4.1% | 4.1% | 5.0% | 5.0% |
| Wdry: | 4727.2 | 4671.6 | 4703 | 4756.1 | 4744.6 | 4709 | 4688 | 4762.7 | 4765.5 | 5801.7 | 5800 | 4715.2 | 4705.6 |
| Wsub: | 2772 | 2727.3 | 2775.2 | 2801.5 | 2811 | 2774 | 2753 | 2814.1 | 2814.2 | 3429.3 | 3430.5 | 2783.4 | 2781.3 |
| Wssd: | 4738 | 4682.1 | 4708.7 | 4767.7 | 4760 | 4730 | 4702 | 4770.8 | 4774 | 5821.8 | 5818.3 | 4728.1 | 4722.4 |
| Gmm: | 2.478 | 2.478 | 2.478 | 2.478 | 2.478 | 2.478 | 2.478 | 2.444 | 2.444 | 2.511 | 2.511 | 2.478 | 2.478 |
| Gsb: | 2.66 | 2.66 | 2.66 | 2.66 | 2.66 | 2.66 | 2.66 | 2.66 | 2.66 | 2.66 | 2.66 | 2.66 | 2.66 |
| Ps: | 95.0% | 95.0% | 95.0% | 95.0% | 95.0% | 95.0% | 95.0% | 94.1% | 94.1% | 95.9% | 95.9% | 95.0% | 95.0% |
| Hini: | 126.09 | 127.14 | 126.43 | 128.19 | 125.77 | 129.91 | 127.77 | 126.95 | 126.71 | 153.96 | 153.93 | 128.29 | 128.29 |
| Hdes: | 113.05 | 113.82 | 112.93 | 114.65 | 112.72 | 116.51 | 115.03 | 113.81 | 113.82 | 138.21 | 138.13 | 114.12 | 114.12 |
| Hmax: | 111.65 | 112.32 | 111.3 | 113.14 | 111.35 | 115.07 | 113.67 | 112.38 | 112.36 | 136.49 | 136.36 | 112.51 | 112.51 |
| **Gmb calculation** | | | | | | | | | | | | | |
| Gmb(measured) at Nmax=Wdry/(Wssd-Wsub) | 2.404 | 2.390 | 2.432 | 2.419 | 2.434 | 2.407 | 2.405 | 2.434 | 2.432 | 2.425 | 2.429 | 2.425 | 2.424 |
| Gmb(estimated) | 2.397 | 2.355 | 2.392 | 2.380 | 2.412 | 2.317 | 2.335 | 2.399 | 2.401 | 2.407 | 2.408 | 2.373 | 2.368 |
| CF | 1.003 | 1.015 | 1.017 | 1.016 | 1.009 | 1.039 | 1.030 | 1.014 | 1.013 | 1.008 | 1.009 | 1.022 | 1.024 |
| Gmb(estimated)@Nd: | 2.367 | 2.324 | 2.358 | 2.349 | 2.383 | 2.288 | 2.307 | 2.369 | 2.370 | 2.377 | 2.377 | 2.339 | 2.335 |
| Gmb(corrected)@Nd: | 2.375 | 2.358 | 2.397 | 2.387 | 2.405 | 2.378 | 2.377 | 2.403 | 2.400 | 2.395 | 2.398 | 2.390 | 2.390 |
| Gmb(estimated)@Nini: | 2.123 | 2.080 | 2.106 | 2.101 | 2.136 | 2.052 | 2.077 | 2.124 | 2.129 | 2.134 | 2.133 | 2.081 | 2.077 |
| Gmb(corrected)@Nini: | 2.129 | 2.111 | 2.141 | 2.135 | 2.155 | 2.132 | 2.140 | 2.155 | 2.156 | 2.150 | 2.152 | 2.126 | 2.126 |
| **Verification of Superpave Criteria at Ndes** | | | | | | | | | | | | | |
| %VMA=100-Gmb(corrected)@Nd*Ps/Gsb | 15.19% | 15.77% | 14.38% | 14.75% | 14.11% | 15.08% | 15.11% | 15.00% | 15.11% | 13.68% | 13.57% | 14.63% | 14.64% |
| %Va@Nd=1-Gmb@Ndes/Gmm | 4.17% | 4.83% | 3.26% | 3.67% | 2.95% | 4.05% | 4.08% | 1.66% | 1.78% | 4.63% | 4.50% | 3.53% | 3.55% |
| %VFA@Nd=100*(VMA-Va)/VMA | 72.6% | 69.4% | 77.3% | 75.1% | 79.1% | 73.2% | 73.0% | 88.9% | 88.2% | 66.2% | 66.8% | 75.8% | 75.7% |
| %Gmm@Nini | 85.9% | 85.2% | 86.4% | 86.2% | 87.0% | 86.1% | 86.4% | 88.2% | 88.2% | 85.6% | 85.7% | 85.8% | 85.8% |
| %Gmm@Ndes | 95.8% | 95.2% | 96.7% | 96.3% | 97.0% | 96.0% | 95.9% | 98.3% | 98.2% | 95.4% | 95.5% | 96.5% | 96.4% |
| %Gmm@Nmax | 97.0% | 96.4% | 98.2% | 97.6% | 98.2% | 97.2% | 97.1% | 99.6% | 99.5% | 96.6% | 96.7% | 97.8% | 97.8% |
| **Air Voids Change** | | | | | | | | | | | | | |
| %Va @Nini = 1-Gmb (corrected @ Nini)/Gmm | 14.1% | 14.8% | 13.6% | 13.8% | 13.0% | 13.9% | 13.6% | 11.8% | 11.8% | 14.4% | 14.3% | 14.2% | 14.2% |
| %Va@Nd=1-Gmb@Ndes/Gmm | 4.2% | 4.8% | 3.3% | 3.7% | 3.0% | 4.0% | 4.1% | 1.7% | 1.8% | 4.6% | 4.5% | 3.5% | 3.6% |
| %Va@Nmax=1-Gmb@Nmax/Gmm | 3.0% | 3.6% | 1.8% | 2.4% | 1.8% | 2.8% | 2.9% | 0.4% | 0.5% | 3.4% | 3.3% | 2.2% | 2.2% |
| **CEI Results** | | | | | | | | | | | | | |
| CEI based on Nmax=160 | 20.043 | 21.839 | 21.717 | 21.308 | 19.985 | 22.054 | 21.083 | 17.27 | 18.586 | 18.441 | 19.585 | 22.579 | 20.875 |
| CEI based on Ndes=100 | 17.086 | 18.826 | 18.514 | 18.283 | 17.115 | 19.44 | 18.614 | 14.275 | 15.658 | 15.343 | 16.632 | 19.432 | 17.321 |
| TEI based on Nmax=160 | 966.39 | 970.54 | 947.48 | 946.99 | 966.15 | 901 | 914.95 | 932.55 | 931.88 | 810.53 | 780.63 | 929.942 | 918.387 |

## Volumetric Analysis and CEI Calculations for Samples of Mix D2

Samples Compacted to N max = 160

| Sample for D2 | D2H1 | D2H2 | D2H3 | D2H4 | D2H5 | D2H6 | D2S1 | D2S2 | D2H10 | D2H11 | D2H14 | D2H15 | D2S9(ch.g) | D2S10(ch.g) |
|---|---|---|---|---|---|---|---|---|---|---|---|---|---|---|
| Asphalt content, Pb by aggregate weight | 6.1% | 6.1% | 6.1% | 6.1% | 6.1% | 6.1% | 6.62% | 6.62% | 7.6% | 7.6% | 5.6% | 5.6% | 6.62% | 6.62% |
| Asphalt content, Pb by mix weight | 5.75% | 5.75% | 5.75% | 5.75% | 5.75% | 5.75% | 6.20% | 6.20% | 7.08% | 7.08% | 5.32% | 5.32% | 6.21% | 6.21% |
| Wdry: | 4745.7 | 4738.2 | 4656.6 | 4738 | 4749.4 | 4758 | 4751.7 | 4742 | 4795 | 4791.1 | 4664 | 4665 | 4656.8 | 4757.4 |
| Wsub: | 2842.8 | 2821.3 | 2783.5 | 2815.1 | 2828.2 | 2842 | 2838.4 | 2835.4 | 2867.2 | 2858.1 | 2787.5 | 2779.8 | 2779.8 | 2850.3 |
| Wssd: | 4762.5 | 4742.4 | 4665.9 | 4750.1 | 4761 | 4776 | 4758 | 4751 | 4804.7 | 4795.5 | 4720.5 | 4712.4 | 4666.3 | 4777.4 |
| Gmm: | 2.567 | 2.567 | 2.567 | 2.567 | 2.567 | 2.567 | 2.548 | 2.548 | 2.514 | 2.514 | 2.585 | 2.585 | 2.548 | 2.548 |
| Gsb: | 2.68 | 2.68 | 2.68 | 2.68 | 2.68 | 2.68 | 2.68 | 2.68 | 2.68 | 2.68 | 2.68 | 2.68 | 2.68 | 2.68 |
| Ps: | 94.25% | 94.25% | 94.25% | 94.25% | 94.25% | 94.25% | 93.8% | 93.8% | 92.92% | 92.92% | 94.68% | 94.68% | 93.8% | 93.8% |
| Hini: | 126.28 | 127.36 | 125.25 | 128.35 | 125.41 | 125.66 | 125.66 | 125.66 | 127.82 | 127.83 | 129.51 | 130.08 | 127.21 | 129.22 |
| Hdes: | 112.99 | 112.99 | 111.5 | 113.83 | 111.8 | 111.81 | 111.81 | 111.81 | 112.99 | 113.62 | 115.54 | 116.08 | 111.97 | 114.12 |
| Hmax: | 111.55 | 111.52 | 109.92 | 112.22 | 110.33 | 110.43 | 110.43 | 110.43 | 111.45 | 112.11 | 113.99 | 114.52 | 110.37 | 112.54 |
| **Gmb calculation** | | | | | | | | | | | | | | |
| Gmb(measured) at Nmax=Wdry/(Wssd-Wsub) | 2.472 | 2.466 | 2.474 | 2.449 | 2.457 | 2.460 | 2.475 | 2.475 | 2.475 | 2.473 | 2.413 | 2.414 | 2.468 | 2.469 |
| Gmb(estimated) | 2.409 | 2.406 | 2.399 | 2.390 | 2.437 | 2.439 | 2.436 | 2.431 | 2.436 | 2.420 | 2.317 | 2.306 | 2.389 | 2.393 |
| CF | 1.026 | 1.025 | 1.031 | 1.024 | 1.008 | 1.009 | 1.016 | 1.018 | 1.016 | 1.022 | 1.042 | 1.047 | 1.033 | 1.031 |
| Gmb(estimated)@Nd: | 2.378 | 2.374 | 2.365 | 2.357 | 2.405 | 2.409 | 2.406 | 2.401 | 2.403 | 2.387 | 2.285 | 2.275 | 2.355 | 2.360 |
| Gmb(corrected)@Nd: | 2.441 | 2.434 | 2.439 | 2.414 | 2.425 | 2.430 | 2.445 | 2.445 | 2.441 | 2.440 | 2.380 | 2.381 | 2.433 | 2.435 |
| Gmb(estimated)@Nini: | 2.128 | 2.106 | 2.105 | 2.090 | 2.144 | 2.144 | 2.141 | 2.137 | 2.124 | 2.122 | 2.039 | 2.030 | 2.073 | 2.084 |
| Gmb(corrected)@Nini: | 2.184 | 2.160 | 2.171 | 2.141 | 2.162 | 2.162 | 2.175 | 2.175 | 2.158 | 2.169 | 2.124 | 2.125 | 2.142 | 2.150 |
| **Verification of Superpave Criteria at Ndes** | | | | | | | | | | | | | | |
| %VMA=100-Gmb(corrected)@Nd*Ps/Gsb | 14.17% | 14.39% | 14.24% | 15.11% | 14.72% | 14.55% | 14.43% | 14.43% | 15.36% | 15.40% | 15.90% | 15.87% | 14.85% | 14.80% |
| %Va@Nd=1-Gmb@Ndes/Gmm | 4.92% | 5.17% | 5.00% | 5.96% | 5.53% | 5.34% | 4.05% | 4.05% | 2.90% | 2.94% | 7.91% | 7.88% | 4.50% | 4.45% |
| %VFA@Nd=100*(VMA-Va)/VMA | 65.2% | 64.1% | 64.9% | 60.5% | 62.4% | 63.3% | 71.9% | 72.0% | 81.1% | 80.9% | 50.2% | 50.4% | 69.7% | 69.9% |
| %Gmm@Nini | 85.1% | 84.1% | 84.6% | 83.4% | 84.2% | 84.2% | 85.4% | 85.4% | 85.8% | 86.3% | 82.2% | 82.2% | 84.1% | 84.4% |
| %Gmm@Ndes | 95.1% | 94.8% | 95.0% | 94.0% | 94.5% | 94.7% | 96.0% | 96.0% | 97.1% | 97.1% | 92.1% | 92.1% | 95.5% | 95.5% |
| %Gmm@Nmax | 96.3% | 96.1% | 96.4% | 95.4% | 95.7% | 95.8% | 97.1% | 97.2% | 98.4% | 98.4% | 93.3% | 93.4% | 96.9% | 96.9% |
| **Air Voids Change** | | | | | | | | | | | | | | |
| %Va @Nini = 1-Gmb (corrected at Nini)/Gmm | 14.93% | 15.87% | 15.43% | 16.60% | 15.79% | 15.78% | 14.63% | 14.62% | 14.17% | 13.73% | 17.85% | 17.79% | 15.95% | 15.62% |
| %Va@Nd=1-Gmb@Ndes/Gmm | 4.92% | 5.17% | 5.00% | 5.96% | 5.53% | 5.34% | 4.05% | 4.05% | 2.90% | 2.94% | 7.91% | 7.88% | 4.50% | 4.45% |
| %Va@Nmax=1-Gmb@Nmax/Gmm | 3.70% | 3.92% | 3.63% | 4.61% | 4.27% | 4.16% | 2.85% | 2.85% | 1.56% | 1.63% | 6.66% | 6.62% | 3.12% | 3.11% |
| **CEI Results** | | | | | | | | | | | | | | |
| CEI based on Nmax=160 | 17.796 | 17.815 | 17.08 | 18.934 | 19.322 | 19.98 | 22.872 | 22.783 | 18.431 | 19.322 | 21.651 | 19.677 | 20.521 | 20.038 |
| CEI based on Ndes=100 | 14.885 | 15.358 | 13.73 | 15.712 | 16.445 | 17.169 | 20.074 | 19.81 | 15.245 | 16.29 | 18.663 | 16.587 | 17.303 | 16.865 |
| TEI based on Nmax=160 | 926.23 | 937.61 | 924.27 | 929.92 | 926.11 | 924.59 | 920.56 | 989.84 | 919.24 | 916.02 | 907.36 | 907.03 | 9191.332 | 913.743 |

## Volumetric Analysis and CEI Calculations for Samples of Mix D3

Samples Compacted to N max = 160

| Sample for D3 | D3H1 | D3H2 | D3H3 | D3H4 | D3H5 | D3S1(ch.gr) | D3S2(ch.gr) | D3S5 | D3S6 |
|---|---|---|---|---|---|---|---|---|---|
| Asphat cntent, Pb by Aggregate weight | 5.0% | 5.0% | 5.0% | 5.0% | 5.0% | 5.0% | 5.0% | 6.0% | 4.0% |
| Asphat cntent, Pb by mix weight | 4.8% | 4.8% | 4.8% | 4.8% | 4.8% | 4.8% | 4.8% | 5.7% | 3.8% |
| Wdry: | 4659.8 | 4741.6 | 4673.6 | 4710.1 | 4709.6 | 4587.4 | 4707.6 | 4709.6 | 4683.3 |
| Wsub: | 2735.4 | 2755 | 2727.2 | 2746.7 | 2733.5 | 2636.6 | 2722.7 | 2739.7 | 2709.4 |
| Wssd: | 4670.2 | 4749.5 | 4682.7 | 4720.5 | 4719.5 | 4590 | 4723.5 | 4726.3 | 4721.8 |
| Gmm: | 2.422 | 2.422 | 2.422 | 2.422 | 2.422 | 2.422 | 2.422 | 2.422 | 2.422 |
| Gsb: | 2.547 | 2.547 | 2.547 | 2.547 | 2.547 | 2.547 | 2.547 | 2.547 | 2.547 |
| Ps: | 95.2% | 95.2% | 95.2% | 95.2% | 95.2% | 95.2% | 95.2% | 94.3% | 96.2% |
| Hini (Nini = 8) | 122.88 | 124.94 | 125.57 | 127.15 | 127.01 | 147.76 | 129.94 | 129.94 | 129.94 |
| Hdes (Ndes = 100) | 112.93 | 114.72 | 114.74 | 116.08 | 115.86 | 115.22 | 117.43 | 117.43 | 117.43 |
| Hmax (Nmax = 160) | 111.79 | 113.78 | 113.32 | 114.81 | 114.46 | 113.92 | 116.08 | 116.08 | 116.08 |
| **Gmb calculations** | | | | | | | | | |
| Gmb(measured) at Nmax=Wdry/(Wssd-Wsub) | 2.408 | 2.377 | 2.390 | 2.386 | 2.371 | 2.348 | 2.353 | 2.371 | 2.327 |
| Gmb(estimated) based on hight at Nmax | 2.360 | 2.359 | 2.335 | 2.323 | 2.330 | 2.280 | 2.296 | 2.297 | 2.284 |
| CF | 1.021 | 1.008 | 1.024 | 1.027 | 1.018 | 1.030 | 1.025 | 1.032 | 1.019 |
| Gmb(estimated)@Nd | 2.336 | 2.340 | 2.306 | 2.297 | 2.301 | 2.254 | 2.270 | 2.271 | 2.258 |
| Gmb(corrected)@Nd | 2.384 | 2.358 | 2.360 | 2.360 | 2.343 | 2.322 | 2.326 | 2.343 | 2.300 |
| Gmb(estimated)@Nini | 2.147 | 2.149 | 2.107 | 2.097 | 2.099 | 1.758 | 2.051 | 2.052 | 2.041 |
| Gmb(corrected)@Nini | 2.191 | 2.165 | 2.157 | 2.155 | 2.137 | 1.811 | 2.102 | 2.118 | 2.079 |
| **Verification of Superpave Criteria at Ndes** | | | | | | | | | |
| %VMA=100-Gmb(corrected)@Nd*Ps/Gsb | 10.9% | 11.8% | 11.7% | 11.7% | 12.4% | 13.2% | 13.0% | 13.2% | 13.2% |
| %Va@Nd=1-Gmb@Ndes/Gmm | 1.6% | 2.6% | 2.5% | 2.6% | 3.3% | 4.1% | 4.0% | 3.2% | 5.0% |
| %VFA@Nd=100*(VMA-Va)/VMA | 85.6% | 77.6% | 78.3% | 78.3% | 73.6% | 68.6% | 69.5% | 75.4% | 61.9% |
| %Gmm@Nini | 90.5% | 89.4% | 89.1% | 89.0% | 88.2% | 74.8% | 86.8% | 87.4% | 85.8% |
| %Gmm@Ndes | 98.4% | 97.4% | 97.5% | 97.4% | 96.7% | 95.9% | 96.0% | 96.8% | 95.0% |
| %Gmm@Nmax | 99.4% | 98.2% | 98.7% | 98.5% | 97.9% | 97.0% | 97.1% | 97.9% | 96.1% |
| **Air Voids Change** | | | | | | | | | |
| %Va @Nini = 1-Gmb (corrected at Nini)/Gmm | 9.5% | 10.6% | 10.9% | 11.0% | 11.8% | 25.2% | 13.2% | 12.6% | 14.2% |
| %Va@Nd=1-Gmb@Ndes/Gmm | 1.6% | 2.6% | 2.5% | 2.6% | 3.3% | 4.1% | 4.0% | 3.2% | 5.0% |
| %Va@Nmax=1-Gmb@Nmax/Gmm | 0.6% | 1.8% | 1.3% | 1.5% | 2.1% | 3.0% | 2.9% | 2.1% | 3.9% |
| **CEI Results** | | | | | | | | | |
| CEI based on Nmax=160 | 9.673 | 8.307 | 18.166 | 10.049 | 12.41 | 22.788 | 23.245 | 19.463 | 18.872 |
| CEI based on Ndes=100 | 7.322 | 6.313 | 16.06 | 7.381 | 9.706 | 20.855 | 19.786 | 17.026 | 16.873 |
| TEI based on Nmax=160 | 857.388 | 843.389 | 840.398 | 837.87 | 834.918 | 824.894 | 819.769 | 835.289 | 840.14 |

# APPENDIX E

**APA Test Results for ITD Mixes**

# REPORT OF TEST ON AGGREGATE

|  |  |
|---|---|
| | Lab No. **02 A0313** |
| Sample of **Gyratory Specimens** | Job Order No. **2A-310** |
| Key No. **8774**    Project No. **SPR-0010(029)** | Source No. |
| Ident No. **B / F02901R  - A - RX / 601-CX** | Contract Item No. |
| Date Sampled ____ By **BAYOMY** | For **BAYOMY** |
| Test Hole No. ____ Depth ____ | County |
| Sampled From **GYO** | Quantity Represented |
| Location | |
| Remarks | |
| Test For **APA** | Date Received **7/20/2002** |

## Test Results

### Gradation-Percent Passing

| Column No. | 1 | 2 | 3 | 4 | 5 | 6 | 7 | 8 | 9 | 10 |
|---|---|---|---|---|---|---|---|---|---|---|
| 75 mm (3 In.) | | | | | | | | | | |
| 50 mm (2 In.) | | | | | | | | | | |
| 37.5 mm (1½ In.) | | | | | | | | | | |
| 25 mm (1 In.) | | | | | | | | | | |
| 19 mm (3/4 In.) | | | | | | | | | | |
| 12.5 mm (1/2 In.) | | | | | | | | | | |
| 9.5 mm (3/8 In.) | | | | | | | | | | |
| 4.75 mm (No.4) | | | | | | | | | | |
| 2.36 mm (No.8) | | | | | | | | | | |
| 1.18 mm (No.16) | | | | | | | | | | |
| 600 µm (No.30) | | | | | | | | | | |
| 300 µm (No.50) | | | | | | | | | | |
| 150 µm (No. 100) | | | | | | | | | | |
| 75 µm (No.200) | | | | | | | | | | |
| Sand Equiv. | | | | | | | | | | |
| T-304 Voids | | | | | | | | | | |
| Liquid Limit | | | | | | | | | | |
| Plastic Index | | | | | | | | | | |

| Resistance Value | | |
|---|---|---|
| Dry (Kg/M³) Max. | | |
| Ethylene Glycol % Ret. | | |

| SP.GR. | +4.75 mm | -4.75 mm | Ave. |
|---|---|---|---|
| Bulk | | | |
| Apparent | | | |
| Absorption | | | |

### Los Angeles Abrasion

| | |
|---|---|
| Grading | |
| 500 Rev. | % |

### Crushed Particles Retained

| | |
|---|---|
| 90% One Face +4.75 mm | % |
| 60% Two Faces +4.75 mm | % |

| | |
|---|---|
| Wt. Kg/M³ Loose. | |
| Cleaness Value | |

### For Further Tests, See Lab No's

| Date Aggregate Delivered | ____ | Date Started | ____ |
|---|---|---|---|
| Date Asphalt Delivered | ____ | Date Due | ____ |
| Date Commericial Report Received | ____ | Date Completed | ____ |

**Remarks:**

Special testing for the University of Idaho Research.  11 Pairs of Gyratory samples prepared at U of I and tested at ITD for Ruttting Characteristic.

Material as Represented is: ☐ Acceptable    ☐ Subject to Rejection    ☐ For Information Only

Recommendations For Mix Design:    Sheet __ of __

Date Mailed  **OCT 1 0 2002**

**JEFF R. MILES, P.E.**

E - 1 _____ ,P.E.

Materials Engineer

# ASPHALT PAVEMENT ANALYZER
## Rutting Test Data Sheet

**PTI**
**PAVEMENT TECHNOLOGY, INC.**

| | | |
|---|---|---|
| Project No. : MIX D-1 | Test No. : R0923-0 | Temperature : 58 (deg. C) |
| Mix ID No. : DI | Test Date: ~~10/08/02~~ 9-25-02 | Wheel Load : 100 (lbs) |
| Mix Type : CORES | Data File : R0923_0.ptd | Hose Pressure : 100 (psi) |
| Operator : M TISH | Run Status : Complete | Run Time 2:15:46 (hh:mm:ss) |

**Left Sample ID D1S4@N40**  **Bulk S Gravity 2.315**  **% Air Void 6.60%**

| Stroke Count | Temperature F | Temperature C | Depth Gauge Reading (mm) 1 | 2 | 3 | 4 | 5 | Manual Average | Net Man Deflection | APA-DAS Average | Percent Change |
|---|---|---|---|---|---|---|---|---|---|---|---|
| 0 | | | | | | | | | 0.000 | 0.000 | |
| 500 | | | | | | | | | | 1.011 | |
| 1,000 | | | | | | | | | | 1.307 | 29.2 |
| 1,500 | | | | | | | | | | 1.478 | 13.1 |
| 2,000 | | | | | | | | | | 1.651 | 11.7 |
| 3,000 | | | | | | | | | | 1.876 | 13.6 |
| 4,000 | | | | | | | | | | 2.134 | 13.8 |
| 5,000 | | | | | | | | | | 2.380 | 11.5 |
| 6,000 | | | | | | | | | | 2.485 | 4.4 |
| 7,000 | | | | | | | | | | 2.612 | 5.1 |
| 8,000 | | | | | | | | | | 2.744 | 5.0 |
| 8,000 | | | | | | | | | | 2.744 | 0.0 |

**Middle Sample ID D1H12@N40**  **Bulk S Gravity 2.317**  **% Air Void 6.50%**

| Stroke Count | Temperature F | Temperature C | Depth Gauge Reading (mm) 1 | 2 | 3 | 4 | 5 | Manual Average | Net Man Deflection | APA-DAS Average | Percent Change |
|---|---|---|---|---|---|---|---|---|---|---|---|
| 0 | | | | | | | | | 0.000 | 0.000 | |
| 500 | | | | | | | | | | 0.726 | |
| 1,000 | | | | | | | | | | 0.875 | 20.6 |
| 1,500 | | | | | | | | | | 0.991 | 13.3 |
| 2,000 | | | | | | | | | | 1.160 | 17.0 |
| 3,000 | | | | | | | | | | 1.282 | 10.6 |
| 4,000 | | | | | | | | | | 1.367 | 6.6 |
| 5,000 | | | | | | | | | | 1.501 | 9.8 |
| 6,000 | | | | | | | | | | 1.671 | 11.3 |
| 7,000 | | | | | | | | | | 1.826 | 9.2 |
| 8,000 | | | | | | | | | | 1.965 | 7.6 |
| 8,000 | | | | | | | | | | 1.965 | 0.0 |

**Right Sample ID D1S3@N40**  **Bulk S Gravity 2.313**  **% Air Void 6.70%**

| Stroke Count | Temperature F | Temperature C | Depth Gauge Reading (mm) 1 | 2 | 3 | 4 | 5 | Manual Average | Net Man Deflection | APA-DAS Average | Percent Change |
|---|---|---|---|---|---|---|---|---|---|---|---|
| 0 | | | | | | | | | 0.000 | 0.000 | |
| 500 | | | | | | | | | | 1.469 | |
| 1,000 | | | | | | | | | | 1.810 | 23.3 |
| 1,500 | | | | | | | | | | 2.086 | 15.3 |
| 2,000 | | | | | | | | | | 2.136 | 2.4 |
| 3,000 | | | | | | | | | | 2.390 | 11.9 |
| 4,000 | | | | | | | | | | 2.441 | 2.1 |
| 5,000 | | | | | | | | | | 2.765 | 13.3 |
| 6,000 | | | | | | | | | | 3.109 | 12.4 |
| 7,000 | | | | | | | | | | 3.371 | 8.4 |
| 8,000 | | | | | | | | | | 3.704 | 9.9 |
| 8,000 | | | | | | | | | | 3.704 | 0.0 |

OCT 1 0 2002          E - 2          JEFF R. MILES, P.E.

# ASPHALT PAVEMENT ANALYZER
## Rutting Test Data Sheet

**PTi**
**PAVEMENT TECHNOLOGY, INC.**

Project No. : MIX D-2  Test No. : R0930-0  Temperature : 64 (deg. C)
Mix ID No. : D-2  Test Date: 10/08/02 9-26-02  Wheel Load : 100 (lbs)
Mix Type : CYLINDERS  Data File : R0930_0.ptd  Hose Pressure : 100 (psi)
Operator : M TISH  Run Status : Complete  Run Time 2:15:42 (hh:mm:ss)

**Left Sample ID D2H8@N95** | Bulk S Gravity 2.413 | % Air Void 6.00%

| Stroke Count | Temperature F | C | Depth Gauge Reading (mm) 1 | 2 | 3 | 4 | 5 | Manual Average | Net Man Deflection | APA-DAS Average | Percent Change |
|---|---|---|---|---|---|---|---|---|---|---|---|
| 0 | | | | | | | | | 0.000 | 0.000 | |
| 500 | | | | | | | | | | 0.854 | |
| 1,000 | | | | | | | | | | 0.950 | 11.2 |
| 1,500 | | | | | | | | | | 1.017 | 7.1 |
| 2,000 | | | | | | | | | | 1.162 | 14.2 |
| 3,000 | | | | | | | | | | 1.268 | 9.1 |
| 4,000 | | | | | | | | | | 1.373 | 8.3 |
| 5,000 | | | | | | | | | | 1.468 | 6.9 |
| 6,000 | | | | | | | | | | 1.701 | 15.9 |
| 7,000 | | | | | | | | | | 1.706 | 0.3 |
| 8,000 | | | | | | | | | | 1.755 | 2.9 |
| 8,001 | | | | | | | | | | 1.760 | 0.3 |

**Middle Sample ID D2H13@N70** | Bulk S Gravity 2.388 | % Air Void 7.00%

| Stroke Count | Temperature F | C | Depth Gauge Reading (mm) 1 | 2 | 3 | 4 | 5 | Manual Average | Net Man Deflection | APA-DAS Average | Percent Change |
|---|---|---|---|---|---|---|---|---|---|---|---|
| 0 | | | | | | | | | 0.000 | 0.000 | |
| 500 | | | | | | | | | | 0.893 | |
| 1,000 | | | | | | | | | | 0.980 | 9.8 |
| 1,500 | | | | | | | | | | 1.131 | 15.4 |
| 2,000 | | | | | | | | | | 1.167 | 3.2 |
| 3,000 | | | | | | | | | | 1.299 | 11.3 |
| 4,000 | | | | | | | | | | 1.462 | 12.5 |
| 5,000 | | | | | | | | | | 1.536 | 5.1 |
| 6,000 | | | | | | | | | | 1.792 | 16.6 |
| 7,000 | | | | | | | | | | 1.845 | 3.0 |
| 8,000 | | | | | | | | | | 1.886 | 2.2 |
| 8,001 | | | | | | | | | | 1.898 | 0.6 |

**Right Sample ID D2S6@N40** | Bulk S Gravity 2.356 | % Air Void 7.50%

| Stroke Count | Temperature F | C | Depth Gauge Reading (mm) 1 | 2 | 3 | 4 | 5 | Manual Average | Net Man Deflection | APA-DAS Average | Percent Change |
|---|---|---|---|---|---|---|---|---|---|---|---|
| 0 | | | | | | | | | 0.000 | 0.000 | |
| 500 | | | | | | | | | | 0.724 | |
| 1,000 | | | | | | | | | | 0.937 | 29.6 |
| 1,500 | | | | | | | | | | 1.129 | 20.4 |
| 2,000 | | | | | | | | | | 0.980 | -13.2 |
| 3,000 | | | | | | | | | | 1.110 | 13.2 |
| 4,000 | | | | | | | | | | 1.416 | 27.6 |
| 5,000 | | | | | | | | | | 1.434 | 1.3 |
| 6,000 | | | | | | | | | | 1.659 | 15.7 |
| 7,000 | | | | | | | | | | 1.727 | 4.1 |
| 8,000 | | | | | | | | | | 1.757 | 1.7 |
| 8,001 | | | | | | | | | | 1.756 | 0.0 |

OCT 10 2002  E - 3  JEFF R. MILES, P.E.

# ASPHALT PAVEMENT ANALYZER
## Rutting Test Data Sheet

**PTI**
**PAVEMENT TECHNOLOGY, INC.**

Project No. : MIX D2 _A_  
Mix ID No. : D-2  
Mix Type : CYLINDERS  
Operator : MTISH  

Test No. : R1001-0  
Test Date: ~~10/08/02~~ 9-29-02  
Data File : R1001_0.ptd  
Run Status : Complete  

Temperature : 64 (deg. C)  
Wheel Load : 100 (lbs)  
Hose Pressure : 100 (psi)  
Run Time 2:15:41 (hh:mm:ss)  

**Left Sample ID** D2H14@N70 | **Bulk S Gravity** 2.388 | **% Air Void** 7.00%

| Stroke Count | Temperature F | Temperature C | Depth Gauge Reading (mm) 1 | 2 | 3 | 4 | 5 | Manual Average | Net Man Deflection | APA-DAS Average | Percent Change |
|---|---|---|---|---|---|---|---|---|---|---|---|
| 0 | | | | | | | | | 0.000 | 0.000 | |
| 500 | | | | | | | | | | 0.777 | |
| 1,000 | | | | | | | | | | 0.904 | 16.4 |
| 1,500 | | | | | | | | | | 0.981 | 8.5 |
| 2,000 | | | | | | | | | | 1.092 | 11.3 |
| 3,000 | | | | | | | | | | 1.260 | 15.5 |
| 4,000 | | | | | | | | | | 1.340 | 6.3 |
| 5,000 | | | | | | | | | | 1.470 | 9.7 |
| 6,000 | | | | | | | | | | 1.514 | 3.0 |
| 7,000 | | | | | | | | | | 1.622 | 7.1 |
| 8,000 | | | | | | | | | | 1.727 | 6.5 |
| 8,000 | | | | | | | | | | 1.727 | 0.0 |

**Middle Sample ID** -- | **Bulk S Gravity** | **% Air Void**

| Stroke Count | Temperature F | Temperature C | Depth Gauge Reading (mm) 1 | 2 | 3 | 4 | 5 | Manual Average | Net Man Deflection | APA-DAS Average | Percent Change |
|---|---|---|---|---|---|---|---|---|---|---|---|
| 0 | | | | | | | | | 0.000 | 0.000 | |
| 500 | | | | | | | | | | 0.000 | |
| 1,000 | | | | | | | | | | 0.000 | |
| 1,500 | | | | | | | | | | 0.000 | |
| 2,000 | | | | | | | | | | 0.000 | |
| 3,000 | | | | | | | | | | 0.000 | |
| 4,000 | | | | | | | | | | 0.000 | |
| 5,000 | | | | | | | | | | 0.000 | |
| 6,000 | | | | | | | | | | 0.000 | |
| 7,000 | | | | | | | | | | 0.000 | |
| 8,000 | | | | | | | | | | 0.000 | |
| 8,000 | | | | | | | | | | 0.000 | |

**Right Sample ID** D2S8@N60 | **Bulk S Gravity** 2.359 | **% Air Void** 7.42%

| Stroke Count | Temperature F | Temperature C | Depth Gauge Reading (mm) 1 | 2 | 3 | 4 | 5 | Manual Average | Net Man Deflection | APA-DAS Average | Percent Change |
|---|---|---|---|---|---|---|---|---|---|---|---|
| 0 | | | | | | | | | 0.000 | 0.000 | |
| 500 | | | | | | | | | | 0.864 | |
| 1,000 | | | | | | | | | | 0.891 | 3.1 |
| 1,500 | | | | | | | | | | 1.078 | 20.9 |
| 2,000 | | | | | | | | | | 1.261 | 17.0 |
| 3,000 | | | | | | | | | | 1.261 | 0.0 |
| 4,000 | | | | | | | | | | 1.492 | 18.3 |
| 5,000 | | | | | | | | | | 1.589 | 6.5 |
| 6,000 | | | | | | | | | | 1.672 | 5.2 |
| 7,000 | | | | | | | | | | 1.849 | 10.6 |
| 8,000 | | | | | | | | | | 1.855 | 0.3 |
| 8,000 | | | | | | | | | | 1.855 | 0.0 |

OCT 10 2002          E - 4          JEFF R. MILES, P.E.

# ASPHALT PAVEMENT ANALYZER
## Rutting Test Data Sheet

**Project No. :** MIX D-3

**Mix ID No. :** D-3

**Mix Type :** CYLINDER

**Operator :** M TISH

**Test No. :** R0925-0

**Test Date:** ~~10/08/02~~ 9-30-02

**Data File :** R0925_0.ptd

**Run Status :** Complete

**Temperature :** 76 (deg. C)

**Wheel Load :** 100 (lbs)

**Hose Pressure :** 100 (psi)

**Run Time** 2:16:50 (hh:mm:ss)

**Left Sample ID** D3H8@N40 | **Bulk S Gravity** 2.269 | **% Air Void** 6.30%

| Stroke Count | Temperature F | Temperature C | Depth Gauge Reading (mm) 1 | 2 | 3 | 4 | 5 | Manual Average | Net Man Deflection | APA-DAS Average | Percent Change |
|---|---|---|---|---|---|---|---|---|---|---|---|
| 0 | | | | | | | | | 0.000 | 0.000 | |
| 500 | | | | | | | | | | 0.915 | |
| 1,000 | | | | | | | | | | 1.174 | 28.2 |
| 1,500 | | | | | | | | | | 1.381 | 17.6 |
| 2,000 | | | | | | | | | | 1.423 | 3.1 |
| 3,000 | | | | | | | | | | 1.659 | 16.5 |
| 4,000 | | | | | | | | | | 1.790 | 7.9 |
| 5,000 | | | | | | | | | | 1.946 | 8.7 |
| 6,000 | | | | | | | | | | 2.104 | 8.1 |
| 7,000 | | | | | | | | | | 2.303 | 9.4 |
| 8,000 | | | | | | | | | | 2.324 | 0.9 |
| 8,000 | | | | | | | | | | 2.324 | 0.0 |

**Middle Sample ID** D3H9@N50 | **Bulk S Gravity** 2.262 | **% Air Void** 6.60%

| Stroke Count | Temperature F | Temperature C | Depth Gauge Reading (mm) 1 | 2 | 3 | 4 | 5 | Manual Average | Net Man Deflection | APA-DAS Average | Percent Change |
|---|---|---|---|---|---|---|---|---|---|---|---|
| 0 | | | | | | | | | 0.000 | 0.000 | |
| 500 | | | | | | | | | | 0.761 | |
| 1,000 | | | | | | | | | | 0.977 | 28.5 |
| 1,500 | | | | | | | | | | 1.182 | 21.0 |
| 2,000 | | | | | | | | | | 1.219 | 3.1 |
| 3,000 | | | | | | | | | | 1.503 | 23.3 |
| 4,000 | | | | | | | | | | 1.618 | 7.7 |
| 5,000 | | | | | | | | | | 1.777 | 9.8 |
| 6,000 | | | | | | | | | | 1.963 | 10.4 |
| 7,000 | | | | | | | | | | 2.192 | 11.7 |
| 8,000 | | | | | | | | | | 2.208 | 0.8 |
| 8,000 | | | | | | | | | | 2.208 | 0.0 |

**Right Sample ID** D3H6@N40 | **Bulk S Gravity** 2.249 | **% Air Void** 7.10%

| Stroke Count | Temperature F | Temperature C | Depth Gauge Reading (mm) 1 | 2 | 3 | 4 | 5 | Manual Average | Net Man Deflection | APA-DAS Average | Percent Change |
|---|---|---|---|---|---|---|---|---|---|---|---|
| 0 | | | | | | | | | 0.000 | 0.000 | |
| 500 | | | | | | | | | | 1.104 | |
| 1,000 | | | | | | | | | | 1.398 | 26.7 |
| 1,500 | | | | | | | | | | 1.850 | 32.3 |
| 2,000 | | | | | | | | | | 2.260 | 22.2 |
| 3,000 | | | | | | | | | | 2.969 | 31.4 |
| 4,000 | | | | | | | | | | 3.290 | 10.8 |
| 5,000 | | | | | | | | | | 3.768 | 14.5 |
| 6,000 | | | | | | | | | | 4.094 | 8.6 |
| 7,000 | | | | | | | | | | 4.495 | 9.8 |
| 8,000 | | | | | | | | | | 4.573 | 1.7 |
| 8,000 | | | | | | | | | | 4.573 | 0.0 |

OCT 1 0 2002

E - 5

JEFF R. MILES, P.E.

Deformation (mm) vs Strokes (x10/point)
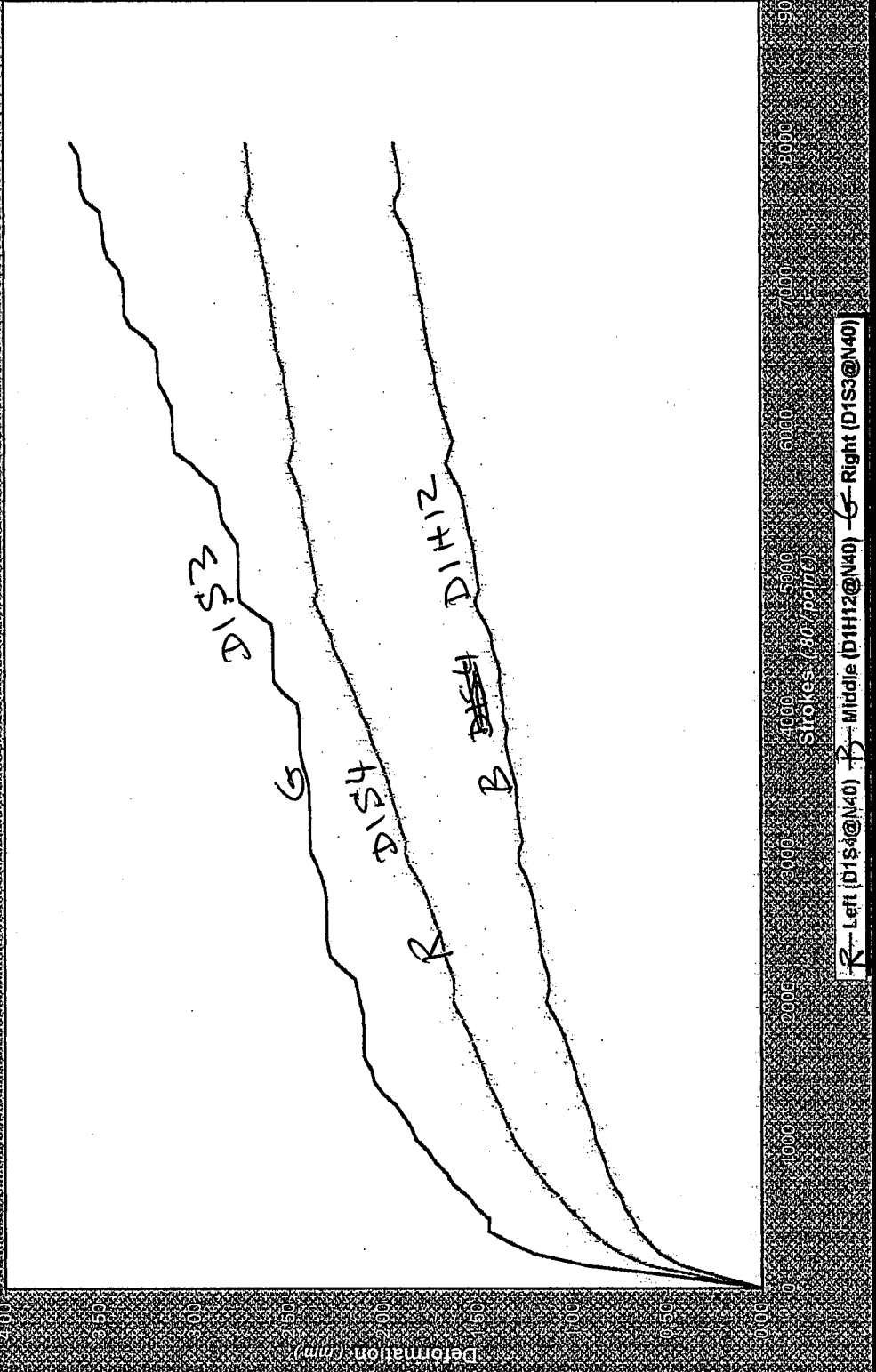
Legend: R— Left (D1S4@N40)  B— Middle (D1H12@N40)  G— Right (D1S3@N40)

Handwritten annotations: D1S3, D1S4, D1H12

| Current Values & Status | Test No. | Stroke Count | Rate | Time Run | Remaining | Est. Complete | Channel Inputs (mm) Left | Middle | Right | Data Link Status | Run Status |
|---|---|---|---|---|---|---|---|---|---|---|---|
| | R0923-0 | 8000 | 59.35 | 2:15:46 | 0:00:00 | 12:35 PM | 2.744 | 1.965 | 3.704 | Inactive | Complete |

Data Link Control: Start, Pause, ABORT, Clear

E - 6

Pavement Technology, Inc.  APA Rut Test  (Deformation vs Stroke Count)

Data Link Control

Start
Pause
ABORT
Clear

Deformation (mm)

Strokes (30 / point)
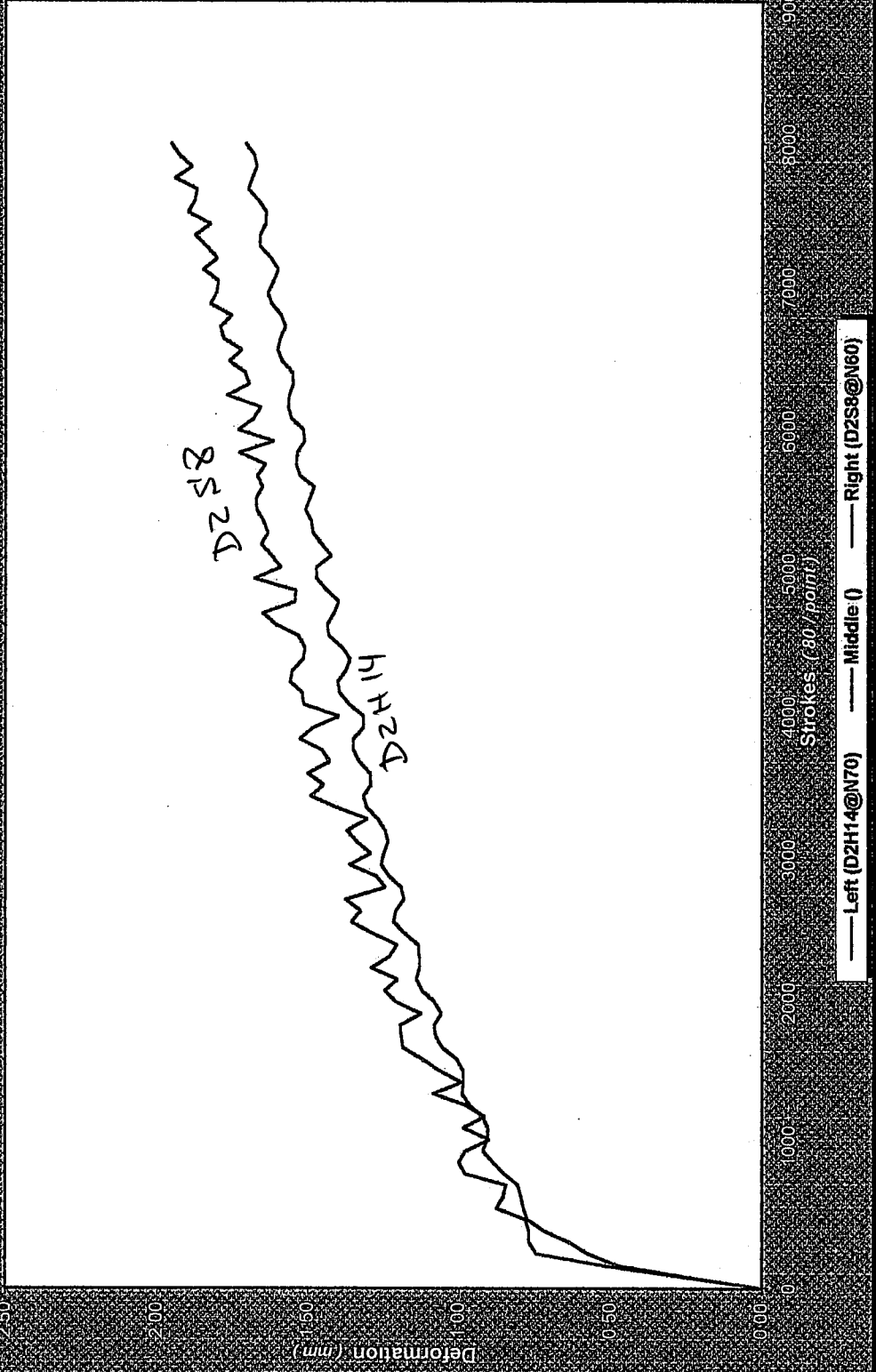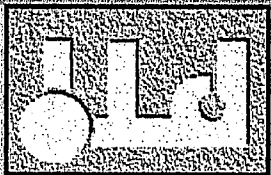
— Left (D2H14@N70)   — Middle ()   — Right (D2S8@N60)

D2S8

D2H14

| Current Values & Status | Test No. | Stroke Count | Rate | Time Run | Remaining | Est Complete | Channel Inputs (mm) Left | Middle | Right | Data Link Status | Run Status |
|---|---|---|---|---|---|---|---|---|---|---|---|
| | ~ | 8000 | 59.41 | 2:15:41 | 0:00:00 | 2:14 PM | 1.727 | 0.000 | 1.855 | Reset | Ready |

Data Link Control

Pavement Technology, Inc.    APA Rut Test    (Deformation vs Stroke Count)

Deformation (mm)

Strokes (60/point)

—— Left (D3H8@N40) —— Middle (D3H9@N50) —— Right (D3H6@N40)
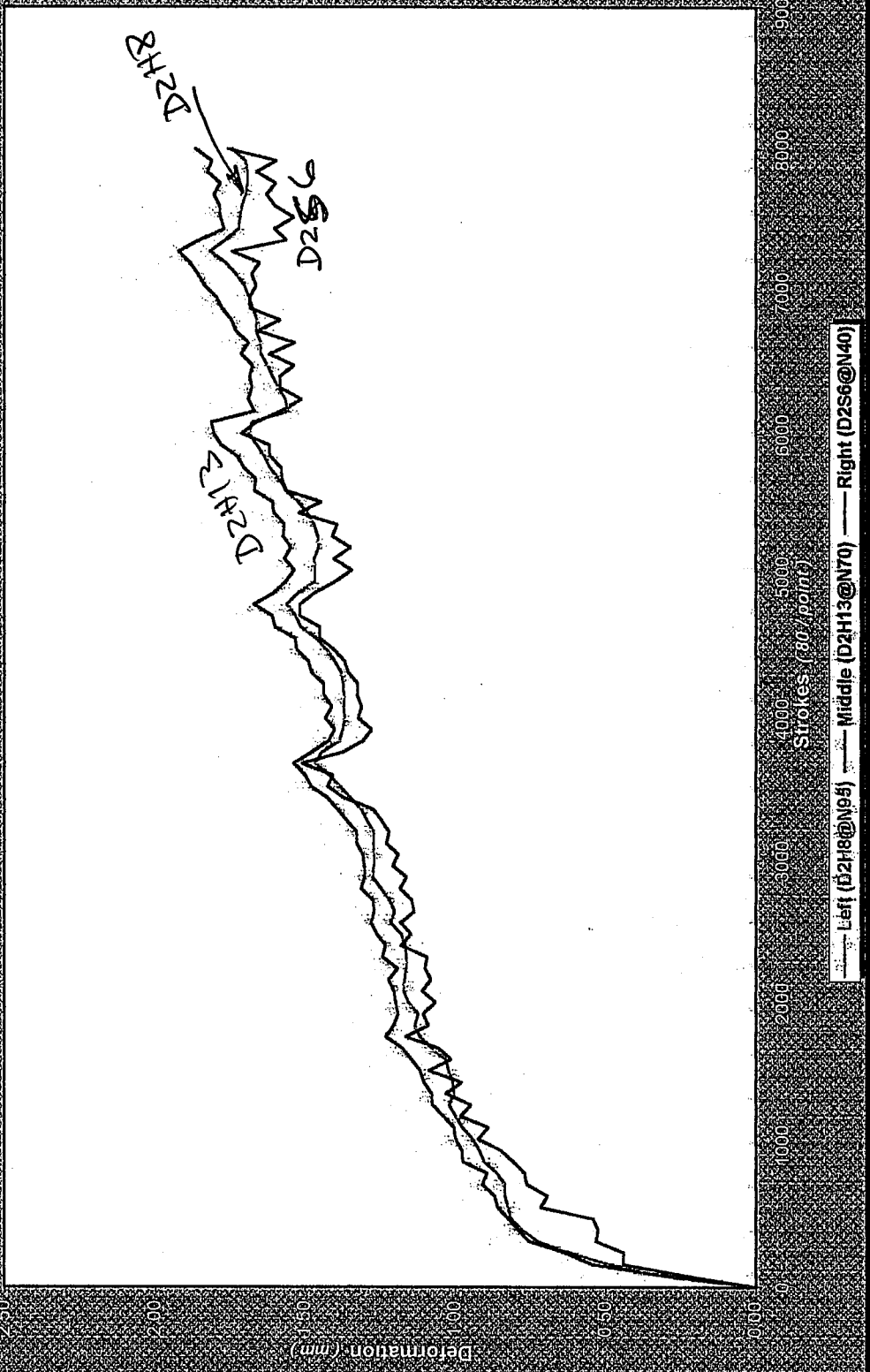
Start
Pause
ABORT
Clear

| Current Values & Status | Test No. | Stroke Count | Rate | Run | Time Remaining | Est. Complete | Channel Inputs (mm) | | | Data Link Status | Run Status |
|---|---|---|---|---|---|---|---|---|---|---|---|
| | | | | | | | Left | Middle | Right | | |
| | R0925-0 | 8000 | 59.41 | 2:16:50 | 0:00:00 | 10:00 AM | 2.324 | 2.208 | 4.573 | Inactive | Complete |

## Mix D1 - Samples for APA Test at Air Viods=7%, PG-58-28

| Sample for D1 | D1H12 at N40 | D1S3 at N40 | D1S4 at N40 |
|---|---|---|---|
| Asphalt content Pb by aggr.WT | 5.3% | 5.25% | 5.25% |
| Asphalt content Pb by mix WT | 5.0% | 5.0% | 5.0% |
| Wdry: | 5830 | 5989 | 6086.5 |
| Wsub: | 3380 | 3433.3 | 3494.2 |
| Wssd: | 5896.2 | 6023 | 6123.7 |
| Gmm: | 2.478 | 2.478 | 2.478 |
| Gsb: | 2.66 | 2.66 | 2.66 |
| Ps: | 95.0% | 95.0% | 95.0% |
| H | 141.83 | 148.61 | 151.15 |
| | | | |
| Gmb=Wdry/Wssd-Wsub | | | |
| Gmb(measured) | 2.317 | 2.313 | 2.315 |
| Gmb(estimated) | 2.327 | 2.282 | 2.280 |
| CF | 0.996 | 1.014 | 1.015 |
| Gmb(estimated)@Nmax: | 2.327 | 2.282 | 2.280 |
| Gmb(corrected)@Nmax: | 2.317 | 2.313 | 2.315 |
| %Va=1-Gmb/Gmm | | | |
| **%Va** | **6.5%** | **6.7%** | **6.6%** |
| %VMA=100-Gmb*Ps/Gsb | | | |
| **%VMA** | **17.3%** | **17.4%** | **17.3%** |
| %VFA=100*(VMA-Va)/VMA | | | |
| **%VFA** | **62.3%** | **61.7%** | **62.0%** |
| Contact Energy Index, **CEI** | **10.061** | **10.219** | **10.279** |
| Total Energy Index, **TEI** | **137.434** | **132.226** | **130.575** |
| APA Rut-Depth, mm | **1.97** | **3.7** | **2.74** |

## Mix D2 - Samples for APA Test at Air Voids=7%, PG-64-34

| Sample for D2 | D2H8 at N95 | D2H13 at N70 | D2H14 at N70 | D2S6 at N60 | D2S8 at N60 |
|---|---|---|---|---|---|
| Asphalt content Pb by aggr.WT | 6.1% | 6.1% | 6.1% | 6.62% | 6.62% |
| Asphalt content Pb by mix WT | 5.75% | 5.75% | 5.75% | 6.20% | 6.20% |
| Wdry: | 5832.8 | 6276.5 | 6302.5 | 6260.1 | 6275.3 |
| Wsub: | 3448 | 3687.5 | 3706 | 3680.2 | 3674.6 |
| Wssd: | 5865.2 | 6308 | 6345.1 | 6302.6 | 6334.9 |
| Gmm: | 2.567 | 2.567 | 2.567 | 2.548 | 2.548 |
| Gsb: | 2.68 | 2.68 | 2.68 | 2.68 | 2.68 |
| Ps: | 94.25% | 94.25% | 94.25% | 93.80% | 93.80% |
| H90: | 140.3 | 151.62 | 153.17 | 152.59 | 154.85 |
|  |  |  |  |  |  |
| Gmb=Wdry/Wssd-Wsub |  |  |  |  |  |
| Gmb(measured) | 2.413 | 2.395 | 2.388 | 2.387 | 2.359 |
| Gmb(estimated) | 2.354 | 2.344 | 2.330 | 2.323 | 2.294 |
| CF | 1.025 | 1.022 | 1.025 | 1.028 | 1.028 |
| Gmb(estimated)@Nmax: | 2.354 | 2.344 | 2.330 | 2.323 | 2.294 |
| Gmb(corrected)@Nmax: | 2.413 | 2.395 | 2.388 | 2.387 | 2.359 |
| %Va=1-Gmb/Gmm |  |  |  |  |  |
| **%Va@N90:** | **6.0%** | **6.7%** | **7.0%** | **6.3%** | **7.42%** |
| %VMA=100-Gmb*Ps/Gsb |  |  |  |  |  |
| **%VMA** | **15.1%** | **15.8%** | **16.0%** | **16.4%** | **17.4%** |
| %VFA=100*(VMA-Va)/VMA |  |  |  |  |  |
| **%VFA** | **60.4%** | **57.5%** | **56.5%** | **61.6%** | **57.4%** |
| Contact Energy Index, **CEI** | **20.746** | **13.412** | **13.658** | **16.432** | **15.817** |
| Total Energy Index, **TEI** | **447.572** | **254.43** | **263.025** | **234.528** | **233.667** |
| APA Rut-Depth, mm | **1.76** | **1.9** | **1.73** | **1.76** | **1.86** |

# Mix D3 - Samples for APA Test at Air Voids=7%, PG-76-28

| Sample for D3 | D3H6 at N40 | D3H8 at N40 | D3H9 at N50 |
|---|---|---|---|
| Asphalt content Pb by aggr.WT | 5.0% | 5.0% | 5.0% |
| Asphalt content Pb by mix WT | 4.8% | 4.8% | 4.8% |
| Wdry: | 5758.2 | 5929.7 | 5937.1 |
| Wsub: | 3290 | 3384 | 3394.1 |
| Wssd: | 5850 | 5996.8 | 6018.6 |
| Gmm: | 2.422 | 2.422 | 2.422 |
| Gsb: | 2.547 | 2.547 | 2.547 |
| Ps: | 95.24% | 95.24% | 95.24% |
| H | 147.07 | 151.04 | 153.04 |
|  |  |  |  |
| Gmb=Wdry/Wssd-Wsub |  |  |  |
| Gmb(measured) | 2.249 | 2.269 | 2.262 |
| Gmb(estimated) | 2.217 | 2.223 | 2.196 |
| CF | 1.015 | 1.021 | 1.030 |
| Gmb(estimated)@Nmax: | 2.217 | 2.223 | 2.196 |
| Gmb(corrected)@Nmax: | 2.249 | 2.269 | 2.262 |
| %Va=1-Gmb/Gmm |  |  |  |
| **%Va** | **7.1%** | **6.3%** | **6.6%** |
| %VMA=100-Gmb*Ps/Gsb |  |  |  |
| **%VMA** | **15.9%** | **15.1%** | **15.4%** |
| %VFA=100*(VMA-Va)/VMA |  |  |  |
| **%VFA** | **55.1%** | **58.4%** | **57.2%** |
| Contact Energy Index, **CEI** | **11.156** | **10.755** | **9.215** |
| Total Energy Index, **TEI** | **150.391** | **147.44** | **128.612** |
| APA Rut-Depth, mm | **4.57** | **2.32** | **2.21** |

This is a blank Page

# APPENDIX F

## Image Analysis Test Results for ITD Mixes

# Mix D1 - Samples for Image Test

| Sample for D1 | D1H1 | D1H4 | D1H13 | D1H14 | D1H115 | D1H116 | D1S1 | D1S2 |
|---|---|---|---|---|---|---|---|---|
| Asphalt content, Pb by aggregate weight | 5.3% | 5.3% | 6.3% | 6.3% | 4.3% | 4.3% | 5.3% | 5.3% |
| Asphalt content, Pb by mix weight | 5.0% | 5.0% | 5.93% | 5.93% | 4.1% | 4.1% | 5.0% | 5.0% |
| Wdry: | 4727.2 | 4756.1 | 4762.7 | 4765.5 | 5801.7 | 5800 | 4709 | 4688 |
| Wsub: | 2772 | 2801.5 | 2814.1 | 2814.2 | 3429.3 | 3430.5 | 2774 | 2753 |
| Wssd: | 4738 | 4767.7 | 4770.8 | 4774 | 5821.8 | 5818.3 | 4730 | 4702 |
| Gmm: | 2.478 | 2.478 | 2.444 | 2.444 | 2.511 | 2.511 | 2.478 | 2.478 |
| Gsb: | 2.66 | 2.66 | 2.66 | 2.66 | 2.66 | 2.66 | 2.66 | 2.66 |
| Ps: | 95.0% | 95.0% | 94.1% | 94.1% | 95.9% | 95.9% | 95.0% | 95.0% |
| Hini: | 126.09 | 128.19 | 126.95 | 126.71 | 153.96 | 153.93 | 129.91 | 127.77 |
| Hdes: | 113.05 | 114.65 | 113.81 | 113.82 | 138.21 | 138.13 | 116.51 | 115.03 |
| Hmax: | 111.65 | 113.14 | 112.38 | 112.36 | 136.49 | 136.36 | 115.07 | 113.67 |
| **Gmb calculation** | | | | | | | | |
| Gmb(measured) at Nmax=Wdry/(Wssd-Wsub) | 2.404 | 2.419 | 2.434 | 2.432 | 2.425 | 2.429 | 2.407 | 2.405 |
| Gmb(estimated) | 2.397 | 2.380 | 2.399 | 2.401 | 2.407 | 2.408 | 2.317 | 2.335 |
| CF | 1.003 | 1.016 | 1.014 | 1.013 | 1.008 | 1.009 | 1.039 | 1.030 |
| Gmb(estimated)@Nd: | 2.367 | 2.349 | 2.369 | 2.370 | 2.377 | 2.377 | 2.288 | 2.307 |
| Gmb(corrected)@Nd: | 2.375 | 2.387 | 2.403 | 2.400 | 2.395 | 2.398 | 2.378 | 2.377 |
| Gmb(estimated)@Nini: | 2.123 | 2.101 | 2.124 | 2.129 | 2.134 | 2.133 | 2.052 | 2.077 |
| Gmb(corrected)@Nini: | 2.129 | 2.135 | 2.155 | 2.156 | 2.150 | 2.152 | 2.132 | 2.140 |
| **Verification of Superpave Criteria at Ndes** | | | | | | | | |
| %VMA=100-Gmb(corrected)@Nd*Ps/Gsb | 15.19% | 14.75% | 15.00% | 15.11% | 13.68% | 13.57% | 15.08% | 15.11% |
| %Va@Nd=1-Gmb@Ndes/Gmm | 4.17% | 3.67% | 1.66% | 1.78% | 4.63% | 4.50% | 4.05% | 4.08% |
| %VFA@Nd=100*(VMA-Va)/VMA | 72.6% | 75.1% | 88.9% | 88.2% | 66.2% | 66.8% | 73.2% | 73.0% |
| %Gmm@Nini | 85.9% | 86.2% | 88.2% | 88.2% | 85.6% | 85.7% | 86.1% | 86.4% |
| %Gmm@Ndes | 95.8% | 96.3% | 98.3% | 98.2% | 95.4% | 95.5% | 96.0% | 95.9% |
| %Gmm@Nmax | 97.0% | 97.6% | 99.6% | 99.5% | 96.6% | 96.7% | 97.2% | 97.1% |
| **Air Voids Change** | | | | | | | | |
| %Va @Nini = 1-Gmb (corrected at Nini)/Gmm | 14.1% | 13.8% | 11.8% | 11.8% | 14.4% | 14.3% | 13.9% | 13.6% |
| %Va@Nd=1-Gmb@Ndes/Gmm | 4.2% | 3.7% | 1.7% | 1.8% | 4.6% | 4.5% | 4.0% | 4.1% |
| %Va@Nmax=1-Gmb@Nmax/Gmm | 3.0% | 2.4% | 0.4% | 0.5% | 3.4% | 3.3% | 2.8% | 2.9% |
| **CEI Results** | | | | | | | | |
| CEI based on Nmax=160 | 20.043 | 21.308 | 17.27 | 18.586 | 18.441 | 19.585 | 22.054 | 21.083 |
| CEI based on Ndes=100 | 17.086 | 18.283 | 14.275 | 15.658 | 15.343 | 16.632 | 19.44 | 18.614 |
| TEI based on Nmax=160 | 966.39 | 946.99 | 932.55 | 931.88 | 810.53 | 780.63 | 901 | 914.95 |

## Mix D2 - Samples for Image Test

| Sample for D2 | D2H2 | D2H6 | D2S1 | D2S2 | D2H10 | D2H11 | D2H14 | D2H15 |
|---|---|---|---|---|---|---|---|---|
| Asphalt content, Pb by aggregate weight | 6.1% | 6.1% | 6.62% | 6.62% | 7.6% | 7.6% | 5.6% | 5.6% |
| Asphalt content, Pb by mix weight | 5.75% | 5.75% | 6.20% | 6.20% | 7.08% | 7.08% | 5.32% | 5.32% |
| Wdry: | 4738.2 | 4758 | 4751.7 | 4742 | 4795 | 4791.1 | 4664 | 4665 |
| Wsub: | 2821.3 | 2842 | 2838.4 | 2835.4 | 2867.2 | 2858.1 | 2787.5 | 2779.8 |
| Wssd: | 4742.4 | 4776 | 4758 | 4751 | 4804.7 | 4795.5 | 4720.5 | 4712.4 |
| Gmm: | 2.567 | 2.567 | 2.548 | 2.548 | 2.514 | 2.514 | 2.585 | 2.585 |
| Gsb: | 2.68 | 2.68 | 2.68 | 2.68 | 2.68 | 2.68 | 2.68 | 2.68 |
| Ps: | 94.25% | 94.25% | 93.8% | 93.8% | 92.92% | 92.92% | 94.68% | 94.68% |
| Hini: | 127.36 | 125.66 | 125.66 | 125.66 | 127.82 | 127.83 | 129.51 | 130.08 |
| Hdes: | 112.99 | 111.81 | 111.81 | 111.81 | 112.99 | 113.62 | 115.54 | 116.08 |
| Hmax: | 111.52 | 110.43 | 110.43 | 110.43 | 111.45 | 112.11 | 113.99 | 114.52 |
| **Gmb calculation** | | | | | | | | |
| Gmb(measured) at Nmax=Wdry/(Wssd-Wsub) | 2.466 | 2.460 | 2.475 | 2.475 | 2.475 | 2.473 | 2.413 | 2.414 |
| Gmb(estimated) | 2.406 | 2.439 | 2.436 | 2.431 | 2.436 | 2.420 | 2.317 | 2.306 |
| CF | 1.025 | 1.009 | 1.016 | 1.018 | 1.016 | 1.022 | 1.042 | 1.047 |
| Gmb(estimated)@Nd: | 2.374 | 2.409 | 2.406 | 2.401 | 2.403 | 2.387 | 2.285 | 2.275 |
| Gmb(corrected)@Nd: | 2.434 | 2.430 | 2.445 | 2.445 | 2.441 | 2.440 | 2.380 | 2.381 |
| Gmb(estimated)@Nini: | 2.106 | 2.144 | 2.141 | 2.137 | 2.124 | 2.122 | 2.039 | 2.030 |
| Gmb(corrected)@Nini: | 2.160 | 2.162 | 2.175 | 2.175 | 2.158 | 2.169 | 2.124 | 2.125 |
| **Verification of Superpave Criteria at Ndes** | | | | | | | | |
| %VMA=100-Gmb(corrected)@Nd*Ps/Gsb | 14.39% | 14.55% | 14.43% | 14.43% | 15.36% | 15.40% | 15.90% | 15.87% |
| %Va@Nd=1-Gmb@Ndes/Gmm | 5.17% | 5.34% | 4.05% | 4.05% | 2.90% | 2.94% | 7.91% | 7.88% |
| %VFA@Nd=100*(VMA-Va)/VMA | 64.1% | 63.3% | 71.9% | 72.0% | 81.1% | 80.9% | 50.2% | 50.4% |
| %Gmm@Nini | 84.1% | 84.2% | 85.4% | 85.4% | 85.8% | 86.3% | 82.2% | 82.2% |
| %Gmm@Ndes | 94.8% | 94.7% | 96.0% | 96.0% | 97.1% | 97.1% | 92.1% | 92.1% |
| %Gmm@Nmax | 96.1% | 95.8% | 97.1% | 97.2% | 98.4% | 98.4% | 93.3% | 93.4% |
| **Air Voids Change** | | | | | | | | |
| %Va @Nini = 1-Gmb (corrected at Nini)/Gmm | 15.87% | 15.78% | 14.63% | 14.62% | 14.17% | 13.73% | 17.85% | 17.79% |
| %Va@Nd=1-Gmb@Ndes/Gmm | 5.17% | 5.34% | 4.05% | 4.05% | 2.90% | 2.94% | 7.91% | 7.88% |
| %Va@Nmax=1-Gmb@Nmax/Gmm | 3.92% | 4.16% | 2.85% | 2.85% | 1.56% | 1.63% | 6.66% | 6.62% |
| **CEI Results** | | | | | | | | |
| CEI based on Nmax=160 | 17.815 | 19.98 | 22.872 | 22.783 | 18.431 | 19.322 | 21.651 | 19.677 |
| CEI based on Ndes=100 | 15.358 | 17.169 | 20.074 | 19.81 | 15.245 | 16.29 | 18.663 | 16.587 |
| TEI based on Nmax=160 | 937.61 | 924.59 | 920.56 | 989.84 | 919.24 | 916.02 | 907.36 | 907.03 |

## Mix D3 - Samples for Image Test

| Sample for D3 | D3H2 | D3H4 | D3S1(ch.gr) | D3S2(ch.gr) |
|---|---|---|---|---|
| Asphalt content, Pb by aggregate weight | 5.0% | 5.0% | 5.0% | 5.0% |
| Asphalt content, Pb by mix weight | 4.8% | 4.8% | 4.8% | 4.8% |
| Wdry: | 4741.6 | 4710.1 | 4587.4 | 4707.6 |
| Wsub: | 2755 | 2746.7 | 2636.6 | 2722.7 |
| Wssd: | 4749.5 | 4720.5 | 4590 | 4723.5 |
| Gmm: | 2.422 | 2.422 | 2.422 | 2.422 |
| Gsb: | 2.547 | 2.547 | 2.547 | 2.547 |
| Ps: | 95.2% | 95.2% | 95.2% | 95.2% |
| Hini: | 124.94 | 127.15 | 147.76 | 129.94 |
| Hdes: | 114.72 | 116.08 | 115.22 | 117.43 |
| Hmax: | 113.78 | 114.81 | 113.92 | 116.08 |
| **Gmb calculation** | | | | |
| Gmb(measured) at Nmax=Wdry/(Wssd-Wsub) | 2.377 | 2.386 | 2.348 | 2.353 |
| Gmb(estimated) | 2.359 | 2.323 | 2.280 | 2.296 |
| CF | 1.008 | 1.027 | 1.030 | 1.025 |
| Gmb(estimated)@Nd: | 2.340 | 2.297 | 2.254 | 2.270 |
| Gmb(corrected)@Nd: | 2.358 | 2.360 | 2.322 | 2.326 |
| Gmb(estimated)@Nini: | 2.149 | 2.097 | 1.758 | 2.051 |
| Gmb(corrected)@Nini: | 2.165 | 2.155 | 1.811 | 2.102 |
| **Verification of Superpave Criteria at Ndes** | | | | |
| %VMA=100-Gmb(corrected)@Nd*Ps/Gsb | **11.8%** | **11.7%** | **13.2%** | **13.0%** |
| %Va @Nd=1-Gmb@Ndes/Gmm | **2.6%** | **2.6%** | **4.1%** | **4.0%** |
| %VFA@Nd=100*(VMA-Va)/VMA | **77.6%** | **78.3%** | **68.6%** | **69.5%** |
| %Gmm@Nini | 89.4% | 89.0% | 74.8% | 86.8% |
| %Gmm@Ndes | 97.4% | 97.4% | 95.9% | 96.0% |
| %Gmm@Nmax | 98.2% | 98.5% | 97.0% | 97.1% |
| **Air Voids Change** | | | | |
| %Va @Nini = 1-Gmb (corrected at Nini)/Gmm | **10.6%** | **11.0%** | **25.2%** | **13.2%** |
| %Va@Nd=1-Gmb@Ndes/Gmm | **2.6%** | **2.6%** | **4.1%** | **4.0%** |
| %Va@Nmax=1-Gmb@Nmax/Gmm | **1.8%** | **1.5%** | **3.0%** | **2.9%** |
| **CEI Results** | | | | |
| CEI based on Nmax=160 | **8.307** | **10.049** | **22.788** | **23.245** |
| CEI based on Ndes=100 | **6.313** | **7.381** | **20.855** | **19.786** |
| TEI based on Nmax=160 | **843.389** | **837.873** | **824.894** | **819.769** |

# APPENDIX G

**e-Files Included on CD-ROM**

The CD ROM includes files for:

- Servopac Gyratory Files for All Samples
- Excel files for CEI calculations for all samples
- Template for CEI Calculation Excel Sheet
- Various Excel files for raw data for volumetric analysis